Journal of Food Quality

Innovative and Emerging Drying Technologies for Enhancing Food Quality

Lead Guest Editor: Hong-Wei Xiao
Guest Editors: Zhongli Pan, Alex Martynenko, Chung-Lim Law, and Prabhat K. Nema

Innovative and Emerging Drying Technologies for Enhancing Food Quality

Journal of Food Quality

Innovative and Emerging Drying Technologies for Enhancing Food Quality

Lead Guest Editor: Hong-Wei Xiao
Guest Editors: Zhongli Pan, Alex Martynenko, Chung-Lim Law, and Prabhat K. Nema

Editorial Board

Contents

Hindawi
Journal of Food Quality
Volume 2018, Article ID 6943078, 2 pages
https://doi.org/10.1155/2018/6943078

Editorial

Innovative and Emerging Drying Technologies for Enhancing Food Quality

Hong-Wei Xiao,[1] **Zhongli Pan**,[2,3] **Alex Martynenko**,[4] **Chung-Lim Law**,[5] **and Prabhat K. Nema**[6]

[1]*College of Engineering, China Agricultural University, Beijing, China*
[2]*Western Regional Research Center, USDA-ARS, Albany, CA, USA*
[3]*University of California, Davis, CA, USA*
[4]*Dalhousie University, Halifax, NS, Canada*
[5]*Department of Chemical and Environmental Engineering, Faculty of Engineering, The University of Nottingham, Malaysia Campus, Jalan Broga, Semenyih, Selangor Darul Ehsan, Malaysia*
[6]*Department of Food Engineering, National Institute of Food Technology Entrepreneurship and Management, Kundli, Sonepat, Haryana 131028, India*

Correspondence should be addressed to Hong-Wei Xiao; xhwcaugxy@163.com

Received 10 April 2018; Accepted 10 April 2018; Published 13 May 2018

Drying is one of the most frequently used methods for food preservation due to prevention of microorganisms' growth and reduction of moisture-mediated deteriorative reactions at low water activity. In addition, food drying provides numerous benefits, such as formation of desirable texture and physical properties, extending shelf life, and minimizing packaging, storage, and transportation costs. Although simplicity and small capital investments make natural open-sun drying and hot air convective drying the most popular practical technologies for drying of agricultural products in developing countries, food quality remains the major issue. For example, open-sun drying has several disadvantages, including long drying time, rewetting or rotting caused by bad weather, contamination by dust and insects, non-uniform drying, and significant color loss and nutrients deterioration due to long exposure to solar radiation. Drawbacks of hot air drying include degradation in nutrients and flavor, shrinkage, fractures and case hardening, color darkening, and decrease of antioxidant and rehydration capacity due to prolonged exposure to high air temperatures. These technologies require critical improvements to improve the product quality and processing sustainability.

With globalization of world economy, food quality became an industry priority since it provides companies competitive advantage in the global market place. Therefore, recent trend in the food drying research focuses on minimizing chemical and thermal degradation and maximizing nutrient retention in food products. Innovative and emerging drying technologies offer key advantages to improve food quality and address growing consumer demand on the global food market. In recent years, a range of novel drying technologies has been developed to improve physicochemical properties of foods by minimizing thermal degradation and time of drying. The primary effort of these innovations is to increase drying efficiency with minimal changes in nutritional value of foods and extension of shelf stability to ensure product safety, quality, and acceptability. Another aspect of innovations is to minimize energy consumption and reduce carbon footprint of drying technologies.

The main goal of this special issue is to provide a platform for the discussion on the latest progress of innovative and emerging drying technologies. Following a call for papers, more than 14 manuscripts were submitted for this special issue, and after being strictly peer reviewed, 8 manuscripts were finally accepted.

Fruit and vegetable chips are very popular with consumers due to its desired texture. The research work from

Min Xiao and corroborators verified that the modifications of pectic polysaccharides of apple chips during drying significantly affect the texture of apple chips. Vacuum frying is a recently developed technique for chips processing with low oil content. The investigation from Aiqing Ren and collaborators focused on using pretreatment to preserve nutrients and reduce oil content of vacuum-fried shiitake mushroom slice. They reported the blanching, osmotic dehydration, and coating pretreatment before vacuum frying could improve color and sensory evaluation and minimize the oil uptake of vacuum-fried shiitake mushroom chips. To avoid intake of excessive energy during consumption of fried chips, the research work from Dr. Jiangyong Yi and collaborators applied a combined freeze drying and instant controlled pressure drop process (FD-DIC) on carrot-potato chips processing, verified that FD-DIC is an alternative method for obtaining desirable restructured fruit and vegetable chips, and optimized the processing conditions of carrot-potato chips by using response surface methodology.

Microencapsulation is widely used to minimize the oxidation of fish oil products. The study from Yuqi Pang and coworkers compared the effects of different drying methods (spray drying, freeze drying, and spray freeze drying) on the microencapsulation of fish oil. The authors found that spray freeze drying obtained high quality and more stability powder, which is a promising method for the preparation of microcapsules, which can improve product storage stability and potential digestibility.

Sun drying and convective drying are still the most frequently used drying methods in many developing countries. The paper of Iva Kučerová and coworkers applied a double-pass solar drier for thin-layer drying of eland and beef, when combined with pretreatment of traditional jerky marinade with fresh pineapple juice, obtained a favorable texture, color, and taste product. The work from Roberto Lemus-Mondaca reported that the hot air drying process is an important processing of abalone, air temperature significantly influenced the physical, chemical, and nutritional properties of osmo-treated abalone slices, discoloration of product was more evident at high drying temperatures, and the drying temperature of 60°C could enhance the final characteristics of the product.

Drying is a complex, dynamic, highly nonlinear, strongly interactive, and multivariable thermal process. The prediction of moisture content and quality parameters is very useful to improve the overall performance of drying process. Artificial neural network (ANN) methodology could precisely predict experimental data. The paper from Dr. Jun-Wen Bai and coworkers modelled the experimental drying kinetics and color changes of ginkgo biloba seeds during its microwave drying process using ANN methodology. The authors verified that ANN methodology could precisely predict experimental data; meanwhile, the established ANN models could be used for online prediction of moisture content and color changes of ginkgo biloba seeds during microwave drying process.

Blanching is an important pretreatment prior to agroproducts drying, to inactivate enzymes and remove air from intercellular space to prevent color and flavor degradation during drying. The paper of Hai-ou Wang and coworkers evaluated the effect of hot water blanching on the drying characteristics and product qualities of apple slices dried with the novel integrated freeze-drying process. It was found that hot water blanching pretreatment is a promising alternative method to decrease drying time and improve product quality of apple slices.

Finally, the research work from Dr. Zhijun Zhang and collaborators revealed the shape effect on the temperature field during microwave heating. They reported that, for the small and big volume samples, spherical sample was better than the cubic ones, and for the intermediate size samples, temperature uniformity of spherical sample is better than that of cubic sample, while the microwave absorption capability of cubic sample is higher than that of spherical sample. Besides, the results also indicated that orientations affect the microwave process significantly. Therefore, an optimal sample shape and orientation could be decided to achieve the goal of high temperature distribution uniformity and low energy consumption.

We hope that this special issue not only contributes to a better understanding of the research status of innovative and emerging drying techniques, but also triggers new research opportunities in this field in order to provide more healthy and nutritious food for the growing global population in a more sustainable way. We hope that the readers will enjoy the reading and this publication will inspire further investigation in this exciting and promising research area.

Hong-Wei Xiao
Zhongli Pan
Alex Martynenko
Chung-Lim Law
Prabhat K. Nema

Acknowledgments

The authors would like to sincerely thank all the authors who contributed to this special issue, as well as the expert reviewers who provided constructive feedback and extremely useful comments.

Hindawi
Journal of Food Quality
Volume 2018, Article ID 6317943, 10 pages
https://doi.org/10.1155/2018/6317943

Research Article

Convective Drying of Osmo-Treated Abalone *(Haliotis rufescens)* Slices: Diffusion, Modeling, and Quality Features

Roberto Lemus-Mondaca,[1] **Sebastian Pizarro-Oteíza**,[2] **Mario Perez-Won**,[2] **and Gipsy Tabilo-Munizaga**[3]

[1]*Departamento de Ciencia de los Alimentos y Tecnología Química, Facultad de Ciencias Químicas y Farmacéuticas, Universidad de Chile, Santos Dumont 964, Independencia, Santiago, Chile*
[2]*Departamento de Ingeniería en Alimentos, Universidad de La Serena, Av. Raúl Bitrán 1305, La Serena, Chile*
[3]*Departamento de Ingeniería en Alimentos, Universidad del Bío-Bío, Av. Andrés Bello 720, Chillán, Chile*

Correspondence should be addressed to Roberto Lemus-Mondaca; roberto.lemus@ciq.uchile.cl

Received 17 October 2017; Revised 6 January 2018; Accepted 14 February 2018; Published 24 April 2018

Academic Editor: Alex Martynenko

The focus of this research was based on the application of an osmotic pretreatment (15% NaCl) for drying abalone slices, and it evaluates the influence of hot-air drying temperature (40–80°C) on the product quality. In addition, the mass transfer kinetics of salt and water was also studied. The optimal time of the osmotic treatment was established until reaching a pseudo equilibrium state of the water and salt content (290 min). The water effective diffusivity values during drying ranged from 3.76 to 4.75 × 10^{-9} m^2/s for three selected temperatures (40, 60, and 80°C). In addition, experimental data were fitted by Weibull distribution model. The modified Weibull model provided good fitting of experimental data according to applied statistical tests. Regarding the evaluated quality parameters, the color of the surface showed a change more significant at high temperature (80°C), whereas the nonenzymatic browning and texture showed a decrease during drying process mainly due to changes in protein matrix and rehydration rates, respectively. In particular, working at 60°C resulted in dried samples with the highest quality parameters.

1. Introduction

The red abalone *(Haliotis rufensces)* is an herbivorous gastropod mollusk living naturally in the bedrock of water between 1 and 30 m depth. The culture of abalone has increased considerably, since it is highly appreciated as a seafood of high commercial value, especially in countries like China and Japan [1], enjoying the firm texture, as well as cooked product tenderness [2]. This species of abalone is considered exotic seafood and is one of the most expensive seafood products (Briones-Labarca et al., 2011). From the above, the Aquaculture in Chile has grown considerably, while exports have been important after copper, forestry, and fruits, considering that for the future it will be one of the most important sources of food for the world. This way, the cultivation has been currently focused on univalve (red abalone), bivalves (oysters), crustaceans (lobsters), cephalopods (cuttlefish), and salmon species, all with growing demand around the world [3].

Marine products are extremely perishable and the time to spoilage depends mainly on species, handling, processing, and storage temperature [4]. Currently, these products are sold as frozen, canned, or cooked frozen. However, the procedures involved can affect the quality attributes such as texture and taste [5]. Therefore, new treatments and/or processes are needed to minimize biological reactions and physicochemical leading to the loss of food quality [5] in order to increase product shelf-life.

Many studies have focused on different methods of preservation, with the hot-air drying being one of the most important processes [6, 7]. This process reduces the water activity through loss of moisture, preventing the growth and reproduction of microorganisms [8]. Convective drying

is one of the most used industrial methods for drying food and biological materials, in order to preserve its quality and stability, so avoiding spoilage and contamination during the storage period [1, 9, 10]. However, it is known that the drying process causes the loss of function of the cell membranes especially when the temperature increases causing significant changes in sensory and nutritional food quality. These disadvantages can be reduced using a combination of different pretreatments. From these pretreatments, the most widely used in convective drying are osmotic dehydration, blanching, microwave drying, and enzyme solution, among others. [11]. Commonly, marine products are immersed in concentrated solutions to impregnate them with salt and/or other curing ingredients (sucrose, glucose, fructose, glycerol, sorbitol, and sodium chloride) to prolong shelf-life [5, 12]. The osmotic pretreatment scarcely affects the color, flavor, and texture of these products. It diminishes also the loss of nourishing substances and does not have a high exigency of energy due to the used temperatures, generally that of the environment.

Knowledge of the drying kinetics is used not only in the evaluation process, but rather to analyze and predict the drying process variables to minimize damage to final product and optimize drying time and excessive energy consumption [1, 9, 13]. This analysis can be performed with different mathematical models such as Newton, Henderson-Pabis, Page, Modified Page, Weibull, Two-Term, Midilli-Kucuk, and Logarithmic models [14, 15]. Nonetheless, in the literature, there is no information available about the use of Weibull distribution model for the marine product dehydration [16]. The Weibull model has been used to describe, among others, the kinetics: high pressure removal of *Bacillus subtilis* [17], rehydration of breakfast cereals [18], loss of water during osmotic dehydration of food [19], and heat resistance of *Bacillus cereus* [20].

Thus, the aim of this research was to study the influence of drying temperature on the mass transfer kinetics of osmotically pretreated abalone slices and to evaluate different quality characteristics such as color, rehydration capacity, texture profile (TPA), no enzymatic browning (NEB), total volatile basic nitrogen (TVBN), and antioxidant capacity of the dried-rehydrated product.

2. Materials and Methods

2.1. Samples Preparation and Osmotic Pretreatment. The red abalone *(Haliotis rufescens)* samples were collected from an aquaculture Company (Live Seafood Chile SA, Coquimbo, Chile). These samples with a weight of 20.0 ± 0.2 g were delivered alive from the company to the university laboratory. Then, they were slaughtered, shucked, cleaned, and washed with fresh water until the blue pigment haemocyanin was removed. Finally, the samples were cut into slices of 10 mm long × 0.1 mm wide × 0.1 thick to consider one dimension and were immersed in a salt solution (NaCl, 15 g/100 mL) at 20°C as proposed by Lemus-Mondaca et al. [13] in the red abalone *(Haliotis rufescens)* and Boudhrioua et al. [21] in sardine fillets. The brine to sample ratio was maintained at 8 : 1 in order to not dilute the osmotic solution by water removal during experiments. The brine was agitated continuously in a water bath (Quimis, Q.215.2, Sao Paulo, Brazil) to maintain a uniform temperature. The osmotic process was made up of regular time intervals (0, 15, 30, 45, 60, 120, 180, 240, 300, 360, and 420 min) until reaching an osmotic pseudo equilibrium. Moisture content was determined by AOAC method n°934.06 (AOAC, 1990) using an analytic balance (Chyo, Jex120, Kyoto, Japan) with a ±0.0001 g accuracy and vacuum drying oven (Gallenkamp, OVA031, Leicester, UK). As to salt content, this one was measured by Mohr method [22], where salt content was expressed as g NaCl/100 g sample. All the experimental determination was performed in triplicate.

2.2. Drying Procedure. Once the osmotic balance of the salt and water content has been reached, convective drying was carried out. The convective drying process was performed in a convective dryer tray designed and fabricated by the Department of Food Engineering at the University of La Serena, Chile [7]. Drying temperatures were 40, 60, and 80°C at a constant air velocity 1.5 ± 0.2 m/s for each test with an environmental condition of 18.0 ± 0.1°C and 68.1 ± 3.8% RH, the latter being measured by a digital hygrothermometer (Extech Instrument Inc., 451112, Waltham, MA, USA). The experiments ended when a state of pseudo equilibrium was reached at a constant weight between 22–18% humidity and 0.73–0.62 water activity according to the temperatures evaluated. The samples were sealed in polyethylene bags and each experiment was made in triplicate. The samples were sealed in polyethylene bags and each experiment was made in triplicate.

2.3. Diffusion Coefficient. In order to study the phenomena of mass transfer during osmotic dehydration and convective drying process of abalone samples, two components were considered in each process: (a) the water loss and salt gain for OD and (b) the water loss for convective drying. Fick's second law has been widely used to describe the dynamics of the different drying processes for biological materials [23]. The mathematical solution of Fick's second law was used to describe the period, when internal mass transfer (water or salt) is the controlling mechanism and one-dimensional transport in an infinite slab [24], shown in (1), which corresponds to the geometry of a semi-infinite slab. Thus, the variables of diffusion model are moisture loss (MR) (see (2)) and salt gain rate (SR) (see (3)) [25], represented as follows:

$$\text{MR\_or\_SR} = \sum_{i=0}^{\infty} \frac{8}{(2i+1)\,\pi^2} \exp\left(\frac{D_e\,(2i+1)\,\pi^2 t}{4L^2}\right). \quad (1)$$

For sufficiently long drying times, the first term ($i = 0$) in the series expansion of (1) gives a good estimation of the solution and can be applied to determine the water and salt diffusion coefficients, (2) and (3), respectively [25]. Then, Fick's 2nd law (see (1)) can be linearized, from the slope ($=\pi^2 D_e/4L^2$), where D_{we} and D_{se} are moisture loss or salt gain, respectively, that can be obtained.

$$\mathrm{MR} = \frac{M_t}{M_o} = \frac{8}{\pi^2}\exp\left(\frac{D_{we}\pi^2 t}{4L^2}\right), \quad (2)$$

$$\mathrm{SR} = \frac{S_t}{S_o} = \frac{8}{\pi^2}\exp\left(\frac{D_{se}\pi^2 t}{4L^2}\right). \quad (3)$$

The influence of drying temperature was determined according to the Arrhenius type equation (4), where kinetic parameters (E_a and D_o) of this model can be estimated from the slope and intercept of the plot in D_e versus the reciprocal of absolute temperature [10, 23]:

$$D_e = D_o\exp\left(\frac{-E_a}{RT}\right). \quad (4)$$

2.4. Mathematical Modeling. Commonly, the authors propose some simple and complex mathematical models to simulate drying curves of foods that can provide an adequate representation of the experimental results [26]. Several models exist in the literature to predict this process [27]. Among these models, the Weibull distribution model has been used to describe diverse cases, for example, the removal of *Bacillus subtilis* for a high pressure treatment (Knorr, 1996), rehydration of breakfast cereals [18], and pressure inactivation of bacteria [28]. The mathematical expression was based on the diffusional mechanism of water, expressed in

$$\mathrm{MR}_{\mathrm{or}_{\mathrm{SR}}} = \exp\left(-\left[\frac{t}{\beta}\right]\right)^{\alpha}. \quad (5)$$

3. Quality Characteristics

3.1. Proximate Analysis and Water Activity (a_w). The moisture content determination was performed according to AOAC methodology number 934.06 using an analytical balance (Chyo, Jex120, Kyoto, Japan) with an accuracy of ±0.0001 g and a vacuum drying oven at 60°C (Gallenkamp, OVA031, Leicester, UK). The crude protein content was determined by the Kjeldahl method (AOAC number 920.39), applying a conversion factor of 6.25. The fat content was determined by the Soxhlet method (AOAC number 920.39) and total ash by oxidation of the organic matter at 550°C (AOAC number 923.08). The methods were performed according to the AOAC (1990) methodology and all the analyses were done in triplicate. In addition, water activity (a_w) was measured (AQUA LAB, 4TE, Pullman, WA, USA).

3.2. Nonenzymatic Browning (NEB) and Total Volatile Basic Nitrogen (TVBN). The proposed methodology for determining the NEB compounds dissolved in water rehydration was proposed by Vega-Gálvez et al. [29]. The samples were rehydrated at a ratio (1 : 10) g sample/g water × 12 h. Then, the procedure was divided into three stages. The first was a clarification of rehydration water with centrifugation at 3500 rpm × 15 min. The second step was a dilution (1 : 1) of this supernatant with ethanol (Sigma Chemical Co., St. Louis, MO, USA) at 95% (pa) centrifuged again to the same conditions and finally the third was read (absorbance at 420 nm) from the extracts that was determined to clear quartz in buckets using a spectrophotometer (Spectronic 20 Genesys, Illinois, USA). All measurements were done in triplicate and NEB was expressed as Abs/g d.m [29]. Total volatile basic nitrogen (TVBN) was determined on 5–16 g of chopped abalone samples using direct distillation with MgO with a Kjeldahl distillation apparatus and titration according to previous work [30]. All measurements were done in triplicate.

3.3. Surface Color. Total color change (ΔE) was calculated from the initial sample surface color (fresh sample) versus the surface color of the processed product (rehydrated sample) (see (6)) using a Colorimeter (HunterLab, model MiniScan™ XE Plus, Reston, VA, USA). Color was determined by CIELab method, where L^* is whiteness or brightness, a^* is redness/greenness, and b^* is yellowness/blueness coordinates; standard illuminant D_{65} and observer 10° [29] were obtained, where L_o, a_o, and b_o are the control values determined for fresh sample.

$$\Delta E = \sqrt{\left(a^*_r - a_o\right)^2 + \left(b^*_r - b_o\right)^2 + \left(L^*_r - L_o\right)^2}. \quad (6)$$

3.4. Rehydration Indexes. Dry samples were rehydrated using a solid/liquid mass ratio of 1 : 50, within a time of 12 hours at room temperature. The rehydration ratio (RR) was calculated according to (7) and expressed as g absorbed water/g dry matter. The water holding capacity (WHC) of the samples rehydrated with the same above condition was centrifuged at 3500g × 20 min at 5°C in tubes equipped with a plastic mesh centrally placed, allowing water to drain from the sample during centrifugation. This water holding capacity expressed as retained water/100 g water was determined according to (8) [29]. All measurements were done in triplicate.

$$\mathrm{RR} = \frac{W_r \times X_r - W_d \times X_d}{W_d\left(1 - X_d\right)} \times 100, \quad (7)$$

$$\mathrm{WHC} = \frac{W_r \times X_r - W_l}{W_r \times X_r} \times 100. \quad (8)$$

3.5. Texture Profile Analysis (TPA). The texture profile of samples, as an indicator of chewiness, springiness, resilience, cohesiveness, and hardness, was measured using a Texture Analyzer (Texture Technologies Corp., TA XT2 Scardale, NY, USA). The probe had a puncture diameter of 2.0 mm that was P/100 with a distance of 20 mm and test speed of 1.7 mm/s. The maximum force was measured by making 1 puncture in each abalone sample, using 10 slices per treatment. TPA parameters, including hardness, gumminess, chewiness elasticity, cohesiveness, and resilience, were evaluated by a typical force-time curve [2].

3.6. Antioxidant Activity. A lipid extraction was performed with the Soxhelt method (AOAC N° 920.39). This extract was reconstituted with ether: ethanol 50% v/v 50 mL flask to react with the reagent 1,1′-diphenyl-2-picrylhydrazyl (DPPH), modified according to Brand-Williams et al. [31]. The solution of radical (DPPH) was prepared by dissolving 2.0 mg DPPH

in 100 mL of ether-ethanol (50%). Then, 0.1 mL of sample was extracted with 3.9 mL of the DPPH solution. Control sample was prepared without adding extract. Once the samples spiked with DPPH, it was placed in the darkness for 30 minutes and the absorbance was measured at 517 nm, using a spectrophotometer (Spectronic 20 Genesys, Illinois, USA). Results were expressed in micromoles of Trolox equivalents TE [32]. All measurements were done in triplicate.

3.7. Statistical Analysis. The fit quality of all models was evaluated using the sum square error (SSE) (see (9)) and Chi-square (χ^2, see (10)) tests [33]. The effect of air-drying temperature on each quality parameter was estimated by Statgraphics Plus v.5 (Statistical Graphics Corp., Herndon, VA, USA). The results were analyzed by an Analysis of Variance (ANOVA) using a factorial design to one single factor (temperature) with 3 levels (40, 60, and 80°C) at a confidence interval of 95% with a Multiple Range Test (MRT).

$$\mathrm{SSE} = \frac{1}{N}\sum_{i=0}^{\infty}\left(\mathrm{MR\_or\_SR}_{ei} - \mathrm{MR\_or\_SR}_{ci}\right)^2, \quad (9)$$

$$\chi^2 = \frac{\sum_{i=0}^{\infty}\left(\mathrm{MR\_or\_SR}_{ei} - \mathrm{MR\_or\_SR}_{ci}\right)^2}{N-m}. \quad (10)$$

4. Results and Discussion

4.1. Effective Moisture and Salt Diffusivity. According to the kinetics of mass transfer of salt and water in the osmotic process (Figure 1), the optimum time was observed, based on (2) and (3). This osmotic equilibrium was between 270 and 300 minutes. These values were similar to those estimated by Telis et al. [34] in caiman fillet and Mujaffar and Sankat [35] in shark muscle. The values of the effective water and salt diffusivity in the osmotic process ((4) and (5)) were of 2.74×10^{-10} m^2/s and 7.19×10^{-10} m^2/s, respectively. This occurs by the simultaneous movements of NaCl and water in the tissue, that is, the concentration differences and osmotic pressure exerted between the cell and the solution [36]. Although there is few data about this process applied to the abalone samples, a similar tendency was obtained by Corzo and Bracho [27], in the case of the sardine for value of D_{we}; and in the OD of sardine fillets, Boudhrioua et al. [21] observed that the D_{we} values ranged from 2.40×10^{-10} to 1.9×10^{-8} m^2/s.

Concerning the effective moisture diffusivity in the drying process, the values oscillated from 3.76×10^{-9} to 4.76×10^{-9} m^2/s, according to the drying temperatures. These values agreed with those found by Panagiotou et al. [37] in seafood drying, which varied from 10^{-11} to 10^{-9} m^2/s. Ortiz et al. [38] attained similar results with the salmon drying *(Salmon salar* L.*)* at temperatures that ranged from 40 to 60°C, with values between 1.08×10^{-10} and 1.90×10^{-10} m^2/s; Vega-Gálvez et al. [29] also obtained similar results in the jumbo squid drying, at temperatures from 40 to 90°C with values of 0.78×10^{-9} to 3.22×10^{-9} m^2/s, together with Medina-Vivanco et al. [39] for tilapia fillets drying. The differences among these values could be explained by the diversity of seafood species that presented changes in temperature, muscular type and position, fat content, and presence or absence of skin [39].

Arrhenius equation ($r^2 > 0.85$) was proposed by Vega-Gálvez et al. [29]. The Arrhenius factor (D_0) that attained a value of 3.17×10^{-8} m^2/s and the activation energy (E_a) of 5.48 kJ/mol were calculated in agreement with (7). Such values showed a clear dependence on the drying temperature, demonstrating that (D_{we}) values increase meaningfully as temperature increases. Furthermore, it can be concluded that abalone was more sensitive to temperature than other species according to its E_a low-value, if it is compared to the jumbo squid [29], which attained a value of 28.93 (kJ/mol), and salmon [38] that showed a value of 24.57 (kJ/mol). The abalone's value was lower, due to the difference in the composition of its protein content, compared to the other seafood species mentioned before; therefore, it is concluded that, during the drying period, there would be a lower denaturalization that would not hinder the water diffusional transfer (crustening), considering that a lower E_a value means a higher sensitivity within the evaluated temperature range [26, 40].

4.2. Weibull Model Applied to Osmotic Dehydration. Figure 1 shows the transfer of kinetic mass (water and salt) in a pseudo equilibrium state experimental and calculated by using the Weibull model to 15% NaCl, with $\chi^2 = 0.000595$, SSE = 0.000463, and $r^2 = 0.94$. The β parameter, both for salt gain and for water loss, was 0.0093 ± 0.0103 to 7659 ± 1492.2 (min), respectively. With respect to the values of α parameter for salt gain and water loss, they were in a range of 0.101 ± 0.010 to 0.404 ± 0.024, respectively. Similar results were reported by Corzo and Bracho [16] regarding sardine's water loss with α values ranging from 0.665 to 0.469, under similar concentrations.

4.3. Weibull Model Applied to Drying Procedure. The complexity of mass transfer process makes it difficult to obtain an accurate prediction because they depend on parameters and equilibrium conditions as well as the effective water diffusivity. Thus, the Weibull's model was used (Figure 2), which shows the drying curves of 40, 60, and 80°C of abalone samples pretreated osmotically and adjusted according to this model ($0.0002 < \chi^2 < 0.00048$; $0.00021 < \mathrm{SSE} < 0.0004$; $0.981 < r^2 < 0.993$). It can be seen that all curves are exponential being typical for drying food [1]. The behavior of the drying curves was also reported by other authors when they worked with lobster [29]. The drying curves 60 and 80°C that have a similar tendency are explained by the formation of a crust in the area of the abalone samples surface associated with osmotic pretreatment and thermal chock. This crust has a significant resistance to water migration [35]. Drying curves or drying rates depend on several factors, some of them being directly related to the product and others related to the air-drying temperature [41]. Table 1 shows the moisture diffusivity coefficient, which was the most significant parameter in the food drying [42], based on Fick's second law [23].

In particular, the values of α and β Weibull parameters showed significant differences among evaluated temperatures, with a p value < 0.05. Similar results were obtained by Vega-Gálvez et al. [29] in the jumbo squid drying at the same

Table 1: Kinetic parameters of Weibull and Fick models for drying process.

Model	Parameter	Drying temperature (°C)		
		40	60	80
Weibull	β	146.03 ± 1.929^{a}	94.84 ± 2.282^{b}	67.32 ± 1.701^{c}
	α	0.827 ± 0.022^{a}	0.733 ± 0.014^{b}	0.685 ± 0.018^{c}
Fick	$D_{we} \times 10^{-9}$	3.76 ± 0.146^{a}	4.64 ± 0.246^{b}	4.75 ± 0.052^{b}

Identical letters above the values indicate no significant difference ($p < 0.05$). Values are mean ± standard deviation ($n = 3$).

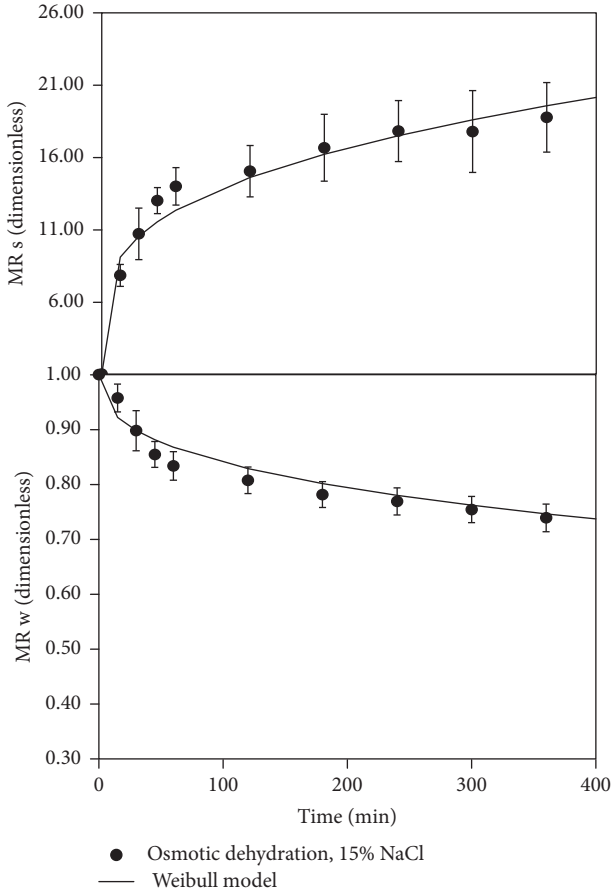

Figure 1: Experimental water and salt transfer during osmotic process and calculated by Weibull model.

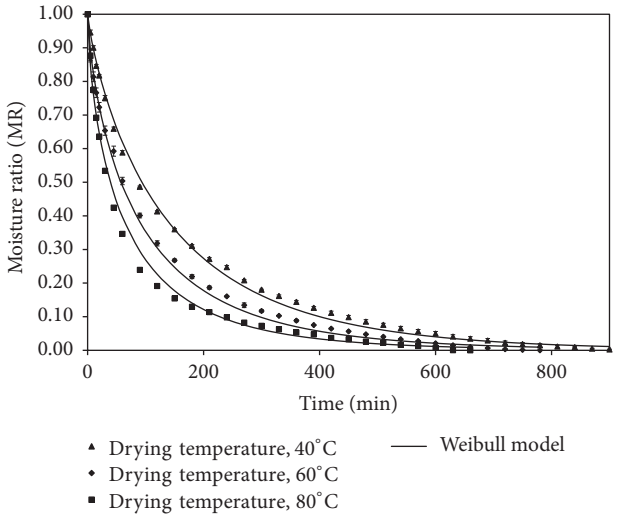

Figure 2: Experimental drying curves modeled by the Weibull model.

temperatures. Cunningham et al. [43] explained that the β parameter represents the time required for 63% of the whole drying process, approximately. Furthermore, this parameter was related to the mass transfer (min) at the beginning of the process; therefore, if the β value was lower, the transference speed was faster [44], and a reduction of α parameter indicates greater water absorption and desorption of the dehydrated product.

4.4. Quality Characteristics

4.4.1. Proximate Analysis and Water Activity (a_w). The proximate composition of osmotically treated samples was 76.6 for the moisture content, 13.3 for the protein content, 1.73 for the lipid content, and 5.83 for the carbohydrate content (g/100 g d.m.); furthermore, the water activity value was 0.97. While the moisture content values of dried samples ranged between 26.45 and 18.03 g/100 g d.m., the lipid content varied from 7.26 to 3.16 (g/100 g d.m.), the carbohydrate content varied from 28.24 to 32.58 g/100 g d.m., and at last, the protein content showed values from 55.94 to 35.93 g d.m, according to the temperatures applied. These values have a similar tendency to the ones reported by other authors who studied drying and brining jumbo squid [45]. The safety limit for a_w in the foods is 0.6 [46]. This research yielded values of 0.77 ± 0.02 to 0.67 ± 0.04. Chiou et al. [45] obtained the same trend in cuttlefish drying subjected to a pretreatment salt. From the microbiological point of view, there might be some chemical, biochemical, or metabolic reactions of growth due to the quantity of water that is available. However, owing to the fact that the abalone was subjected to an osmotic pretreatment at 15% NaCl, it will cause a slower growth of some microorganism because of the difference in the osmotic pressure or because of chloride ions that are deadly for some pathogens [47], affecting the enzymatic systems and consequently the chemical reaction speed will be reduced.

4.4.2. Surface Color and Nonenzymatic Browning (NEB). Color changes are in connection with the changes in the structural protein that bring about a difference in light dispersion properties on the surface of abalone samples,

Table 2: Quality parameters such as TPA, TVBN, and antioxidant activity of fresh and dehydrated samples.

Quality parameters	Fresh	Drying temperature (°C)		
		40	60	80
Texture profile analysis (TPA)				
Chewiness (mm)	2040 ± 976^{a}	1308 ± 527^{a}	2016 ± 246^{b}	3833.25 ± 1693^{a}
Springiness (mm)	0.68 ± 0.14^{a}	0.70 ± 0.11^{ab}	0.77 ± 0.08^{bc}	0.85 ± 0.08^{c}
Resilience	0.30 ± 0.07^{b}	0.24 ± 0.03^{a}	0.31 ± 0.02^{a}	0.34 ± 0.04^{c}
Cohesiveness	0.52 ± 0.09^{a}	0.63 ± 0.05^{a}	0.70 ± 0.03^{c}	0.74 ± 0.04^{b}
Hardness (N/mm)	21.43 ± 15.95^{a}	29.57 ± 10.24^{ab}	37.06 ± 15.16^{b}	55.22 ± 18.16^{c}
TVBN (mg N/100 mg)	10.57 ± 0.03^{a}	45.24 ± 0.09^{b}	47.66 ± 0.64^{c}	53.65 ± 0.34^{d}
Antioxidant activity (μmol TE/d.m.)	28.82 ± 0.003^{a}	8.70 ± 0.003^{b}	8.55 ± 0.273^{b}	8.08 ± 0.151^{c}

Identical letters above the values indicate no significant difference ($p < 0.05$). Values are mean ± standard deviation ($n = 3$).

like browning reactions [47]. Figure 3 shows the changes of L^*, a^*, b^*, ΔE, and NEB parameters from fresh and rehydrated samples. According to ANOVA, the luminosity (L^*) attained statistically significant differences in all the treatments, resulting in their decrease, which were observed at 95% confidence level ($p < 0.05$), among the mean values that resulted in two homogeneous groups (40-60-80°C and fresh), which can be explained because the luminosity was affected mainly by NaCl osmotic pretreatment [47] and the drying temperature [1, 29]. The yellowness (b^*) increased during the drying temperature due to the browning [48]; that is, it was proved that the temperatures used affected the b^* parameter, since these ones showed significant differences ($p < 0.05$) in the average value for each temperature. Similar values were obtained by Ortiz et al. [38] in salmon drying and by Vega-Gálvez et al. [1, 29] in jumbo squid osmo-treated drying. This also occurs in a^* parameter, where there were significant statistical differences that attained a confidence value of 95% ($p < 0.05$). As in the case of color variation (ΔE), it also increased with the drying temperatures [38] from 12.35 to 14.15. However, the statistical study revealed that no significant differences were found among treatments that had a value $p > 0.05$, with a homogeneous group (40-60-80°C).

Maillard type reactions or nonenzymatic browning (NEB) occurs because carbonyl compounds react with amino-groups when thermal treatments are applied on the muscular tissues that usually contain carbohydrates like glycogen, reducing sugars, and nucleotides [49], which was evidenced by the decrease in the value of L^* and increase of b^* parameter. The abalone is abundant in proteins and free amino-acids; therefore, it can be observed that temperature increase brought about an important chestnut colored compound formation. This was observed because the NEB compounds increased with the increase in temperature resulting in brown compounds. The NEB treatment at 80°C obtained a 0.27 ± 0.023 value Abs/g d.m. like Rahman [49] that evaluated other seafood products.

4.5. Texture Profile Analysis (TPA). Seafood muscle tissue is formed by muscle fibers cells located in the interstitial medium and capillary space medium. Muscular cells are mainly fibrils, sarcoplasm, and the connective tissue, specifically collagen [50]. The principal structural factors that affect

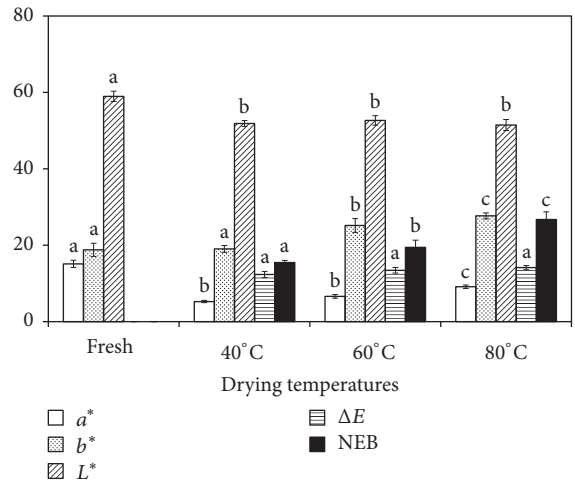

Figure 3: Effect of drying temperature on color differences (ΔE), chromaticity coordinates L^*, a^*, and b^* (whiteness or brightness, redness/greenness, and yellowness/blueness), and nonenzymatic browning (NEB × 10^{-2}) of fresh and rehydrated abalone. Different letters above the bars indicate significant differences ($p < 0.05$).

the texture are associated with the connective tissues and myofibrils proteins (actins and myosin) [51]. The myofibrils proteins such as the myosin play an important role in the quality of meat owing to their capacity to hold water [52].

Based on the above, the texture is one of the most important characteristics that affect the quality of the product when it is chewed by the consumer [53]. Table 2 shows the effects of drying temperature on the fresh and rehydrated texture samples. The latter display a significant influence with increasing temperature [29]. Comparable results have been reported in baking squid [53] and during shrimp drying [54]. Drying causes protein denaturation by irreversible structural changes that lead to a change in texture [2]. Dried abalone samples firmness is a critical parameter affecting the quality and hence the acceptability of the product. All treatments prior to drying showed an increase compared to the fresh sample and can be explained by the effect of the drying temperature, the NaCl concentration on tissue proteins [55]. Firmness values between a fresh abalone and a dried-hydrated one at the highest drying temperature varied

from 21.43 to 54.12 N/mm. The same tendency was reported by Vega-Gálvez et al. [29], for the osmo-treated cuttlefish drying and by Ortiz et al. [38], on salmon drying.

4.6. Rehydration Indexes. Most products dehydrated are rehydrated before consumption. Rehydration can be regarded as an indirect measure of tissue damage caused by drying [29]. Figure 4 shows the rehydration ratio (RR) together with the water holding capacity (WHC) for different treatments used. This figure indicated that treatment at 60°C obtained RR increased compared to the other treatments (1.26 g absorbed water/g dry matter). The treatment at 40°C reveals slightly lower value as compared to 60 to 80°C. Moreover, it is generally accepted that the degree of rehydration depends on the degree of cell structural alteration [47], because if the drying temperature increases, the higher the rehydration capacity will be, due to its lower water retention capacity that was caused by structural damage at the cellular level, resulting, among other effects, in leaching of soluble solids [56].

WHC value shows a tendency to decrease as the treatment temperature increases; thus, at 40°C the treatment has the highest water holding capacity (98.96 g retained water/100 g water) and the lowest at 80°C (95.25 g retained water/100 g water). Similar results were reported by other authors who described that drying temperature was the main factor of WHC decrease, becoming an obstacle to retain this water. In particular, Vega-Gálvez et al. [29] working in cuttlefish found similar results. Besides, it must be pointed out that abalone and all the meat species have a good water holding capacity, due to their protein feature of a myofibril origin [52].

4.7. Antioxidant Capacity. The results in Table 2 show that the antioxidant capacity obtained a decrease with the process temperatures; that is, it can be observed that the variable temperature has a significant effect on the antioxidant activity of the abalone samples. These results also were reported by Bennett et al. [57] concluding that the drying and processing conditions affect the antioxidant capacity of foods. All the treatments showed a diminishing of such an activity as compared to a fresh sample that obtained 28.824 μmol TE/g d.m. A similar behavior was also observed at 60°C and 80°C due to the same period under thermal process. This can be explained by the osmotic pretreatment that the abalone has, which might produce NaCl crystals, as a barrier to the water outlet (Collignan et al., 2000), affecting the drying process. The antioxidant activity of seafood has been related to proteins and has been reported of different peptides having antioxidant effects [58]. However, the relationship between antioxidant activity and content of active peptide has not been fully studied yet in the process [58].

4.8. Total Volatile Basic Nitrogen (TVBN). TVBN values that are reported in this research are in a range from 10.57 to 53.65 mg N/100 g from samples fresh and dehydrated, which can be better valued from Table 2. These values vary according to the fishtailed species, the environment, physiological conditions, processing, and storage conditions [48].

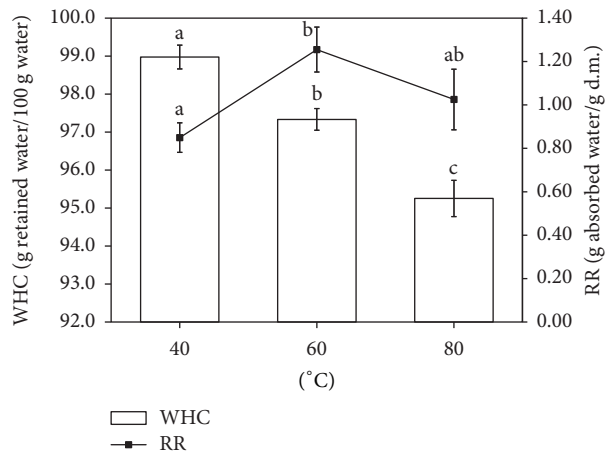

Figure 4: Effect of air-drying temperature on the rehydration ratio (RR) and the water holding capacity (WHC) for dry-rehydrated abalone samples. Identical letters above the bars indicate no significant difference ($p < 0.05$).

Table 2 shows an increase in the amount of TVBN as the temperature increases, due to the low molecular weight volatile compounds that increase the amount of nitrogen considerably with the heat treatment [29]. Similar results were found by Robles et al. [59] when applying thermal treatments on crabs *(Homalaspis plana)*. The total basic volatile nitrogen content (TVBN) has been worldwide used as an indicator of fish quality [60]. The fresh value was 10.57 ± 0.03 mg N/100 g, sample that can be compared to fresh seafood reported by other authors [59].

TVBN content increases by the thermal treatment due to the longer heat exposition, according to Gallardo et al. [61, 62]. During thermal treatment, the composition and proportion of the nitrogenous compounds cause changes in the amine's molecular weight contents; that is, TVBN increases as a consequence of some amino-acids degradation [59]. TVBN values of meat subjected to a thermal treatment are always higher than fresh meat [61]. Studies carried out in canned mussels and squids and other fish species that underwent some thermal treatment showed TVBN values of 42.5–57.3 mg/100 g of muscles [62]. According to ANOVA ($p < 0.05$), there was a significant difference between the average values of the total content of volatile nitrogen for treatments studied.

5. Conclusion

This study has shown that the concentration of the osmotic treatment influences directly the diffusional coefficient of water and salt in the process, obtaining a balance between $270 < \text{min} < 300$. These values ranged from 2.74 to 7.19×10^{-10} m^2/s, respectively. As for the effective diffusivity of water in the drying process, there was a tendency to increase regarding the evaluated temperatures, whose values oscillated from 3.76 to 4.76×10^{-9} m^2/s. The Weibull model obtained a good fit in the OD and drying, corroborating with statistical test $0.0006 < \chi^2 < 1.09$, $0.0005 < \text{SSE} < 0.8934$, and $0.91 < r^2 < 0.94$. The drying temperature significantly influenced the

physical, chemical, and nutritional properties of abalone samples. Discoloration of product was more evident at high drying temperatures, where combined effects of nonenzymatic browning as well as protein denaturation modified the abalone samples original color. According to the drying temperature, the RR and WHC indexes showed a decrease, while the texture presented an increase. TVBN and antioxidant activity values presented a decrease with increased temperature. Therefore, the results of this work indicate that the drying kinetics along with quality aspects of dried abalones can be used to improve the final characteristics of the product and predict a suitable drying treatment at 60°C under an osmotic pretreatment (15% NaCl).

Nomenclature

OD: Osmotic dehydration
D_e: Mass effective diffusivity (m^2/s)
S_t: Salt content (g NaCl/g dry matter, d.m.)
M_t: Water content (g water/g d.m.)
SR: Salt ratio (dimensionless)
MR: Moisture ratio (dimensionless)
L: Sample thickness (m)
E_a: Activation energy (kJ/mol)
L^*: Whiteness/darkness color parameter
a^*: Redness/greenness color parameter
b^*: Yellowness/blueness color parameter
RH: Relative humidity (%)
RR: Rehydration ratio (g absorbed water/g dry matter)
WHC: Water holding capacity (g retained water/100 g water)
TE: μmol of trolox equivalents
R: Universal gas constant (8.314 J/mol K)
D_o: Arrhenius factor (m^2/s)
T: Temperature (°C or K)
W: Weight of the sample (g)
t: Time (min)
N: Number of data.

Greek Letters

α: Shape parameter of Weibull model (dimensionless)
β: Scale parameter of Weibull model (min).

Subscripts

w: Water
s: Salt
t: At time
o: Initial
r: Rehydrated sample
d: Dried sample
l: Drained liquid after centrifugation
i: Number of terms
c: Calculated
e: Experimental.

Conflicts of Interest

The authors declare that there are no conflicts of interest regarding the publication of this paper as well as the received funding.

Acknowledgments

The authors gratefully acknowledge the financial support provided by Concurso DIULS Apoyo Tesis de Postgrado Project no. PT14332 and FONDECYT Regular Project no. 1140067.

References

[1] A. Vega-Gálvez, R. Lemus-Mondaca, D. Plaza-Sáez, and M. Pérez-Won, "Effect of air-temperature and diet composition on the drying process of pellets for japanese abalone (haliotis discus hannai) feeding," *Ciência e Tecnologia de Alimentos*, vol. 31, no. 3, pp. 694–702, 2011.

[2] B. Zhu, X. Dong, L. Sun et al., "Effect of thermal treatment on the texture and microstructure of abalone muscle (Haliotis discus)," *Food Science and Biotechnology*, vol. 20, no. 6, pp. 1467–1473, 2011.

[3] Sernapesca. 2015. Servicio nacional de Pesca de Chile. Leyes y Reglamentos; Normativas y Valparaíso: Ministerio de Economia, Fomento y Turismo. Disponible en: http://www.sernapesca.cl;. Acesso em: Jun 10, 2015.

[4] T. Tsironi, I. Salapa, and P. Taoukis, "Shelf life modelling of osmotically treated chilled gilthead seabream fillets," *Innovative Food Science and Emerging Technologies*, vol. 10, no. 1, pp. 23–31, 2009.

[5] A. Z. Valencia-Pérez, M. H. García-Morales, J. L. Cárdenas-López, J. R. Herrera-Urbina, O. Rouzaud-Sández, and J. M. Ezquerra-Brauer, "Effect of thermal process on connective tissue from jumbo squid (Dosidicus gigas) mantle," *Food Chemistry*, vol. 107, no. 4, pp. 1371–1378, 2008.

[6] B. S. M. Mahmoud, K. Yamazaki, K. Miyashita, Y. Kawai, I.-S. Shin, and T. Suzuki, "Preservative effect of combined treatment with electrolyzed NaCl solutions and essential oil compounds on carp fillets during convectional air-drying," *International Journal of Food Microbiology*, vol. 106, no. 3, pp. 331–337, 2006.

[7] A. Vega-Gálvez, K. Di Scala, K. Rodríguez et al., "Effect of air-drying temperature on physico-chemical properties, antioxidant capacity, colour and total phenolic content of red pepper (*Capsicum annuum*, L. var. *Hungarian*)," *Food Chemistry*, vol. 117, no. 4, pp. 647–653, 2009.

[8] S. Bellagha, A. Sahli, A. Farhat, N. Kechaou, and A. Glenza, "Studies on salting and drying of sardine (Sardinella aurita): Experimental kinetics and modeling," *Journal of Food Engineering*, vol. 78, no. 3, pp. 947–952, 2007.

[9] E. K. Akpinar, "Determination of suitable thin layer drying curve model for some vegetables and fruits," *Journal of Food Engineering*, vol. 73, no. 1, pp. 75–84, 2006.

[10] K. Di Scala and G. Crapiste, "Drying kinetics and quality changes during drying of red pepper," *LWT- Food Science and Technology*, vol. 41, no. 5, pp. 789–795, 2008.

[11] N. E. Perez and M. E. Schmalko, "Convective drying of pumpkin: Influence of pretreatment and drying temperature," *Journal of Food Process Engineering*, vol. 32, no. 1, pp. 88–103, 2009.

[12] R. Lemus-Mondaca, M. Miranda, A. Andres Grau, V. Briones, R. Villalobos, and A. Vega-Gálvez, "Effect of osmotic pretreatment on hot air drying kinetics and quality of Chilean papaya (Carica pubescens)," *Drying Technology*, vol. 27, no. 10, pp. 1105–1115, 2009.

[13] R. Lemus-Mondaca, S. Noma, N. Igura, M. Shimoda, and M. Pérez-Won, "Kinetic Modeling and Mass Diffusivities during Osmotic Treatment of Red Abalone (Haliotis rufescens) Slices," *Journal of Food Processing and Preservation*, vol. 39, no. 6, pp. 1889–1897, 2015.

[14] I. Doymaz, "Drying of leek slices using heated air," *Journal of Food Process Engineering*, vol. 31, no. 5, pp. 721–737, 2008.

[15] L. Ait Mohamed, C. S. Ethmane Kane, M. Kouhila, A. Jamali, M. Mahrouz, and N. Kechaou, "Thin layer modelling of Gelidium sesquipedale solar drying process," *Energy Conversion and Management*, vol. 49, no. 5, pp. 940–946, 2008.

[16] O. Corzo and N. Bracho, "Application of Weibull distribution model to describe the vacuum pulse osmotic dehydration of sardine sheets," *LWT- Food Science and Technology*, vol. 41, no. 6, pp. 1108–1115, 2008.

[17] V. Heinz and D. Knorr, "High pressure inactivation kinetics of Bacillus subtilis cells by a three-state-model considering distributed resistance mechanisms," *Food Biotechnology*, vol. 10, no. 2, pp. 149–161, 1996.

[18] M. F. Machado, F. A. R. Oliveira, and L. M. Cunha, "Effect of milk fat and total solids concentration on the kinetics of moisture uptake by ready-to-eat breakfast cereal," *Int J Food Sci Tech.34*, pp. 47–57, 1999.

[19] L. M. Cunha, F. A. R. Oliveira, A. P. Aboim, and J. M. Frías, "a.Stochastic approach to the modelling of water losses during osmotic dehydration and improved parameter estimation," in *Proceedings of the a.Stochastic approach to the modelling of water losses during osmotic dehydration and improved parameter estimation. International J Food Sci Tech. 36: 253–262*, vol. 36, pp. 253–262, 2001.

[20] A. Fernández, J. Collado, L. M. Cunha, M. J. Ocio, and A. Martinez, "Empirical model building based on Weibull distribution to describe the joint effect of pH and temperature on the termal resistance of Bacillus cereus in vegetable substrate," *Int J Food Micr*, pp. 77–147, 2002.

[21] N. Boudhrioua, N. Djendoubi, S. Bellagha, and N. Kechaou, "Study of moisture and salt transfers during salting of sardine fillets," *Journal of Food Engineering*, vol. 94, no. 1, pp. 83–89, 2009.

[22] J. M. Barat, L. Gallart-Jornet, A. Andrés, L. Akse, M. Carlehög, and O. T. Skjerdal, "Influence of cod freshness on the salting, drying and desalting stages," *Journal of Food Engineering*, vol. 73, no. 1, pp. 9–19, 2006.

[23] Y. Wang, M. Zhang, and A. S. Mujumdar, "Convective drying kinetics and physical properties of silver carp (Hypophthalmichthys molitrix) fillets," *Journal of Aquatic Food Product Technology*, vol. 20, no. 4, pp. 361–378, 2011.

[24] J. Crank, *The Mathematics of Diffusion*, Clarendon Press, Oxford, UK, 2nd edition, 1975.

[25] E. Uribe, M. Miranda, A. Vega-Gálvez, I. Quispe, R. Clavería, and K. Di Scala, "Mass Transfer Modelling During Osmotic Dehydration of Jumbo Squid (Dosidicus gigas): Influence of Temperature on Diffusion Coefficients and Kinetic Parameters," *Food and Bioprocess Technology*, vol. 4, no. 2, pp. 320–326, 2011.

[26] S. Simal, A. Femenia, M. C. Garau, and C. Rosselló, "Use of exponential, Page's and diffusional models to simulate the drying kinetics of kiwi fruit," *Journal of Food Engineering*, vol. 66, no. 3, pp. 323–328, 2005.

[27] O. Corzo and N. Bracho, "Application of Normalized Weibull Model in the Osmotic Dehydration of Sardine Sheets," *Revista Científica*, vol. XIX, no. 4, pp. 400–407, 2009.

[28] S. Buzrul, H. Alpas, and F. Bozoglu, "Use of Weibull frequency distribution model to describe the inactivation of Alicyclobacillus acidoterrestris by high pressure at different temperatures," *Food Research International*, vol. 38, no. 2, pp. 151–157, 2005.

[29] A. Vega-Gálvez, M. Miranda, R. Clavería et al., "Effect of air temperature on drying kinetics and quality characteristics of osmo-treated jumbo squid (Dosidicus gigas)," *LWT- Food Science and Technology*, vol. 44, no. 1, pp. 16–23, 2011.

[30] J. R. BOTTA, J. T. LAUDER, and M. A. JEWER, "Effect of Methodology on Total Volatile Basic Nitrogen (TVB-N) Determination as an Index of Quality of Fresh Atlantic Cod (Gadus morhua)," *Journal of Food Science*, vol. 49, no. 3, pp. 734–736, 1984.

[31] W. Brand-Williams, M. E. Cuvelier, and C. Berset, "Use of a free radical method to evaluate antioxidant activity," *LWT - Food Science and Technology*, vol. 28, no. 1, pp. 25–30, 1995.

[32] P. Molyneux, "The use of the stable radical Diphenylpicrylhydrazyl (DPPH) for estimating antioxidant activity," *Songklanakarin Journal of Science and Technology*, vol. 26, no. 2, pp. 211–219, 2004.

[33] Y. Wang, J. Yue, Z. Liu et al., "Impact of Far-Infrared Radiation Assisted Heat Pump Drying on Moisture Distribution and Rehydration Kinetics of Squid Fillets During Rehydration," *Journal of Aquatic Food Product Technology*, vol. 25, no. 2, pp. 147–155, 2016.

[34] V. R. N. Telis, P. F. Romanelli, A. L. Gabas, and J. Telis-Romero, "Salting kinetics and salt diffusivities in farmed Pantanal caiman muscle," *Pesquisa Agropecuária Brasileira*, vol. 38, no. 4, pp. 529–535, 2003.

[35] S. Mujaffar and C. K. Sankat, "The mathematical modelling of the osmotic dehydration of shark fillets at different brine temperatures," *International Journal of Food Science & Technology*, vol. 41, no. 4, pp. 405–416, 2006.

[36] M. F. Villacís, N. K. Rastogi, and V. M. Balasubramaniam, "Effect of high pressure on moisture and NaCl diffusion into turkey breast," *LWT- Food Science and Technology*, vol. 41, no. 5, pp. 836–844, 2008.

[37] N. M. Panagiotou, M. K. Krokida, Z. B. Maroulis, and G. D. Saravacos, "Moisture diffusivity: Literature data compilation for foodstuffs," *International Journal of Food Properties*, vol. 7, no. 2, pp. 273–299, 2004.

[38] J. Ortiz, R. Lemus-Mondaca, A. Vega-Gálvez et al., "Influence of air-drying temperature on drying kinetics, colour, firmness and biochemical characteristics of Atlantic salmon (Salmo salar L.) fillets," *Food Chemistry*, vol. 139, no. 1-4, pp. 162–169, 2013.

[39] M. Medina-Vivanco, P. J. A. Do Sobral, and M. D. Hubinger, "Osmotic dehydration of tilapia fillets in limited volume of ternary solutions," *Chemical Engineering Journal*, vol. 86, no. 1-2, pp. 199–205, 2002.

[40] I. Doymaz, "Drying characteristics and kinetics of okra," *Journal of Food Engineering*, vol. 69, no. 3, pp. 275–279, 2005.

[41] P. Fito, A. M. Andrés, J. M. Barat, A. M. Albors, and A. M. Andrés, *Introducción al Secado de Alimentos por Aire Caliente*, Editorial U.P.V, Valencia, España, 2001.

[42] A. Vega, P. Fito, A. Andrés, and R. Lemus, "Mathematical modeling of hot-air drying kinetics of red bell pepper (var.

Lamuyo)," *Journal of Food Engineering*, vol. 79, no. 4, pp. 1460–1466, 2007.

[43] S. E. Cunningham, W. A. M. McMinn, T. R. A. Magee, and P. S. Richardson, "Modelling water absorption of pasta during soaking," *Journal of Food Engineering*, vol. 82, no. 4, pp. 600–607, 2007.

[44] M. F. Machado, F. A. R. Oliveira, V. Gekas, and R. P. Singh, "Kinetics of moisture uptake and soluble-solids loss by puffed breakfast cereals immersed in water," *International Journal of Food Science & Technology*, vol. 33, no. 3, pp. 225–237, 1998.

[45] T. Chiou, H. Chang, L. Lo, H. Lan, and C. Shiau, "Changes in chemical constituents and physical índices during processing of dried-seasoned squid," *Fish Sci*, pp. 66–708, 2000.

[46] A. Vega-Gálvez, M. Palacios, F. Boglio, C. Pássaro, C. Jeréz, and R. Lemus-Mondaca, "Deshidratación osmótica de la papaya chilena (Vasconcellea pubescens) e influencia de la temperatura y concentración de la solución sobre la cinética de transferencia de materia," *Ciência e Tecnologia de Alimentos*, vol. 27, no. 3, pp. 470–477, 2007.

[47] N. Guizani, A. O. Al-Shoukri, A. Mothershaw, and M. S. Rahman, "Effects of salting and drying on shark (Carcharhinus sorrah) meat quality characteristics," *Drying Technology*, vol. 26, no. 6, pp. 705–713, 2008.

[48] S.-C. Shen, K.-C. Tseng, and J. S.-B. Wu, "An analysis of Maillard reaction products in ethanolic glucose-glycine solution," *Food Chemistry*, vol. 102, no. 1, pp. 281–287, 2007.

[49] S. Rahman, "Drying of fish and seafood," in *Handbook of industrial drying*, A. S and Mujumdar., Eds., CRC Press, Boca Raton, FL, USA, 3 edition, 2006.

[50] S. K. Øiseth, C. Delahunty, M. Cochet, and L. Lundin, "Why is abalone so chewy? structural characterization and relationship to textural attributes," *Journal of Shellfish Research*, vol. 32, no. 1, pp. 73–79, 2013.

[51] F. Erdogdu and M. Balaban, "Thermal processing effects on the textural attributes of previously frozen shrimp," *J Aquat Food Prod Tech*, pp. 67–84, 2000.

[52] N. Chapleau, C. Mangavel, J.-P. Compoint, and M. De Lamballerie-Anton, "Effect of high-pressure processing on myofibrillar protein structure," *Journal of the Science of Food and Agriculture*, vol. 84, no. 1, pp. 66–74, 2004.

[53] W. S. Otwell and D. D. Hamann, "Textural characterizati, on of squid (loligo pealei l.): instrumental and panel evaluations," *Journal of Food Science*, vol. 44, no. 6, pp. 1636–1643, 1979.

[54] Y. Namsanguan, W. Tia, S. Devahastin, and S. Soponronnarit, "Drying kinetics and quality of shrimp undergoing different two-stage drying processes," *Drying Technology*, vol. 22, no. 4, pp. 759–778, 2004.

[55] L. Gallart-Jornet, J. M. Barat, T. Rustad, U. Erikson, I. Escriche, and P. Fito, "Influence of brine concentration on Atlantic salmon fillet salting," *Journal of Food Engineering*, vol. 80, no. 1, pp. 267–275, 2007.

[56] P. García-Pascual, N. Sanjuán, R. Melis, and A. Mulet, "*Morchella esculenta* (morel) rehydration process modelling," *Journal of Food Engineering*, vol. 72, no. 4, pp. 346–353, 2006.

[57] L. E. Bennett, H. Jegasothy, I. Konczak, D. Frank, S. Sudharmarajan, and P. R. Clingeleffer, "Total polyphenolics and antioxidant properties of selected dried fruits and relationships to drying conditions," *Journal of Functional Foods*, vol. 3, no. 2, pp. 115–124, 2011.

[58] S. Jongberg, C. U. Carlsen, and L. H. Skibsted, "Peptides as antioxidants and carbonyl quenchers in biological model systems," *Free Radical Research*, vol. 43, no. 10, pp. 932–942, 2009.

[59] V. Robles, L. Abugoch, J. Vinagre et al., "Efecto de tratamientos térmicos sobre las características químicas de carne de jaiba mora," *Homalaspis plana*, vol. 53, pp. 191–223, 2003.

[60] L. Pivarnik, P. Ellis, X. Wang, and T. Reilly, "Standardization of the ammonia electrode method for evaluating seafood quality by correlation to sensory analysis," *Journal of Food Science*, vol. 66, no. 7, pp. 945–952, 2001.

[61] J. M. Gallardo, R. I. Perez-Martin, J. M. Franco, S. Aubourg, and C. G. Sotelo, "Changes in volatile bases and trimethylamine oxide during the canning of albacore (Thunnus alalunga)," *International Journal of Food Science & Technology*, vol. 25, no. 1, pp. 78–81, 1990.

[62] J. M. Gallardo, R. Perez-Martin, J. M. Franco, and S. Aubourg, "Chemical composition and evolution of nitrogen compounds during the processing and storage of canned albacore (Thunnus alalunga," in *Proc. M.O.C.C.A*, pp. 51–58, Chemical composition and evolution of nitrogen compounds during the processing and storage of canned albacore (Thunnus alalunga). Proc. M.O.C.C.A. 1, 51-58, 1984.

Hindawi
Journal of Food Quality
Volume 2018, Article ID 1067672, 10 pages
https://doi.org/10.1155/2018/1067672

Research Article

Solar Drying and Sensory Attributes of Eland *(Taurotragus oryx)* Jerky

Iva Kučerová, Štěpán Marek, and Jan Banout

Department of Sustainable Technologies, Faculty of Tropical AgriSciences, Czech University of Life Sciences Prague, Kamycka 129, Suchdol, 16521 Praha 6, Czech Republic

Correspondence should be addressed to Jan Banout; banout@ftz.czu.cz

Received 29 September 2017; Revised 3 February 2018; Accepted 8 March 2018; Published 23 April 2018

Academic Editor: Alex Martynenko

A double-pass solar drier (DPSD) and a laboratory oven (LO) were used for thin-layer drying of eland and beef. Prior to drying, the physicochemical characteristics of the raw meat were determined, such as pH, dry matter content (%), Warner-Bratzler shear force (N), pigment concentration (mg·kg^{-1}), weight loss during cooking (%), water holding capacity (%), colour (L, a, b), and crude fat content (%). Both meats were pretreated with traditional jerky marinade (TM), TM with fresh pineapple juice (TMP), TM with honey (TMH), and TM with Coca Cola© (TMCCL) and compared to an untreated control (C). The sensory properties of the eland and beef jerky were assessed in a two-stage process. The surface colour values of the jerky samples were measured in the CIE L^* a^* b^* colour space and the effect of the different pretreatments on the overall combined colour (ΔE) was calculated. Significant differences ($p < 0.05$) between raw eland and beef samples were found in case of pH, pigment concentration, water holding capacity, crude fat content, and colour (L and b). Jerky from TMP pretreated meat had the highest scores for texture, colour, and taste. Generally, for both meats dried in both driers, TMH marinade was evaluated as the one with the highest total difference ΔE compared to meat dipped in TMP pretreatment, which had the lowest total difference ΔE.

1. Introduction

Drying, particularly open sun drying, agricultural products such as fruit, vegetables, or meat is one of the oldest and still widespread conservation techniques used for food processing [1]. Drying in the sun is still a popular method in many developing countries, chiefly where no cold chain is available. Although, from the point of view of the sensory properties, dried meat cannot be compared with fresh meat, most nutritional properties, in particular the protein content, remain unchanged through drying [2]. Dried meats are traditional in different parts of the world and they are known as "cecina" in Spain, "biltong" in South Africa, "bresaola" in Italy, or "jerky" in America [3, 4]. Nowadays, jerky is more of a convenient snack food with a great variety of products where safe preservation, flavour, and texture are important. The market for meat snacks has rapidly grown in the past decade, and of those meat snacks, meat jerky is very popular because it can be purchased easily in retail shops worldwide and has long shelf stability and high protein content [5]. In developing countries the consumption of dried meat (in fresh meat equivalency) has continuously increased from a modest average annual per capita consumption of 10 kg in the 1960s to 26 kg in 2000 and it is projected to reach 37 kg around the year 2030 [2].

The simplest method to make jerky is to cut meat into strips and dry it. More typically, spices or marinades are used to flavour the meat, and curing or smoking might be used in combination with drying to make jerky [4]. Jerky can be made from different animal species (beef, pork, fish, chicken, turkey, and/or venison) but more than 70% of jerky is produced from beef. Nowadays consumers are increasingly becoming concerned about healthy, natural, and safe products and the demand for these products is escalating.

Game meat and venison meet most of the criteria demanded by a discerning consumer [6]. One of the prospective venison and/or game animals is eland *(Taurotragus oryx)*. The eland is the largest kind of antelope comparable to the domestic ox not only in size but also in its placid nature and its meat is comparable to beef. Further, eland

meat has a lower content of intramuscular fat, with fat content averaging around 2.4% [7]. Lower fat content is better from the point of view of drying (faster drying), the lower presence of pathogens [8], and healthiness (a desirable ratio of polyunsaturated and saturated fatty acids) [6, 9]. Finally, game meat was not associated with BSE. These properties make eland meat a good perspective as a source of human nutrition as well as an alternative product to traditional beef, even in the dried form.

There is a lack of any detailed research and information in the scientific literature on drying behaviour and drying pretreatments for jerky prepared from eland meat. It is also reasonable to investigate the solar drying process, mainly because dried meat is a potentially important part of the diet of rural inhabitants in developing countries where a connection to the electricity grid is unavailable. The advantages of solar driers, enabling them to compete with traditional open-to-sun drying techniques and/or conventional driers powered by energy from fossil fuels, have been previously reported in the literature [10–13]. This study focuses on the influence of different drying pretreatments on the behaviour of solar drying whilst processing eland and beef meat, the sensory properties, and the quality of the final product.

2. Materials and Methods

2.1. Meat Samples. Fresh beef (steer, *Bos taurus*, Fleckvieh Breed, 16 months old) from biceps femoris was purchased from the Institute of Animal Sciences (Prague (Uhříněves), Czech Republic). Fresh eland (steer, *Taurotragus oryx*, 16 months old) meat from biceps femoris was purchased from the school farm of the Czech University of Life Sciences Prague (Lány, Czech Republic). Both groups of animals had been fed with a similar diet based on a mix of corn silage, lucerne haylage, meadow hay, and barley straw ad libitum.

2.2. Physicochemical Characteristics of Raw Meat. Meat samples for physicochemical analysis were obtained 24 hours after slaughter, packed into low density polyethylene (LDPE) bags, and stored at 4 to 7°C for seven days. Data from a duplicate analysis for pH, dry matter content (%), Warner-Bratzler shear force (N), pigment concentration ($mg \cdot kg^{-1}$), weight loss during cooking (%), water holding capacity (%), colour (L, a, b), and fat content (%) were averaged.

The pH value was measured 24 hours after slaughter using a Testo 205 pH meter (Lenzkirch, Germany). Analyses were done in triplicate.

The sea sand reference method ISO 1442:1997 [14] was used to dry 60 g of meat at 103 ± 2°C for 24 hours. Analyses were done in triplicate.

Shear force values were determined with a Warner-Bratzler shear attachment on a texture analyser (Instron Model 5544, software Series IX, Instron Co., USA). Samples of muscles were cleared from connective tissues and cut into pieces of 15 × 20 × 60 mm. Test speeds were set at $2\ mm \cdot s^{-1}$. Data were collected and analysed from the shear force values to obtain the maximum force required to shear through each sample and were then converted into Newton (N). Analyses were done on four samples.

Haem pigments were extracted in a solution of acetone and HCl [15], and pigment concentration was determined using a UV-2900 PC spectrophotometer (Tsingtao Unicom-Optics Instruments Co., Ltd., China) and expressed as total haem pigments content [16]. Analyses were measured in two replications.

Samples of meat (separately for eland and beef) were placed in glass tubes, weighted, covered with aluminium foil, and placed in a water bath at a temperature of 80°C for 30 min. Water loss was measured gravimetrically. Analyses were done in two replications.

Water holding capacity was determined using the Grau and Hamm's filter paper press method modified by Brendl [17]. Meat and total fluid areas were measured with a Planix 7 digital planimeter (Tamaya Technics Inc., Japan) [18]. Analyses were done in twelve replications.

Reflectance was measured with a Minolta CM206d spectrophotometer (Minolta Co. Ltd., Japan). Muscle samples were cleared from connective tissues and cut crosswise. Data were obtained immediately from a freshly sliced cut of sample [16]. Measurements were done in triplicate. Reflectance was measured again after the drying procedure with twenty replications.

Fat content was obtained gravimetrically after extraction from dried samples with petrol ether for 4 hours according to the Soxhlet method [19]. Analyses were done in triplicate.

2.3. Sample Preparation and Drying Pretreatments. The meat samples used for the drying experiment were cleaned from connective tissues 24 h after the slaughter, packed into LDPE bags, and stored at 4 to 7°C for 7 days. Afterwards both meat samples were stored at −18°C for 4 days and then thawed at 4°C overnight. This semithawed meat was cut with a food slicer (Concept KP 3530, FS-82T) into uniform samples of size 5 × 80 × 25 mm. A sample size of 5 mm was cut through the fibre. Meat slices were vacuum-packaged (MAGIC VAC Champion, Elaem Nuova) in bags and stored at −18°C for 1 month for later use.

After one month of storage, the samples were thawed, treated in marinades, and subsequently dried in two driers. The following drying pretreatments were used in this study: traditional jerky marinade (TM), TM with pineapple juice (TMP), TM with honey (TMH), TM with Coca Cola (TMCCL), and control samples, without marinade (C).

Traditional jerky marinade [20, 21] consisted of 60 mL soy sauce (Kikkoman Foods), 15 mL Worcestershire sauce (Vitana, Czech Republic), 0.6 g black pepper, 1.25 g garlic powder, 1.5 g onion powder, and 4.35 g old hickory-smoked salt. Meat samples were dipped for 10 min at ambient temperature (24°C) in different marinades as presented in Table 1.

2.4. Drying Experiment. The fresh meat slices were dried out in a double-pass solar drier (DPSD) (Figure 1) designed at the Faculty of Tropical AgriSciences, Czech University of Life Sciences Prague, and previously described by Banout et al. [22].

Table 1: Classification of pretreatments used.

Pretreatment	Content
(1) TM	Traditional jerky marinade (TM)
(2) TMP	TM and freshly prepared pineapple juice (50% fresh pineapple juice/50% TM)
(3) TMH	TM and bee honey solution (50% bee honey solution/50% TM), bee honey solution (50% bee honey/50% distilled water)
(4) TMCCL	TM and Coca Cola (50% Coca Cola/50% TM), Coca Cola (The Coca-Cola Company). Ingredients of Coca Cola original: sugar, caramel colour E150d, caffeine, phosphoric acid, carbonated water, and flavour

Table 2: Climatic and drying conditions of all solar drying experiments (SD: standard deviations; A, B, C: set of experiments).

	A	B	C
	Mean ± SD	Mean ± SD	Mean ± SD
Average ambient temperature (°C)	24.3 ± 1.7	23.4 ± 1.4	25.5 ± 2.1
Average drying temperature (°C)	48.4 ± 6.0	46.4 ± 5.7	49.2 ± 5.2
Average ambient RH (%)	49.2 ± 8.7	51.3 ± 8.7	46.2 ± 7.7
Average RH of drying air (%)	18.2 ± 5.7	19.7 ± 6.7	17.7 ± 5.7
Average insolation ($W \cdot m^{-2}$)	552.3 ± 219.4	525.4 ± 194.1	615.3 ± 144.1
Average air flow speed in collector ($m \cdot s^{-1}$)	1.0 ± 0.3	0.7 ± 0.1	1.1 ± 0.1

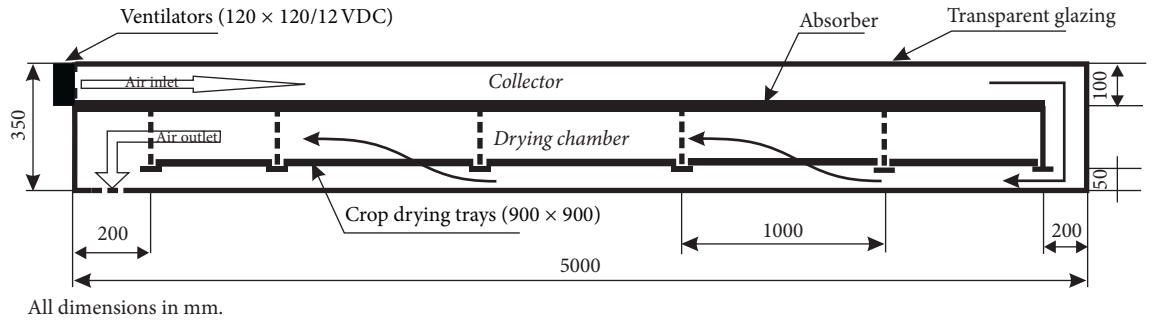

(a)

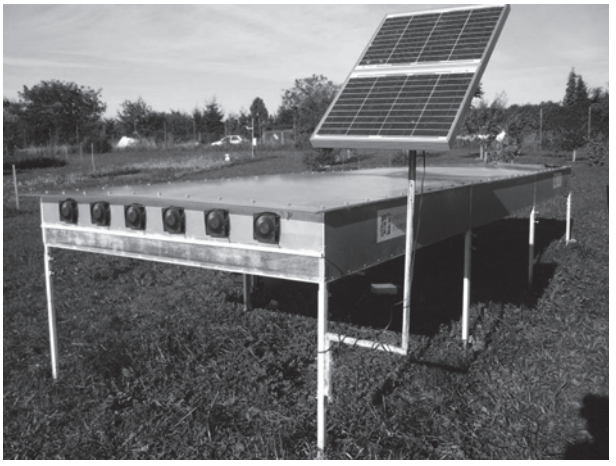

(b)

Figure 1: Double-pass solar drier (DPSD) ((a) schematic diagram of DPSD, (b) photo of DPSD).

A total of three full-scale experimental sets for drying eland and beef were conducted from June to September at the Czech University of Life Sciences Prague (Czech Republic). The climatic and drying conditions are presented in Table 2. Each set of solar drying experiments took 2 days and always started at 10:00 AM and stopped at 6:00 PM. During the night, the samples were collected and placed in a room in closed plastic bags. The following operational parameters were measured every hour during the solar drying experiments:

Table 3: Parameters and orientation.

Parameter/orientation	0	100
General look	Like	Dislike
General likableness of taste	Like	Dislike
General likableness of meat taste*	Like	Dislike
Intensity of meat taste*	Slightly intensive	Extremely intensive
Intensity of fatty taste*	Slightly intensive	Extremely intensive
Colour intensity	Light	Dark
Colour likableness	Like	Dislike
Hardness	Very soft	Very hard
Chewiness	Very good	Bad
Fibrousness*	Soft	Chewy
Sappiness	Juicy	Dry
General structure	Excellent	Bad

*Parameters evaluated only by the first panel whose aim was to evaluate the difference between drying in DPSD and LO and differences between eland and beef.

(i) Drying air temperature (°C) and drying air relative humidity (RH) (%), Temperature-Humidity Logger S3121 (Comet System, Czech Republic)

(ii) Drying air velocity ($m \cdot s^{-1}$), Anemometer Testo 425 (Lenzkirch, Germany)

(iii) Weight loss of reference samples of meat slices (g), Balance Kern 572-30 (Kern & Sohn GmbH)

(iv) Ambient air temperature (°C), ambient air RH (%), Temperature-Humidity Logger S3121 (Comet System, Czech Republic)

(v) Global solar radiation ($W \cdot m^{-2}$), pyranometer CMP 6, along with a solar integrator (Kipp Zonen, Delft, Netherlands).

The solar drying of meat samples from both eland and beef was compared with drying in a laboratory oven (LO), standard dehydrator (Memmert UFE 500 GmbH + Co. KG, Germany), at a constant temperature of 55°C. Experiments conducted in the LO were replicated three times.

At the end of each drying test in the DPSD and LO the control samples of each meat were collected in triplicate and the dry matter content was estimated by the oven method at 105°C for 24 h (Memmert UFE 500 GmbH + Co. KG, Germany). Equation (1) was used to estimate dry matter content on the dry basis [11]:

$$MC_{db} = \frac{\text{water (kg)}}{\text{dry meat (kg)}} * 100\%. \quad (1)$$

The drying rate is an important parameter when assessing the drying process. Kituu et al. [23] evaluated the drying rate (DR) as the decrease of water concentration during the time interval between two subsequent measurements divided by the time interval. The drying rate (DR) is presented by the following equation:

$$DR = \frac{\Delta M}{\Delta T}. \quad (2)$$

2.5. Organoleptic Properties and Sensory Analysis. All the sensory analysis was in accordance with ISO 8586:2012 [24]. Two independent panels, first of 15 expert assessors and second of 22 assessors, were organized. Panellists were selected and trained. Each assessor evaluated the meat samples submitted on a paper tray designated by a digit code. The profile method with a 100 mm unstructured graphic scale was used for evaluation. The parameters evaluated are given in Table 3. The first panel ($n = 15$) evaluated four samples: (1) untreated control sample C of eland dried in DPSD, (2) untreated control sample C of eland dried in LO, (3) untreated control sample C of beef dried in DPSD, and (4) untreated control sample C of beef dried in LO. This sensory panel aimed to investigate if different drying devices and different kinds of meat can influence the results of a sensory profile analysis.

Based on the results of the first panel, the second assessment only focused on eland meat dried in the DPSD and the effect of different drying pretreatments on the organoleptic properties assessed by the 22-member panel. The panellists evaluated samples pretreated with (1) traditional marinade (TM), (2) TM with honey, (3) TM with pineapple, and (4) TM with Coca Cola. Sensory analyses were accomplished in 2 sessions (in separate days) within 1 month.

The surface colour values of the jerky samples were measured with a CM-2600d spectrophotometer (Minolta) in the CIE L^* a^* b^* colour space using Spectra Magic CM-S100w software.

To evaluate the effect of different pretreatments on the overall combined colour of dried meat, the ΔE index, as given by the following equation [25, 26], was calculated by taking the colour of the control sample (C) as the reference value:

$$\Delta E = \sqrt{(\Delta L)^2 + (\Delta a)^2 + (\Delta b)^2}, \quad (3)$$

where $\Delta L = L - L_{base}$, $\Delta a = a - a_{base}$, and $\Delta b = b - b_{base}$ and L, a, and b are the colour coordinates of the sample and L_{base}, a_{base}, and b_{base} are the colour coordinates of the control C sample.

Table 4: Results of physicochemical characteristics of raw meat (SD: standard deviations).

	Eland	Beef	
	Mean ± SD	Mean ± SD	p values
pH 24 hours after slaughter	5.50 ± 0.01	5.55 ± 0.01	0.001
Warner-Bratzler shear force (N)	68.84 ± 15.43	89.32 ± 19.68	0.155
Pigment concentration (mg·kg–1)	4339.36 ± 51.57	3482.41 ± 103.14	0.023
Weight loss during cooking (%)	27.23 ± 0.18	27.55 ± 0.42	0.461
Water holding capacity (%)	44.87 ± 2.17	52.13 ± 5.97	0.001
Water content (%)	75.05 ± 0.05	75.20 ± 0.11	0.121
Crude fat content (%)	0.84 ± 0.09	2.80 ± 0.53	0.021
Colour L	38.88 ± 2.59	42.41 ± 1.64	0.031
a	9.13 ± 1.05	10.33 ± 0.74	0.067
b	6.86 ± 1.02	9.71 ± 0.49	0.001

2.6. Statistical Analysis. Data were analysed with the IBM SPSS Statistics software version 22.0 (IBM, US). For the physicochemical characteristics of raw meat, the data were analysed using the independent samples t-test. Sensory data were analysed using a one-way ANOVA, in the case of the first panel, separately for the main effects of the meat drier by groups, and the kind of meat by groups, the second panel for the treatment by groups. A Tukey test was performed for the separation of mean differences with a 95% confidence level. The results of the sensory profile analysis for the parameter general likableness of taste within the first panel were transformed and processed by the Friedman test. Instrumentally measured colour was analysed by one-way ANOVA for the main effect of different treatments within a drying system, separately for eland and beef with the Tukey test as a post hoc test. The independent t-test was applied to compare different colour parameters within different drying systems, separately for eland and beef.

3. Results and Discussion

3.1. Physicochemical Characteristics of Raw Meat. The results of the physicochemical characteristics of raw meat are presented in Table 4. A comparison of eland and beef meat showed lower pH values in the eland sample, which, according to Huff-Lonergan and Lonergan [27] and Muchenje et al. [28], is one of the aspects related to the development of lower water holding capacity in eland. The Warner-Bratzler shear force for the beef samples was higher, but did not differ statistically from eland. A higher WB shear force for beef, when comparing beef with eland, was already published by Bartoň et al. [29]. Pigment concentrations in muscles of eland were higher and therefore it was darker (lower L value) with lower redness and yellowness. A significant difference was found for yellowness (b), caused by the low accumulation level of carotenoids in eland [30] compared to the high accumulation level in cattle [31]. These data are in accordance with a lighter colour found for beef compared to eland [29] and compared to other venison [32–34]. The muscles of eland contain less crude fat as noted by La Chevallerie et al. [7].

3.2. Drying Performance. The data presented in Table 2 show a relative uniformity, which is due to similar climatic conditions during each solar drying test. For further performance analyses, the data from experiment A were considered to represent optimal average values. Maximum solar radiation on the first day was 954.5 $W{\cdot}m^{-2}$ and on the second day it was 864.3 $W{\cdot}m^{-2}$ with an average for both days of 552.3 $W{\cdot}m^{-2}$. Ambient temperature varied during both days between 20.6 and 26.8°C, with an average of approximately 24.4°C, and ambient relative humidity between 35.7% and 64.1%, with an average of approximately 49.2%. The daily mean values of drying air temperature and relative humidity in the drier (DPSD) varied from 23.6 to 60.8°C and 11.7 to 62.8%, with their average values being 48.1°C and 18.4%. The drying temperatures measured in the solar drier were close to those recommended for the preparation of dried meat [8, 35]. The daily mean values of drying air velocity varied during both days, approximately 0.04 to 1.87 $m{\cdot}s^{-1}$ with an average of 1 $m{\cdot}s^{-1}$ in the collector part of the drier. The relatively large difference between the maximum and minimum drying air velocities was caused by the PV panel being directly connected to fans with no regulatory systems. The system regulates the airflow itself due to the position of the sun during the day. However, this disposition makes the airflow rate highly sensitive to actual insolation.

According to Kucerova et al. [36] where there was no statistically significant difference between the drying behaviour of eland and beef, Figures 2 and 3 present just eland meat dried in the DPSD and LO and the reduction of its moisture content over time.

From Figures 2 and 3, it is evident that, in general, a higher drying rate was achieved in the DPSD as compared to the LO.

Drying rates plotted with moisture contents for solar drying in the DPSD and drying in the LO are presented in Figures 4 and 5. The drying rates were higher at the beginning of the drying process and later decreased with decreasing moisture content. Similarly, as in the case of Figures 2 and 3, a higher drying rate was observed during solar drying of meat samples mainly in the initial stages. The drying rates were fitted by linear trend lines and DR equations (see (4),

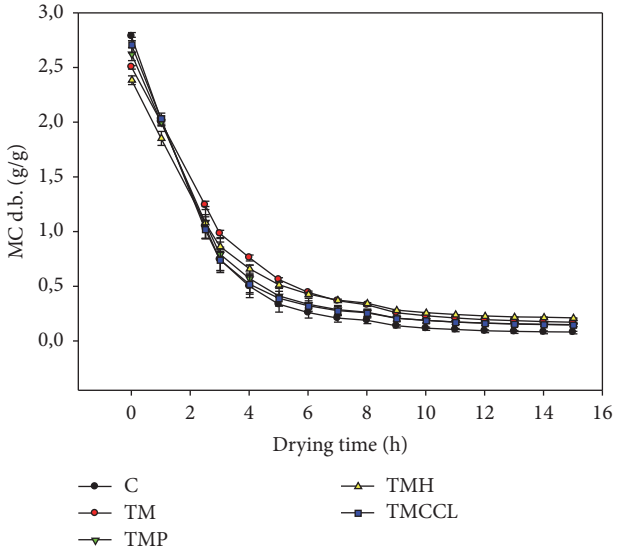

Figure 2: Changes in moisture content (d.b.) of control and pretreated samples of eland in drying time for a typical experimental run in DPSD.

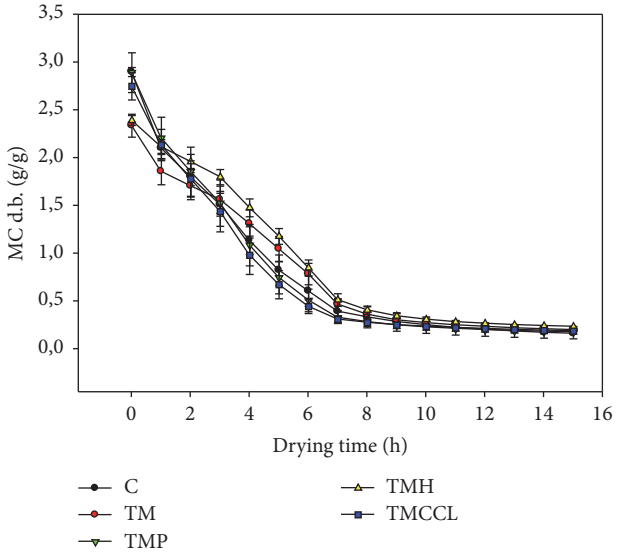

Figure 3: Changes in moisture content (d.b.) of control and pretreated samples of eland in drying time for a typical experimental run in LO.

(5), (6), (7), and (8)) were developed for solar drying and (9), (10), (11), (12), and (13) for LO drying, respectively:

$$\mathrm{DR_C} = 0.4637(M) - 0.0096 \quad \left(R^2 = 0.8553\right) \tag{4}$$

$$\mathrm{DR_{TM}} = 0.3438(M) - 0.0319 \quad \left(R^2 = 0.8351\right) \tag{5}$$

$$\mathrm{DR_{TMP}} = 0.4194(M) - 0.0314 \quad \left(R^2 = 0.7998\right) \tag{6}$$

$$\mathrm{DRT_{TMH}} = 0.3946(M) - 0.0637 \quad \left(R^2 = 0.8649\right) \tag{7}$$

$$\mathrm{DR_{TMCCL}} = 0.4441(M) - 0.0353 \quad \left(R^2 = 0.7943\right) \tag{8}$$

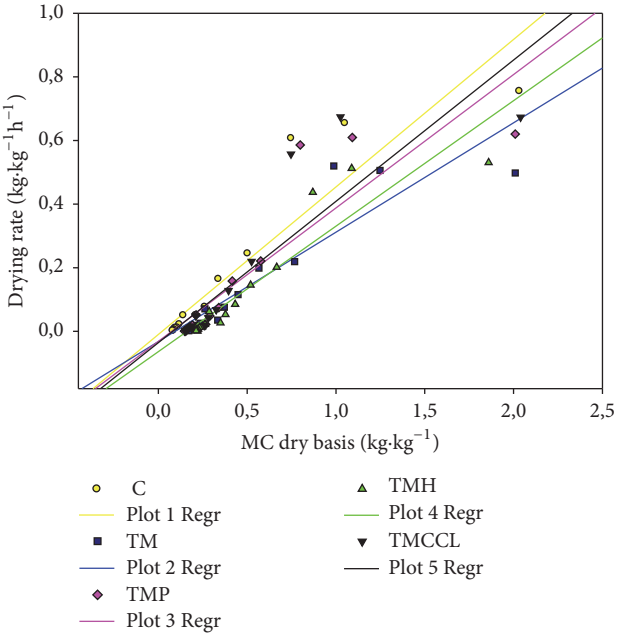

Figure 4: Drying rate curves of eland meat dried in a DPSD.

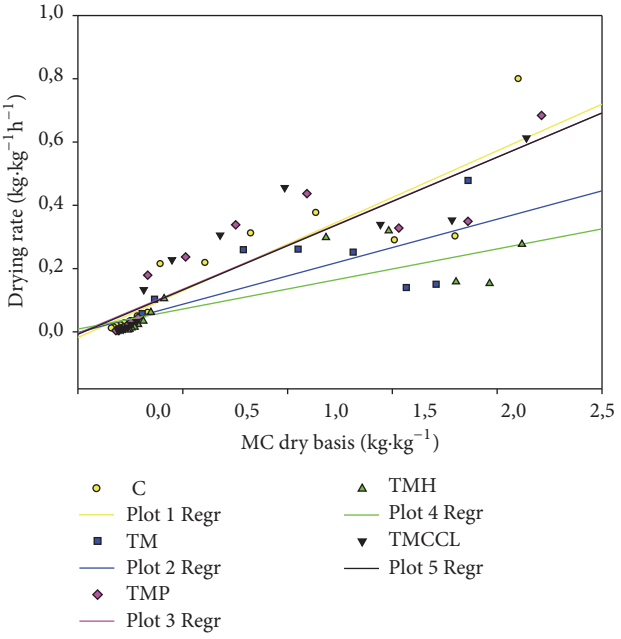

Figure 5: Drying rate curves of eland meat dried in a LO.

$$\mathrm{DR_C} = 0.2951(M) - 0.0179 \quad \left(R^2 = 0.7953\right) \tag{9}$$

$$\mathrm{DR_{TM}} = 0.1791(M) - 2.1887 \quad \left(R^2 = 0.6483\right) \tag{10}$$

$$\mathrm{DR_{TMP}} = 0.2786(M) - 0.0048 \quad \left(R^2 = 0.8236\right) \tag{11}$$

$$\mathrm{DR_{TMH}} = 0.1267(M) + 0.0088 \quad \left(R^2 = 0.6510\right) \tag{12}$$

$$\mathrm{DR_{TMCCL}} = 0.2798(M) - 0.0076 \quad \left(R^2 = 0.8171\right). \tag{13}$$

Table 5: Overall sensory evaluation of eland meat samples dried in DPSD ($n = 22$).

	Pretreatments							
	TM		TMP		TMH		TMCCL	
	Mean	SD	Mean	SD	Mean	SD	Mean	SD
General look	4.24[a]	2.17	**3.24**[a]	1.92	4.5[a]	2.46	3.90[a]	2.05
General likableness of taste	**2.65**[a]	0.76	3.38[ab]	1.83	4.61[b]	1.69	4.34[ab]	1.48
Colour intensity	5.46[ab]	2.32	**4.97**[a]	2.31	7.63[c]	1.97	7.06[bc]	1.87
Colour likableness	5.12[b]	1.95	**3.64**[a]	1.98	4.07[ab]	1.81	3.81[ab]	1.64
Hardness	5.42[ab]	2.45	**5.11**[a]	2.35	6.99[b]	1.92	6.39[ab]	2.07
Chewiness	4.96[a]	2.04	5.23[a]	1.88	5.55[a]	2.5	5.96[a]	2.18
Sappiness	5.56[a]	2.3	5.72[a]	2.09	5.59[a]	1.76	5.45[a]	2.52
General texture	4.83[ab]	1.37	**3.89**[a]	1.81	6.05[b]	1.39	5.3[ab]	2.14

[a–c]Mean values with different superscripts within a same row are significantly different ($p < 0.05$). Extrabold type signs the best evaluated parameter for the pretreatment.

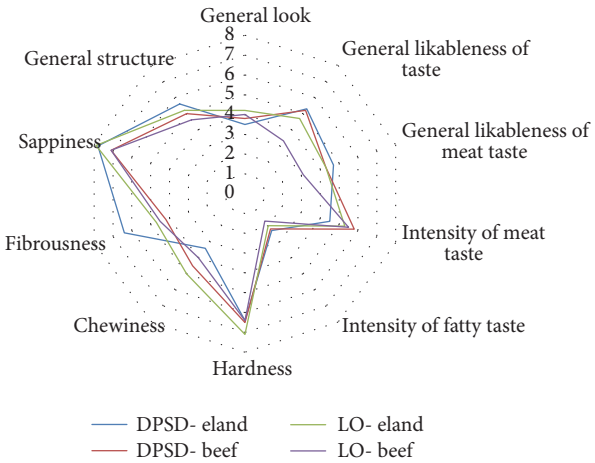

Figure 6: Sensory evaluation by profile method of control samples. C of both eland and beef meat dried in DPSD and LO ($n = 15$).

3.3. Sensory Analysis. The results of the first sensory panel are presented in Figure 6.

For the parameter general likableness of taste transformed by the Friedman test, the sample of beef meat dried in LO scored the highest, and differences between samples of beef dried in LO and eland dried in DPSD as well as beef dried in LO and beef dried in DPSD ($p < 0.05$) were found. This could be due to the lower drying rate in LO. According to Bejerholm and Aaslyng [37], it could affect the flavour and odour components, especially the humidity, which influences the odour, flavour, and colour of the meat where a high humidity will prevent Maillard reactions from taking place and will dilute the flavour and odour components.

All sensory attributes with higher water holding capacity (see Table 4) in beef can therefore be influenced by changes in the drying technique. On the other hand, eland meat dried in DPSD scored in the parameter general look; even the differences between samples were not significant. These findings are in accordance with data published by Speth [38], where eland meat is considered to be very similar to beef. Assessors could not distinguish differences in the intensity of fatty taste, even if beef meat contained more fat (as noticed in Table 4). In contrast they assessed the beef samples as juicier than the eland samples, which is in accordance with Ruiz-Carrascal et al. [39], who pointed out that intramuscular fat plays a decisive role in most features of dry-cured products directly linked to their sensory characteristics, such as marbling and juiciness. Consumers are concerned about diet and health and a fat low-content is desirable [40]; nevertheless juiciness, more precisely a higher fat content, could even affect the assessment of general likableness of taste. The most important sensory attributes of this type of snack food are texture, colour, and flavour all together. As determined by the selection of the raw material and the effect of numerous technological factors [41], generally it is not possible to state that there is a statistical difference ($p < 0.05$) between samples dried in DPSD and LO and between beef and eland meat. This result is in agreement with those obtained by Mapesa et al. [42] where beef dried in a solar drier was not statistically different ($p < 0.05$) from that dried in an oven. The difference between eland and beef was evaluated by Bartoň et al. [29] and their results on the texture are in agreement with the dried meat in this study.

Based on the first sensory analysis, in most cases there was no significant difference between beef and eland meat samples; the results from the second assessment are presented in Table 5.

The sample treated with traditional jerky marinade with fresh pineapple juice (TMP) was considered to be the best from the samples of eland meat dried in DPSD. This treatment scored in all categories. Fresh pineapple juice contains bromelain, which is known to degrade myosin [43]. Therefore, meat treated with fresh pineapple juice is more tender. This is also evident in the evaluation of the hardness of the meat samples or their general texture too. Even such parameters as chewiness or juiciness were not significantly different; they did not influence the result of the parameter general texture. The TMP sample also scored in the parameter colour likableness, whereas in the correlation with the results for colour intensity it is clear that a lighter colour is considered better, or rather the one with a more pleasant colour in terms of assessing meat.

Table 6: Colour of dried eland and beef in DPSD and LO ((a) eland; (b) beef).

(a)

	DPSD		
	L	*a*	*b*
C	$30.24 \pm 4.3^{b.c}$	5.07 ± 0.93^{d}	9.27 ± 2.19^{b}
TM	20.65 ± 2.74^{a}	$2.11 \pm 0.74^{a.b}$	6.03 ± 1.51^{a}
TMP	30.95 ± 4.23^{c}	$2.6 \pm 0.82^{b.c}$	4.54 ± 1.49^{a}
TMH	21.21 ± 3.5^{a}	1.44 ± 0.56^{a}	4.75 ± 1.14^{a}
TMCCL	$27.21 \pm 4.01^{b.c}$	2.25 ± 1.00^{b}	5.05 ± 1.84^{a}
	LO		
	L	*a*	*b*
C	29.98 ± 3.61^{b}	3.14 ± 1.04^{d}	5.17 ± 3.10^{a}
TM	28.80 ± 3.51^{b}	3.31 ± 1.30^{d}	10.46 ± 3.19^{b}
TMP	22.62 ± 4.44^{a}	$2.09 \pm 1.22^{a.b.c}$	6.89 ± 3.19^{a}
TMH	20.04 ± 2.31^{a}	1.26 ± 0.87^{a}	6.20 ± 1.39^{a}
TMCCL	22.32 ± 2.51^{a}	$2.46 \pm 1.22^{b.c.d}$	7.33 ± 2.20^{a}

$^{a–d}$Mean values with different superscripts within the same column are significantly different ($p < 0.05$).

(b)

	DPSD		
	L	*a*	*b*
C	$25.20 \pm 3.95^{b.c}$	4.49 ± 1.15^{c}	$8.86 \pm 1.75^{c.d}$
TM	$22.83 \pm 4.74^{a.b.c}$	3.11 ± 1.12^{b}	$8.83 \pm 2.35^{c.d}$
TMP	25.71 ± 4.49^{c}	3.61 ± 1.37^{b}	$8.31 \pm 2.36^{c.d}$
TMH	20.41 ± 3.25^{a}	1.49 ± 0.6^{a}	$6.49 \pm 1.36^{a.b}$
TMCCL	30.3 ± 4.6^{d}	3.21 ± 1.6^{b}	4.76 ± 2.53^{a}
	LO		
	L	*a*	*b*
C	28.80 ± 3.63^{c}	4.45 ± 1.22^{c}	$7.99 \pm 2.61^{b.c}$
TM	$26.86 \pm 5.01^{b.c}$	4.09 ± 1.43^{c}	12.41 ± 3.44^{d}
TMP	$24.45 \pm 3.10^{a.b}$	$1.98 \pm 1.20^{a.b}$	5.12 ± 2.41^{a}
TMH	20.79 ± 3.33^{a}	1.64 ± 0.88^{a}	$6.96 \pm 1.86^{a.b}$
TMCCL	$24.35 \pm 3.22^{a.b}$	3.04 ± 1.31^{b}	9.06 ± 2.50^{c}

$^{a–d}$Mean values with different superscripts within the same column are significantly different ($p < 0.05$).

As mentioned above, colour is one of the most important attributes of jerky [44] and is strongly associated with the concept of quality [45]. The meat of eland and beef contains a large quantity of free amino acids [29] that, in combination with the sugar in pretreatments, can, under relevant conditions of concentration, pH, and temperature, start Maillard reactions and form dark pigments [46]. A comparison of the colours of different treatments within a drying system for eland and beef is presented in Table 6.

The lightness value *L* and the value of the parameter *a* of the dried beef are similar to the values of beef jerky reported by Farouk and Swan [47]. It is also possible to compare some other colour values reported in the literature with the results of this study. The values of *L*, *a*, and *b* for beef jerky reported by Konieczny et al. [41] were 30.66, 13.42, and 4.24, respectively; for ostrich jerky, they were 27.2, 2.0, and 2.3, respectively [48].

The results of comparing the *L*, *a*, and *b* parameters within different drying systems separately for eland and beef are as follows. In the case of eland, significant differences ($p < 0.05$) between DPSD and LO were found in the C sample (*a*, *b* parameters), the TM sample (*L*, *a*, and *b* parameters), TMP, TMCCL (*L*, *b* parameters), and TMH (*b* parameter). Significant differences ($p < 0.05$) between DPSD and LO in the case of beef were also identified: sample C (*L* parameter), TM (*L*, *a*, and *b* parameters), TMP (*a*, *b* parameters), and TMCCL (*L*, *b* parameters). Thus, it is evident that the type of drier can influence the final colour of the product.

The total colour difference ΔE as determined by (3) can be classified analytically according to Cserhalmi et al. [49] as not noticeable (0–0.5), slightly noticeable (0.5–1.5), noticeable (1.5–3.0), well visible (3.0–6.0), and great (>6.0). The results of ΔE for eland and beef dried in DPSD and LO are presented in Figure 7.

Generally, for both meats dried in both driers, the TMH marinade was evaluated as the one with the highest total difference ΔE; in contrast meat dipped in the TMP pretreatment has the lowest total difference in ΔE. This result

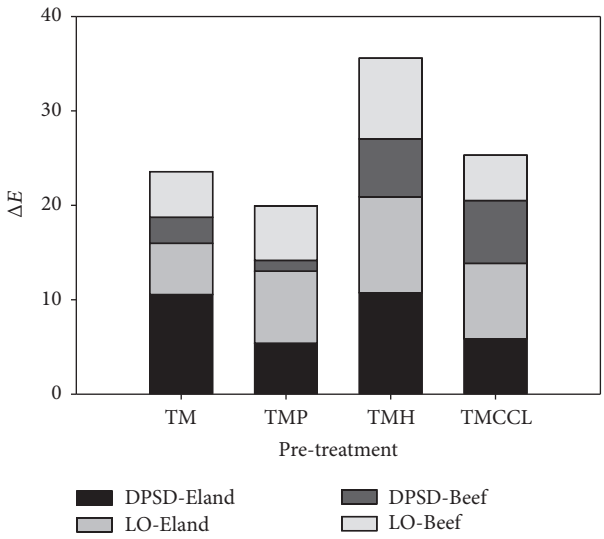

Figure 7: Total colour difference ΔE.

correlates with the result of the sensory panel, where the TMP sample was evaluated as the lightest one and therefore it is possible to point out that the assessors preferred lighter meat with a lower total colour change than the darker one.

4. Conclusion

This study brings new findings about the sensory analysis and organoleptic properties, including colour change whilst drying eland jerky, which might be important for possible industrial processing. Further, it can be concluded that solar drying technology brings compatible results as with a standard laboratory drier. Finally, the study indicates that the organoleptic properties of eland jerky are similar to widely recognized traditional beef jerky.

Conflicts of Interest

The authors declare that they have no conflicts of interest.

Acknowledgments

The authors wish to express their gratitude to the Internal Grant Agency of the Faculty of Tropical AgriSciences, Czech University of Life Sciences Prague (Project no. 20175013).

References

[1] L. Imre, "Solar dryers," in *Industrial drying of food*, L. Baker, Ed., pp. 210–238, Blackie academic and professional, London, UK, 1997.

[2] G. Heinz and P. Hautzinger, "Meat processing technology. For small to medium-scale producers," *Food and Agriculture Organization of the United Nations*, 2007.

[3] E. Hierro, L. De La Hoz, and J. A. Ordóñez, "Headspace volatile compounds from salted and occasionally smoked dried meats (cecinas) as affected by animal species," *Food Chemistry*, vol. 85, no. 4, pp. 649–657, 2004.

[4] B. A. Nummer, J. A. Harrison, M. A. Harrison, P. Kendall, J. N. Sofos, and E. L. Andress, "Effects of preparation methods on the microbiological safety of home-dried meat jerky," *Journal of Food Protection*, vol. 67, no. 10, pp. 2337–2341, 2004.

[5] M.-J. Kim and H.-Y. Kim, "Species identification of commercial jerky products in food and feed using direct pentaplex PCR assay," *Food Control*, vol. 78, pp. 1–6, 2017.

[6] L. C. Hoffman and E. Wiklund, "Game and venison - meat for the modern consumer," *Meat Science*, vol. 74, no. 1, pp. 197–208, 2006.

[7] M. La Chevallerie, J. M. Erasmus, J. D. Skinner, and J. H. M. van Zyl, "A note on the carcass composition of the Common Eland (Taurotragus oryx)," *South African Journal of Animal Science*, no. 1, pp. 129–131, 1971.

[8] N. G. Faith, N. S. Le Coutour, M. B. Alvarenga, M. Calicioglu, D. R. Buege, and J. B. Luchansky, "Viability of Escherichia coli O157:H7 in ground and formed beef jerky prepared at levels of 5 and 20% fat and dried at 52, 57, 63, or 68∘C in a home-style dehydrator," *International Journal of Food Microbiology*, vol. 41, no. 3, pp. 213–221, 1998.

[9] J. D. Wood, R. I. Richardson, G. R. Nute et al., "Effects of fatty acids on meat quality: a review," *Meat Science*, vol. 66, no. 1, pp. 21–32, 2004.

[10] V. T. Karathanos and V. G. Belessiotis, "Sun and artificial air drying kinetics of some agricultural products," *Journal of Food Engineering*, vol. 31, no. 1, pp. 35–46, 1997.

[11] V. Belessiotis and E. Delyannis, "Solar drying," *Solar Energy*, vol. 85, no. 8, pp. 1665–1691, 2011.

[12] B. K. Bala, M. R. A. Mondol, B. K. Biswas, B. L. Das Chowdury, and S. Janjai, "Solar drying of pineapple using solar tunnel drier," *Journal of Renewable Energy*, vol. 28, no. 2, pp. 183–190, 2003.

[13] M. A. Hossain and B. K. Bala, "Drying of hot chilli using solar tunnel drier," *Solar Energy*, vol. 81, no. 1, pp. 85–92, 2007.

[14] *ISO 1442:1997 Meat and meat products — Determination of moisture content (Reference method)*, International Organization for Standardization, Geneva, 1997.

[15] H. C. Hornsey, "The colour of cooked cured pork. I.—Estimation of the Nitric oxide-Haem Pigments," *Journal of the Science of Food and Agriculture*, vol. 7, no. 8, pp. 534–540, 1956.

[16] AMSA, "Guidelines for Meat Color Evaluation," in *Paper presented at the Reciprocal Meat Conference Proceedings*, 1991.

[17] J. Brendl, *Vaznost masa*, ČAZ- VÚPP, Prague, 1970.

[18] K. Hofmann, R. Hamm, and Blüchel E., "Neues über die Bestimmung der Wasserbindung des Fleisches mit Hilfe der Filterpapierpressmethode," *Fleischwirtschaft*, vol. 62, no. 1, pp. 87–94, 1982.

[19] A.O.A.C., *Official method of analysis of the Association of Official Analytical Chemists International*, vol. 16th, 1997.

[20] E. L. Andress and J. A. Harrison, *So Easy to Preserve*, Cooperative Extension Service, University of Georgia, Athens, GA, 4th edition, 1999.

[21] Y. Yoon, M. Calicioglu, P. A. Kendall, G. C. Smith, and J. N. Sofos, "Influence of inoculum level and acidic marination on inactivation of Escherichia coli O157:H7 during drying and storage of beef jerky," *Food Microbiology*, vol. 22, no. 5, pp. 423–431, 2005.

[22] J. Banout, P. Ehl, J. Havlik, B. Lojka, Z. Polesny, and V. Verner, "Design and performance evaluation of a Double-pass solar drier for drying of red chilli (*Capsicum annum* L.)," *Solar Energy*, vol. 85, no. 3, pp. 506–515, 2011.

[23] G. M. Kituu, D. Shitanda, C. L. Kanali et al., "Thin layer drying model for simulating the drying of Tilapia fish (*Oreochromis niloticus*) in a solar tunnel dryer," *Journal of Food Engineering*, vol. 98, no. 3, pp. 325–331, 2010.

[24] *ISO 8586:2012 Sensory Analysis – General Guidelines for the Selection, Training and Monitoring of Selected Assessors and Expert Sensory Assessors*, International Organization for Standardization, Geneva, 2012.

[25] M. Kashaninejad and L. G. Tabil, "Drying characteristics of purslane (Portulaca oleraceae L.)," *Drying Technology*, vol. 22, no. 9, pp. 2183–2200, 2004.

[26] K. J. Chua, A. S. Mujumdar, S. K. Chou, M. N. A. Hawlader, and J. C. Ho, "Convective drying of banana, guava and potato pieces : effect of cyclical variations of air temperature on drying kinetics and color change," *Drying Technology*, vol. 18, no. 4-5, pp. 907–936, 2000.

[27] E. Huff-Lonergan and S. M. Lonergan, "Mechanisms of water-holding capacity of meat: the role of postmortem biochemical and structural changes," *Meat Science*, vol. 71, no. 1, pp. 194–204, 2005.

[28] V. Muchenje, K. Dzama, M. Chimonyo, P. E. Strydom, A. Hugo, and J. G. Raats, "Some biochemical aspects pertaining to beef eating quality and consumer health: A review," *Food Chemistry*, vol. 112, no. 2, pp. 279–289, 2009.

[29] L. Bartoň, D. Bureš, R. Kotrba, and J. Sales, "Comparison of meat quality between eland (Taurotragus oryx) and cattle (Bos taurus) raised under similar conditions," *Meat Science*, vol. 96, no. 1, pp. 346–352, 2014.

[30] K. A. Slifka, P. E. Bowen, M. Stacewicz-Sapuntzakis, and S. D. Crissey, "A survey of serum and dietary carotenoids in captive wild animals," *Journal of Nutrition*, vol. 129, no. 2, pp. 380–390, 1999.

[31] K. Urich, *Comparative Animal Biochemistry*, Springer Berlin Heidelberg, Berlin, Heidelberg, 1994.

[32] R. M. Koch, H. G. Jung, J. D. Crouse, V. H. Varel, and L. V. Cundiff, "Growth, digestive capability, carcass, and meat characteristics of Bison bison, Bos taurus, and Bos x Bison.," *Journal of Animal Science*, vol. 73, no. 5, pp. 1271–1281, 1995.

[33] P. J. Rincker, P. J. Bechtel, G. Finstadt, R. G. C. Van Buuren, J. Killefer, and F. K. Mckeith, "Similarities and differences in composition and selected sensory attributes of reindeer, caribou and beef," *Journal of Muscle Foods*, vol. 17, no. 1, pp. 65–78, 2006.

[34] M. M. Farouk, M. Beggan, S. Hurst, A. Stuart, P. M. Dobbie, and A. E. D. Bekhit, "Meat quality attributes of chilled venison and beef," *Journal of Food Quality*, vol. 30, no. 6, pp. 1023–1039, 2007.

[35] K. Allen, D. Cornforth, D. Whittier, M. Vasavada, and B. Nummer, "Evaluation of high humidity and wet marinade methods for pasteurization of jerky," *Journal of Food Science*, vol. 72, no. 7, pp. C351–C355, 2007.

[36] I. Kucerova, A. Hubackova, B.-A. Rohlik, and J. Banout, "Mathematical Modeling of Thin-Layer Solar Drying of Eland (Taurotragus oryx) Jerky," *International Journal of Food Engineering*, vol. 11, no. 2, pp. 229–242, 2015.

[37] C. Bejerholm and M. D. Aaslyng, "The influence of cooking technique and core temperature on results of a sensory analysis of pork - Depending on the raw meat quality," *Food Quality and Preference*, vol. 15, no. 1, pp. 19–30, 2004.

[38] J. D. Speth, "Big-Game Hunting: Protein, Fat, or Politics?" in *The Paleoanthropology and Archaeology of Big-Game Hunting*, Interdisciplinary Contributions to Archaeology, pp. 149–161, Springer New York, New York, NY, 2010.

[39] J. Ruiz-Carrascal, J. Ventanas, R. Cava, A. I. Andrés, and C. García, "Texture and appearance of dry cured ham as affected by fat content and fatty acid composition," *Food Research International*, vol. 33, no. 2, pp. 91–95, 2000.

[40] A. V. A. Resurreccion, "Sensory aspects of consumer choices for meat and meat products," *Meat Science*, vol. 66, no. 1, pp. 11–20, 2004.

[41] P. Konieczny, J. Stangierski, and J. Kijowski, "Physical and chemical characteristics and acceptability of home style beef jerky," *Meat Science*, vol. 76, no. 2, pp. 253–257, 2007.

[42] O. J. Mapesa, S. K. Mbugua, and S. M. Mahungu, "Sensory evaluation of dried beef strips treated with acetic acid or brine and monosodium glutamate," *Journal of Food Processing and Preservation*, vol. 34, no. 1, pp. 272–286, 2010.

[43] H.-J. Kim and I. A. Taub, "Specific degradation of myosin in meat by bromelain," *Food Chemistry*, vol. 40, no. 3, pp. 337–343, 1991.

[44] S. N. Albright, P. A. Kendall, J. S. Avens, and J. N. Sofos, "Pretreatment effect on inactivation of Escherichia coli O157:H7 inoculated beef jerky," *LWT- Food Science and Technology*, vol. 36, no. 4, pp. 381–389, 2003.

[45] S. Wibowo, L. Vervoort, J. Tomic et al., "Colour and carotenoid changes of pasteurised orange juice during storage," *Food Chemistry*, vol. 171, pp. 330–340, 2015.

[46] E. Marquez-Rios, V. M. Ocaño-Higuera, A. N. Maeda-Martínez, M. E. Lugo-Sánchez, M. G. Carvallo-Ruiz, and R. Pacheco-Aguilar, "Citric acid as pretreatment in drying of Pacific Lion's Paw Scallop (Nodipecten subnodosus) meats," *Food Chemistry*, vol. 112, no. 3, pp. 599–603, 2009.

[47] M. M. Farouk and J. E. Swan, "Boning and storage temperature effects on the attributes of soft jerky and frozen cooked free-flow mince," *Journal of Food Science*, vol. 64, no. 3, pp. 465–468, 1999.

[48] S.-W. Lee and C.-S. Kang, "Effects of moisture content and drying temperature on the physicochemical properties of ostrich jerky," *Nahrung-Food*, vol. 47, no. 5, pp. 330–333, 2003.

[49] Z. Cserhalmi, A. Sass-Kiss, M. Toth-Markus, and N. Lechner, "Study of pulsed electric field treated citrus juices," *Innovative Food Science & Emerging Technologies*, vol. 7, pp. 49–54, 2006.

Hindawi
Journal of Food Quality
Volume 2018, Article ID 4510242, 11 pages
https://doi.org/10.1155/2018/4510242

Research Article

Modification of Cell Wall Polysaccharides during Drying Process Affects Texture Properties of Apple Chips

Min Xiao,[1] Jianyong Yi,[1] Jinfeng Bi,[1] Yuanyuan Zhao,[1] Jian Peng,[1] Chunhui Hou,[1,2] Jian Lyu,[1] and Mo Zhou[1]

[1]*Institute of Food Science and Technology, Chinese Academy of Agricultural Science (CAAS), Key Laboratory of Agro-Products Processing, Ministry of Agriculture, Beijing 100193, China*
[2]*College of Food Engineering and Biotechnology, Tianjin University of Science & Technology, Tianjin 300457, China*

Correspondence should be addressed to Jianyong Yi; yijianyong_caas@yeah.net and Jinfeng Bi; bjfcaas@126.com

Received 28 October 2017; Accepted 5 February 2018; Published 29 March 2018

Academic Editor: Chung-Lim Law

The influences of hot air drying (AD), medium- and short-wave infrared drying (IR), instant controlled pressure drop drying (DIC), and vacuum freeze drying (FD) on cell wall polysaccharide modification were studied, and the relationship between the modifications and texture properties was analyzed. The results showed that the DIC treated apple chips exhibited the highest crispness (92) and excellent honeycomb-like structure among all the dried samples, whereas the FD dried apple chips had low crispness (10), the minimum hardness (17.4 N), and the highest volume ratio (0.76) and rehydration ratio (7.55). Remarkable decreases in the contents of total galacturonic acid and the amounts of water extractable pectin (WEP) were found in all the dried apple chips as compared with the fresh materials. The highest retention of WEP fraction (102.7 mg/g AIR) was observed in the FD dried apple chips, which may lead to a low structural rigidity and may be partially responsible for the lower hardness of the FD apple chips. In addition, the crispness of the apple chips obtained by DIC treatment, as well as AD and IR at 90°C, was higher than that of the samples obtained from the other drying processes, which might be due to the severe degradation of pectic polysaccharides, considering the results of the amounts of pectic fractions, the molar mass distribution, and concentrations of the WEP fractions. Overall, the data suggested that the modifications of pectic polysaccharides of apple chips, including the amount of the pectic fractions and their structural characteristics and the extent of degradation, significantly affect the texture of apple chips.

1. Introduction

Apple, one of the most cultivated and consumed fruits in China, is a significant part of the human diet. It has been identified as one of the main dietary sources of food antioxidants, mainly due to the phenolic compounds such as flavonoids and phenolic acids. These functional substances may contribute to the nutritional effects; for example, they could reduce risk of cancer, heart disease, and asthma [1]. From the health benefit point of view, a variety of technologies have been applied to develop different types of apple products, including apple juices, purees, and apple chips.

Since drying has been used as an effective method to process apples, a large number of studies have been focused on the qualities of dehydrated apple, such as color, flavor, taste, and texture, as well as nutrition and functionality. Among these quality aspects, texture is one of the vital organoleptic properties which is closely related to consumer acceptability. Complex physicochemical and biological reactions occur during drying process which could greatly affect the microstructure and texture of material tissues. To be specific, the volume of a material would decline continuously due to the loss of osmotic pressure caused by the evaporation of inner moisture. Additionally, the shrinkage of tissues is also related to the loss of vacuolar pressure and further damage to the integrity of cell wall, thus resulting in textural changes that could play an important role in the quality of dried fruit and vegetable products [2]. Generally, it is recognized that the microstructure and porosity of materials are the most important properties of dried food that affect its texture. Therefore, there are great interests in the development of methods to predict and control the texture of plant-based foods during

drying. The correlation between textural properties and the microstructure has also been the subject of many research efforts [3–5].

Texture is the result of complex interaction among food components relating to molecular, supramolecular, and the microstructural levels [6]. Plant cell wall and the middle lamella are known to control the way in which plant tissues undergo mechanical deformation and failure during mastication [7, 8]. The plant cell wall is made up of complex polysaccharides, phenolic compounds, and proteins stabilized by covalent and noncovalent (e.g., ionic) linkages. The cell wall of apples is generally depicted as a pectin-rich structure, containing high amounts of rhamnose [9]. Pectin is a complex polysaccharide which generally consists of three domains, that is, homogalacturonan (HG) (smooth region), rhamnogalacturonan-I (RG-I), and rhamnogalacturonan-II (RG-II) (hairy regions) [10]. The evolution of texture occurs during the processing of plant materials or some physiological events, which are related to the increased solubility of cell wall polysaccharides and the microstructure changes, such as the loss of the integrity in cell wall and middle lamella, changes on cell adhesion, and structural changes on pectin fraction.

Recently, the structural changes on cell wall polysaccharides during drying have also been reported for several fruits. The rehydration property of air-dried broccoli substantially affected by the amount and structure of cell wall pectin polysaccharides was reported [11]. Latorre et al. [12] claimed that microwave treatment modified the structure of cell wall polysaccharides in such a manner that produced an increase in their hydrophilicity. Yi et al. [13] studied the relationship between the modification in composition, structure, and extractability of cell wall polysaccharides and the alteration in volume expansion, microstructure, T_g, and rehydration behaviors, confirming that cell wall polysaccharide played a significant role in the physicochemical and physical properties of pitaya fruit chips. During sun-drying process, the molecular size distribution of water extractable pectin was affected by the degradation of arabinogalactan and arabinan side chains [14]. However, the impact of structural modification of cell wall polysaccharides on the texture of dehydrated fruits and vegetables is still obscure. A better understanding of the biochemical changes occurring during drying, and how these changes are related to texture variation, is expected to lead ultimately to a better process control and final product quality, valorisation, and acceptance.

The objective of this study was to investigate the effects of four different drying methods on the characteristics of cell wall polysaccharides of apple chips and to study the relationship between cell wall polysaccharides and texture of apple chips.

2. Materials and Methods

2.1. Sample Preparation. Apples (*Malus pumila* Mill var. Qin) were bought from the Xiaoying market in Beijing. Moisture content of fresh apple was 7.0 ± 0.3 kg/kg d.b. The peel was removed from the apples and they were cut into slices with 10 mm thickness and 20 mm diameter uniformly.

2.2. Methods

2.2.1. Drying Methods. Hot air drying (AD) was carried out using a convective dryer (DHG-9203, Yiheng Technical Co. Ltd., Shanghai, China). The dryer was loaded with 750 g (6.79 kg/m^2) of apple slices that were spread on a tray in single layer. The samples were flipped over during drying to avoid sticking to the tray and allow equal dehydration from all sides. Fresh apple slices were dried at 60°C, 75°C, and 90°C, respectively.

Infrared drying (IR) was operated using a laboratory medium- and short-wave infrared dryer (STC-5, Senttech Infrared Technology Co. Ltd., Jiangsu, China). The dryer consists of three infrared lights with powers of 0.48, 0.60, and 0.90 kW and wavelengths of 3.15, 3.10, and 1.40 μm, respectively. The samples were dried at 60°C, 75°C, and 90°C, respectively. The power density of IR process was 1.8 KW/kg, the air velocity was 2.11 m/s, and the distance from the emitters to the sample tray was 12 cm. For AD and IR drying, the moisture at equilibrium was measured when the weight of samples became constant. In this study, the drying times were 450 min, 300 min, and 250 min for AD at 60, 75, and 90°C, respectively, and 200, 120, and 100 min for IR at 60, 75, and 90°C, respectively.

Freeze drying (FD) was conducted using an experimental freezing dryer (Alphal-4L plus, Christ Col, Osterode am Harz, German) with a drying area of 0.42 m^2. Before freeze drying, the apple samples were prefrozen at −80°C for 12 h and then freeze-dried for 15 h [16]. The pressure was around 0.12 mbar with the condenser temperature of −56°C. The heating plate temperature was 35°C.

Instant controlled pressure drop (French: Détente Instantannée Contrôlée, DIC), also known as explosion puffing drying (EPD), was developed since 1988 [17, 18]. Prior to DIC treatment, samples were predried by AD at the same condition as the abovementioned AD drying. Apple chips were predried to the moisture content of 0.3 kg/kg w.b. by hot air drying at 70°C. After predrying, the samples were tightly wrapped in polyethylene bags and equilibrated in a thermostatic chamber at 20°C for 24 h. The above equilibrated semidried samples were removed to an experimental DIC dryer (QDPH10-1, Tianjin Qin-de New Material Scientific Development Co. Ltd., Tianjin, China), which was depicted in a previous study [13]. Prior to DIC treatment, the samples were equilibrated at 90°C for 10 min under the atmospheric pressure. Meanwhile, the vacuum tank was evacuated to approximate 3 kPa, producing enough vapor pressure, thus contributing to the expansion of the apple slices during the next stages of DIC drying. Then, the snuffle valves were opened to obtain an abrupt pressure drop to vacuum (around 3 kPa) in the treatment chamber, namely, instant pressure drop. Then, the apple slices were dried under a continuous vacuum at 65°C for 2 h. Each drying process was performed in triplicate.

2.2.2. Moisture Content. Moisture content was determined by drying the samples at 105°C until reaching constant weight [19].

2.2.3. Texture Analysis. The hardness and crispness of apple chips were measured by a TA-XT2i/50 Texture Analyzer (Stable Micro Systems Ltd., Surry, UK). A cylinder penetrometer probe (5 mm diameter) was used and the test parameters were set as follows: 2 mm/s of the prespeed and postspeed, 1 mm/s of the test speed, and 100 g trigger. In the test, hardness is the maximum force required to break the sample [17] and the crispness is characterized by the number of peaks [20]. Twelve measurements were performed for each treatment.

2.2.4. Volume Ratio (VR) and Rehydration Ratio (RR). The VR was measured using quartz sand displacement method [21]. VR was evaluated as volume change of apple cylinders affected by drying methods. The VR of dried apple chips can be determined by

$$\mathrm{VR} = \frac{V_m}{V_0}, \tag{1}$$

where V_0 and V_m are the initial and dried sample volumes, respectively.

The RR of dried products is one of important indications for the occurrence of physical and chemical changes during drying process due to drying conditions, pretreatment, and sample composition [22]. Five grams of dried samples was put in 50 mL distilled water in 250 mL beaker. Samples were taken out after 2 h and filter papers were used to wipe the excess water on the surface of the samples. The weights of the samples were recorded before and after rehydration. The RR was calculated according to

$$\mathrm{RR} = \frac{m_r}{m_0}, \tag{2}$$

where m_0 and m_r are the initial and dried sample weights, respectively.

2.2.5. Scanning Electron Microscopy (SEM). Microstructure characterization was performed using a scanning electron microscope (SEM S-570, Hitachi Ltd., Tokyo, Japan) at 150 kV accelerated voltage and 10–15 mm working distance. The microstructure of the samples was magnified 50 times.

2.2.6. Extraction of Cell Wall Polysaccharides and Fractionation. The cell wall polysaccharides of dried apple slices, namely, alcohol insoluble residue (AIR), were prepared following the procedure described by Gwanpua et al. [23]. About 30 g of dried apple chips was weighed and homogenized in 180 mL of 95% ethanol using a mixer (Joyoung Co. Ltd., Shandong, China). The residue was filtered and resuspended in 90 mL of 95% ethanol. The insoluble cell wall fraction was washed with 90 mL of acetone and filtered. To obtain AIR, the suspension was dried at 40°C for 36 h. AIR fractionation was performed according the procedure of Christiaens et al. [24]. For water extractable pectin (WEP), 1.0 g AIR samples were weighed exactly and suspended in 180 ml boiling water for 5 min. The solution was cooled and filtered using a filter paper (Machery-Nagel, MN615, 90 mm) and then adjusted to 200 mL with distilled water. The residue was further fractionated in 180 mL, 0.05 mol/L cyclohexane-trans-1,2-diamine tetraacetic acid (CDTA) in 0.1 mol/L potassium acetate (PH 6.5) for 6 h at 28°C in a shaking water bath. The solution was adjusted to 200 mL with distilled water, which was labeled as CDTA extractable pectin (CEP). The residue was sequentially incubated in 180 mL 0.05 mol/L Na_2CO_3 containing 0.02 mol/L $NaBH_4$ and stirred for 16 h at 4°C. The solution was filtered and the filtrate was adjusted to 200 mL. The filtration of the suspension was designated as Na_2CO_3 extractable pectin (NEP). All extracts were filtered, dialyzed exhaustively in distilled water, and finally lyophilized [25]. The samples were stored in a desiccator over P_2O_5.

2.2.7. Galacturonic Acid (GalA) Content. The AIRs and the corresponding fractions obtained thereof (WEP, CEP, and NEP) were first hydrolyzed using concentrated sulfuric acid (95–98%) according to the method described by Ahmed and Labavitch [26]. GalA contents of the hydrolyzates were measured by a colorimetric hydroxyl-phenyl-phenol method using a UV/Vis spectrophotometer (UV1800, Shimadzu, Kyoto, Japan) at 520 nm, according to the procedure by Blumenkrantz and Asboe-Hansen [27]. The GalA content measurement was conducted in triplicate.

2.2.8. Degree of Methoxylation (DM). The DM of the fractions of the AIR fractions were calculated as the ratio of the molar amount of methoxy groups to the molar amount of GalA content and expressed as a percentage. Before the measurement of the concentration of methanol, 20 mg of each dried AIR faction was weighed and was first hydrolyzed according to the description of Ng and Waldron [28]. The amount of methanol was spectrophotometrically determined by the method of Klavons and Bennett [29]. Determination of DM was conducted in triplicate.

2.2.9. Neutral Sugar Composition. Analyses of neutral sugars including fucose (Fuc), rhamnose (Rha), arabinose (Ara), galactose (Gal), and xylose (Xyl) were performed using the method described by Njoroge et al. [30]. Five grams of lyophilized AIR fractions (i.e., WEP, CEP, and NEP) was hydrolyzed with 0.5 mL 4 mol/L trifluoroacetic acid for 1.5 h at 110°C. After cooling and evaporation of the trifluoroacetic acid, samples were diluted with demineralized water to a concentration of 1 mg/mL. Quantification of the neutral sugars of the fractions was performed via high-performance anion exchange chromatography (HPAEC) using a Dionex Bio-LC System including a quaternary gradient pump (Dionex Bio-LC System, Dionex Co., Sunnyvale, CA, USA). An ED_{50} electrochemical detector equipped with a gold electrode was used in the pulsed amperometric detection mode, performing a quadruple potential waveform. After equilibration of the system for 5 min with 100 mmol/L NaOH and 5 min with 4 mmol/L NaOH, the diluted hydrolyzate (10 μL) was eluted at 30°C on a CarboPac PA20 column (Dionex) with 4 mmol/L NaOH at a flow rate of 0.5 mL/min. Thereafter, column wash was performed for 10 min with 500 mmol/L NaOH. Commercial neutral sugar standards were used for identification and quantification. Correction for degradation of monosaccharide during acid hydrolysis was performed

Table 1: Moisture content, hardness, crispness, volume ratio, and rehydration ratio of the dried apple chips obtained by different drying methods.

Drying method	Drying condition	*Moisture content ($\times 10^{-2}$ kg/kg, d.b.)	Hardness (N)	Crispness	Volume ratio	Rehydration ratio
AD	60°C	8.30 ± 0.01^{d}	86.9 ± 8.1^{d}	4 ± 1^{a}	0.19 ± 0.00^{a}	4.56 ± 0.18^{a}
	75°C	6.50 ± 0.01^{bc}	43.7 ± 4.7^{b}	38 ± 3^{b}	0.21 ± 0.01^{ab}	4.95 ± 0.11^{b}
	90°C	5.76 ± 0.50^{ab}	43.4 ± 5.6^{b}	74 ± 10^{c}	0.21 ± 0.03^{b}	4.99 ± 0.10^{b}
IR	60°C	7.03 ± 0.11^{c}	57.7 ± 3.6^{c}	5 ± 1^{a}	0.19 ± 0.00^{a}	4.82 ± 0.10^{ab}
	75°C	5.95 ± 0.13^{abc}	50.3 ± 2.5^{bc}	69 ± 7^{c}	0.21 ± 0.03^{ab}	5.08 ± 0.13^{b}
	90°C	5.72 ± 0.21^{ab}	53.5 ± 2.0^{bc}	74 ± 6^{c}	0.25 ± 0.01^{ab}	5.04 ± 0.18^{b}
FD		5.29 ± 0.23^{ab}	17.4 ± 1.8^{a}	10 ± 3^{a}	0.76 ± 0.01^{d}	7.55 ± 0.09^{d}
DIC		5.03 ± 0.51^{a}	44.4 ± 2.3^{bc}	92 ± 4^{d}	0.31 ± 0.01^{c}	5.48 ± 0.35^{c}

Results are presented as mean values ± standard deviation of triplicate tests. Samples in the same column with different letters differ significantly at $p < 0.05$.
∗ represents the moisture content of dried apple slices produced by different drying methods.

by the estimation of recovery values [31]. Measurement of neutral sugar compositions was conducted in duplicate.

2.2.10. Molecular Mass Distribution. Molar mass analysis was performed according to the method described by Yang et al. [32]. Dialyzed and lyophilized fraction (3.0 mg) was dissolved in 1 mL of 0.1 mol/L 4-morpholineethanesulfonic acid monohydrate buffer solution (MES), pH 6.5, containing 0.1 mol/L NaCl. Molar mass distribution was determined using a high-performance size exclusion chromatography (HPSEC) coupled with multiangle laser light scattering (Malls, Dawn-EOS, Wyatt Tech. Co., Santa Barbara, USA) and refractive index (RI) detector (OptiLab-DSP, Wyatt Tech. Co., Santa Barbara, USA). The abovementioned solution sample (100 μL) was injected and separated by a TSK-Gel G3000SW$_{XL}$ column (7.8 mm × 300 mm) (Tosoh Co., Tokyo, Japan), eluting with 0.1 mol/L MES buffer (pH 6.5) containing 0.1 mol/L NaCl at flow rate of 0.45 mL/min at 35°C. RI intensity and light scattering intensity at different angles were used to calculate cell wall polysaccharide concentration and molar mass distribution, respectively [33].

2.2.11. Statistical Analysis. Statistical analysis of the experimental data was conducted by using SPSS Statistics (Version 17.0, SPSS Inc., Chicago, USA), applying one-way analysis of variance (ANOVA) and Duncan's multiple range tests. Significant differences were defined at $p < 0.05$.

3. Results and Discussion

3.1. Physicochemical Properties. The effects of drying methods and drying temperature on hardness, crispness, water content, volume ratio (VR), and rehydration ratio (RR) of dried apple chips are presented in Table 1. The moisture contents of the samples dried under different conditions ranged from 5.03 to 8.30 × 10^{-2} kg/kg d.b. The hardness of the apple chips was reduced and the crispness was increased as rising of the drying temperature of AD and IR process; such behavior was reported in few similar studies regarding constant temperature drying of bulbus of *Tulipa edulis* [34] and air drying of bell pepper [35]. FD dried samples had the minimum value in hardness (17.4 N) and low crispness (10). Several earlier studies also reported that samples produced using hot air drying were characterized as having higher hardness when compared to freeze drying ([36], Giri et al. 2006). This phenomenon was probably because higher temperature accelerates removal of water from the tissues, but also results in case hardening [37]. Besides, the capillary force which causes water removal and loss of turgor pressure in the cell during HAD resulted in more severe shrinkage than in the process of FD, during which process the material was frozen and the structure became more rigid without collapse [36]. It is worthy to note that the DIC treated apple chips represented the highest crispness value (92) and a modest hardness value (44.4 N). Conversely, the highest hardness (86.9 N) and lowest crispness (4) were observed in the treatment of AD 60°C. This might be attributed to the hard and dry crust formed in the surface area and the shrinkage of the tissue, due to the rate of inner water transferring to the surface being limited during AD at 60°C. The volume ratio (VR) of the samples dried by all the selected drying methods is smaller than 1.0, suggesting that all of the drying processes would lead to shrinkage for apple slices. The VR of the FD dried samples (0.76) was the highest, followed by the DIC finished samples (0.31), and the samples dried by AD at 60°C and IR at 60°C had the lowest VR, which were both 0.19. The highest VR of the FD dried samples may be due to the maintaining of freezing or solid state of the samples throughout the FD process. During FD process, the ice was sublimated in the vacuum and frozen condition; then the homogeneous voids were left within the structure [38]. As expected, the VR of the DIC treated samples was significantly smaller than that of the FD dried samples. However, for the DIC treatment, though the compact structure could be substantially expanded after instant pressure drop, it still cannot compromise the shrinkage that occurred during the stage of hot air predrying (Mounir et al. 2012), because the cellular structure of the materials and the rigid cell wall networks supporting the plant tissue might be irreversibly damaged by the predrying treatment. On the other hand, during the cooling period of DIC treatment, slight shrinkage may occur due to the viscoelastic behavior of the material.

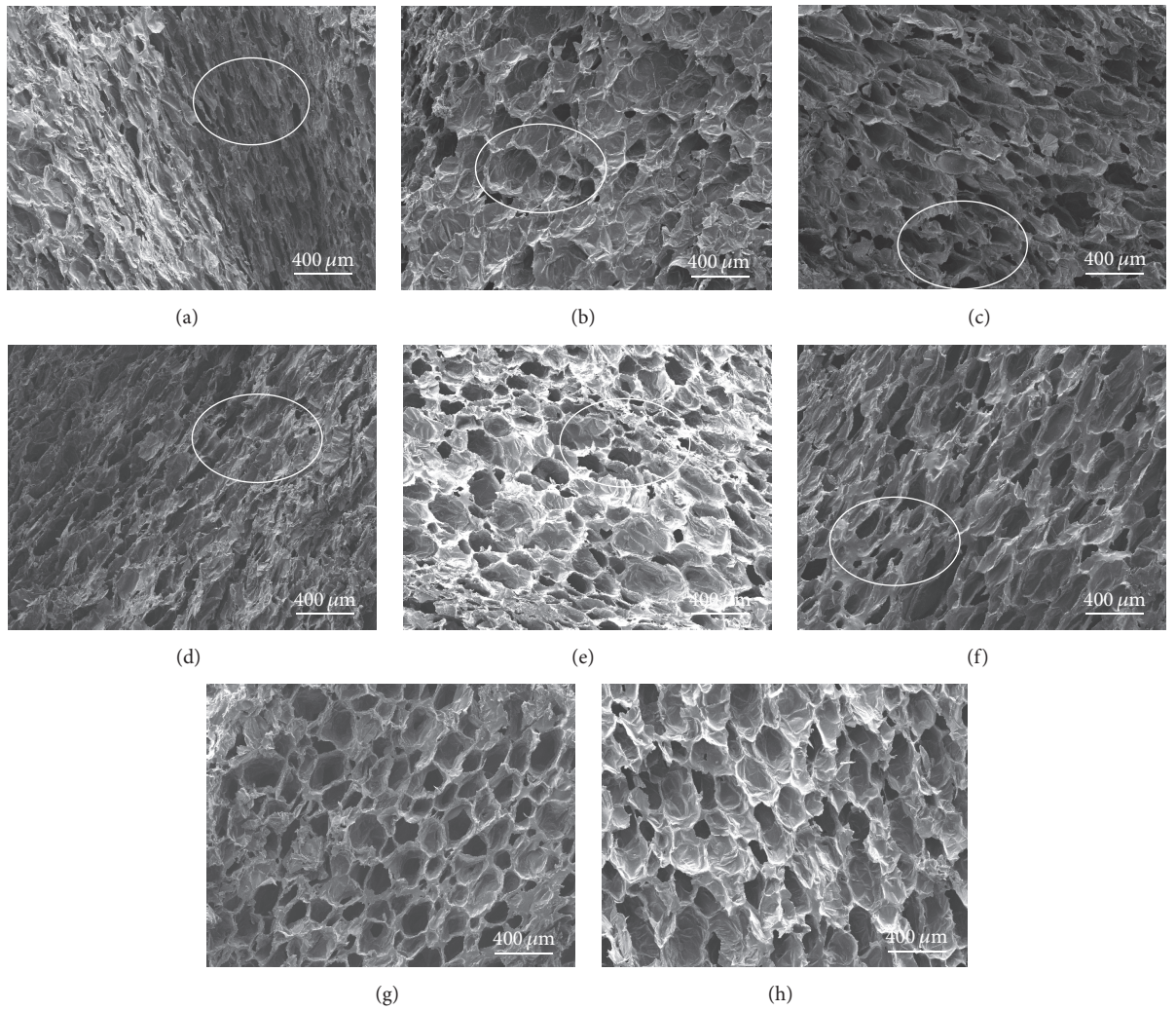

Figure 1: Microstructures of the apple chips dried by hot air drying (AD), medium- and short-wave infrared drying (IR), instant controlled pressure drop drying (DIC), and freeze drying (FD) (×50). (a) AD 60°C, (b) AD 75°C, (c) AD 90°C, (d) IR 60°C, (e) IR 75°C, (f) IR 90°C, (g) FD, and (h) DIC. The white circles added in (a), (b), and (c) were used to point the microstructure changes of apple chips, as well as in (d), (e), and (f).

Generally, during the stage of dropping in temperature of DIC drying, the material evolved from high temperature-high moisture state towards a low temperature-low moisture state; then, the state of the product could transfer from rubber state to vitreous state [39]; as a result, the new expanded structure can be maintained during the following vacuum drying [40]. Both the VR of the apple chips dried by AD and IR were lower than those of FD and DIC treated samples, and no significant differences in VR were observed between the samples dried by AD and IR at the same temperature. In addition, the VR of the apple chips dried by AD or IR showed an increasing trend with increasing of drying temperature. The smaller shrinkage for apple slices that dried at relatively higher temperature might be ascribed to the fact that apple slices took a shorter time for drying as the temperature and water diffusivity were high [41].

The rehydration ratio (RR) of the FD dried apple chips was 7.55 (Table 1), which was significantly higher than that of the samples dried by the other drying methods, followed by that of DIC samples (5.48). The fact that higher RR was found in the FD and DIC dried samples was due to the homogenous porous structure and big specific surface area of the samples, which allowed a large amount of water molecules to be absorbed during rehydration [42]. The AD and IR dried apple chips showed the minimum of RR, which ranged within 4.56–4.99 and 4.82–5.08, respectively. This could be explained by the hard crust on the outer layer and smaller number of pores inside the samples. Unlike VR, the RR of the samples dried by AD and IR showed a trend that it decreased with increase of the drying temperature.

3.2. Microstructure. The microstructure of dried apples produced by different drying methods was observed by scanning electron microscope to further analyze the texture characteristic of the dried apples chips (Figure 1). There was no pronounced difference between the microstructures of the

Table 2: Effect of drying methods on the galacturonan acid contents of water extractable pectin (WEP), CDTA extractable pectin (CEP), and Na_2CO_3 extractable soluble pectin (NEP) of the apple chips obtained by different drying methods.

Drying method	Drying condition	Galacturonan acid (mg/g AIR)			
		WEP	CEP	NEP	Total GalA
AD	60°C	86.9 ± 2.8^{d}	41.5 ± 0.1^{b}	75.0 ± 6.0^{e}	203.4
	75°C	74.6 ± 1.8^{c}	40.3 ± 1.7^{b}	65.1 ± 5.2^{d}	180.0
	90°C	33.8 ± 5.8^{a}	47.3 ± 4.2^{c}	45.8 ± 5.2^{b}	126.9
IR	60°C	85.0 ± 0.9^{d}	37.9 ± 1.2^{ab}	53.4 ± 2.0^{bc}	176.3
	75°C	75.3 ± 3.2^{c}	36.0 ± 0.1^{ab}	61.0 ± 1.6^{cd}	172.3
	90°C	65.4 ± 2.1^{b}	71.0 ± 4.2^{e}	61.5 ± 3.0^{cd}	197.9
FD		102.7 ± 1.8^{e}	38.8 ± 1.1^{b}	33.6 ± 7.3^{a}	174.4
DIC		64.2 ± 0.8^{b}	56.1 ± 2.9^{d}	51.8 ± 1.9^{b}	171.9
Fresh		112.7 ± 0.9^{f}	32.0 ± 2.8^{a}	73.4 ± 1.4^{e}	218.1

Results are presented as mean values ± standard deviation of triplicate tests. Samples in the same column with different letters differ significantly at $p < 0.05$.

AD and IR dried samples at the same drying temperature. As the white circles point in Figures 1(a) and 1(d), among these samples, dense areas were observed in the apple chips dried by AD at 60°C and IR at 60°C, revealing significant collapse of tissues after the drying process, thus expecting harder texture and lower RR for these samples. With increasing of the drying temperature for AD (Figures 1(a)–1(c)) and IR (Figures 1(d)–1(f)) process, typical porous structure was formed apparently, which could be attributed to the enhanced water-removing rate at the elevated temperature. Moreover, obvious honeycomb-like network and superior porous structure were observed in both the FD and DIC treated samples, pointing to limited shrinkage for the cellular and tissue structure of the apple slices. In addition, it is suggested that the differences in the microstructure of the apples derived from various drying methods could be related to the modification of its chemical constitution and functionality of middle lamella, affecting cellular adhesive properties [43] and thus the texture of the dried apple chips.

3.3. Galacturonic Acid Contents. As GalA is dominant pectic saccharide in the AIR of apple; the amount of GalA found in AIR was estimated to evaluate the amount of pectin in each fraction of AIR. Table 2 summarizes the amount of GalA in different fractions (WEP, CEP, and NEP) of the apple chips dried by various methods. The contents and proportions of WEP, CEP, and NEP varied from drying methods and drying conditions ($p < 0.05$). The contents of the WEP, CEP, and NEP extracted from the fresh apples were 112.7 mg/g AIR, 32.0 mg/g AIR, and 73.4 mg/g AIR, respectively. The contents of the total GalA and WEP of the dried samples (126.9–203.4 mg/g AIR, 33.8–102.7 mg/g AIR) were lower than those of the fresh samples (218.1 mg/g AIR, 112.7 mg/g AIR), while the amount of the CEP fraction was higher. The deviation in total GalA might be partially due to the conversion among different fractions of pectin during the different drying process. In addition, it is supposed that the ratio or efficiency of pectin extraction could be affected by the differences of the microstructure of the apple chips, illustrated above (Figure 1).

The amount of WEP for AD and IR dried samples decreased with increasing of drying temperature, while the CEP contents increased. This might be explained by the fact that leaching of WEP occurred with certain amount of fluid flowing out of the tissue during the drying process or partially converted into CEP fraction. The amount of WEP of the apple chips dried by AD at 90°C, IR at 90°C, and DIC significantly decreased compared with the fresh samples. This was consistent with the result that degradation of WSP and leaching occurred in the drying process with high temperature [44]. The decrease of cell wall macromolecules, for example, pectic polysaccharides, might lead to decrease in T_g of the matrix [45]. For the DIC treated sample, the drying temperature was higher than T_g; therefore, the apple slices entered a viscoelastic state (Welti-Chanes et al. 1999) during the equilibrium process. Due to the high viscoelasticity and plasticity, porous structure was formed when instant pressure drop treatment was introduced. With the moisture content decreased, the products changed from rubbery state to glassy state [39], contributing to the preservation of the expanding and porous structure, thus resulting in superior porous microstructure. In addition, relatively low amount of WEP was found in the DIC treated sample, implying that limited amount of soluble pectin existed for this sample. This could be in favor of cell separation during expansion [46]. The FD dried apple chips exhibited the highest content of WEP fraction (102.7 mg/g AIR) among the selected drying methods. The apple slices were quickly frozen before sublimation, and the matrix stayed in frozen or solid state throughout the FD process. Consequently, the leaching of WEP was avoided during the FD process, and the WEP fraction was well retained, whose amount is comparable to the fresh samples. The relatively high amount of WEP in the FD dried sample might partially contribute to the low mechanical strength and the minimum hardness of the products. This may be due to the fact that the WEP is generally made up of high esterified pectic polymers, loosely bound to the cell wall through noncovalent and nonionic bonds, and it could be one of the explanations that FD apple chips presented the highest rehydration ratio [30].

Table 3: Effect of drying methods on the degree of methoxylation of water extractable pectin (WEP), CDTA extractable pectin (CEP), and Na_2CO_3 extractable pectin (NEP) from dehydrated apple chips obtained by different drying methods.

Drying method	Drying condition	Degree of methoxylation (%)		
		WEP	CEP	NEP
AD	60°C	59.7 ± 3.2^{a}	37.6 ± 3.6^{bcd}	1.3 ± 0.0^{bcd}
	75°C	60.5 ± 0.7^{ab}	34.6 ± 0.1^{bc}	1.2 ± 0.3^{bc}
	90°C	71.8 ± 0.7^{cd}	24.86 ± 1.2^{a}	0.7 ± 0.0^{ab}
IR	60°C	66.2 ± 1.8^{bc}	43.4 ± 0.9^{d}	2.0 ± 0.1^{de}
	75°C	72.4 ± 1.8^{cd}	40.2 ± 1.2^{cd}	0.9 ± 0.1^{b}
	90°C	73.2 ± 6.2^{d}	17.5 ± 5.1^{a}	0.1 ± 0.0^{a}
FD		80.8 ± 0.7^{e}	33.8 ± 0.1^{bc}	5.0 ± 0.8^{f}
DIC		77.5 ± 2.0^{f}	23.3 ± 0.4^{a}	2.3 ± 0.2^{d}
Fresh		69.8 ± 0.6^{cd}	36.4 ± 5.8^{bcd}	1.7 ± 0.3^{cde}

Results are presented as mean values ± standard deviation of triplicate tests. Samples in the same column with different letters differ significantly at $p < 0.05$.

3.4. Degree of Methoxylation. The DM of pectin, a key functional parameter, was estimated as the ratio of the molar amount of methanol groups to the molar amount of GalA. The DM affects the hydrogen bonding between pectin molecular interactions and might also influence the texture of dried fruits and vegetable. The DM of the WEP, CEP, and NEP fractions are represented in Table 3. Generally, the DM of the WEP fraction was the highest (59.7%–80.8%), followed by the CEP fraction (17.5%–43.4%) and NEP fraction (0.1%–5.0%). This observation was corresponding to the fact that the NEP was extracted from the AIR using aqueous Na_2CO_3, a reagent that broke various types of ester linkages [47]. It was found that the DM of the WEP fraction increased with increasing of the temperature for AD and IR. This might be ascribed to the inactivation of pectin methylesterase at higher temperature; thus de-esterification was limited at drying temperature of 75°C and 90°C compared with drying at 60°C. On the contrary, the DM of the CEP fractions displayed an opposite trend. It could be due to the consequence of de-esterification of the WEP fraction, which might be partially cross-linked with free divalent ionic and thus transferred to CEP factions. In addition, CEP fractions with low DE would contain more carboxyl groups, with higher amount of crosslinking with metal ions such as Ca^{2+} [48], and such effects could contribute to the rigidity of the microstructure of apple chips. This could be a partial explanation for the fact that the crispness of the apple chips obtained by AD at 90°C, IR at 90°C, and DIC was higher than that by the other drying methods, and vice versa for the hardness.

3.5. Sugar Ratio. Pectin is a kind of cell wall polysaccharide that mainly consists of a linear chain of covalently linked galacturonic acid. Various amounts of neutral sugars are attached to these regions as side chains, including fucose, rhamnose, arabinose, galactose, and xylose. Based on the amount and linkage types of side chains, pectin is generally described as homogalacturonan (HG), rhamnogalacturonan-I (RG-I), and rhamnogalacturonan-II (RG-II) [10]. In general, HG is composed of a linear chain of (1,4)-linked-*D*-galacturonic acid. RG-I consists of repeats of disaccharide (1,2)-*α*-*L*-rhamnose-(1,4)-*α*-*D*-galacturonic acid. RG-II is a branched pectic domain containing an HG backbone. The use of "sugar ratios" can help to interpret the sugar information on the polymeric level. Sugar ratios 1, 2, and 3 are formulated specifically for pectin, assuming a linear pectin structure, in which the backbones of RG-I and RG-II are continuous with the linear HG structure [49]. As shown in Table 4, the amount of GalA to neutral sugars in side chains (sugar ratio 1) can be an indication for the linearity of pectin; sugar ratio 2 is embodied by the ratio of Rha to GalA, a measurement for the contribution of RG to the entire pectin population. The proportion of RG-I side-chain sugars to Rha (sugar ratio 3) is indicative for the extent of branching of RG-I [15]. The linearity of the WEP and CEP fractions of the fresh samples was 13.62 and 26.63, respectively. The linearity of the WEP of the dried apple slices was lower than that of the fresh samples, and the opposite was found in the CEP fractions. Meanwhile, in the case of AD and IR dried samples, the linearity of the WEP decreased with increasing of the temperature, while CEP showed the opposite trend, implying fraction on the WEP backbone and side chain of the CEP fractions. In addition, based on the fact that the amount of WEP fraction was reduced after drying, it is speculated that significant degradation of the pectic polysaccharides occurred during drying process, and these residues with small molecular mass might not be included in the WEP fraction after extraction process. It can be observed that the sugar ratio 2 of the WEP, CEP, and NEP fraction from all of the samples was small, ranging from 0.01 to 0.04, indicating that the proportion of RG is small for apple pectic polysaccharides. The WEP exhibited the highest extent of RG-I branching (sugar ratio 3) among all the pectic fractions, ranging from 6.87 to 10.31, indicating that the WEP fractions were loosely bound to the cell wall and thus were extracted by a relatively moderate condition.

3.6. Molar Mass Distribution. Figure 2 illustrates the molar mass distribution and concentration profiles of the cell wall polysaccharides in the WEP fractions of the apple chips. The molar mass distributions of the cell wall polysaccharides extracted from different samples were similar for all the WEP fractions of different samples. The MALLS and RI signals

Table 4: Effect of drying methods on sugar ratios of water extractable pectin (WEP), CDTA extractable pectin (CEP), and Na_2CO_3 extractable pectin (NEP) from dehydrated apple chips obtained by different drying methods.

	Sugar ratio	AD			IR			FD	DIC	Fresh
		60°C	75°C	90°C	60°C	75°C	90°C			
WEP	1	11.83	10.35	6.05	12.35	9.24	7.02	7.19	5.64	13.62
	2	0.01	0.01	0.01	0.01	0.01	0.01	0.02	0.02	0.01
	3	10.31	8.50	9.78	9.05	8.79	9.80	6.87	6.92	7.18
CEP	1	37.05	35.02	44.27	30.76	31.27	49.42	27.03	33.55	26.63
	2	0.00	0.01	0.00	0.00	0.01	0.00	0.01	0.00	0.01
	3	5.61	4.42	5.90	5.62	4.28	4.31	4.21	3.98	5.12
NEP	1	13.54	8.67	6.04	10.78	9.86	6.76	3.79	6.56	5.65
	2	0.01	0.02	0.02	0.01	0.01	0.02	0.04	0.03	0.03
	3	3.84	3.88	4.90	3.35	4.87	4.97	3.74	3.21	4.65

Note. Sugar ratio 1 = GalA/(Fuc + Rha + Ara + Xyl), representing the linearity of pectin; sugar ratio 2 = Rha/Gala, representing the contribution of RG to pectin population; sugar ratio 3 = (Ara + Gal)/Rha, representing the branching of RG-I [15].

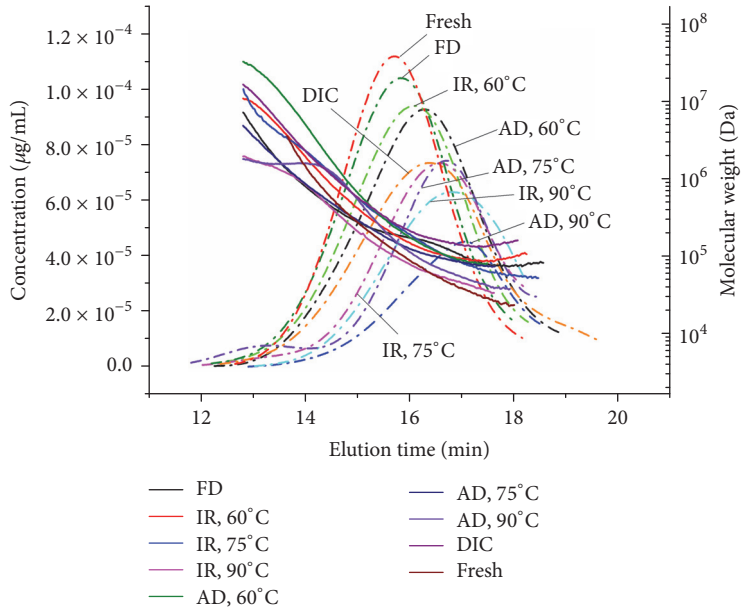

Figure 2: Molar mass distribution of the water extractable pectins of the apple chips dried by hot air drying (AD), medium- and short-wave infrared drying (IR), instant controlled pressure drop drying (DIC), and vacuum freeze drying (FD). Solid lines indicate molecular weight of the WEP fraction, and dash-dotted lines indicate the concentration of the WEP fraction.

of CEP fractions were low; thus the data were not shown. The elution times of the WEP fractions of the fresh samples and FD dried chips (around 15.5–15.7 min) were generally shorter than those of the AD, IR, and DIC dried samples, suggesting that the molar mass of WEP fraction from fresh and FD dried samples was higher than that from other samples. The data corroborated that limited degradation and de-esterification occurred during FD drying process, which contributed to its higher amount of water extractable pectic polysaccharides with high DM (Tables 2 and 3). Interestingly, peak shifting to longer elution times in the WEP fractions was observed with increasing of the drying temperature for AD and IR process, together with the apparent decrease in the concentrations of the samples. It implied that the extent of cell wall polysaccharide degradation was raised correspondingly. Moreover, the elution times of the peaks for AD dried products were generally longer than those of the IR dried chips at the same drying temperature. The corresponding concentrations of the AD dried products were generally lower than those of the IR dried products, which was consistent with the results of the amounts of WEP fraction (Table 2). This phenomenon might be attributed to the longer drying time for the AD process compared with IR process when performed at the same drying temperature. For the DIC treated apple chips, significant decrease in molar mass was also found.

The modifications in cell wall polysaccharides could affect the physicochemical and physical properties of the apple

chips. Firstly, the occurrence of polysaccharide depolymerization and the modification of cell wall polysaccharide intermolecular interactions (Table 2) suggested that cell wall polysaccharide network might be disorganized and misaligned to certain extent due to the drying process. This might damage the integrity of the primary cell wall and/or middle lamella of apple slices, leading to the decrease in the strength of intercellular adhesion. Consequently, the reduction in intercellular adhesion strength might be in favor of tissue/cell separation and reduce the internal structural resistance for volume expansion during instant pressure drop treatment or AD and IR drying at elevated temperature, that is, 90°C. This, consequently, could contribute to a more porous microstructure as well as a crispier texture for the apple chips. Secondly, polysaccharide degradation could provide higher amounts of pectic residues with smaller molecular mass, leading to a better hydrophilicity for cell wall polysaccharides, which was a partial explanation for the improvement of rehydration rate and capacity. This was in good agreement with the report of Latorre et al. [12], who found that the modification of cell wall polysaccharide structure induced by microwave drying led to a significant increase in the hydrophilicity of cell wall polysaccharide. In addition, the superior porous microstructure in the DIC treated samples, as well as the AD and IR (90°C) dried sample, could facilitate a faster capillary suction during immersing, which was another reason for their superior rehydration properties (Table 1). On the other hand, cell wall polysaccharide depolymerization produced chemical residues with smaller molecular mass, which could increase the molecular mobility of a system, thus decreasing the glass transition point (T_g) of the matrix. Moreover, the damage and misalignment of cell wall polysaccharide network might liberate part of structural polysaccharides from cell wall, which could also increase molecular mobility and contribute to decreasing T_g, and these effects might bring adverse effects for volume expansion. Overall, data from the results of the texture and microstructure (Table 1 and Figure 1), as well as the amount of pectic fractions, DM, and the sugar ratios (Tables 2, 3, and 4) suggested that the modifications of cell wall polysaccharides induced by the drying process significantly contributed to the final texture of apple chips.

4. Conclusions

Apple chips were produced by AD, IR, FD, and DIC, respectively. The influences of the modification in the extractability, composition, and structure of cell wall polysaccharide induced by various drying processes on the volume expansion, microstructure, rehydration behavior, and so on suggested that cell wall polysaccharides modification played a significant role in the texture properties of the apple chips. The amounts and structural properties of the WEP and CEP fractions obviously related to the texture properties of the dried samples. Based on the data, the apple chips exhibited higher crispness and better microstructure when there was less amount of WEP fraction, which might be partially attributed to depolymerization and leaching of the pectic polysaccharides. Cell wall polysaccharide degradation was in favor of volume expansion during instant pressure drop treatment, as well as AD and IR drying at elevated temperatures, consequently, contributing to a superior porous structure and crispier texture. Since cell wall polysaccharides are a nonnegligible factor affecting the formation and hardening of the porous structure for dried products, the influences of cell wall polysaccharide modification during different stages of drying process, for example, pretreatment, predrying, DIC, and final drying, on texture evolution can be better understood by further study using model system.

Additional Points

Practical Applications. Nowadays, a rapid increase in the fruit and vegetable chips is witnessed because of their health benefits. Instant controlled pressure drop drying (DIC) is one of the available industrial technologies for producing fruit and vegetable chips. Currently, apple chips are the main products in the Chinese market due to their crispy texture and pleasant flavor. However, the texture of apple chips is unstable during industrial manufacturing due to limited information about the fundamentals of texture evolution, which, except for the final microstructure and moisture content, is supposed to be related to pectic polysaccharides. Therefore, better understanding of the relationship between the texture of apple chips and the modification of pectic polysaccharides could be helpful to guarantee excellent crispy texture of the products.

Conflicts of Interest

The authors declare that they have no conflicts of interest.

Acknowledgments

The authors acknowledge the National Key R&D Program of China (2016YFD0400700 and 2016YFD0400704).

References

[1] D. A. Hyson, "A comprehensive review of apples and apple components and their relationship to human health," *Advances in Nutrition*, vol. 2, no. 5, pp. 408–420, 2011.

[2] M. U. Joardder, A. Karim, C. Kumar, and R. J. Brown, "Effect of cell wall properties of plant tissue on porosity and shrinkage during drying," in *1st International Conference on Food Properties*, Kuala Lumpur, Malaysia, 2014.

[3] J.-Y. Yi, L.-Y. Zhou, J.-F. Bi, P. Wang, X. Liu, and X.-Y. Wu, "Influence of number of puffing times on physicochemical, color, texture, and microstructure of explosion puffing dried apple chips," *Drying Technology*, vol. 34, no. 7, pp. 773–782, 2016.

[4] A. Vega-Gálvez, L. Zura-Bravo, R. Lemus-Mondaca et al., "Influence of drying temperature on dietary fibre, rehydration properties, texture and microstructure of Cape gooseberry (Physalis peruviana L.)," *Journal of Food Science and Technology*, vol. 52, no. 4, pp. 2304–2311, 2015.

[5] M. Akbarian, B. Ghanbarzadeh, M. Sowti, and J. Dehghannya, "Effects of pectin-CMC-based coating and osmotic dehydration pretreatments on microstructure and texture of the hot-air

dried quince slices," *Journal of Food Processing and Preservation*, vol. 39, no. 3, pp. 260–269, 2015.

[6] V. Singh, N. Guizani, A. Al-Alawi, M. Claereboudt, and M. S. Rahman, "Instrumental texture profile analysis (TPA) of date fruits as a function of its physico-chemical properties," *Industrial Crops and Products*, vol. 50, pp. 866–873, 2013.

[7] D. J. Karakurt, "Cell wall-degrading enzymes and pectin solubility and depolymerization in immature and ripe watermelon (Citrullus lanatus) fruit in response to exogenous ethylene," *Physiologia Plantarum*, vol. 116, no. 3, pp. 398–405, 2002.

[8] D. N. Sila, T. Duvetter, A. De Roeck et al., "Texture changes of processed fruits and vegetables: potential use of high-pressure processing," *Trends in Food Science & Technology*, vol. 19, no. 6, pp. 309–319, 2008.

[9] J. P. Moore, J. M. Farrant, and A. Driouich, "A role for pectin-associated arabinans in maintaining the flexibility of the plant cell wall during water deficit stress," *Plant Signaling and Behavior*, vol. 3, no. 2, pp. 102–104, 2008.

[10] D. N. Sila, S. Van Buggenhout, T. Duvetter et al., "Pectins in processed fruits and vegetables: part II—structure-function relationships," *Comprehensive Reviews in Food Science and Food Safety*, vol. 8, no. 2, pp. 86–104, 2009.

[11] A. Femenia, M. J. Bestard, N. Sanjuan, C. Rosselló, and A. Mulet, "Effect of rehydration temperature on the cell wall components of broccoli (Brassica oleracea L. Var. italica) plant tissues," *Journal of Food Engineering*, vol. 46, no. 3, pp. 157–163, 2000.

[12] M. E. Latorre, M. F. de Escalada Plá, A. M. Rojas, and L. N. Gerschenson, "Blanching of red beet (Beta vulgaris L. var. conditiva) root. Effect of hot water or microwave radiation on cell wall characteristics," *LWT- Food Science and Technology*, vol. 50, no. 1, pp. 193–203, 2013.

[13] J. Yi, L. Zhou, J. Bi, Q. Chen, X. Liu, and X. Wu, "Impacts of pre-drying methods on physicochemical characteristics, color, texture, volume ratio, microstructure and rehydration of explosion puffing dried pear chips," *Journal of Food Processing and Preservation*, vol. 40, no. 5, pp. 863–873, 2016.

[14] M. A. Asgar, R. Yamauchi, and K. Kato, "Structural features of pectins from fresh and sun-dried Japanese persimmon fruit," *Food Chemistry*, vol. 87, no. 2, pp. 247–251, 2004.

[15] K. Houben, R. P. Jolie, I. Fraeye, A. M. Van Loey, and M. E. Hendrickx, "Comparative study of the cell wall composition of broccoli, carrot, and tomato: structural characterization of the extractable pectins and hemicelluloses," *Carbohydrate Research*, vol. 346, no. 9, pp. 1105–1111, 2011.

[16] Z.-W. Cui, C.-Y. Li, C.-F. Song, and Y. Song, "Combined microwave-vacuum and freeze drying of carrot and apple chips," *Drying Technology*, vol. 26, no. 12, pp. 1517–1523, 2008.

[17] J.-F. Bi, X. Wang, Q.-Q. Chen et al., "Evaluation indicators of explosion puffing Fuji apple chips quality from different Chinese origins," *LWT- Food Science and Technology*, vol. 60, no. 2, pp. 1129–1135, 2015.

[18] L. B. H. Said, S. Bellagha, and K. Allaf, "Measurements of texture, sorption isotherms and drying/rehydration kinetics of dehydrofrozen-textured apple," *Journal of Food Engineering*, vol. 165, pp. 22–33, 2015.

[19] K. Zou, J. Teng, L. Huang, X. Dai, and B. Wei, "Effect of osmotic pretreatment on quality of mango chips by explosion puffing drying," *LWT—Food Science and Technology*, vol. 51, no. 1, pp. 253–259, 2013.

[20] K. Rungthip, D. Sakamon, and C. Naphaporn, "Effect of starch retrogradation on texture of potato chips produced by low-pressure superheated steam drying," *Journal of Food Engineering*, vol. 89, no. 1, pp. 72–79, 2008.

[21] A. Nath and P. K. Chattopadhyay, "Effect of process parameters and soy flour concentration on quality attributes and microstructural changes in ready-to-eat potato-soy snack using high-temperature short time air puffing," *LWT- Food Science and Technology*, vol. 41, no. 4, pp. 707–715, 2008.

[22] L. Seremet, E. Botez, O.-V. Nistor, D. G. Andronoiu, and G.-D. Mocanu, "Effect of different drying methods on moisture ratio and rehydration of pumpkin slices," *Food Chemistry*, vol. 195, pp. 104–109, 2016.

[23] S. G. Gwanpua, S. Van Buggenhout, B. E. Verlinden et al., "Pectin modifications and the role of pectin-degrading enzymes during postharvest softening of Jonagold apples," *Food Chemistry*, vol. 158, pp. 283–291, 2014.

[24] S. Christiaens, S. Van Buggenhout, K. Houben, D. Chaula, A. M. Van Loey, and M. E. Hendrickx, "Unravelling process-induced pectin changes in the tomato cell wall: an integrated approach," *Food Chemistry*, vol. 132, no. 3, pp. 1534–1543, 2012.

[25] T. Stolle-Smits, J. G. Beekhuizen, K. Recourt, A. G. J. Voragen, and C. Van Dijk, "Changes in pectic and hemicellulosic polymers of green beans (Phaseolus vulgaris L.) during industrial processing," *Journal of Agricultural and Food Chemistry*, vol. 45, no. 12, pp. 4790–4799, 1997.

[26] A. E. R. Ahmed and J. M. Labavitch, "A simplified method for accurate determination of cell wall uronide content," *Journal of Food Biochemistry*, vol. 1, pp. 361–365, 2010.

[27] N. Blumenkrantz and G. Asboe-Hansen, "New method for quantitative determination of uronic acids," *Analytical Biochemistry*, vol. 54, no. 2, pp. 484–489, 1973.

[28] A. Ng and K. W. Waldron, "Effect of cooking and pre-cooking on cell-wall chemistry in relation to firmness of carrot tissues," *Journal of the Science of Food and Agriculture*, vol. 73, no. 4, pp. 503–512, 1997.

[29] J. A. Klavons and R. D. Bennett, "Determination of methanol using alcohol oxidase and its application to methyl ester content of pectins," *Journal of Agricultural and Food Chemistry*, vol. 34, no. 4, pp. 597–599, 1986.

[30] D. M. Njoroge, P. K. Kinyanjui, A. O. Makokha et al., "Extraction and characterization of pectic polysaccharides from easy- and hard-to-cook common beans (Phaseolus vulgaris)," *Food Research International*, vol. 64, pp. 314–322, 2014.

[31] A. Arnous and A. S. Meyer, "Comparison of methods for compositional characterization of grape (Vitis vinifera L.) and apple (Malus domestica) skins," *Food and Bioproducts Processing*, vol. 86, no. 2, pp. 79–86, 2008.

[32] C. Yang, Y. Gou, J. Chen, J. An, W. Chen, and F. Hu, "Structural characterization and antitumor activity of a pectic polysaccharide from Codonopsis pilosula," *Carbohydrate Polymers*, vol. 98, no. 1, pp. 886–895, 2013.

[33] L. C. Vriesmann, R. F. Teófilo, and C. L. D. O. Petkowicz, "Optimization of nitric acid-mediated extraction of pectin from cacao pod husks (*Theobroma cacao* L.) using response surface methodology," *Carbohydrate Polymers*, vol. 84, no. 4, pp. 1230–1236, 2011.

[34] X.-H. Yang, Q.-S. Guo, Z.-B. Zhu et al., "Effects of different drying methods on processing performance and quality in bulbus of Tulipa edulis," *Journal of Chinese Meteria Medica*, vol. 40, no. 20, pp. 3974–3980, 2015.

[35] Oduneye, "Effects of drying methods on rehydration and textural properties of bell pepper (capsicum annuum)," Tech. Rep., 2014.

[36] G. Rajkumar, S. Shanmugam, M. D. S. Galvâo et al., "Comparative evaluation of physical properties and volatiles profile of cabbages subjected to hot air and freeze drying," *Drying Technology*, vol. 35, no. 6, pp. 699–708, 2017.

[37] S. K. Giri, "Quality and sorption characteristics of microwave-vacuum, air and freeze dried button mushrooms," in *ASABE Annual International Meeting*, 066206, Portland, Ore, USA, 2006.

[38] B. Koc, İ. Eren, and F. K. Ertekin, "Modelling bulk density, porosity and shrinkage of quince during drying: the effect of drying method," *Journal of Food Engineering*, vol. 85, no. 3, pp. 340–349, 2008.

[39] S. Mounir, C. Besombes, N. Al-Bitar, and K. Allaf, "Study of instant controlled pressure drop DIC treatment in manufacturing snack and expanded granule powder of Apple and Onion," *Drying Technology*, vol. 29, no. 3, pp. 331–341, 2011.

[40] D. Turnbull and M. H. Cohen, "Free-volume model of the amorphous phase: glass transition," *The Journal of Chemical Physics*, vol. 34, no. 1, pp. 120–125, 1961.

[41] M. Maskan, "Drying, shrinkage and rehydration characteristics of kiwifruits during hot air and microwave drying," *Journal of Food Engineering*, vol. 48, no. 2, pp. 177–182, 2001.

[42] S. Parthasarathi and C. Anandharamakrishnan, "Modeling of shrinkage, rehydration and textural changes for food structural analysis: a review," *Journal of Food Process Engineering*, vol. 37, no. 2, pp. 199–210, 2014.

[43] V. Marsilio, B. Lanza, C. Campestre, and M. De Angelis, "Oven-dried table olives: textural properties as related to pectic composition," *Journal of the Science of Food and Agriculture*, vol. 80, no. 8, pp. 1271–1276, 2000.

[44] J. Lyu, *Quality evaluation of peach chips and anticancer activity of pectin extracted from chips dehydrated by explosion puffing drying*, Université de Liège, Liège, Belgique, 2017.

[45] V. N. Novikov and E. A. Rössler, "Similar dependence of glass transition temperature on molecular mass in molecular glasses and polymers," in *International Conference on Times of Polymers & Composites*, vol. 1599, pp. 130–133, American Institute of Physics, 2014.

[46] D. N. Sila, C. Smout, F. Elliot, A. Van Loey, and M. Hendrickx, "Non-enzymatic depolymerization of carrot pectin: toward a better understanding of carrot texture during thermal processing," *Journal of Food Science*, vol. 71, no. 1, pp. E1–E9, 2010.

[47] R. R. Selvendran and M. A. O'Neill, "Isolation and analysis of cell walls from plant material," *Methods of Biochemical Analysis*, vol. 32, pp. 25–153, 1987.

[48] M.-C. Ralet, M.-J. Crépeau, H.-C. Buchholt, and J.-F. Thibault, "Polyelectrolyte behaviour and calcium binding properties of sugar beet pectins differing in their degrees of methylation and acetylation," *Biochemical Engineering Journal*, vol. 16, no. 2, pp. 191–201, 2003.

[49] K. H. Caffall and D. Mohnen, "The structure, function, and biosynthesis of plant cell wall pectic polysaccharides," *Carbohydrate Research*, vol. 344, no. 14, pp. 1879–1900, 2009.

Hindawi
Journal of Food Quality
Volume 2018, Article ID 3278595, 8 pages
https://doi.org/10.1155/2018/3278595

Research Article

Artificial Neural Network Modeling of Drying Kinetics and Color Changes of Ginkgo Biloba Seeds during Microwave Drying Process

Jun-Wen Bai,[1] **Hong-Wei Xiao**,[2] **Hai-Le Ma**,[1] **and Cun-Shan Zhou**[1]

[1]*School of Food and Biological Engineering, Jiangsu University, Zhenjiang 212013, China*
[2]*College of Engineering, China Agricultural University, Beijing 100083, China*

Correspondence should be addressed to Cun-Shan Zhou; cunshanzhou@163.com

Received 21 September 2017; Revised 16 January 2018; Accepted 28 January 2018; Published 21 February 2018

Academic Editor: Egidio De Benedetto

Ginkgo biloba seeds were dried in microwave drier under different microwave powers (200, 280, 460, and 640 W) to determinate the drying kinetics and color changes during drying process. Drying curves of all samples showed a long constant rate period and falling rate period along with a short heating period. The effective moisture diffusivities were found to be 3.318×10^{-9} to 1.073×10^{-8} m^2/s within the range of microwave output levels and activation energy was 4.111 W/g. The L^* and b^* values of seeds decreased with drying time. However, a^* value decreased firstly and then increased with the increase of drying time. Artificial neural network (ANN) modeling was employed to predict the moisture ratio and color parameters (L^*, a^*, and b^*). The ANN model was trained for finite iteration calculation with Levenberg-Marquardt algorithm as the training function and tansig-purelin as the network transfer function. Results showed that the ANN methodology could precisely predict experimental data with high correlation coefficient (0.9056–0.9834) and low mean square error (0.0014–2.2044). In addition, the established ANN models can be used for online prediction of moisture content and color changes of ginkgo biloba seeds during microwave drying process.

1. Introduction

Ginkgo biloba (GB) is the oldest relict plant of the extant gymnosperms and is referred to as an archaic living fossil. GB is native to China, and the cultivation area in China accounts for 90% of the worldwide cultivated land of GB trees [1]. In some oriental countries, including China, Japan, and Korea, GB seeds are regarded as delicious food and tonic medicine, which is a rich source of health-promoting compounds such as flavonoids, ginkgo acid, bilobol, and ginkgolides as well as carbohydrates, protein, fats, vitamins, and mineral elements [2]. As a seasonal nut, in China, GB is generally harvested in late September to October, which is a typical seasonal crop. Although it is wrapped by a hard shell, GB seed cannot be stored for a long time due to its relative high moisture content. Drying is one of the most frequently used methods to prolong the shelf life of GB seeds. The dried products can be used as materials for further processing for other products such as GB seeds powers.

The traditional drying methods for GB seeds are natural sun drying and hot air drying. Although both methods are relatively simple and inexpensive, they have several disadvantages such as long drying time, low energy efficiency, and substantial deterioration of food quality, such as degradation of color and loss of nutrients. Microwave drying is a technique that can be used as an alternative to shorten the drying time, improve the quality of the dried products, and reduce energy consumption [3]. Microwaves can penetrate into the material with the effect known as volumetric hearting [4], which can increase the drying rate in the falling drying rate period [5]. Microwave drying technology has been applied to several fruits and vegetables, such as carrot [6], nut seed [7], blueberry [8], apple slices [9], thyme leaves [10], and jujube [11].

Drying is a complex, dynamic, highly nonlinear, strongly interactive, and multivariable thermal process [12]. Therefore, the prediction of moisture content and quality parameters are very useful and necessary to improve the overall performance of drying process. Researchers usually develop mathematical

models which can be classified as theoretical, semitheoretical, and empirical models to describe the drying kinetics and quality changes. Although these models can give good regression to experimental data in very specific conditions, there is no way to obtain general equations to describe the drying process of every product [13].

Artificial neural networks (ANN) offer several advantages over conventional modeling techniques because of the learning ability and being suitable to the nonlinear process. ANN models have been developed to model the moisture content and quality parameters in drying process. Jafari et al. [14] observed that ANN model was more productive and precise than mathematical modeling method for predicting changes in the moisture ratio of green bell pepper during hot air fluidized bed drying. Sarimeseli et al. [10] used ANN to describe microwave drying kinetics of thyme leaves. Behroozi Khazaei et al. [15] applied machine vision and ANN for modeling and controlling of the grape drying process in hot air dryer. Nadian et al. [16] developed an ANN model to predict the color changes of apple slices during hot air drying. Guiné et al. [17] employed ANN to characterize the antioxidant activity and phenolic compounds degradation kinetics of bananas under different drying conditions.

The objectives of current work are (i) to explore the drying characteristic and color changes kinetic of GB seeds at different microwave powers, (ii) to calculate effective moisture diffusivity and the activation energy to highlight the effect of microwave power, and (iii) to model the experimental drying kinetics and color changes of GB seeds during its microwave drying process using ANN methodology.

2. Materials and Methods

2.1. Materials. Fresh GB seeds were purchased from a local market in Taixing, China. The cultivar of GB is Dafozi. To ensure uniformity of physical characteristics of the experimental materials, the samples were carefully selected with the same size (average major axis, middle axle, and minor axis were 22.07 mm, 13.84 mm, and 12.03 mm, resp.). The initial moisture content of samples was determined by vacuum drying at 70°C for 24 h following the standard method (AOAC, 1990). The initial moisture content of the samples was reported as 53.02% in wet basis (w.b.) or 1.13 kg/kg in dry basis (d.b.). Prior to experiments, the kernel (nut meat) of the GB seed was obtained by shelling and removing the bronzing pellicle. All the GB seeds were stored in a refrigerator at 5 ± 1°C and 90% relative humidity before the experiments were carried out.

2.2. Drying Experiments. Drying experiments were carried out in a domestic digital microwave oven with maximum power output capacity of 700 W at 2450 MHz (P70d2otl, Galanz, China). The microwave oven has a capability to operate at four different microwave output powers (200, 280, 460, and 640 W), with measurement accuracy of ±10 W. Processing time and microwave output power were adjusted with the digital control on the microwave oven. GB seeds of 80 g were placed in a single layer on a rotating glass plate in the oven. The weight loss was periodically recorded by taking out the rotating glass and weighing it on an electronic balance within the accuracy of ±0.01 g during drying. Drying was stopped when the moisture content of the samples reached the final moisture content of 0.15 kg/kg (d.b.). All the drying experiments were conducted in triplicate.

2.3. Calculation of Moisture Ratio and Drying Rate. The moisture ratio (MR) of the samples was calculated according to [23]

$$\mathrm{MR} = \frac{M_t - M_e}{M_0 - M_e}, \tag{1}$$

where M_t, M_0, and M_e are moisture content at any time of drying (kg water/kg dry matter), initial moisture content (kg water/kg dry matter), and equilibrium moisture content (kg water/kg dry matter), respectively. The equilibrium moisture content was assumed to be zero for microwave drying as stated by Maskan [24].

The drying rate (DR) of samples during drying experiments was computed using [18]

$$\mathrm{DR} = \frac{M_{t+dt} - M_t}{dt}, \tag{2}$$

where M_t and M_{t+dt} are the moisture content at t and moisture content at $t + dt$ (kg water/kg dry matter), respectively, and t is drying time (min).

2.4. Calculation of Effective Moisture Diffusivity. Weibull distribution can be used to calculate the effective moisture diffusivity, regardless of the characteristics of moisture migration during drying process. The MR curves were fitted to the Weibull distribution [25]

$$\mathrm{MR} = \exp\left[-\left(\frac{t}{\alpha}\right)^{\beta}\right], \tag{3}$$

where MR is moisture ratio of GB seeds; t is the drying time; α is the scale parameter of Weibull distribution (min); β is the shape parameter of Weibull distribution.

Effective moisture diffusivity (D_{eff}) can be calculated with the following equation [25, 26]:

$$D_{\mathrm{eff}} = \frac{D_{\mathrm{cal}}}{R_g} = \frac{r^2}{\alpha R_g}, \tag{4}$$

where D_{eff} is the effective moisture diffusivity (m^2/s); D_{cal} is the estimate moisture diffusivity (m^2/s); r is the volume equivalent radius of GB seeds, with 0.769×10^{-2} m as its value; α is the scale parameter of Weibull distribution; R_g is the physical dimension constant. For agriculture products with a shape of sphere, the value of R_g is 18.6 [27].

2.5. Estimation of Activation Energy. Activation energy (E_a) is the minimum energy that must be supplied to break water-solid and/or water-water interactions and to move water molecules from one point to another in solid [3]. The dependence of effective moisture diffusivity on drying temperature

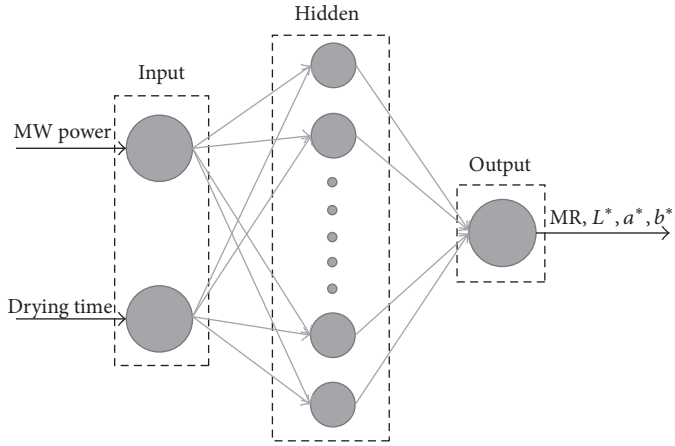

Figure 1: Artificial neural network configuration.

has been shown to follow an Arrhenius relationship presented as follows:

$$D_{\text{eff}} = D_0 \exp\left(-\frac{E_a}{R\,(T + 273.15)}\right), \tag{5}$$

where D_0 is the preexponential factor of Arrhenius equation (m^2/s); E_a is the activation energy (kJ/mol); R is the universal gas constant (kJ/mol K); T is temperature (°C).

However, during the microwave drying processes, the temperature is not a directly measured variable. The Arrhenius equation was used in a modified form to illustrate the relationship between the effective moisture diffusion and the ratio of the microwave output power to sample weight (m/P) instead of the temperature for calculation of the activation energy. The modified Arrhenius equation (6) derived by Dadalı et al. [18] can be effectively used as follows:

$$D_{\text{eff}} = D_0 \exp\left(-\frac{E_a m}{P}\right), \tag{6}$$

where D_0 is the preexponential factor of Arrhenius equation (m^2/s); D_{eff} is the effective moisture diffusivity (m^2/s); E_a is the activation energy (W/g); m is the mass of raw sample (g); P is the microwave power (W).

Equation (6) can be expressed in a logarithmic form as follows:

$$\ln D_{\text{eff}} = \ln D_0 - \frac{E_a m}{P}. \tag{7}$$

So the activation energy can be calculated from the slope of $\ln(D_{\text{eff}})$ versus the ratio of the microwave output power to sample weight (m/P).

2.6. Color Measurement. A CIE standard illuminant D65 and observer 10° were used to determine CIE color space coordinates, L^* (whiteness or brightness), a^* (redness/greenness), and b^* (yellowness/blueness). GB seed samples color was measured using a colorimeter (Color Quest X, Hunter Lab, USA) before drying and prespecified time intervals during drying. Three samples were randomly selected for color measurement. L^*, a^*, and b^* values of each sample were average of 6 readings.

2.7. ANN Modeling. MATLAB software (Version 7.8, MathWorks, USA) was used for the design and testing of various ANN models. The ANN configuration used in this work (Figure 1) was a multilayer "feed-forward," consisting of one input layer, one hidden layer, and one output layer with a convergence criterion for training purposes. The input variables in the input layer are microwave power and drying time and the output variables in the output layer are moisture content and the color parameters (L^*, a^*, and b^*) of GB seeds at any time. After trial and error, network unit with hyperbolic tangent sigmoid transfer function "tansig" for neurons of hidden layer, 10 neurons in the hidden layer, linear transfer function "purelin" for neuron of output layer, and Levenberg-Marquardt training algorithm "trainlm" for the training function were selected.

In this study, input-output data sets collected in the experiment were totally 120 and 114 for MR and color parameters (L^*, a^*, and b^*), respectively. For ANN model building, the available data were randomly divided into 3 subsets: training (70%), validation (15%), and testing (15%) subset. The networks performance was evaluated by correlation coefficient (R^2) and mean square error (RMSE). These statistical values can be calculated as follows:

$$R^2 = 1 - \frac{\sum_{i=1}^{N}\left(C_{\text{pre},i} - C_{\text{exp},i}\right)^2}{\sum_{i=1}^{N}\left(\overline{C_{\text{pre}}} - C_{\text{exp},i}\right)^2},$$
$$\text{RMSE} = \left[\frac{1}{N}\sum_{i=1}^{N}\left(C_{\text{pre},i} - C_{\text{exp},i}\right)^2\right]^{1/2}, \tag{8}$$

where $C_{\text{exp},i}$ is the ith experimental data, $C_{\text{pre},i}$ is the ith predicted data by ANN model, and N is the number of experimental data.

3. Result and Discussion

3.1. Drying Curves. To investigate the effects of microwave power on moisture ratio and drying time, the curves of MR versus drying time are shown in Figure 2. From Figure 2,

Table 1: Moisture effective diffusion coefficients of GB seeds by different microwave powers.

Powers (W)	α (min)	β	R^2	D_{eff} (10^{-9} m^2/s)
200	15.97	1.909	0.9999	3.318
280	9.337	1.850	0.9999	5.675
460	6.530	1.884	1.0000	8.114
640	4.941	2.038	0.9999	10.73

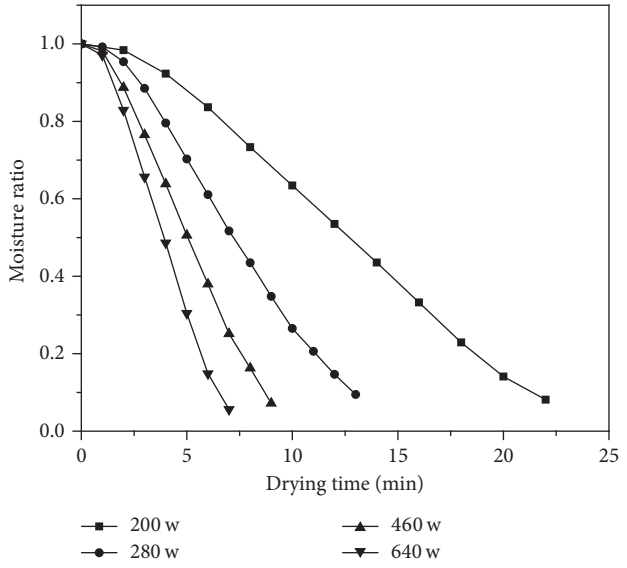

Figure 2: Drying kinetics of GB seeds under different microwave powers.

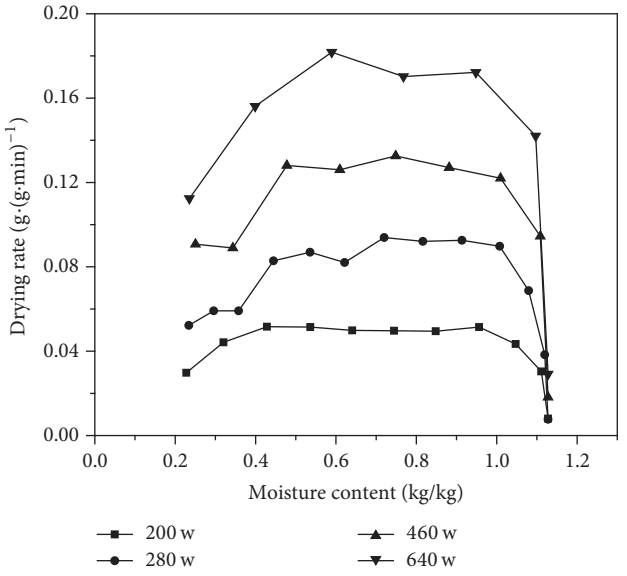

Figure 3: Drying rate of GB seeds under different microwave powers.

it was shown that drying time required to reduce the moisture from the initial moisture content to desired moisture content for GB seeds was approximately 22, 13, 9, and 7 min, respectively, in relation to the microwave power of 200, 280, 460, and 640 W. The drying time was approximately 3.14 times more at 200 W than that at 640 W. Therefore, it can be concluded that microwave power had significant effect on the drying time. The results indicated that mass transfer is rapid during the higher microwave power heating as a result of more energy transfer to the samples, causing an increase in temperature of the product [28, 29]. This phenomenon was in agreement with reported literatures for drying parsley [30], sardine fish [19], and tea [31].

The drying rate curves for GB seeds under different microwave powers were given in Figure 3. As can be seen from this figure, the drying rate of samples was apparently increased as the microwave power level was increased. After a short preheating period, a long constant drying rate period was observed in all cases and the average drying rates at constant rate period ranged from about 0.04 to 0.16 (g water/g solid min) for the microwave power between 200 and 640 w, respectively. As the drying processed, when the material moisture content was lower than about 0.42 (g water/g solid min), a constant rate period was followed by a falling rate period which was controlled by the internal liquid diffusion. The loss of moisture content of samples caused a decrease in the absorption of microwave power and led to a descending in the drying rate [32, 33]. These results were in agreement with the study of microwave drying of okra [34], coriander leaves [35], onion slices [20], and daylily flower buds [33], which indicated that a long constant rate period and falling rate period were observed after a short heating period. On the other hand, these results were not the same as the studies performed by Ozkan et al. [32] and Balbay and Şahin [36], both of the investigations claimed that microwave drying of liquorice root or spinach occurred only in the falling rate period. The reason for differences may be ascribed to the different structures and sizes of materials.

3.2. Effective Moisture Diffusivity and Activation Energy. The effective moisture diffusivity values of GB seeds were calculated using Weibull distribution and (4) and are shown in Table 1. The D_{eff} values of dried samples were varied in the range of 3.318×10^{-9} to 1.073×10^{-8} m^2/s under different microwave powers. The values of the Weibull scale parameter (α) ranged from 4.941 to 15.97 min and values of the shape parameter (β) varied from 1.8502 to 2.0378. It was noted that D_{eff} values increased greatly with increasing microwave powers. When samples were dried at higher microwave power, increased heating energy would increase the activity of water molecules leading to higher moisture diffusivity [37]. The values of D_{eff} obtained from this study lie within the general range from 10^{-12} to 10^{-8} m^2/s for food materials [37].

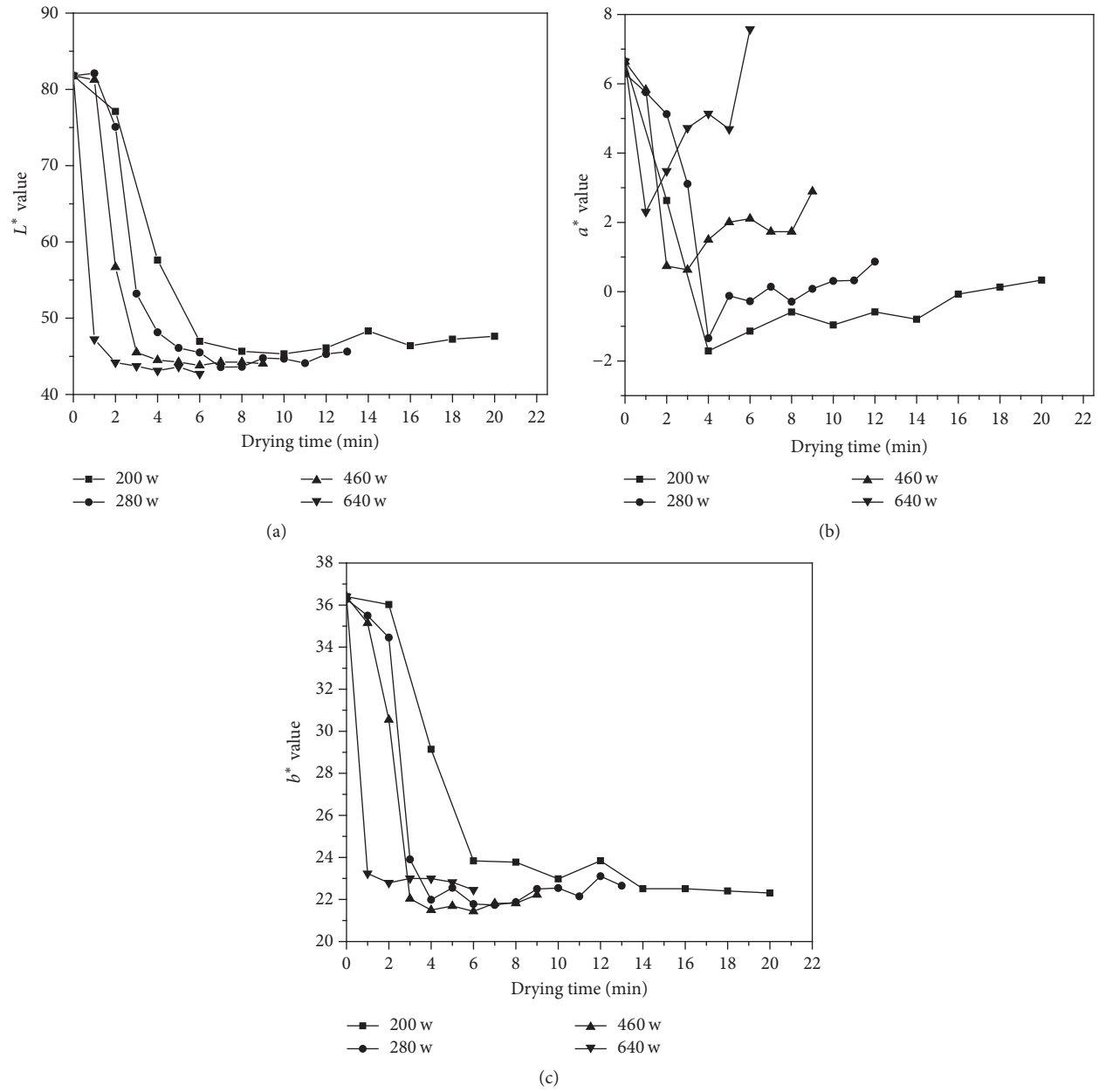

Figure 4: Color changes of (a) L^* value, (b) a^* value, and (c) b^* value as a function of drying time at various microwave powers for sample amount of 80 g.

The activation energy is the energy required to initiate moisture diffusion from inside to the outside of the drying product. The E_a value for GB seeds was determined to be 4.111 W/g, which can be calculated from the slope of $\ln(D_{\text{eff}})$ versus the ratio of the microwave power to sample weight (m/P). To compare the activation energy of GB seeds with other agricultural products, the activation energy of various agricultural materials is presented in Table 2. Table 2 shows that GB seeds have lower activation energy than that for sardine fish, mint leaves, okra, and onion slices. And the value of E_a found from this study was quite similar to the value of apple slices (4.140 W/g). A lower E_a value indicates greater temperature sensitivity of diffusion coefficient and less energy required to remove moisture from the product [3]. In general, the factors such as the components, variety, and tissue structures of the samples have a significant effect on activation energy.

3.3. Color Change Kinetics during Drying Process. The color change curves of L^*, a^*, and b^* value as a function of drying time under various microwave powers were shown in Figures 4(a)–4(c). The L^* value is illustrated in Figure 4(a). As can be seen from this figure, L^* value decreased with drying time and all dried GB seeds were obviously darker than the fresh samples. It has been stated that the decrease of the brightness of dried samples can be taken as an indicator of browning

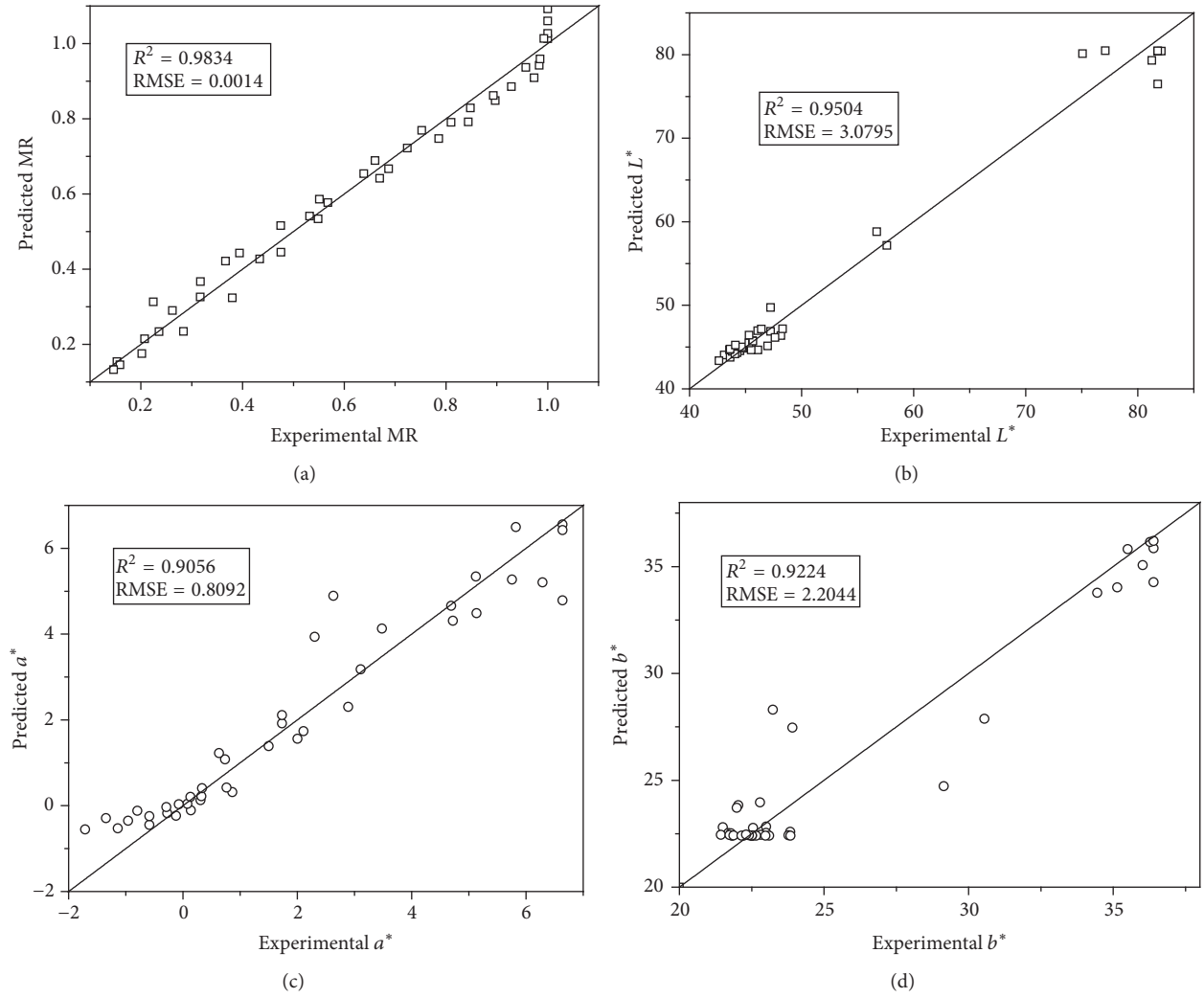

Figure 5: Comparison of predicted and experimental moisture ratio and color parameters (L^*, a^*, and b^*) on testing step for the optimal ANN topology.

[38]. Besides, the L^* values of final dried samples were about 47.62, 45.62, 44.05, and 42.63 under the microwave power of 200, 280, 460, and 640 W, respectively. The differences might be due to the Maillard reaction, which was accelerated at higher temperature. Similar phenomenon was in agreement with the study for drying spinach published by Dadalı et al. [39] and for drying tea published by Demirhan and Ozbek [40].

The results for a^* value are shown in Figure 4(b). It was found that a^* value of GB seeds decreased firstly and then increased with the increase of drying time in all cases. The lowest a^* of samples were about −1.71, −1.34, 0.63, and 2.31 under the microwave power of 200, 280, 460, and 640 W, respectively. The negative a^* value appeared when drying for 4 min under the microwave power of 200 and 280 w, indicating that the samples turned to be greenish. It may be due to that the surface of GB seeds became transparent and showed the color of internal germ. After a^* value reached its lowest point, it had begun to increase with the drying time, which indicated that the color of the samples became more reddish. Figure 4(b) also showed that, at the end of drying, a^* value increased as the microwave power increased. The final a^* values of dried samples were about 0.34, 2.58, 2.89, and 7.57 under the microwave power of 200, 280, 460, and 640 W, respectively. This phenomenon could be attributed to the creation of red-brown pigments in the effect of nonenzymatic reaction [41, 42].

The results for b^* values are shown in Figure 4(c). As can be seen from this figure, b^* values decreased with drying time and indicate that the yellowness of sample decreased due to microwave power applied. In addition, the change rate of b^* value was faster at the initial drying stage than that at the intermediate and final drying stages.

3.4. ANN Modeling. The BP neural network model was trained for finite iteration calculation with Levenberg-Marquardt algorithm as the training function and tansig-purelin as the network transfer function. The experimental and predicted moisture ratio and color parameters (L^*, a^*, and b^*) values for the optimal ANN topology were shown in Figure 5. The determination coefficient (R^2) and root mean squared error (RMSE) between the predicted and

Table 2: Activation energies of GB seeds and other products under microwave drying.

Products	Microwave power (W)	Activation energy (W/g)	References
GB seeds	200–640	4.111	Present work
Okra	180–900	5.540	[18]
Sardine fish	200–500	11.14	[19]
Onion slices	328–557	7.900	[20]
Mint leaves	180–900	11.04	[21]
Apple slices	200–600	4.140	[22]

measured values were 0.9834 and 0.0014 for moisture content, 0.9504 and 3.0795 for L^* value, 0.9056 and 0.8092 for a^* value, and 0.9224 and 2.2044 for b^* value, respectively. An acceptable level of statistical parameters of R^2 and RMSE was obtained by employing the selected ANN. The best and worst estimations were obtained for the moisture ratio and a^* value. In general, there was a good agreement between experimental and estimated values, demonstrating that the selected ANN topology had an acceptable capability to predict the network outputs with the inconsiderable error. Therefore, according to the results of this experimental study as well as ANN modeling, the online prediction moisture content and color evaluation would be proposed as a promising methodology for GB seeds drying process.

4. Conclusions

Ginkgo biloba seeds were dried in microwave drier to determinate the drying kinetics and color changes during drying process. Microwave power had significant effect on the drying time, and higher microwave power results in higher drying rate and shorter drying time. Within the range of microwave output levers (200, 280, 460, and 640 w), effective moisture diffusivities were found to be 3.318×10^{-9} to 1.073×10^{-8} m^2/s and activation energy was estimated to be 4.111 W/g. The L^* and b^* values of GB seeds decreased with drying time. However, a^* value decreased firstly and then increased with the increase of drying time. ANN modeling was applied to predict the moisture ratio and color parameters (L^*, a^*, and b^*). The results showed that the ANN methodology could precisely model the microwave drying process of GB seeds with correlation coefficient higher than 0.9056. The findings in current work demonstrated that the selected ANN topology had an acceptable capability to predict the network outputs with the inconsiderable error.

Conflicts of Interest

The authors declare that they have no conflicts of interest.

Acknowledgments

The authors acknowledge the financial support provided by the National Natural Science Foundation of China (31601578), the National Key Research and Development Plan (2017YFD0400905), and the Natural Science Foundation of Jiangsu Province (BK20160504).

References

[1] M. Miao, H. Jiang, B. Jiang, S. W. Cui, Z. Jin, and T. Zhang, "Structure and functional properties of starches from Chinese ginkgo (Ginkgo biloba L.) nuts," *Food Research International*, vol. 49, no. 1, pp. 303–310, 2012.

[2] C. H. Zhang, L. X. Huang, C. P. Wang, and A. S. Mujumdar, "Experimental and numerical investigation of spray-drying parameters on the dried powder properties of ginkgo biloba seeds," *Drying Technology*, vol. 28, no. 3, pp. 380–388, 2010.

[3] V. Kumar, H. K. Sharma, and K. Singh, "Mathematical Modeling of Thin Layer Microwave Drying of Taro Slices," *Journal of The Institution of Engineers (India): Series A*, vol. 97, no. 1, pp. 53–61, 2016.

[4] D. Wray and H. S. Ramaswamy, "Novel Concepts in Microwave Drying of Foods," *Drying Technology*, vol. 33, no. 7, pp. 769–783, 2015.

[5] G. R. Nair, Z. Li, Y. Gariepy, and V. Raghavan, "Microwave drying of corn (Zea mays L. ssp.) for the seed industry," *Drying Technology*, vol. 29, no. 11, pp. 1291–1296, 2011.

[6] H. Pu, Z. Li, J. Hui, and G. S. V. Raghavan, "Effect of relative humidity on microwave drying of carrot," *Journal of Food Engineering*, vol. 190, pp. 167–175, 2016.

[7] A. C. da Silva, H. J. Sarturi, E. L. Dall'Oglio et al., "Microwave drying and disinfestation of Brazil nut seeds," *Food Control*, vol. 70, pp. 119–129, 2016.

[8] M. Zielinska and M. Markowski, "The influence of microwave-assisted drying techniques on the rehydration behavior of blueberries (Vaccinium corymbosum L.)," *Food Chemistry*, vol. 196, pp. 1188–1196, 2016.

[9] M. Zarein, S. H. Samadi, and B. Ghobadian, "Investigation of microwave dryer effect on energy efficiency during drying of apple slices," *Journal of the Saudi Society of Agricultural Sciences*, vol. 14, no. 1, pp. 41–47, 2015.

[10] A. Sarimeseli, M. A. Coskun, and M. Yuceer, "Modeling Microwave Drying Kinetics of Thyme (Thymus Vulgaris L.) Leaves Using ANN Methodology and Dried Product Quality," *Journal of Food Processing and Preservation*, vol. 38, no. 1, pp. 558–564, 2014.

[11] S. Fang, Z. Wang, X. Hu et al., "Energy requirement and quality aspects of Chinese jujube (Zizyphus jujuba Miller) in hot air drying followed by microwave drying," *Journal of Food Process Engineering*, vol. 34, no. 2, pp. 491–510, 2011.

[12] M. Aghbashlo, S. Hosseinpour, and A. S. Mujumdar, "Application of Artificial Neural Networks (ANNs) in Drying Technology: A Comprehensive Review," *Drying Technology*, vol. 33, no. 12, pp. 1397–1462, 2015.

[13] V. Martínez-Martínez, J. Gomez-Gil, T. S. Stombaugh, M. D. Montross, and J. M. Aguiar, "Moisture Content Prediction in the Switchgrass (Panicum virgatum) Drying Process Using Artificial Neural Networks," *Drying Technology*, vol. 33, no. 14, pp. 1708–1719, 2015.

[14] S. M. Jafari, V. Ghanbari, M. Ganje, and D. Dehnad, "Modeling the Drying Kinetics of Green Bell Pepper in a Heat Pump Assisted Fluidized Bed Dryer," *Journal of Food Quality*, vol. 39, no. 2, pp. 98–108, 2016.

[15] N. Behroozi Khazaei, T. Tavakoli, H. Ghassemian, M. H. Khoshtaghaza, and A. Banakar, "Applied machine vision and

artificial neural network for modeling and controlling of the grape drying process," *Computers and Electronics in Agriculture*, vol. 98, pp. 205–213, 2013.

[16] M. H. Nadian, S. Rafiee, M. Aghbashlo, S. Hosseinpour, and S. S. Mohtasebi, "Continuous real-time monitoring and neural network modeling of apple slices color changes during hot air drying," *Food and Bioproducts Processing*, vol. 94, pp. 263–274, 2015.

[17] R. P. F. Guiné, M. J. Barroca, F. J. Gonçalves, M. Alves, S. Oliveira, and M. Mendes, "Artificial neural network modelling of the antioxidant activity and phenolic compounds of bananas submitted to different drying treatments," *Food Chemistry*, vol. 168, pp. 454–459, 2015.

[18] G. Dadalı, D. K. Apar, and B. Özbek, "Microwave drying kinetics of okra," *Drying Technology*, vol. 25, no. 5, pp. 917–924, 2007.

[19] H. Darvishi, M. Azadbakht, A. Rezaeiasl, and A. Farhang, "Drying characteristics of sardine fish dried with microwave heating," *Journal of the Saudi Society of Agricultural Sciences*, vol. 12, no. 2, pp. 121–127, 2013.

[20] E. Demiray, A. Seker, and Y. Tulek, "Drying kinetics of onion (Allium cepa L.) slices with convective and microwave drying," *Heat and Mass Transfer*, vol. 53, no. 5, pp. 1817–1827, 2017.

[21] B. Özbek and G. Dadali, "Thin-layer drying characteristics and modelling of mint leaves undergoing microwave treatment," *Journal of Food Engineering*, vol. 83, no. 4, pp. 541–549, 2007.

[22] N. Aghilinategh, S. Rafiee, A. Gholikhani et al., "A comparative study of dried apple using hot air, intermittent and continuous microwave: Evaluation of kinetic parameters and physicochemical quality attributes," *Food Science & Nutrition*, vol. 3, no. 6, pp. 519–526, 2015.

[23] E. E. Abano, H. Ma, and W. Qu, "Influence of combined microwave-vacuum drying on drying kinetics and quality of dried tomato slices," *Journal of Food Quality*, vol. 35, no. 3, pp. 159–168, 2012.

[24] M. Maskan, "Microwave/air and microwave finish drying of banana," *Journal of Food Engineering*, vol. 44, no. 2, pp. 71–78, 2000.

[25] L. Xie, A. S. Mujumdar, X.-M. Fang et al., "Far-infrared radiation heating assisted pulsed vacuum drying (FIR-PVD) of wolfberry (Lycium barbarum L.): Effects on drying kinetics and quality attributes," *Food and Bioproducts Processing*, vol. 102, pp. 320–331, 2017.

[26] J.-W. Dai, J.-Q. Rao, D. Wang et al., "Process-Based Drying Temperature and Humidity Integration Control Enhances Drying Kinetics of Apricot Halves," *Drying Technology*, vol. 33, no. 3, pp. 365–376, 2015.

[27] A. Marabi, S. Livings, M. Jacobson, and I. S. Saguy, "Normalized Weibull distribution for modeling rehydration of food particulates," *European Food Research and Technology*, vol. 217, no. 4, pp. 311–318, 2003.

[28] L. M. Bal, A. Kar, S. Satya, and S. N. Naik, "Drying kinetics and effective moisture diffusivity of bamboo shoot slices undergoing microwave drying," *International Journal of Food Science & Technology*, vol. 45, no. 11, pp. 2321–2328, 2010.

[29] A. S. Kipcak, "Microwave drying kinetics of mussels (Mytilus edulis)," *Research on Chemical Intermediates*, vol. 43, no. 3, pp. 1429–1445, 2017.

[30] Y. Soysal, "Microwave drying characteristics of parsley," *Biosystems Engineering*, vol. 89, no. 2, pp. 167–173, 2004.

[31] D. Hatibaruah, D. C. Baruah, and S. Sanyal, "Microwave drying characteristics of assam ctc tea (camellia assamica)," *Journal of Food Processing and Preservation*, vol. 37, no. 4, pp. 366–370, 2013.

[32] I. A. Ozkan, B. Akbudak, and N. Akbudak, "Microwave drying characteristics of spinach," *Journal of Food Engineering*, vol. 78, no. 2, pp. 577–583, 2007.

[33] S. Ding, J. You, K. An, Y. Li, and Z. Wang, "Effective diffusivities and energy consumption of daylily in microwave drying," *International Journal of Food Science & Technology*, vol. 47, no. 12, pp. 2648–2654, 2012.

[34] G. Dadalı, D. K. Apar, and B. Özbek, "Color change kinetics of okra undergoing microwave drying," *Drying Technology*, vol. 25, no. 5, pp. 925–936, 2007.

[35] A. Sarimeseli, "Microwave drying characteristics of coriander (*Coriandrum sativum* L.) leaves," *Energy Conversion and Management*, vol. 52, no. 2, pp. 1449–1453, 2011.

[36] A. Balbay and Ö. Şahin, "Microwave Drying Kinetics of a Thin-Layer Liquorice Root," *Drying Technology*, vol. 30, no. 8, pp. 859–864, 2012.

[37] I. Doymaz, "Thin-layer drying characteristics of sweet potato slices and mathematical modelling," *Heat and Mass Transfer*, vol. 47, no. 3, pp. 277–285, 2011.

[38] E. Demirhan and B. Özbek, "Color change kinetics of microwave-dried basil," *Drying Technology*, vol. 27, no. 1, pp. 156–166, 2009.

[39] G. Dadalı, E. Demirhan, and B. Özbek, "Color change kinetics of spinach undergoing microwave drying," *Drying Technology*, vol. 25, no. 10, pp. 1713–1723, 2007.

[40] E. Demirhan and B. Ozbek, "Color change kinetics of tea leaves during microwave drying," *International Journal of Food Engineering*, vol. 11, no. 2, 2015.

[41] H.-W. Xiao, C.-L. Law, D.-W. Sun, and Z.-J. Gao, "Color Change Kinetics of American Ginseng (Panax quinquefolium) Slices During Air Impingement Drying," *Drying Technology*, vol. 32, no. 4, pp. 418–427, 2014.

[42] M. Shahabi, S. Rafiee, S. S. Mohtasebi, and S. Hosseinpour, "Image analysis and green tea color change kinetics during thin-layer drying," *Food Science and Technology International*, vol. 20, no. 6, pp. 465–476, 2014.

Hindawi
Journal of Food Quality
Volume 2018, Article ID 9169875, 24 pages
https://doi.org/10.1155/2018/9169875

Research Article

Shape Effect on the Temperature Field during Microwave Heating Process

Zhijun Zhang, Tianyi Su, and Shiwei Zhang

School of Mechanical Engineering and Automation, Northeastern University, Shenyang 110004, China

Correspondence should be addressed to Zhijun Zhang; zhjzhang@mail.neu.edu.cn

Received 9 November 2017; Revised 2 January 2018; Accepted 11 January 2018; Published 11 February 2018

Academic Editor: Hong-Wei Xiao

Aiming at improving the food quality during microwave process, this article mainly focused on the numerical simulation of shape effect, which was evaluated by microwave power absorption capability and temperature distribution uniformity in a single sample heated in a domestic microwave oven. This article only took the electromagnetic field and heat conduction in solid into consideration. The Maxwell equations were used to calculate the distribution of microwave electromagnetic field distribution in the microwave cavity and samples; then the electromagnetic energy was coupled as the heat source in the heat conduction process in samples. Quantitatively, the power absorption capability and temperature distribution uniformity were, respectively, described by power absorption efficiency (PAE) and the statistical variation of coefficient (COV). In addition, we defined the comprehensive evaluation coefficient (CEC) to describe the usability of a specific sample. In accordance with volume or the wave numbers and penetration numbers in the radial and axial directions of samples, they can be classified into different groups. And according to the PAE, COV, and CEC value and the specific need of microwave process, an optimal sample shape and orientation could be decided.

1. Introduction

Microwave is a common process treatment of food products as an approach to accelerate the processes or improve the food quality. It can be used as a heat source in processes like heating [1–5], drying [6, 7], thawing, puffing [8, 9], and so on; besides microwave can be also used as an assisting method in other processes like sterilization [10], moist measurement [11], and so on [12]. Compared with the conventional heating process microwave heating has many advantages, such as high heating efficiency, good uniformity, being controllable, easy maintenance, and being environment friendly [13, 14]; thus microwave heating process has been applied in plenty of processes in food, nonmetal, and advanced materials industry since the 1950s. Although using microwave heating can achieve better uniformity compared with the conventional methods, hot spots and cold spots still occur in the sample, which seriously affect the quality of material during the process [15]. Improving temperature uniformity is still an urgent problem in microwave heating processes.

Microwave is an electromagnetic wave with a frequency range of 0.3 GHZ to 300 GHZ, corresponding to the wavelength range of 0.001 m to 1 m. The commonly used microwave frequencies are 0.915 GHZ, 2.45 GHz, and 5.8 GHz, and most equipment designed for microwave processing is operated at 2.45 GHz [16]. Electromagnetic field distribution of the microwave treatment process can be described by Maxwell's equations or Lambert's law [13]. The propagation and absorption of microwave electromagnetic field can be described by Maxwell's equations and the accuracy of Lambert's law which is based on an assumption of semi-infinite critical sample length [17], which is verified when the thickness of the sample is more than three times the microwave penetration depth of the sample [18]. Taking the scope of application and accuracy into account, Maxwell's equations are the best choice to describe the electromagnetic field distribution.

Materials placed in the microwave environment are classified as insulators, conductors, semiconductors, and superconductors [19]. Most of foodstuff are in the category of insulators and have low internal wavelength decided by dielectric properties and electromagnetic frequency [20]. Chemical component and physical structure of foodstuff determine the dielectric properties [13]. Food materials

interact with microwave electromagnetic field to generate heat, and the dielectric constant and dielectric loss coefficient of the material are used to characterize the electromagnetic energy storage capability and the ability to convert electromagnetic energy into heat of the materials. So electromagnetic distribution can directly influence the temperature generation and distribution in the foodstuff heated by microwave [19]. Therefore, studying the rules from foodstuff heating phenomena in microwave oven has significant meaning for improving the quality of various foodstuff.

After the foodstuff treatment processes, the compositions of food product are main indicators to measure the quality. Enzymes, trace elements, proteins, and other substances in food are sensitive to temperature, and the high temperature during processing will destroy the food structure and even produce harmful substances, which seriously influences the food quality. Temperature nonuniformity in foodstuff leads to hot spots and cold spots. At the location of hot spots the temperature may be too high to damage the nutrient substance, and at the cold spots the low temperature may fail to reach the damage temperature of microorganisms, which raises the risk of food deterioration. Therefore, both hot spots and cold spots are drawbacks of the overall quality of the product [13]. In addition, compared with a single homogeneous material or synthetic material, foodstuff is more complex and anisotropic, so the interaction between microwave electromagnetic wave and food material becomes less uniform during the whole processing, which results in uneven distribution of temperature. Therefore, it is very important to study the temperature uniformity of food microwave processing.

Researches on foodstuff microwave treatment processes are mostly concentrated on two aspects: one aspect is the dielectric properties of the object itself, including factors affecting dielectric properties [18, 21], shape effect [22–24], and deformation effect [25]. Researches on aspects other than the target object like microwave equipment structure [26, 27], microwave properties [28], microwave processing strategies [20, 29], and experimental verifications [30, 31] are also being performed at the same time. Even though all factors affect the results in the microwave treatment process, it is too complex to take overall consideration of them. Therefore, researchers tend to select the dominant elements which may convert to each other to conduct studies. Foodstuff can be divided into four groups by the microwave heating characteristics, and potato can present the most commonly used vegetable materials [20] with a relatively complete system of characteristic parameters as well as representative properties [15, 16, 20, 21, 23, 32].

In this article, we studied the temperature field distribution of potato samples with different shapes, sizes, and position orientations using a domestic microwave oven with one 2.45 GHz microwave source in TE10 mode rectangular waveguide in three dimensions. The basically physical model of the microwave oven is consistent with the Microwave Oven in COMSOL Multiphysics software, but the shape, size, and position orientations of potato samples change in a wide range. This article described and summed up the general rules of the sample microwave heating processing from the perspective of the interaction between microwave electromagnetic field and sample's dielectric properties. The temperature distribution of various samples at different times was intuitively drawn from the qualitative point of view. Quantitatively, the ratio of absorbed power and input power named power absorption efficiency (PAE) was used to describe the microwave energy absorption capability of samples, and the ratio of internal temperature standard deviation and average value, namely, coefficient of variation (COV) [15, 29, 33], measured the temperature distribution uniformity of a sample at a given moment. A lower coefficient of variation (COV) means a better internal temperature uniformity, and, in addition, defining the comprehensive evaluation coefficient (CEC) which was the ratio of power absorption efficiency to temperature COV value. The CEC value can measure the samples' usability at a certain condition, and a higher CEC value presents a sample with a high PAE and/or low COV, which could be chosen according to specific needs of microwave process.

2. Materials and Methods

2.1. Basic Assumption. In order to simplify the calculation process and save calculation time, the following assumptions were made for the simulation process within the allowable error range:

(i) The samples are isotropic homogeneous. The samples of different sizes or shapes can be considered as isotropic homogeneous.

(ii) The influence of mass transfer and phase transformation of the process is ignored. The aim of this study is to obtain the temperature field distribution during the initial stage sample, so the temperature is below the phase transition temperature at atmospheric pressure.

(iii) The dielectric constant and conductivity are constant. The dielectric properties of foodstuff are mainly affected by the moisture [25]. In this paper, the temperature is below the phase transition point, so the moisture content of the sample changed a little; thus the dielectric constant can be regarded as constant. Similarly, thermal conductivity of the sample is also regarded as a constant.

(iv) The heat transfer occurs only in the sample. Because of the shorter research time, and the thermal conductivity of the stationary air being smaller than the solid thermal conductivity, the heat transfer of the air in the microwave oven can be neglected in this study.

2.2. Physical Model. As shown in Figure 1, the physical model consisted of a microwave oven cavity, a waveguide, a glass tray, and a potato sample (with different shapes other than the one shown in Figure 1), and the cavity and rectangular waveguide were made of copper and the size of cavity was length $w_O = 0.267$ m, width $d_O = 0.27$ m, and height $h_O = 0.188$ m and the rectangular waveguide was length $w_g = 0.05$ m, width $d_g = 0.078$ m, and height $h_g = 0.018$ m. Glass tray in the microwave electromagnetic field was regarded as transparent medium, and no heat was generated. In

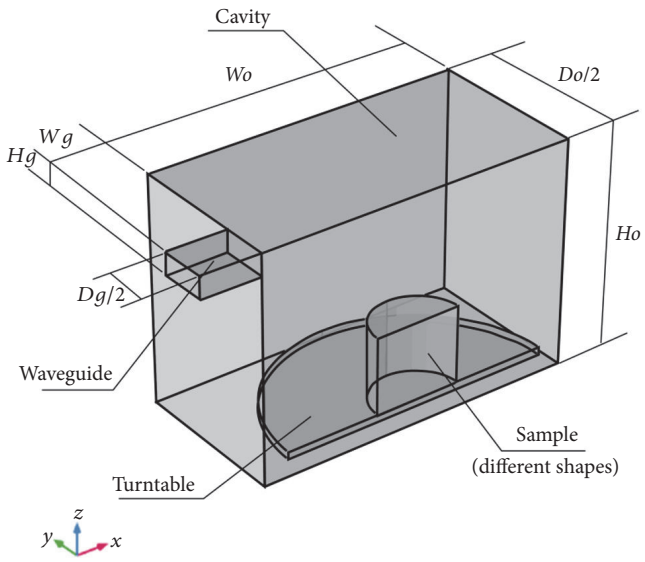

Figure 1: Schematic diagram of physical model.

order to reduce the amount of calculation and improve the computational efficiency, a symmetric model was established. The potato samples were in different shapes (sphere, ellipsoid, cylinder, cuboid, etc.), different sizes, and different position orientations.

2.3. Mathematical Model

2.3.1. Electromagnetic Field Model Establishment. The electromagnetic field distribution in the sample, microwave cavity, and waveguide was described by the Maxwell equations as follows:

$$\begin{aligned} \nabla \cdot \vec{D} &= \rho_{\text{ele}} \\ \nabla \times \vec{E} &= -\frac{\partial \vec{B}}{\partial t} \\ \nabla \cdot \vec{B} &= 0 \\ \nabla \times \vec{H} &= \vec{j} + \frac{\partial \vec{D}}{\partial t}, \end{aligned} \tag{1}$$

where $\vec{D}$ is the electric flux density, $\vec{E}$ is the electric field intensity, $\vec{B}$ is the magnetic flux density, $\vec{H}$ is the magnetic field intensity, ρ_{ele} is the source of the electric field, and $\vec{j}$ is the current density.

The constitutive equations describing the interaction between material and electromagnetic wave in electromagnetic field were presented as follows:

$$\begin{aligned} \vec{D} &= \varepsilon_0 \varepsilon_r \cdot \vec{E} \\ \vec{B} &= \mu_0 \mu_r \cdot \vec{H} \\ \vec{j} &= \sigma \cdot \vec{E}, \end{aligned} \tag{2}$$

where ε_r is the relative permittivity, μ_r is the relative permeability, σ is the conductivity, ε_0 is the permittivity of free space ($\varepsilon_0 = 8.854 \times 10^{-12}$ F/m), and μ_0 is the permeability of free space ($\mu_0 = 4\pi \times 10^{-7}$ H/m).

In the physical model, no conduction current existed in the microwave cavity and sample, and both of the electric and magnetic field were passive field; thus in this case the following can be concluded: $\rho_{\text{ele}} = 0$, $\vec{j} = 0$. The wave equation in microwave cavity was as follows:

$$\nabla \times \mu_r^{-1} (\nabla \times E) - k_0^2 \varepsilon_r E = 0, \tag{3}$$

where k_0 is electromagnetic wave in free space, described as

$$k_0 = \omega \sqrt{\varepsilon_0 \mu_0}. \tag{4}$$

2.3.2. Heat Transfer Model Establishment. The samples were treated as solid, interacted with electric field, and generated heat in the food interior. The electromagnetic heat then transferred to the low temperature part in the way of conduction. The heat transferred ability of the sample and its surrounding environment was low because of still air around the sample. Therefore, only heat conduction in the sample was considered, and that in the surrounding environment was neglected. Besides, water evaporation of the sample was also neglected due to the low water evaporation rate in the period before the phase transition temperature of the hot spot. The microwave electromagnetic energy was used as heat source to couple the electromagnetic energy with the energy equation. The heat transfer process was described as follows [29, 34]:

$$\begin{aligned} \rho C_p \frac{\partial T}{\partial t} &= \nabla \cdot (k \nabla T) + Q_{\text{mic}} \\ Q_{\text{mic}} &= \frac{1}{2} \omega \varepsilon_o \varepsilon'' |E|^2, \end{aligned} \tag{5}$$

where ρ is the density of the sample, C_p is the specific heat capacity, k is the thermal conductivity of the sample, T is the temperature, Q_{mic} is the microwave heat source, and ω is the angular frequency of microwave.

2.3.3. Initial Condition. Initial values of electromagnetic field components were all zero except the initial value of z directional electric field component, which was described as follows:

$$E_{z0} = \cos \frac{\pi y}{dg}. \tag{6}$$

Besides, initial ambient temperature was $T_{\text{atm0}} = 20^{\circ}\text{C}$, and the initial temperature of sample was $T_0 = 8^{\circ}\text{C}$.

2.3.4. Boundary Condition. The cavity and waveguide were considered as the copper wall resistance loss, using impedance boundary conditions to define the wall, described as follows:

$$\begin{aligned} &\sqrt{\frac{\mu_0 \mu_r}{\varepsilon_0 \varepsilon_r - j(\sigma/\omega)}} n \times H + E - (n \cdot E) n \\ &\quad = (n \cdot E_s) n - E_s. \end{aligned} \tag{7}$$

Table 1: Physical parameters of potato samples.

Symbol	Value	Unit	Description
ε'	58	1	Dielectric constant
ε''	13	1	Dielectric loss coefficient
μ_r	1	1	Magnetic permeability
σ	0	S/m	Conductivity
k	0.648	W/(m·K)	Thermal conductivity
ρ	1067	kg/m^3	Density
C_p	3630	J/(kg·K)	Specific heat capacity

The plane of symmetry used electrical conductor boundary conditions to eliminate the influence on the imaginary plane of the simulation process, by the following formula:

$$n \times H = 0. \tag{8}$$

The propagation constant of electromagnetic field was expressed by

$$\beta = \frac{2\pi}{c}\sqrt{f^2 - \frac{c^2}{4dg^2}}. \tag{9}$$

The whole simulation process was carried out under atmospheric pressure, and the pressure boundary conditions were set to 1 atm.

2.3.5. Sample Parameters. The sample was potato, and the related parameters of the sample were shown in Table 1 [35].

3. Results and Discussion

In order to verify the accuracy of the mathematical model of this article, this model was used to calculate the physical model in [27]; the specific calculation process was not expressed in this article. The calculated results were compared with the results in [27], as shown in Figure 2. It can be seen from the diagram that the results obtained by the mathematical model in this paper are close to the results in the literature, but the temperature rise rate is slightly larger than that in literature. Therefore, the mathematical model selected in this paper could basically meet the needs of the research.

In Figure 3, there were several typical temperature distribution results of potato examples with same calculation conditions except for shape or orientation. It can be clearly seen in the figures that examples with different shapes or orientations formed some hot spots in different position in different time. Obviously, the hot spots must be the first positions to reach the phase transition temperature, and at the same time temperature at other positions of the food sample would be lower than that of hot spots. In Figure 3, the deeper red color indicated the lower temperature, and on the contrary the brighter yellow color indicated the higher temperature. Meanwhile, the images in the same row showed the whole heating process from the beginning to the time that the maximum temperature of the hot spots reached the

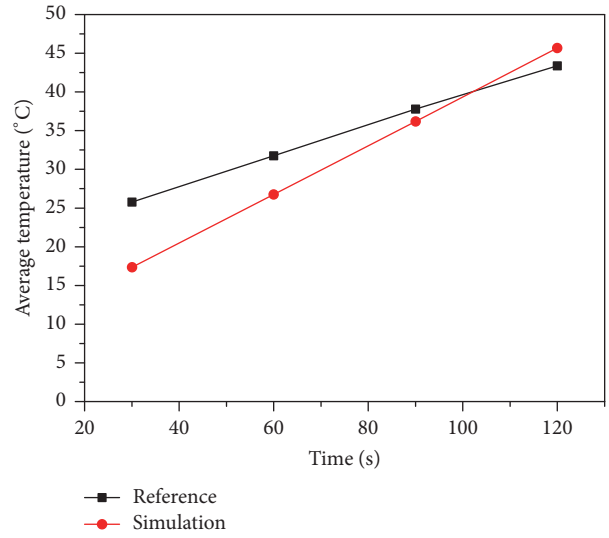

Figure 2: Model validation.

phase transition temperature. It is not difficult to conclude from Figure 3 that when the hot spots reach the phase transition temperature, the internal temperature distribution of the potato samples changes with shape or orientation of the sample. For the microwave treatment process of different samples, a process with good uniformity, high absorption power efficiency, small temperature difference, and short time is expected. Therefore, it is of great practical significance to study the influence of sample shape on the initial temperature field establishment of microwave process.

3.1. Microwave Power Input Effect. Heating power is the energy applied to the samples, partially producing dielectric heating effect [36]. The increasing or decreasing of input power directly affects the heat generated in the sample per unit time, then the heating rate of the sample is affected as well. The hot spots formed in the sample, as shown in Figure 3, would firstly reach the boiling point at each input power. There were some microwave power distribution grayscale color map images of the elliptical sample in reference [22], which was corresponding to the hot spots in the ellipsoid shaped samples in 2D. Studies focused on the period before the phase transition temperature was conducted and obtained the temperature field establishment process.

From Figure 4 it can be seen that the maximum temperature within a cylinder sample with radius 0.016 m and height 0.05 m reached the phase transition temperature after being heated by different input power within 200 s (except for 10 W). The greater the input power, the shorter the time it takes to reach the phase transition temperature. The PAE of microwave power is about 0.63 and remains constant during the process due to the constant dielectric loss coefficient of the sample and constant input power under the specific study condition. Therefore, before the hot spots reach the phase transition temperature, input power of the microwave has little effect on PAE of the potato samples. The direct effect of the input power is the time it spent on reaching the phase

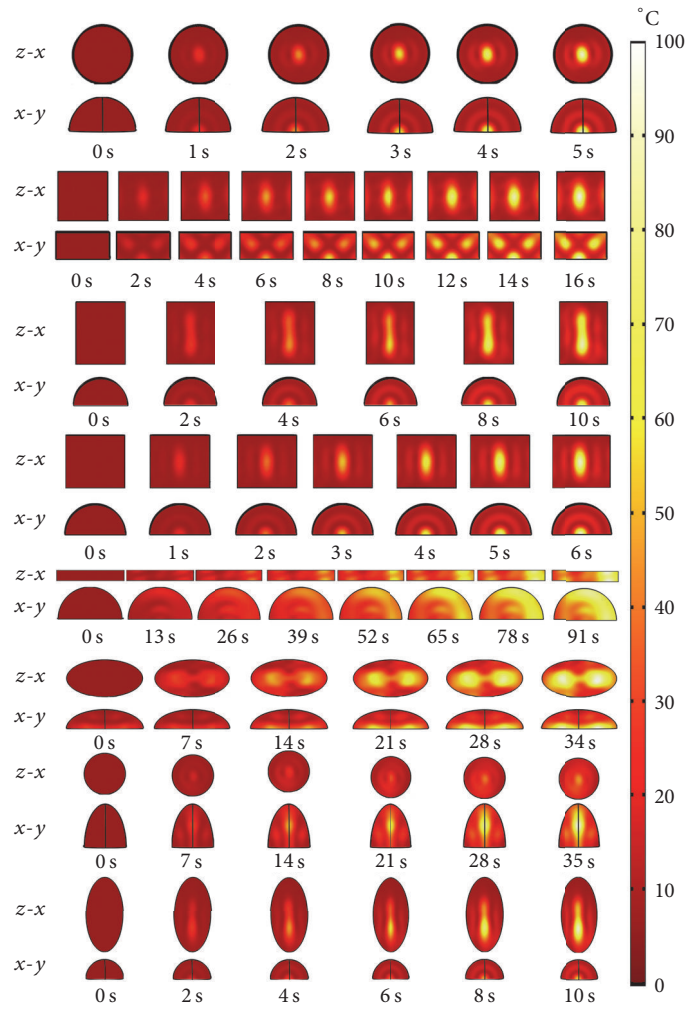

Figure 3: Hot spot in different samples.

transition temperature as shown in Figure 4; this is consistent with [30].

As we all know, energy consumption is an important measurement to a productive process, so the total energy of different input power consumed before the phase transition temperature should be considered to choose an optimal input power. As the curve has shown in Figure 5, it indicates that when the internal hot spots reach the phase transition temperature, the total energy consumption decreases from 4116 J to 630 J corresponding to the input power increasing from 10 W to 200 W. Besides, when the input power is larger than 80 W, the total energy consumption tends to be stable from the curve in Figure 5. Taking the previous work into consideration, it suggests that properly increasing input power will reduce energy consumption.

Figures 6 and 7 show the potato samples' temperature uniformity. In Figure 6, curves indicate the COV time variation of different input power before the internal hot spots reach the phase transition temperature (except 10 W). It can be grasped that COV history of the sample internal temperature distribution tends to be level-off for the relatively lower input power but increases linearly for the higher ones; both of the phenomena can be seen in [29]. For the lower input power, it takes a relatively long time to reach the phase transition temperature, and during this period heat generated in the penetration depth is conducted to the lower temperature locations, which makes a positive effect of the temperature uniformity. As for the higher input power, hot spots reach the phase transition temperature in a short time, during which the heat generated in the penetration depth cannot be adequately conducted to the lower temperature locations; as a consequence the temperature uniformity is worse under these circumstances.

The final COV-input power curve at the hot spots phase transition moment can be seen in Figure 7. It demonstrates that when input power is larger than 80 W, the final COV remains about 0.5 as the input power rises, while when the input power is less than 80 W, the final COV increases from about 0.3 to 0.5 as the input power rises. The reason why the final COV tends to be stable can be attributed to same penetration depth [24] and short time before the hot spots phase transition moment. From the equations in [24], the penetration depth of a microwave process depends on the microwave frequency and the sample's dielectric properties

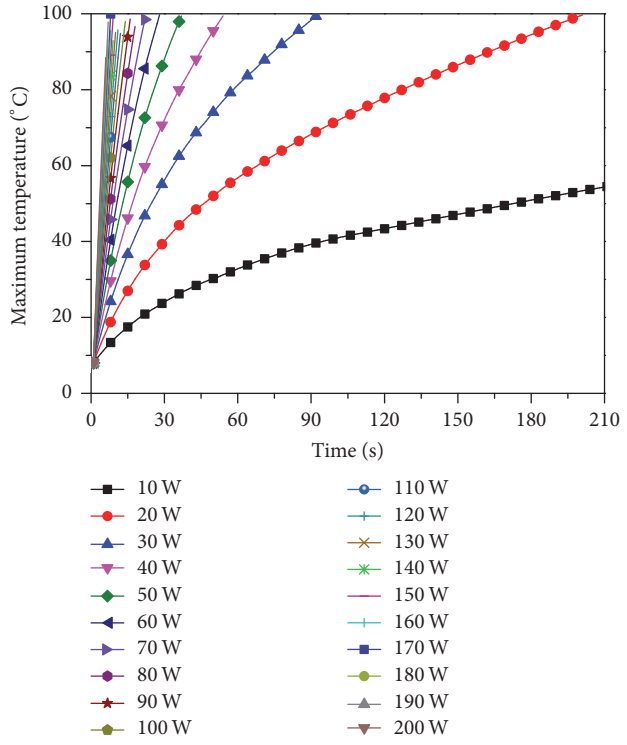

Figure 4: Maximum temperature of different input power.

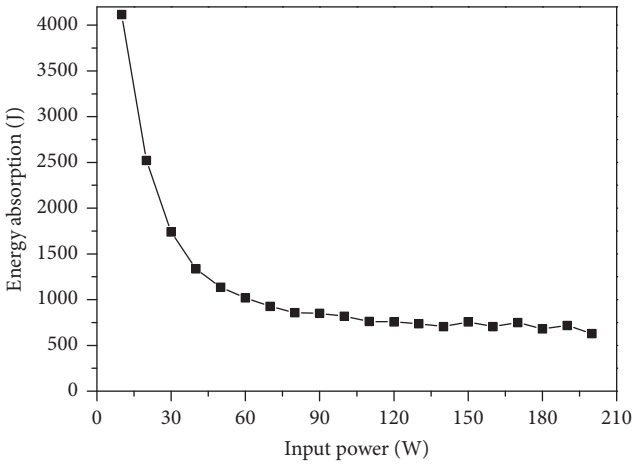

Figure 5: Energy consumption of different input power.

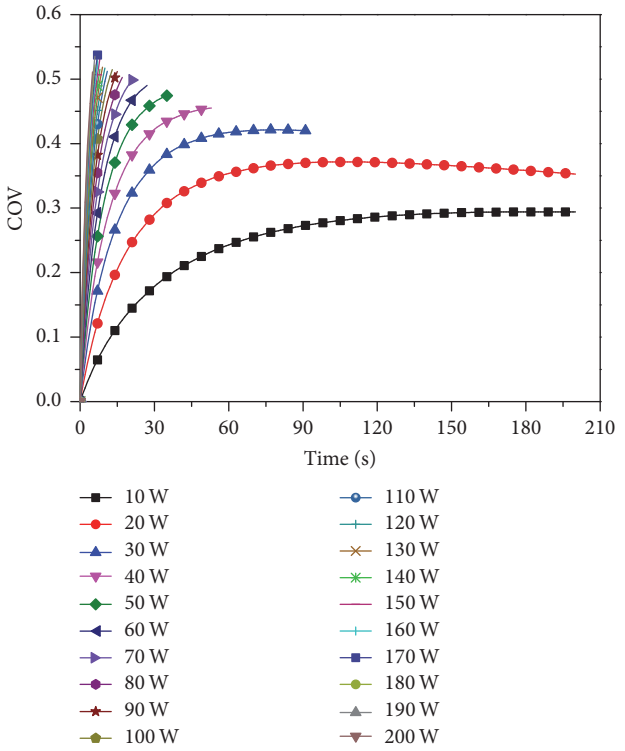

Figure 6: Time variation of temperature uniformity.

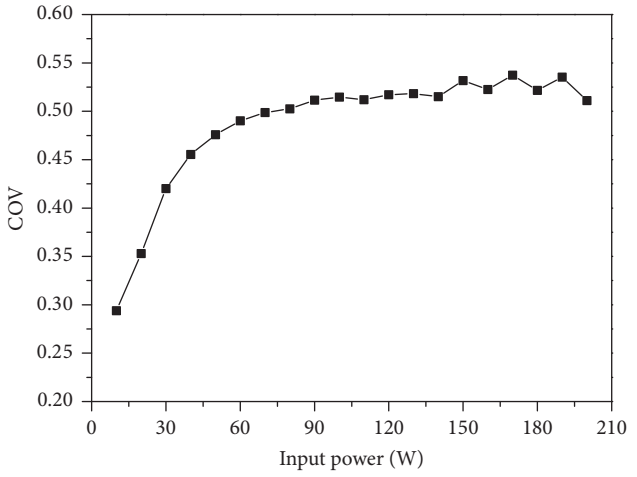

Figure 7: Temperature uniformity of different input power.

which in our study remain constant, so it can be concluded that during the microwave process in this case the heat generated in the penetration depth of the potato sample remains constant, too. Besides, when input power is larger than 80 W, the time for rising temperature is shorter than that used to heat conduction, so the heat generated almost stays within the area of penetration depth. Thus, the COV values of internal temperature distribution stay constant. From Figure 7, it can be also concluded that lower input power can make a better temperature uniformity, and with the increasing of input power, the uniformity of temperature becomes worse, the same conclusion was drawn in reference [30].

To sum up, relatively low input power leads to a more uniform temperature distribution in potato samples, but excessive pursuit of uniform temperature reduces heating efficiency and increases energy consumption. Relatively high input power can dramatically shorten heating time and decrease energy consumption, but the uniformity in potato samples at the phase transition time becomes worse. Therefore, in order to consume less energy and get more uniform temperature distribution, it is necessary to choose a proper input power for specific samples.

Table 2: Geometric characteristics dimension of different shape potato samples.

Number	Shape	Characteristics dimension (10^{-3} m)		
		V1 (m^3) = 1.64×10^{-5}	V2 (m^3) = 6.25×10^{-5}	V3 (m^3) = 13.11×10^{-5}
(1)	Sph.	*R*19.851	*R*31.018	*R*39.702
(2)	Cub.	L32	L50	L64
(3)	Cyl.1	*R*16 – *H*40.7	*R*16 – *H*155.4	
(4)	Cyl.2	*R*25 – *H*16.7	*R*25 – *H*63.7	*R*25 – *H*133.5
(5)	Cyl.3	*R*32 – *H*10.2	*R*32 – *H*38.9	*R*32 – *H*81.5
(6)	Cyl.4	*R*50 – *H*4.2	*R*50 – *H*15.9	*R*50 – *H*33.4
(7)	Cyl.5	*R*64 – *H*2.5	*R*64 – *H*9.7	*R*64 – *H*20.4
(8)	Ell.1	*x*32 – *yz*15.6	*x*32 – *yz*30.5	*x*32 – *yz*44.2
(9)	Ell.2	*y*32 – *xz*15.6	*y*32 – *xz*30.5	*y*32 – *xz*44.2
(10)	Ell.3	*z*32 – *xy*15.6	*z*32 – *xy*30.5	*z*32 – *xy*44.2
(11)	Ell.4	*x*50 – *yz*12.5	*x*50 – *yz*24.4	*x*50 – *yz*35.4
(12)	Ell.5	*y*50 – *xz*12.5	*y*50 – *xz*24.4	*y*50 – *xz*35.4
(13)	Ell.6	*z*50 – *xy*12.5	*z*50 – *xy*24.4	*z*50 – *xy*35.4
(14)	Ell.7	*x*64 – *yz*11.1	*x*64 – *yz*21.6	*x*64 – *yz*31.3
(15)	Ell.8	*y*64 – *xz*11.1	*y*64 – *xz*21.6	*y*64 – *xz*31.3
(16)	Ell.9	*z*64 – *xy*11.1	*z*64 – *xy*21.6	*z*64 – *xy*31.3

3.2. Sample Shapes Effect. In microwave processing various shapes of samples may be dealt with. This part mainly focused on the samples' shape effect on microwave power absorption capability and temperature distribution uniformity of potato samples before the internal hot spots reach the phase transition temperature. The sample shape can be simplified as sphere, cube, cylinder, ellipsoid, and cuboid. In the course of this section, except for the sample shape, all properties including physical and geometric properties of the sample were set to be the same. Input power was 90 W. There were three groups of samples classified by volume, as shown in Table 2 (the blank indicates the characteristics size of the sample is beyond the computational domain). These samples were placed in the middle of the glass tray. Samples number 1 and number 2 are sphere and cube, which have only one characteristics dimension. The samples who have more than one characteristics dimension, namely, number 3 to number 7, are cylindrical samples with increasing radius and decreasing height, and number 8 to number 16 are three groups of ellipsoidal samples placed in different axis directions. When the internal hot spots reached the phase transition temperature, samples' power absorption efficiency (PAE) and temperature distribution uniformity (COV) were shown in Figures 8 and 9, respectively.

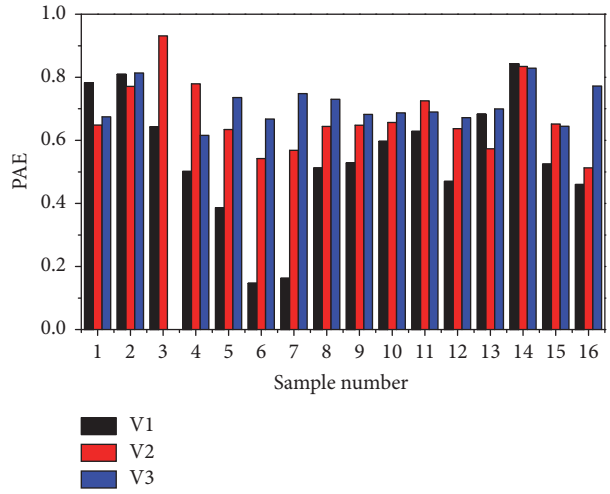

Figure 8: PAE of different shape.

In Figures 8 and 9, it can be clearly seen that the PAE and COV values of spherical samples are less than those of isometric volume cubic samples. In detail, the sphere samples' PAE of V1, V2, and V3 are 0.78, 0.65, and 0.67, respectively, which are less than those of corresponding cubic samples 0.81, 0.77, and 0.81. Similarly, the sphere samples' COV values of V1, V2, and V3 are 0.45, 0.42, and 0.47, respectively, which are less than those of cubic samples 0.50, 0.56, and 0.56. Therefore, there is an enhancement of power absorption capability and a detriment of temperature distribution uniformity for cubic samples in contrast to spherical ones. The differences between spherical and cubic samples on power absorption capability and temperature distribution uniformity mainly originate from the focusing tendency of microwave at the samples' corners and were concluded in the two-dimension simulation of reference [37] and can be also seen in the result diagram of cubic sample in Figure 3. Further comparison between spherical and cubic samples will be discussed in Section 3.2.1.

Contrasting the PAE and COV values of number 3 to number 7 isometric volume cylindrical samples in Figures 8 and 9, an obvious fluctuation with the increasing radius and decreasing height can be seen, but the position of extreme values is unfixed for different volume sample groups. Similar phenomena can be seen by contrasting the samples of number 8, number 11, and number 14 (similar comparisons

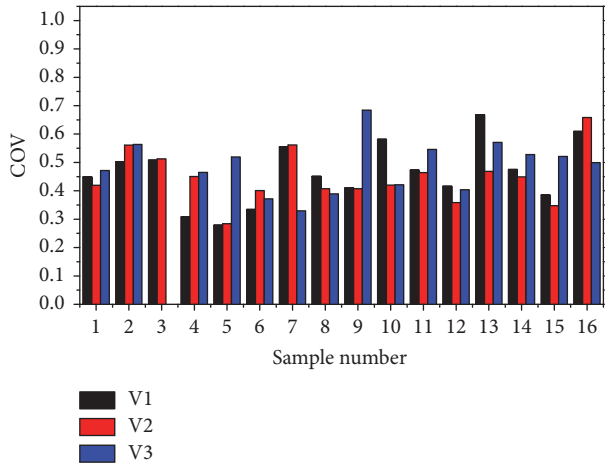

Figure 9: COV of different shape samples.

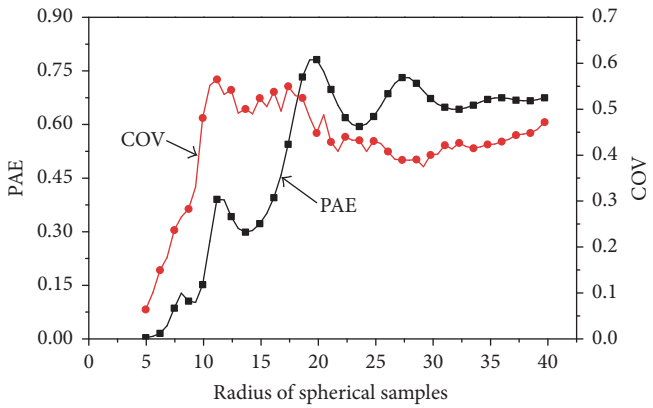

Figure 10: PAE and COV of sphere.

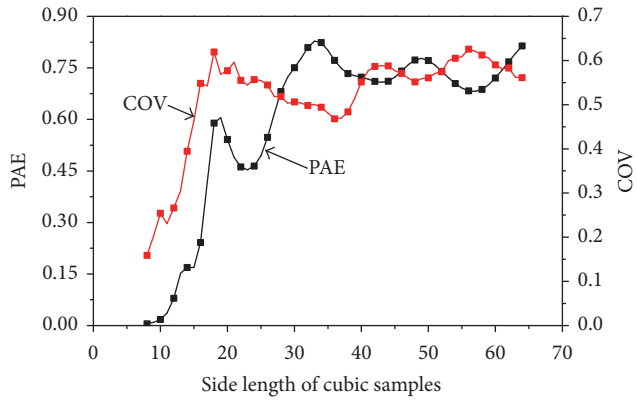

Figure 11: PAE and COV of cube.

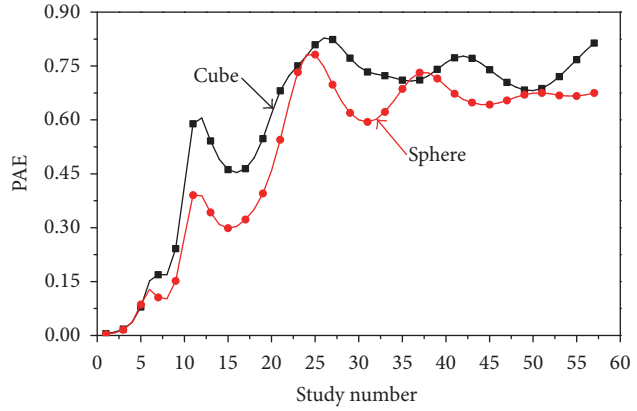

Figure 12: PAE comparison of cubic and spherical sample.

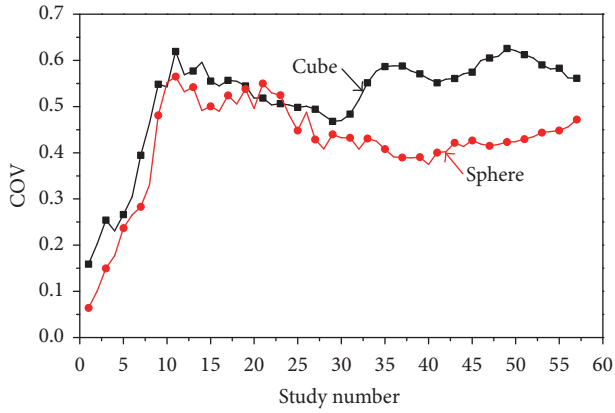

Figure 13: COV comparison of cubic and spherical sample.

are number 9, number 12, and number 15, or number 10, number 13, and number 16). It will be discussed further in Section 3.2.2.

By contrasting the PAE and COV values of number 8 to number 10 samples (similar comparisons are number 11 to number 13, or number 14 to number 16), there are obvious changes of different placement directions, and the variation tendency may increase, wave, or decrease. Therefore, being treated in a single port microwave oven, placement direction of a sample has also a significant effect on samples' power absorption capability and temperature distribution uniformity, which will be discussed in Section 3.3.

3.2.1. Spherical and Cubic Sample. In this section, a comparative study of spherical and cubic samples was conducted. Spherical samples' radii were from 0.005 m to 0.04 m, and the corresponding isometric volume cubic samples' side length were from 0.008 m to 0.064 m at an interval of 0.001 m, and the isometric volume samples were numbered from number 1 to number 57. The input power was 90 W, and the two groups of samples were heated to the moment when the temperature of the internal hot spots reached phase transition temperature. Figures 10 and 11 presented the PAE and COV values of the two series of samples, separately. PAE and COV values comparisons between cubic and spherical samples are shown in Figures 12 and 13. Figures 14 and 15 indicate some typical intuitive calculation results of electromagnetic field and temperature distribution.

The black curve in Figure 10 indicates the PAE values of spherical samples with increasing radii. It can be clearly seen that small radii spherical samples' capacity of absorbing

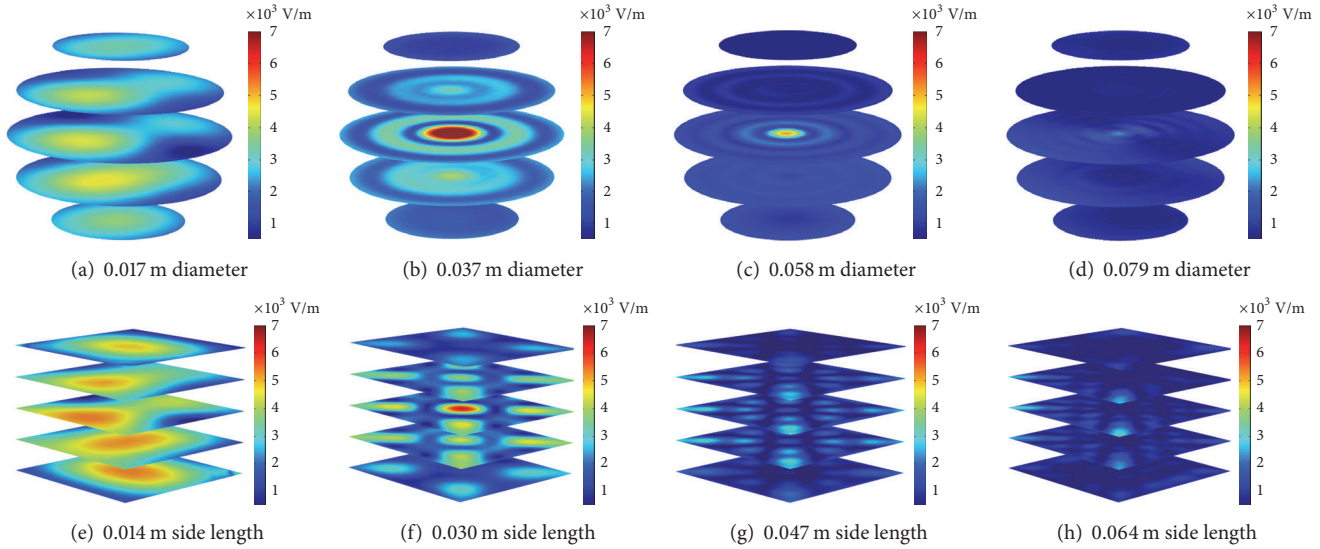

(a) 0.017 m diameter (b) 0.037 m diameter (c) 0.058 m diameter (d) 0.079 m diameter

(e) 0.014 m side length (f) 0.030 m side length (g) 0.047 m side length (h) 0.064 m side length

Figure 14: Spatial distribution of electromagnetic field in samples.

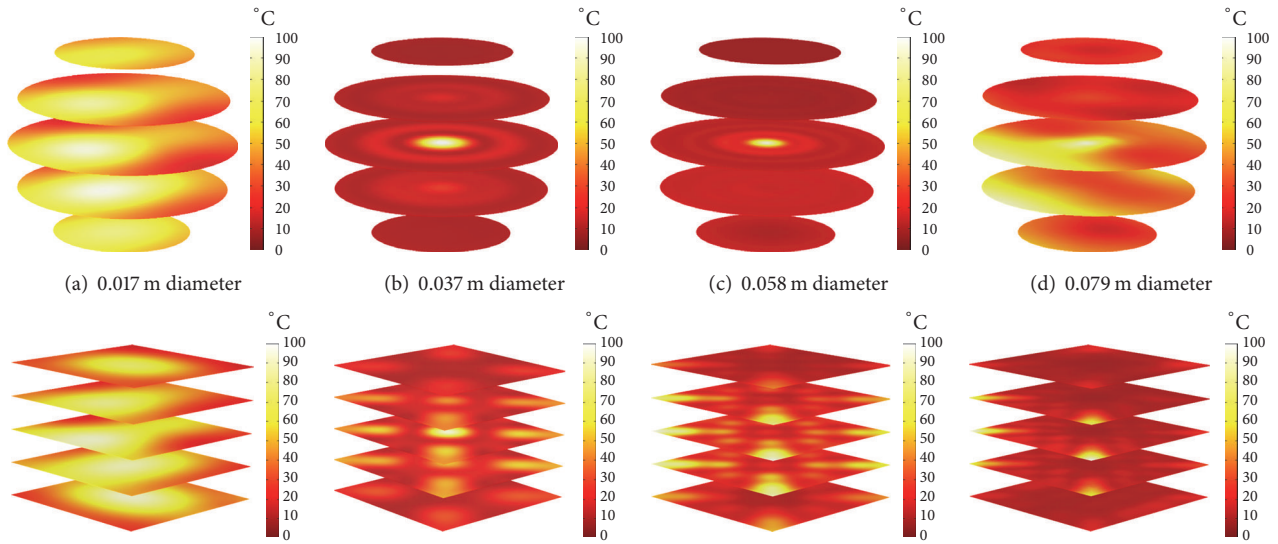

(a) 0.017 m diameter (b) 0.037 m diameter (c) 0.058 m diameter (d) 0.079 m diameter

(e) 0.014 m side length (f) 0.030 m side length (g) 0.047 m side length (h) 0.064 m side length

Figure 15: Spatial distribution of temperature in samples.

energy is low in contrast to the larger ones, and the PAE values of spherical samples increase as the radii rise. These phenomena were also shown in [38]. The lower PAE values of small spherical samples are resulting from the low temperature rising rate of these samples and lead to a better temperature distribution uniformity in the smaller samples. Likewise, higher PAE values of larger spherical samples would lead to worse temperature uniformity. Therefore, the red curve in Figure 10 represents the COV values being lower in the small samples and rises to higher values when the radii increase.

Interestingly, by contrasting the two curves in Figure 10, when spherical samples' radii increase, the COV curve firstly reaches an extreme value when the corresponding PAE value is still at a lower position. This maxima of COV values resulted from the focusing effect at internal local positions of samples [38]. Then when the samples' volume becomes large, the PAE curve stays stable, while the COV curve tends to increase. This phenomenon is due to the samples' large size which leads to heating only near the surface [38]. For the cubic samples' power absorption efficiency and COV curves in Figure 11, we can also find similar phenomena to the previous study of spherical samples. So phenomena in Figure 11 can be explained by the previous theory as well.

By contrasting the corresponding curve values of these two kinds of samples shown in Figures 12 and 13, there exist enormous differences caused by shape. Figure 12 shows the PAE values of equal volume cubic and spherical samples; it

can be directly seen that most of the red curve is below the black one which means that in most cases cubic samples' capacity of absorbing microwave power is better than that of spherical ones. Similarly in Figure 13 the red curve is below the black one at most locations, which indicates that in most cases the temperature distribution uniformity of spherical samples is better than cubic samples.

Quantitatively, the PAE values of spherical samples range from 0.004 to 0.782, while those of cubic samples range from 0.005 to 0.828. Only for number 4, number 5, number 24, and number 36 to number 38 studies, cubic samples' values are lower than the spherical ones. Meanwhile, the COV values of spherical samples range from 0.064 to 0.565, and those of cubic samples range from 0.159 to 0.626. Only for number 10 and number 21 to number 23 studies, cubic samples' COV values are lower than the spherical ones. Combining with the above two phenomena, for number 4, number 5, number 24, and number 36 to number 38 studies, spherical samples are better than cubic ones due to the high PAE and low temperature COV, and for number 10, and number 21 to number 23 studies, cubic samples are better than spherical ones because of the same reason. Except for the above samples the cubic samples all have higher PAE and higher temperature COV values, which means a better power absorption capability and worse temperature distribution uniformity. Therefore, in most cases when a microwave process needs a high PAE, cubic sample is better, while if temperature uniformity is more important, it is recommended to choose spherical samples.

For example, choosing four sizes that represent the small, intermediate, and large samples (number 7, number 23, number 40, and number 57 samples) from the spherical samples and the corresponding cubic samples, Figures 14 and 15 show the spatial distribution of electromagnetic field and temperature of the four kinds of samples. Results shown in Figures 14(a)–14(d) and 15(a)–15(d) are quite similar with that of reference [38, 39], which verify the correctness of this model. Contrasting Figures 14(a) and 14(e), 15(a) and 15(e), it can be concluded that when the samples are small, the internal electromagnetic field and temperature distribution are similar between cubic and spherical samples. Contrasting Figures 14(b) and 14(f), or Figures 14(c) and 14(g), the electromagnetic field distribution of intermediate size samples is quite different between cubic and spherical samples. In spherical samples the focusing appears in the center, while in the cubic samples the focusing appears in the center as well as near the corners, which tend to be cyclical generation as the side length increases. Therefore in Figures 15(b) and 15(f), or Figures 15(c) and 15(g), hot spots in spherical and cubic samples are different in the aspect of position and number. Contrasting Figures 14(d) and 14(h), the electromagnetic field of spherical samples moves towards the outer surface direction and that of cubic samples is mostly focused on the corners, the corresponding temperature distribution in Figures 15(d) and 15(h) shows similar phenomena.

According to Figures 10–15, the samples can be divided into four groups. (1) Small volume samples, whose PAE and COV value are both low; besides, internal electromagnetic field focusing and hot spots are not obvious, as shown in Figures 14(a) and 14(e) and Figures 15(a) and 15(e), respectively. (2) Low intermediate volume samples, whose PAE values are low, while the COV values are high due to the concentrated internal hot spots, which are caused by the intense focusing effect of electromagnetic field, as shown in Figures 14(b) and 14(f) and Figures 15(b) and 15(f). (3) High intermediate volume samples, whose PAE values are high, while the COV values are low. The reasons that caused these phenomena are less concentrated hot spots and less intense electromagnetic focusing effect, as shown in Figures 14(c) and 14(g) and Figures 15(c) and 15(g). (4) Big volume samples, whose PAE values tend to be low or stable, and the COV values increase. The electromagnetic focusing and hot spots move to the outer surfaces and sharp corners, as shown in Figures 14(d) and 14(h) and Figures 15(d) and 15(h). In this section, samples in Study 1~Study 7 can be classified into the first group, those in Study 8~Study 25 can be classified into the second group, those in Study 26~Study 40 can be classified into the third group, and those in Study 41~Study 57 can be classified into the last group.

In summary, when the isometric volume spherical and cubic samples' sizes are small, the microwave power absorption capability of both shapes is similar, but the temperature distribution uniformity of cubic samples is worse than that of spherical samples. So on this condition, it is recommended to make samples sphere in microwave heating progress. In the case of intermediate size, the spherical samples' electromagnetic field focusing is in the center, while that of cubic ones locates both in center and on corners that result in multiple hot spots, so the PAE values of cubic samples are higher, and COV values of spherical samples are lower or comparable to the cubic ones. Thus, for the intermediate size samples, it is recommended to select the shape of the sample according to the demand for power absorbing capability or temperature uniformity. As for the big size samples, electromagnetic field distribution of spherical samples moves towards outer surface and that of cubic samples focuses on corners. The PAE values of cubic samples are higher than spherical ones, but the internal temperature uniformity gets worse and worse. Therefore, for the big size cubic samples are unpractical due to the worse temperature uniformity resulting from the focusing on corners.

3.2.2. Cylindrical, Cuboidal, and Ellipsoidal Sample. For cylindrical, cuboidal, and ellipsoidal samples, the same volume may have a variety of size combinations; namely, same volume samples may have different combinations of axial size and radial cross-sectional area. Therefore, in this section, the cylindrical, cuboidal, and ellipsoidal samples are of the same volume of $1.64 \times 10^{-5}\,\mathrm{m}^3$; the samples' axial size is from 0.004 m to 0.163 m. The radial cross sections of cylindrical and ellipsoidal samples are circular, whose diameters are from 0.016 m to 0.100 m and from 0.0196 m to 0.1225 m, respectively, while the cross section of cuboidal sample is square, whose side length is from 0.0143 m to 0.0886 m.

As shown in Figure 16, cylindrical, cuboidal, and ellipsoidal samples of the same volume were placed in three directions. The correlation results can be obtained by contrasting

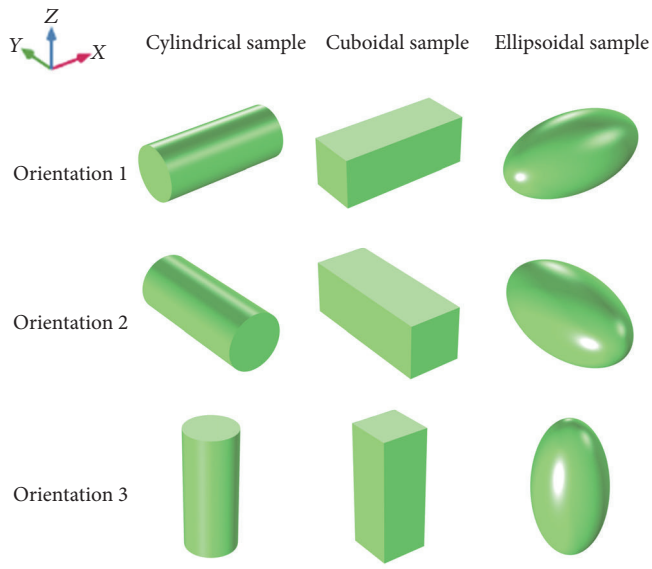

Figure 16: Sample diagram.

the different samples in same directions (horizontal) as well as the same sample in different directions (vertical), as discussed in this section and Section 3.3, respectively.

The thickness of samples can be described by wave number N_w and penetration number N_p defined as (10) in 2D problems [37]:

$$N_w = \frac{L}{\lambda_m}$$
$$N_p = \frac{L}{D_p}, \tag{10}$$

where L is the characteristic dimension, and for circular cross section samples L is the diameter, and for square cross section samples L is the side length. In addition, λ_m and D_p are the wavelength and penetration depth of microwave within the food material, which can be obtained from the following equations [37]:

$$\lambda_m = \frac{c\sqrt{2}}{f\left[\sqrt{\left(\varepsilon'\right)^2 + \left(\varepsilon''\right)^2} + \varepsilon'\right]^{1/2}}$$
$$D_p = \frac{c}{\sqrt{2}\pi f\left[\sqrt{\left(\varepsilon'\right)^2 + \left(\varepsilon''\right)^2} - \varepsilon'\right]^{1/2}}. \tag{11}$$

Thus, The wavelength and penetration depth within the potato samples of this section are 0.016 m and 0.023 m, respectively.

In the 2D study in [37], different shape food samples could be classified as thin ($N_w \leq 0.1$), intermediate ($N_w > 0.1$, $N_p < 3$), and thick ($N_p \geq 3$) size according to samples' wave number and penetration number on the cross-section plane. Similarly, in the 3D study of this section, potato samples can be classified on the XY-plane, YZ-plane, and ZX-plane in the same way. The wave numbers of three shapes samples on axial direction section are from 0.261 to 10.186, and the penetration numbers are from 0.181 to 7.086. The wave numbers on cylindrical, cuboidal, and ellipsoidal samples' radial middle cross section are, respectively, from 1 to 6.250, from 0.886 to 5.539, and from 1.225 to 7.655. The penetration numbers of them are, respectively, from 0.696 to 4.348, from 0.617 to 3.853, and from 0.852 to 5.352.

For the thin size samples the temperature distribution uniformity is invariant of the shape [37]. Therefore, in this section, all the samples locate in the regions of intermediate and thick size. Besides, according to the radial and axial wave number and penetration number, the samples can be further divided into three categories, namely, (1) Group 1: radial thick-axial medium samples, whose radial penetration number is $N_p^r > 3$ and the axial wave numbers and penetration numbers are $N_w^a > 0.1$ and $N_p^a < 3$; (2) Group 2: radial medium-axial medium samples, whose wave numbers and penetration numbers in radial and axial directions are all $N_w > 0.1$ and $N_p < 3$; (3) Group 3: radial medium-axial thick samples, whose radial penetration numbers are $N_w^r > 0.1$ and $N_p^r < 3$, and axial penetration numbers are $N_p^a > 3$. Intuitively, samples of Group 1 tend to be more flat, while those belonging to the Group 3 are more slender.

When the samples are placed in Orientation 1, the electromagnetic field distribution on radial middle cross section (YZ section) demonstrates unique characteristics of different samples; some typical results are shown in Figure 17. Images in Figure 17(a) belong to Group 1; the electromagnetic field focusing almost locates near the circular's surface and square's surface and corners. Images in Figures 17(b) and 17(c) show the inward focusing trend of samples in Group 2. Images in Figure 17(d) exhibit the electromagnetic focusing in the center of samples in Group 3. The above results are consistent with 2D results of thick turnip samples in [37].

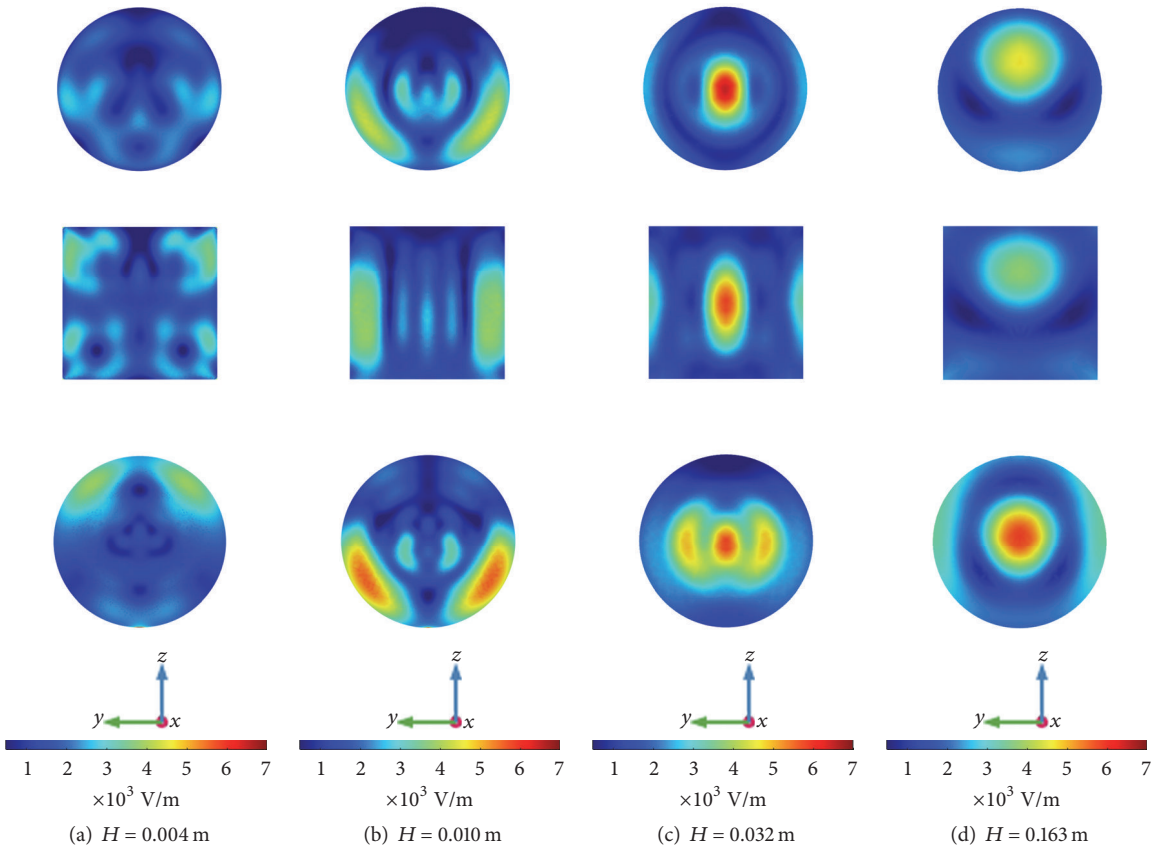

Figure 17: Electromagnetic field distribution on *YZ* radial middle cross section in Orientation 1.

Besides, the corresponding axial cross sections (*XY* section and *ZX* section) of these samples are shown in Figures 18 and 19. Considering the geometric optical properties of microwave, electromagnetic field in the cavity consists of the superposition of the original electromagnetic wave with that reflected by walls and samples' surfaces. Besides, the electromagnetic field in the foodstuff originates from the electromagnetic wave refracted from its surfaces [36]. In this section, the refraction surfaces of samples include two end surfaces and a cambered surface (as for cuboidal samples the cambered surfaces are those except for the two end surfaces).

Therefore, it is clear that when the size of axis is less than penetration depth and wavelength, the focusing is mainly caused by the microwave refracted from the cambered surface as shown in Figures 18(a) and 19(a).

As shown in Figures 18(b) and 19(b), sample's radial size is bigger than penetration depth and the axial size is comparable to wavelength, so the focusing appears separately near cambered surface as well as in the internal space due to the microwave refracted from cambered surface and end surfaces, respectively. For samples whose radial size and axial size are both close to the penetration depth, the microwave refracted from the cambered surface and the two end surfaces all play important roles in the internal electromagnetic wave propagation, and the results of intensive superposition are shown in Figures 18(c) and 19(c).

In Figures 18(d) and 19(d), sample's radial sizes are comparable to the wavelength, while the axial sizes are bigger than penetration depth. Thus, the electromagnetic focusing along the axis is mainly caused by the microwave refracted from the cambered surface, and only within the penetration depth region near end surfaces may microwave refraction from two end surfaces have an effect on the microwave superposition.

In Figures 17–19, we can find that the electromagnetic field distribution of same axial size samples presents similar tendency and local differences, and from the electromagnetic field distribution images it is not hard to obtain the distribution of temperature. However, from the intuitional visual images it is difficult to determine the optimal samples of high power absorption and uniform temperature distribution. Therefore, parameter of power absorption efficiency (PAE) is used to measure the samples' microwave power absorbing capability, and a higher PAE value is desired. Besides, coefficient of variation (COV) of samples' temperature is used for evaluating the internal temperature of samples, and the low COV value demonstrates a better temperature uniformity. Moreover, optimal sample should own high power absorption efficiency and low temperature COV value; thus the ratio of power absorption efficiency to temperature COV value (named comprehensive evaluation coefficient, CEC) can measure the samples' usability at a certain condition, and a

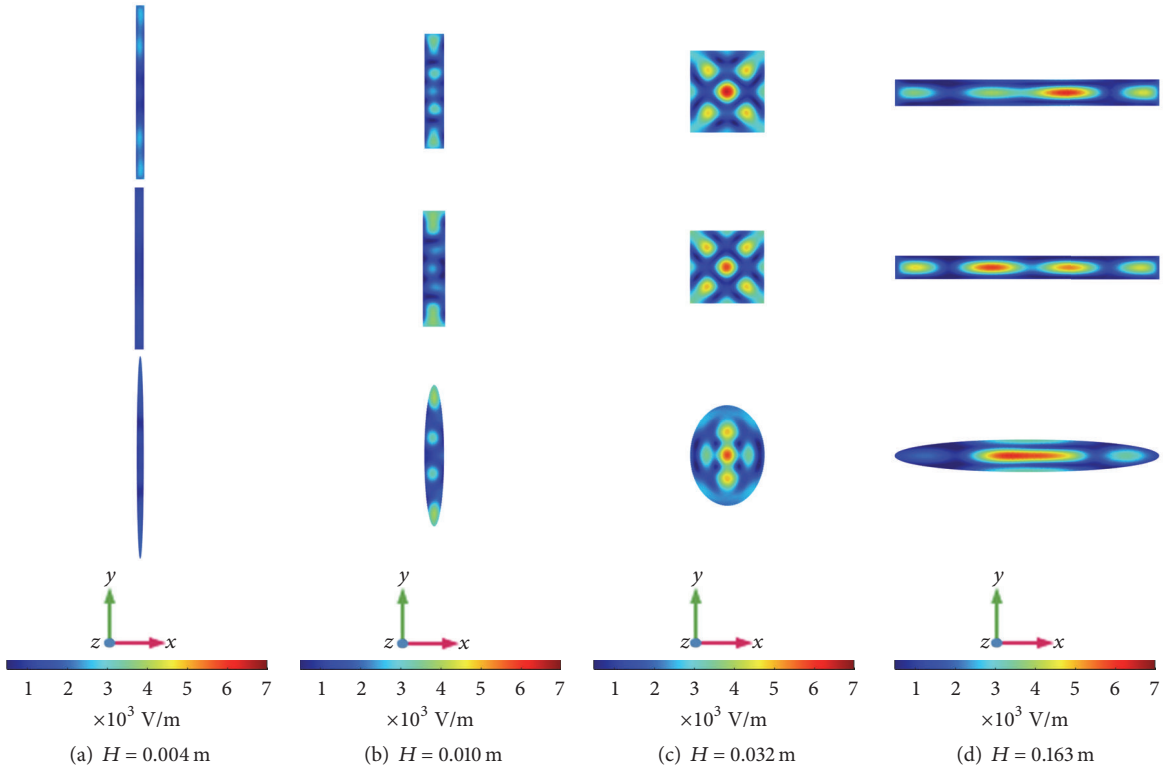

(a) $H = 0.004$ m (b) $H = 0.010$ m (c) $H = 0.032$ m (d) $H = 0.163$ m

FIGURE 18: Electromagnetic field distribution on *XY* axial middle cross section in Orientation 1.

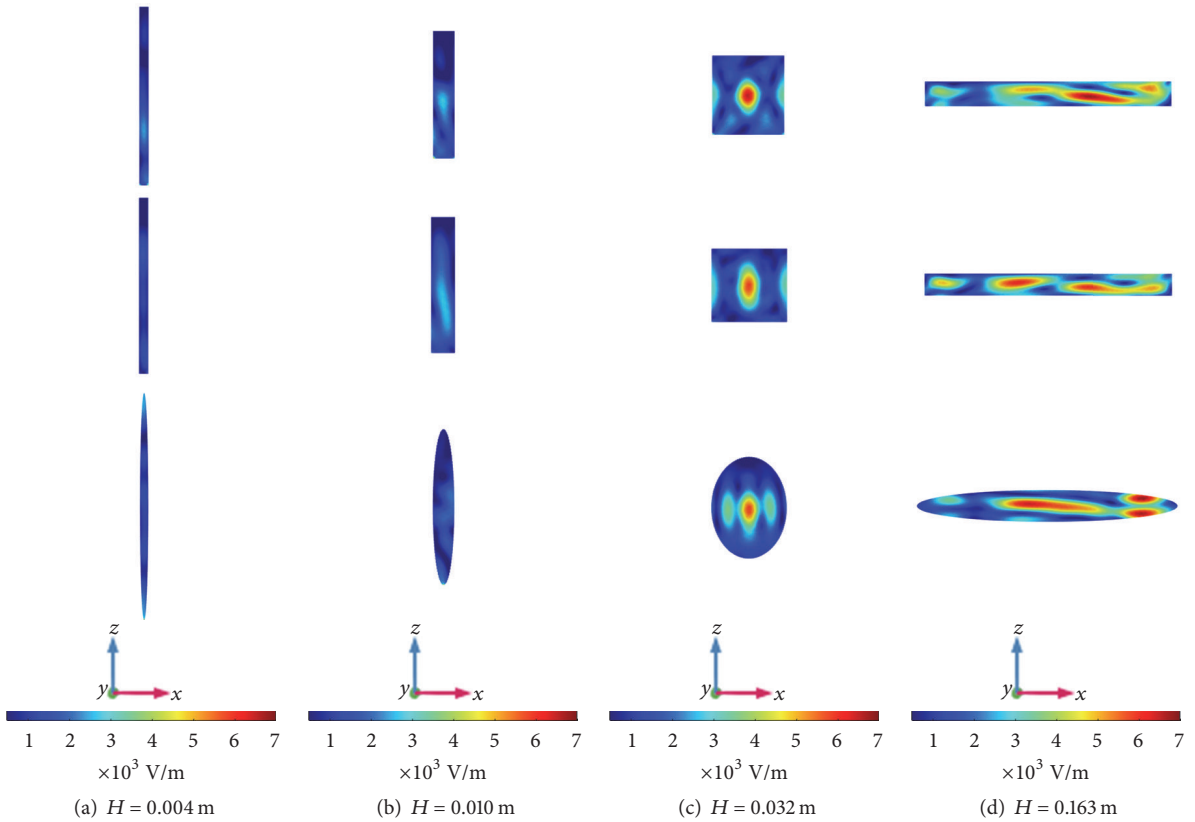

(a) $H = 0.004$ m (b) $H = 0.010$ m (c) $H = 0.032$ m (d) $H = 0.163$ m

FIGURE 19: Electromagnetic field distribution on *ZX* axial middle cross section in Orientation 1.

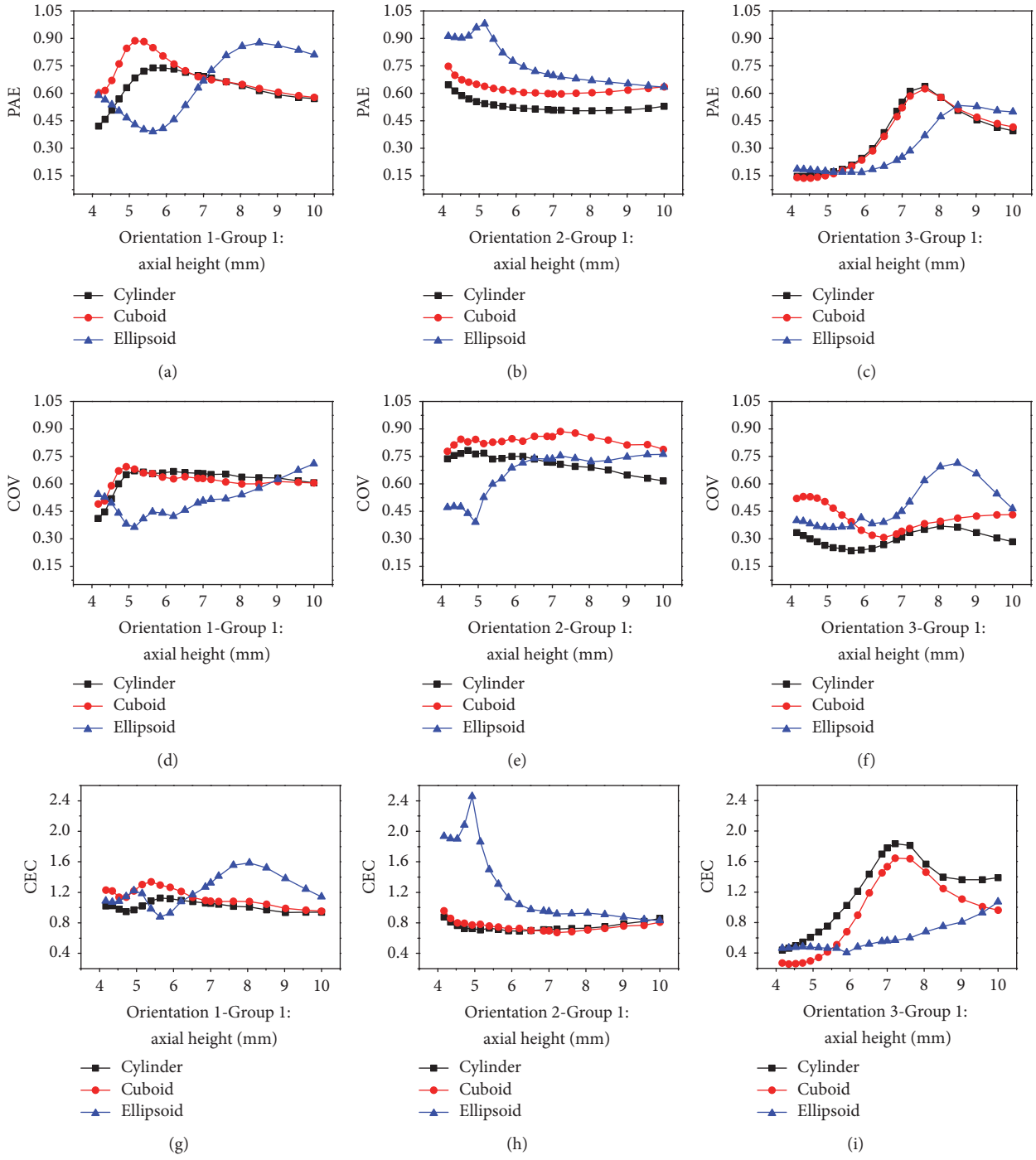

Figure 20: Different samples in the same orientations, Group 1.

higher CEC value presents a sample with a high PAE and/or low COV, which could be chosen according to specific needs of microwave process.

Curves in Figures 20(a)–20(c) (similarly in Figures 21(a)–21(c) and Figures 22(a)–22(c)) give the PAE values of these three shape samples in different orientations. Besides, when the internal hot spots reach the phase transition temperature, curves in Figures 20(d)–20(f) (similarly in Figures 21(d)–21(f) and Figures 22(d)–22(f)) demonstrate the temperature COV values of three shape samples in different orientations. Figures 20(g)–20(i) (similarly Figures 21(g)–21(i) and Figures 22(g)–22(i)) give the corresponding CEC curves of the three shape samples in different orientations.

In Figures 20(a), 20(d), and 20(g), the figures suggest that, in Orientation 1, cylindrical, cuboidal, and ellipsoidal samples' PAE values have maximal values which are 0.74, 0.89, and 0.88, and the corresponding COV values are also located

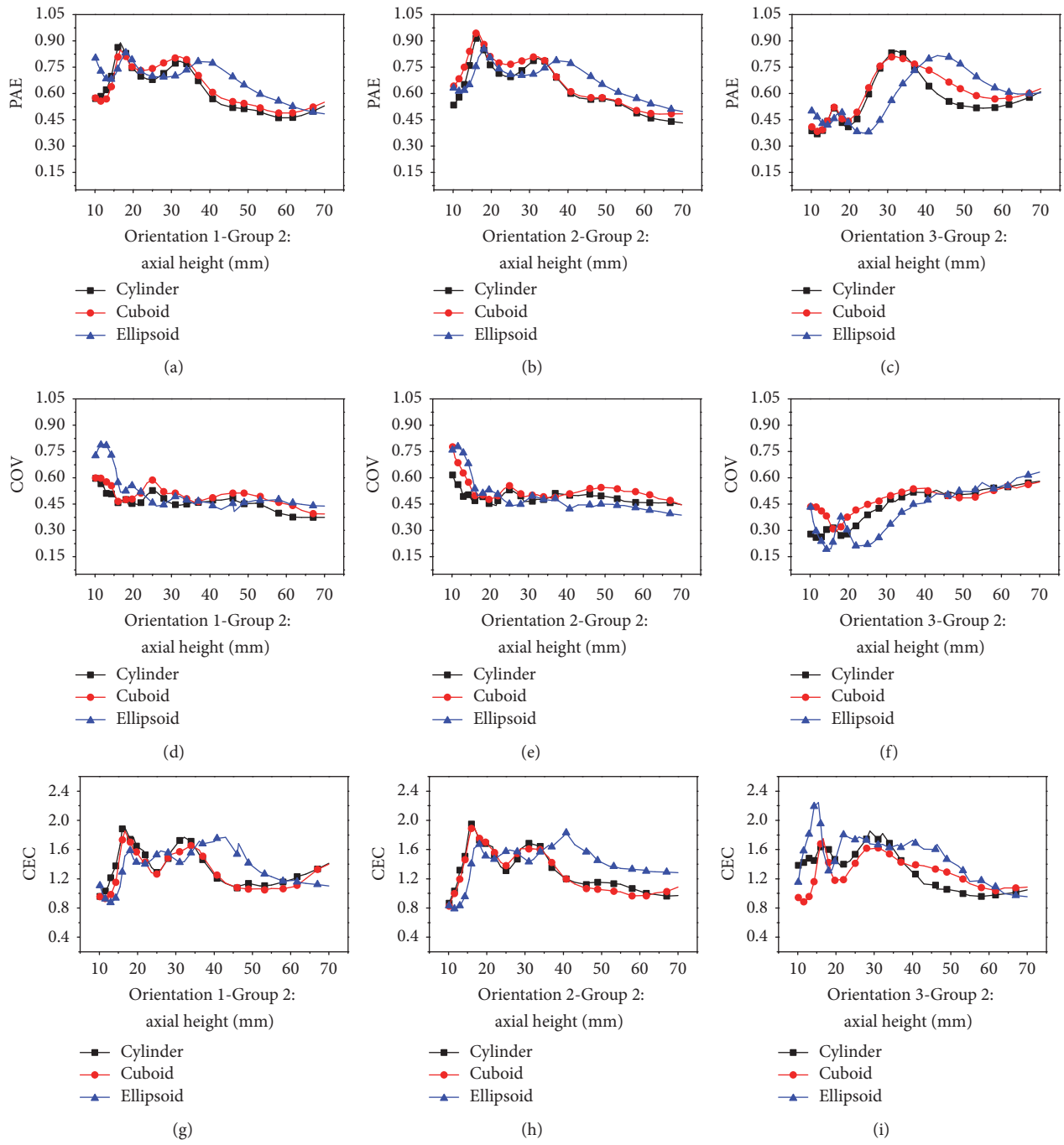

Figure 21: Different samples in the same orientations, Group 2.

near the maximal values except ellipsoidal sample. Thus from Figure 20(g) it can be concluded that when samples of Group 1 are placed in Orientation 1, sample of ellipsoidal shape is better than cylindrical and cuboidal ones due to relatively high PAE and low temperature COV. Similarly, in Figures 20(b), 20(e), and 20(h), when samples are placed in Orientation 2, ellipsoidal shape is also the best choice. However when samples are placed in Orientation 3 as shown in Figures 20(c), 20(f), and 20(i), cylindrical shape samples are better than the other two shapes for the same reason.

PAE, COV, and CEC value curves of different samples in Group 2 are shown in Figure 21. From the curves in Figures 21(g)–21(i), it can be concluded that when samples' axial sizes are lower than 0.040 m, samples' CEC values are all comparable. The reason causing this phenomenon is that the radial and axial sizes of samples are all comparable to the penetration depth or wavelength, and thus intensively electromagnetic field focusing would happen to enhance the heating effect. Among this range, samples' shape effect can be ignored, and all these three shape samples can obtain good

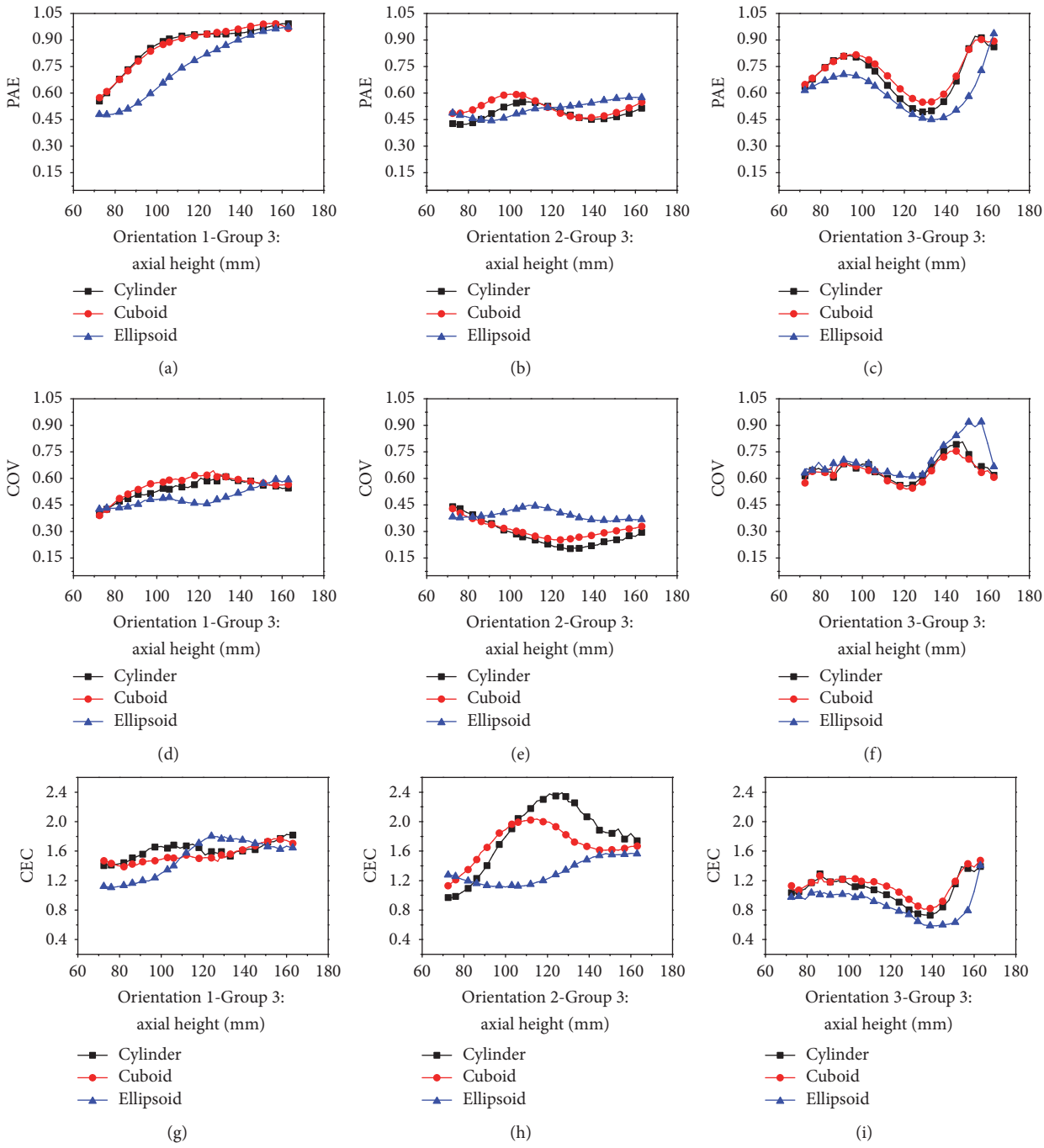

Figure 22: Different samples in the same orientations, Group 3.

heating results. Beyond this range ellipsoidal shape would be better because of the higher PAE and/or lower COV.

PAE, COV, and CEC of samples in Group 3 are shown in Figure 22. When placed in Orientation 1, cylindrical samples are the first choice due to the higher PEA and relatively lower COV as shown in Figures 22(a), 22(d), and 22(g). Cylindrical and cuboidal shapes are better than ellipsoidal shape when placed in Orientation 2. Besides, if temperature uniformity is more decisive, cylindrical shape is the best. When placed in Orientation 3, cuboidal shape should be firstly selected.

Taking all samples in the three groups into consideration, in Figures 23–25, every curve is divided into three parts: the left unmarked part separately indicates the PAE, COV, and CEC values of the samples belonging to Group 1 and the middle part and right part represent Group 2 and Group 3 as marked in figures.

In Figure 23(a), it can be seen that, for all samples whose axial sizes are in the range of 0.004 m to 0.163 m, cylindrical and cuboidal samples' PAE values are almost equal to each other in Orientation 1. The PAE value curve of ellipsoidal

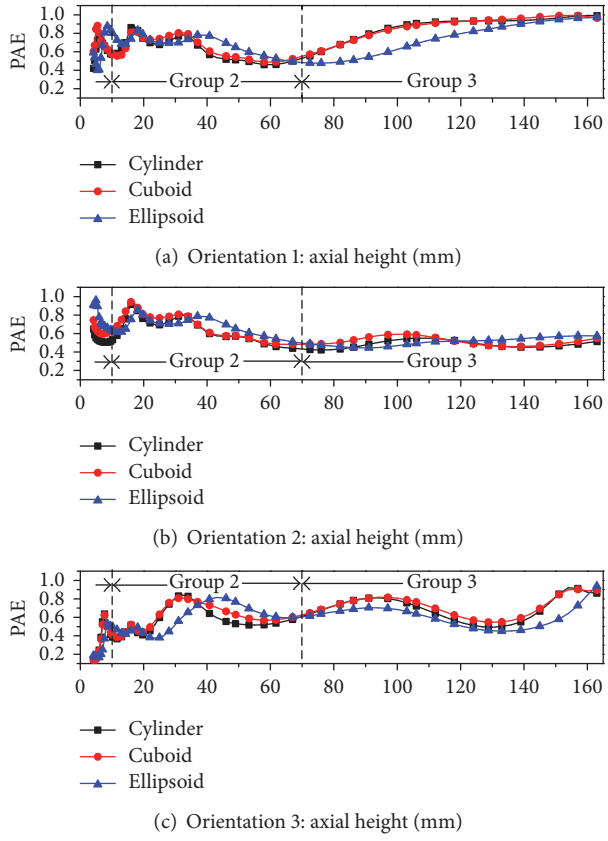

(a) Orientation 1: axial height (mm)

(b) Orientation 2: axial height (mm)

(c) Orientation 3: axial height (mm)

Figure 23: PAE of different shapes.

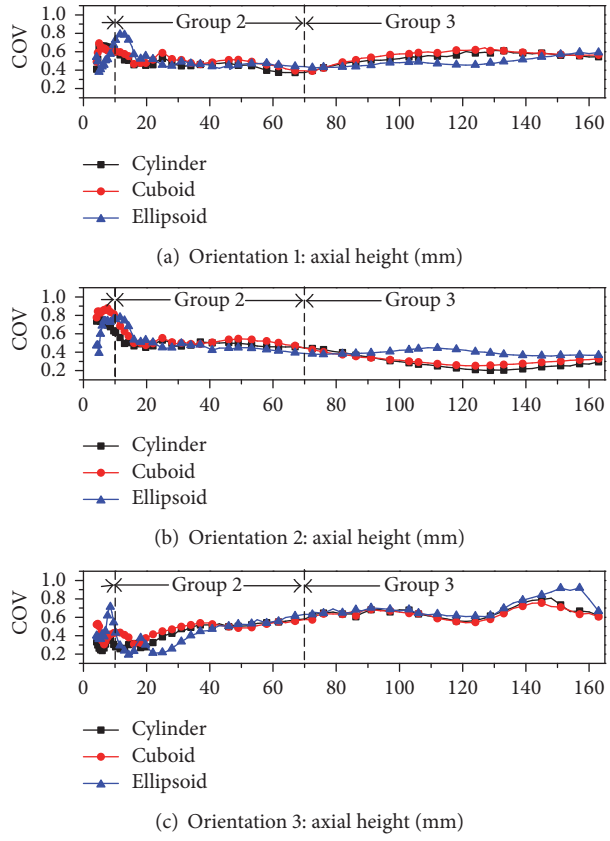

(a) Orientation 1: axial height (mm)

(b) Orientation 2: axial height (mm)

(c) Orientation 3: axial height (mm)

Figure 24: COV of different shapes.

samples is interlaced with those of the other two shapes. This phenomenon is caused by the equal radial cross section areas of cylindrical and cuboidal samples whose axial sizes are equal and of cylindrical and ellipsoidal samples whose axial sizes are not equal. Similar phenomena are also shown in Figures 23(b) and 23(c).

In Figures 24(a)–24(c), when samples' axial sizes are lower than 0.020 m, the temperature COV curves show intense volatility. As the axial sizes of samples are bigger than 0.020 m, COV curves in Figure 24(a) are relatively flat, those in Figure 24(b) show downward tendency, and those in Figure 24(c) show upward tendency. Therefore, when samples' axial sizes increase from Group 1 to Group 3, samples' temperature uniformity becomes stable in Orientation 1, gets better in Orientation 2, and gets worse in Orientation 3. It suggests that different shape samples in the same orientation have the same temperature uniformity variation tendency.

In Figures 25(a)–25(c), it can be concluded that in every sample group there exist extreme values, which means there are optimal sample shape in a certain range as discussed previously. In Figures 25(a) and 25(b), some of the CEC values in Group 3 are bigger than those in Group 2, but the causes of the maximal values of these two groups are different. So when selecting sample shapes, only considering CEC value is not enough; PAE and COV values should be considered as well. As discussed previously, the optimal shape in Group 2 is selected due to the two optimal values of PAE and COV, namely, higher PAE and lower COV. However, in Group 3, due to the fact that the optimal values of PAE and COV cannot be obtained synchronously, optimal shape should be selected according to specific need of temperature uniformity or microwave power absorption capability.

To sum up, in this section microwave heating properties of samples of different shapes placed in the same orientation were elaborated by means of intuitive figures and quantificational curves. Different shape samples were classified into three categories according to the radial and axial wave number and penetration number. Samples belonging to different groups demonstrate different electromagnetic field and temperature distribution. PAE, COV, and CEC curves are used to comprehensively evaluate the usability of a sample. PAE, COV, and CEC curves of different shape samples in same orientation have similar variation tendency. For samples belonging to Group 1, ellipsoidal shape sample is the optimal shape when placed in Orientation 1 and Orientation 2, and when the sample is placed in Orientation 3, cylinder is the best shape. For samples belonging to Group 2, when samples' axial sizes are lower than 0.040 m, the effect of sample shape is small enough to be negligible, and beyond this range ellipsoidal shape would be a better choice. For samples in Group 3, cylindrical samples are better when placed in Orientation 1 and Orientation 2, and when in Orientation 3, cuboid would be a better shape.

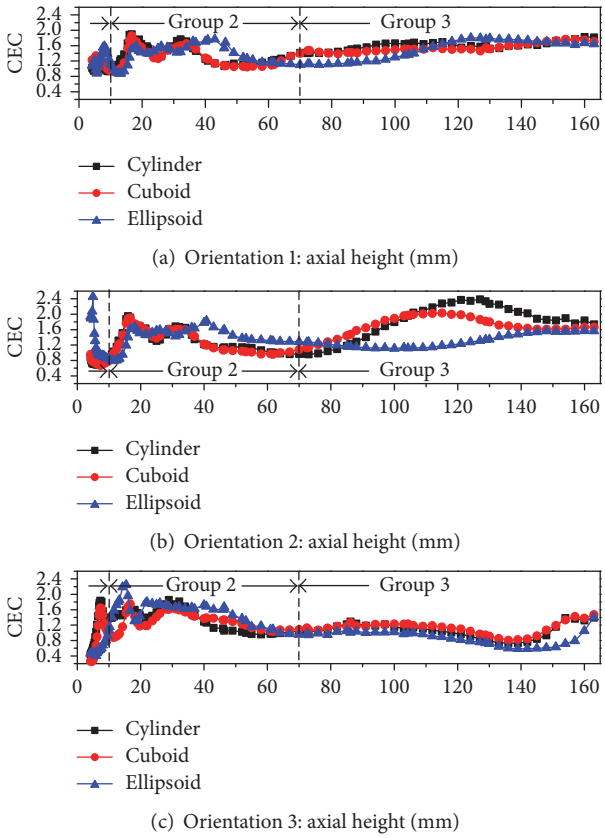

Figure 25: CEC of different shapes.

3.3. Position Orientation Effect. In Section 3.2.2, microwave heating properties of samples of different shapes placed in the same orientation have been discussed. During the studies, it is clear that when samples' shapes changed, the quantificational curve differed significantly. Meanwhile, differences between samples of the same shape in different orientations were also obvious. Therefore, in this section the microwave heating properties of the same samples placed in three orientations (shown in Figure 16) are discussed as follows.

PAE, COV, and CEC values of samples in Group 1 placed in different orientations are shown in Figure 26. From Figures 26(a), 26(d), and 26(g), it can be seen that PAE values of cylindrical samples placed in Orientation 1 are bigger than other orientations, but the corresponding temperature COV values of cylindrical samples placed in Orientation 3 are better than the others. Besides, the CEC values of cylindrical samples placed in Orientation 3 are better than those placed in Orientation 1. Therefore, if the microwave heating process prefers a high power absorption capability, cylindrical samples in Group 1 should be placed in Orientation 1. If temperature uniformity is a more decisive factor, cylindrical samples in Group 1 should be placed in Orientation 3. The same conclusion can be drawn for the cuboidal samples in Group 1. For ellipsoidal samples, when sample axial size is small enough, Orientation 2 would be a good choice due to a higher PAE and lower COV. Otherwise, Orientation 1 is better for the same reasons.

PAE, COV, and CEC values of samples in Group 2 placed in different orientations are shown in Figure 27. From Figures 27(a)–27(f), it can be seen that when samples' axial sizes are lower than 0.040 m, the PAE and COV values of samples placed in Orientation 3 are lower than the other two orientations. When the axial sizes are bigger than 0.040 m, those values of Orientation 3 are larger than the others. Thus, in Figures 27(g)–27(i), the CEC values of different orientations are close to each other. Therefore, when selecting the orientations of samples in Group 2, users should firstly confirm whether the microwave absorption efficiency or the temperature uniformity is the decisive factor. If high PAE is more important, samples should be placed in Orientation 1 and Orientation 2 for those whose axial sizes are lower than 0.040 m and in Orientation 3 for those whose axial sizes are bigger than 0.040 m. Otherwise, the lower COV values would be the dominant factor. As the conclusion drawn in former section, the effect of sample shape in Group 2 is less important than that of orientation.

PAE, COV, and CEC values of samples in Group 3 placed in different orientations are shown in Figure 28. It is clear that samples' PAE values of Orientation 1 are the highest and those of Orientation 3 are the lowest as shown in Figures 28(a)–28(c). Besides, the COV values of Orientation 2 are the best and those of Orientation 3 are the worst as shown in Figures 28(d)–28(f). Thus, from the CEC value shown in Figures 28(g)–28(i), the first conclusion that can be drawn is for the samples in Group 3: Orientation 3 is the worst choice to place the samples. Secondly, taking the PAE and COV values into consideration, if the microwave process needs higher PAE, Orientation 1 is the best choice. If temperature COV value is the dominant factor, it is better to place the samples in Orientation 2 though the PAE values are only around 0.45 on this condition.

PAE, COV, and CEC values of samples in three groups are shown in Figures 29–31, respectively. In these images, positions of Group 2 and Group 3 have been marked and the unmarked part is belonging to the Group 1.

In Figure 29, it can be seen that when samples' axial sizes are lower than 0.040 m, the PAE values of samples placed in Orientation 3 are lower than those of samples placed in the other two orientations. When the axial sizes are bigger than 0.040 m, the PAE curves of Orientation 1 tend to a fixed value of about 0.9, curves of Orientation 2 fluctuate around 0.52, 0.55, and 0.56 for cylindrical, cuboidal, and ellipsoidal samples, respectively, and curves of Orientation 3 fluctuate around 0.67, 0.70, and 0.64 for cylindrical, cuboidal, and ellipsoidal samples, respectively. Obviously, from the perspective of microwave power absorption capability of samples, Orientation 1 is the best choice for all the three groups of samples.

In Figure 30, when samples' axial sizes are lower than 0.040 m, the temperature COV values of samples placed in Orientation 3 are the lowest among three orientations; namely, samples could obtain the best temperature uniformity on this condition. However, when the axial sizes of samples are bigger than 0.040 m, the temperature COV values of Orientation 3 get worse which are of average values of about 0.61, 0.60, and 0.65 separately of cylindrical,

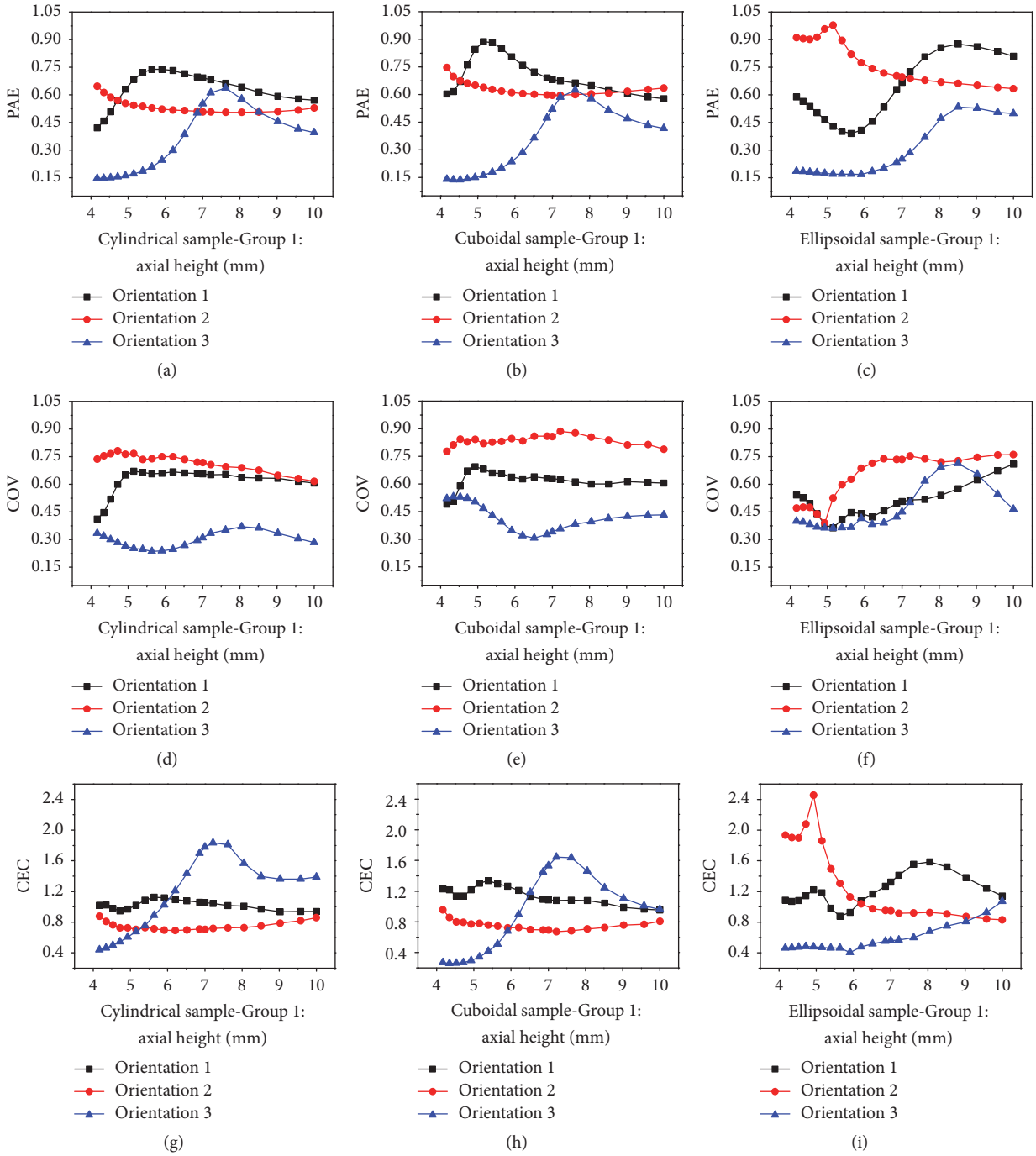

Figure 26: Same samples in different orientations, Group 1.

cuboidal, and ellipsoidal samples. Those of Orientation 2 get better which are of average values about 0.34, 0.37, and 0.40 separately of cylindrical, cuboidal, and ellipsoidal samples. And values of Orientation 1 keep stable average values of 0.50, 0.53, and 0.48, respectively. Therefore, if a microwave process has a higher requirement for temperature uniformity, Orientation 2 is the best choice for samples whose axial sizes are bigger than 0.040 m, and Orientation 3 is better when the axial sizes are lower than 0.040 m.

In Figure 31, when samples' axial sizes are lower than 0.040 m, the CEC values of three orientations are close to each other; thus the PAE and COV values should be taken into consideration. Under this situation, if a higher PAE value is needed, samples should be placed in Orientation 1 and Orientation 2, and if a lower COV value is needed, samples should be placed in Orientation 3. When samples' axial sizes are bigger than 0.040 m, Orientation 3 is not recommended due to the lower PAE and higher COV. If there is a specific

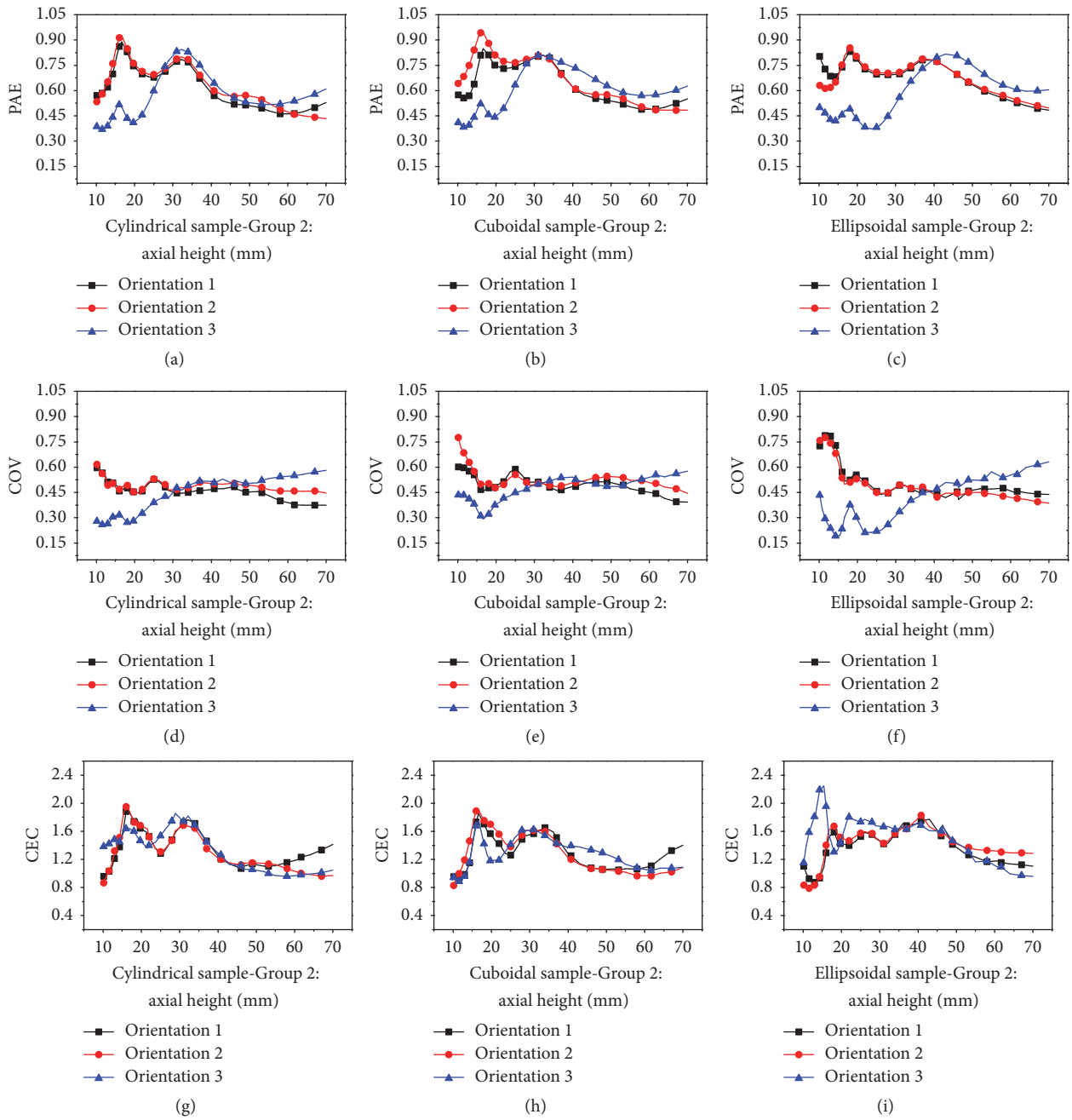

Figure 27: Same samples in different orientations, Group 2.

need for temperature uniformity, Orientation 2 is better; otherwise, Orientation 1 is better on this condition.

To sum up, in this section samples of the same shape are placed in different orientations, and the corresponding PAE, COV, and CEC curves indicate that orientation influences the microwave process significantly. PAE, COV, and CEC values should be taken into consideration, when selecting orientations. From the study in this section, it can be concluded that when samples' axial sizes are bigger than 0.040 m, Orientation 3 is the worst choice, Orientation 2 could be chosen only for the special needs of temperature uniformity, and Orientation 1 is the best choice due to the higher PAE and relatively lower temperature COV value. When samples' axial sizes are lower than 0.040 m, Orientation 3 is recommended if temperature uniformity is important, and if microwave power absorption is more decisive, Orientation 1 and Orientation 2 are better.

4. Conclusion

Based on the above calculation results, it can be seen that, in the microwave heating cavity, samples with equal volume and

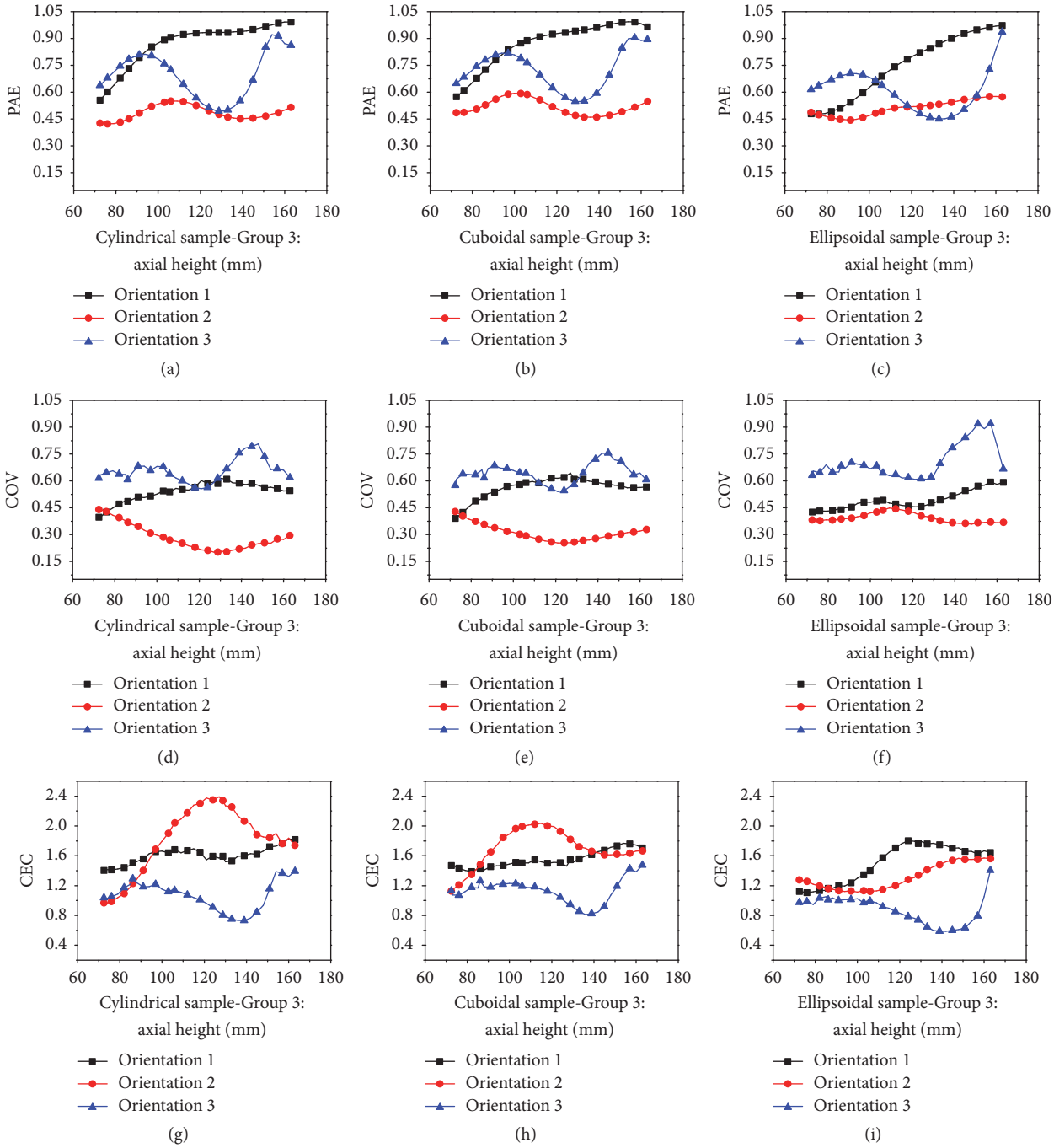

Figure 28: Same samples in different orientations, Group 3.

different shapes form hot spots at different positions in the center or near the surface of samples. Choosing proper input power can achieve the goal of high temperature distribution uniformity and low energy consumption. When the input power is larger than a certain value (which may change with sample's material), the final internal temperature uniformity tends to be constant.

The samples of spherical and cubic shapes can be classified into four groups according to the PAE and COV values as well as the locations of electromagnetic focusing and hot spots. For the small and big volume groups samples, spherical samples are better than the cubic ones. For the intermediate size samples, if temperature uniformity of samples is more important, spherical samples is the best choice, while if the decisive factor is the high microwave power absorption capability, cubic samples are recommended.

As for the isometric volume cylindrical, cuboidal, and ellipsoidal samples, they can be classified into three groups by the wave numbers and penetration numbers in the radial and axial directions. Intuitively, samples of Group 1 tend to be

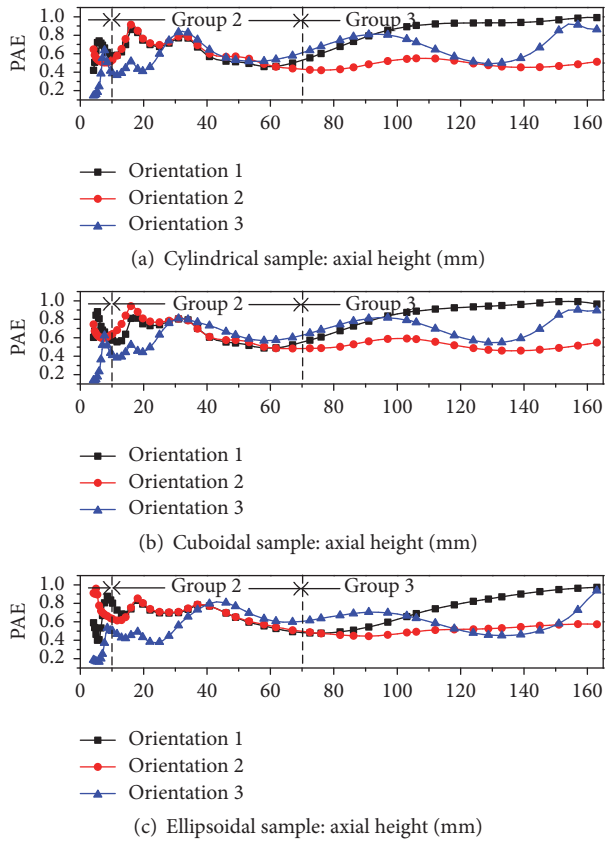

Figure 29: PAE of the same samples in different orientations.

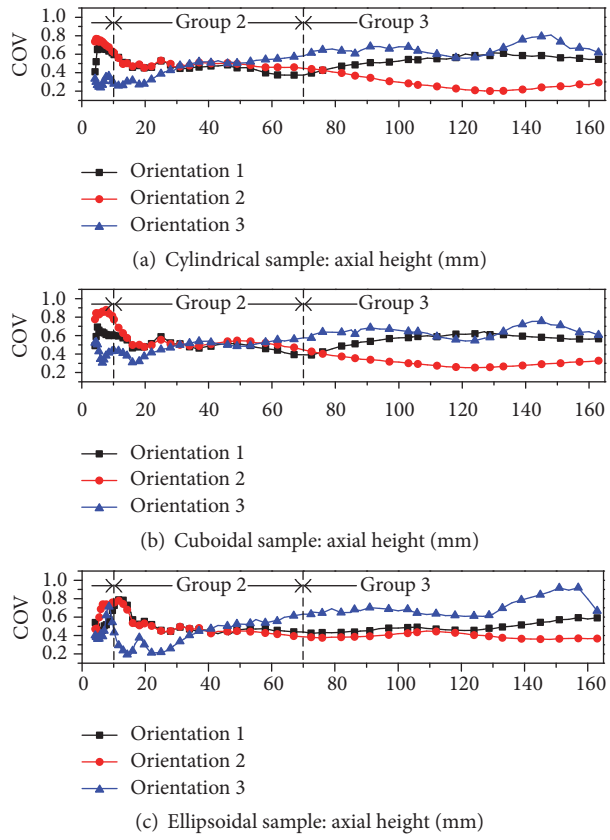

Figure 30: COV of the same samples in different orientations.

more flat, while those belonging to Group 3 are more slender. Quantitatively, in Group 1, samples' radial and axial wave numbers and penetration numbers are $N_p^r > 3$, $N_w^a > 0.1$, and $N_p^a < 3$. In Group 2, samples' radial and axial wave numbers and penetration numbers are $N_w > 0.1$ and $N_p < 3$. In Group 3, samples' radial and axial wave numbers and penetration numbers are $N_w^r > 0.1$, $N_p^r < 3$, and $N_p^a > 3$.

Microwave heating properties of samples of different shapes placed in the same orientation were elaborated by the means of intuitive figures and quantificational curves. PAE, COV, and CEC curves are used to comprehensively evaluate the usability of a sample. PAE, COV, and CEC curves of different shape samples in the same orientation have similar variation tendency. For samples belonging to Group 1, ellipsoidal shape sample is the optimal shape when placed in Orientation 1 and Orientation 2, and when the sample is placed in Orientation 3, cylinder is the best shape. For samples belonging to Group 2, when samples' axial sizes are lower than 0.040 m, the effect of sample shape is small enough to be negligible; namely, every shape of samples could be chosen, and beyond this range ellipsoidal shape would be a better choice. For samples in Group 3, cylindrical samples are better when placed in Orientation 1 and Orientation 2, and when in Orientation 3, cuboid would be a better shape.

The PAE, COV, and CEC curves of samples of same shape placed in different orientations indicate that orientations affect the microwave process significantly. PAE, COV,

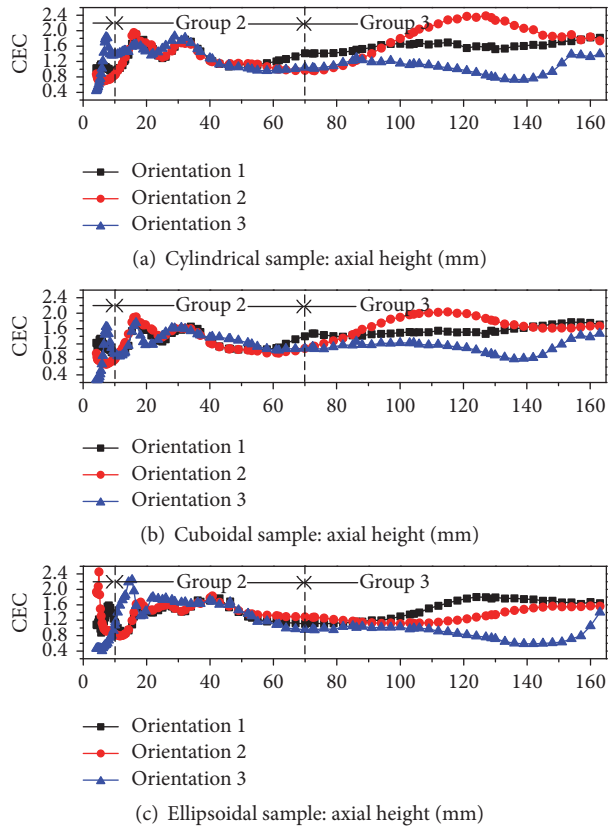

Figure 31: CEC of the same samples in different orientations.

and CEC values should be taken into consideration when selecting orientations. When samples' axial sizes are bigger than 0.040 m, Orientation 3 is the worst choice, Orientation 2 could be chosen only for the special needs of temperature uniformity, and Orientation 1 is the best choice due to the higher PAE and relatively lower temperature COV value. When samples' axial sizes are lower than 0.040 m, Orientation 3 is recommended if temperature uniformity is important, and if microwave power absorption is more decisive, Orientation 1 and Orientation 2 are better.

Conflicts of Interest

The authors declare that there are no conflicts of interest regarding the publication of this paper.

Acknowledgments

This research was supported by the National Natural Science Foundation of China (Grant nos. 31371873, 31000665, 51176027, and 31300408).

References

[1] S. Begum and M. S. Brewer, "Physical, chemical and sensory quality of microwave-blanched snow peas," *Journal of Food Quality*, vol. 24, no. 6, pp. 479–493, 2001.

[2] W. H. Wu and D. A. Lillard, "Cholesterol and proximate composition of channel catfish (Ictalurus punctatus) fillets - Changes following cooking by microwave heating, deep-fat frying, and oven baking," *Journal of Food Quality*, vol. 21, no. 1, pp. 41–51, 1998.

[3] S. B. M. S. Brewer and A. Bozeman, "Microwave and Conventional Blanching Effects on Chemical, Sensory, and Color Characteristics of Frozen Broccoli," *Journal of Food Quality*, vol. 18, no. 6, pp. 479–493, 1995.

[4] B. P. K. M. S. Brewer, K. Bharati, and A. K. Perry, "Microwave Blanching Effects on Chemical Sensory and Color Characteristics of Frozen Green Beans," *Journal of Food Quality*, vol. 17, pp. 245–259, 1994.

[5] T. P. W. H. S. Ramaswamy, "Temperature Distribution in Microwave Heated Food Models," *Journal of Food Quality*, vol. 15, pp. 435–448, 1992.

[6] J. F. Song, C. Q. Liu, X. Q. Jiang, and D. J. Li, "Quality Evaluation of Vacuum Microwave-Dried Immature Vegetable Soybean (Glycine Max [L.] Merr.)," *Journal of Food Quality*, vol. 38, no. 5, pp. 337–346, 2015.

[7] E. E. Abano, H. Ma, and W. Qu, "Influence of combined microwave-vacuum drying on drying kinetics and quality of dried tomato slices," *Journal of Food Quality*, vol. 35, no. 3, pp. 159–168, 2012.

[8] N. Therdthai, P. Ritthiruangdej, and W. Zhou, "Effect of Microwave Assisted Baking on Quality of Rice Flour Bread," *Journal of Food Quality*, vol. 39, no. 4, pp. 245–254, 2016.

[9] R. G. M. van der Sman and J. R. Bows, "Critical factors in microwave expansion of starchy snacks," *Journal of Food Engineering*, vol. 211, pp. 69–84, 2017.

[10] M. C. Law, E. L. Liew, S. L. Chang, Y. S. Chan, and C. P. Leo, "Modelling microwave heating of discrete samples of oil palm kernels," *Applied Thermal Engineering*, vol. 98, pp. 702–726, 2016.

[11] I. E. Marques, C. A. Bizzi, F. B. Lucion et al., "Are Infrared and Microwave Drying Suitable Alternatives for Moisture Determination of Meat Products?" *Journal of Food Quality*, vol. 39, no. 4, pp. 391–397, 2016.

[12] C. Conesa, L. Seguí, N. Laguarda-Miró, and P. Fito, "Microwaves as a pretreatment for enhancing enzymatic hydrolysis of pineapple industrial waste for bioethanol production," *Food and Bioproducts Processing*, vol. 100, pp. 203–213, 2016.

[13] S. Chandrasekaran, S. Ramanathan, and T. Basak, "Microwave food processing—a review," *Food Research International*, vol. 52, no. 1, pp. 243–261, 2013.

[14] R. R. Mishra and A. K. Sharma, "Microwave-material interaction phenomena: Heating mechanisms, challenges and opportunities in material processing," *Composites Part A: Applied Science and Manufacturing*, vol. 81, pp. 78–97, 2016.

[15] S. S. R. Geedipalli, V. Rakesh, and A. K. Datta, "Modeling the heating uniformity contributed by a rotating turntable in microwave ovens," *Journal of Food Engineering*, vol. 82, no. 3, pp. 359–368, 2007.

[16] M. S. Venkatesh and G. S. V. Raghavan, "An overview of microwave processing and dielectric properties of agri-food materials," *Biosystems Engineering*, vol. 88, no. 1, pp. 1–18, 2004.

[17] H. W. Yang and S. Gunasekaran, "Comparison of temperature distribution in model food cylinders based on Maxwell's equations and Lambert's law during pulsed microwave heating," *Journal of Food Engineering*, vol. 64, no. 4, pp. 445–453, 2004.

[18] K. G. Ayappa, H. T. Davis, E. A. Davis, and J. Gordon, "Analysis of microwave heating of materials with temperature-dependent properties," *AIChE Journal*, vol. 37, no. 3, pp. 313–322, 1991.

[19] C. A. Balanis, *Advanced Engineering Electromagnetics*, John Wiley & Sons, Inc., New York, NY, USA, 1989.

[20] T. Basak, M. Bhattacharya, and S. Panda, "A generalized approach on microwave processing for the lateral and radial irradiations of various Groups of food materials," *Innovative Food Science and Emerging Technologies*, vol. 33, pp. 333–347, 2016.

[21] J. Chen, K. Pitchai, D. Jones, and J. Subbiah, "Effect of decoupling electromagnetics from heat transfer analysis on prediction accuracy and computation time in modeling microwave heating of frozen and fresh mashed potato," *Journal of Food Engineering*, vol. 144, pp. 45–57, 2014.

[22] T. Basak, "Role of various elliptical shapes for efficient microwave processing of materials," *AIChE Journal*, vol. 53, no. 6, pp. 1399–1412, 2007.

[23] H. Zhu, T. Gulati, A. K. Datta, and K. Huang, "Microwave drying of spheres: Coupled electromagnetics-multiphase transport modeling with experimentation. Part I: Model development and experimental methodology," *Food and Bioproducts Processing*, vol. 96, pp. 314–325, 2015.

[24] M. Bhattacharya, T. Basak, and S. Sriram, "Generalized characterization of microwave power absorption for processing of circular shaped materials," *Chemical Engineering Science*, vol. 118, pp. 257–279, 2014.

[25] M. U. H. Joardder, M. A. Karim, and C. Kumar, "Multiphase transfer model for intermittent microwave-convective drying of food: considering shrinkage and pore evolution," *International Journal of Multiphase Flow*, vol. 95, pp. 101–119, 2017.

[26] J. Zhang, Y. Luo, C. Liao et al., "Theoretical investigation of temperature distribution uniformity in wood during microwave drying in three-port feeding circular resonant cavity," *Drying Technology*, vol. 35, no. 4, pp. 409–416, 2017.

[27] X. L. Hu, X. Q. Yang, and G. Z. Jia, "Effective optimization of temperature uniformity and power efficiency in two-ports microwave ovens," *The Journal of Microwave Power and Electromagnetic Energy*, vol. 48, no. 4, pp. 261–268, 2014.

[28] D. Luan, Y. Wang, J. Tang, and D. Jain, "Frequency Distribution in Domestic Microwave Ovens and Its Influence on Heating Pattern," *Journal of Food Science*, vol. 82, no. 2, pp. 429–436, 2017.

[29] A. K. D. V. Rakesh, M. H. G. Amin, and L. D. Hall, "Heating uniformity and rates in a domestic microwave combination oven," *Journal of Food Process Engineering*, vol. 32, pp. 398–424, 2007.

[30] Y. D. Hong, B. Q. Lin, H. Li, H. M. Dai, C. J. Zhu, and H. Yao, "Three-dimensional simulation of microwave heating coal sample with varying parameters," *Applied Thermal Engineering*, vol. 93, pp. 1145–1154, 2016.

[31] H. Chen, M. Zhang, Z. Fang, and Y. Wang, "Effects of Different Drying Methods on the Quality of Squid Cubes," *Drying Technology*, vol. 31, no. 16, pp. 1911–1918, 2013.

[32] M. Bhattacharya and T. Basak, "On the analysis of microwave power and heating characteristics for food processing: Asymptotes and resonances," *Food Research International*, vol. 39, no. 10, pp. 1046–1057, 2006.

[33] F. Chen, A. D. Warning, A. K. Datta, and X. Chen, "Susceptors in microwave cavity heating: Modeling and experimentation with a frozen pie," *Journal of Food Engineering*, vol. 195, pp. 191–205, 2017.

[34] C. Kumar, *Modelling Intermittent Microwave Convective Drying (IMCD) of Food Materials [Doctor of Philosophy, Chemistry, Physics and Mechanical Engineering]*, Science and Engineering Faculty Queensland University of Technology, Australia, 2015.

[35] L. Zhou, V. M. Puri, R. C. Anantheswaran, and G. Yeh, "Finite element modeling of heat and mass transfer in food materials during microwave heating - Model development and validation," *Journal of Food Engineering*, vol. 25, no. 4, pp. 509–529, 1995.

[36] *The Microwave Processing of Foods*, Woodhead Publishing Limited and CRC Press LLC, USA, 2005.

[37] M. Bhattacharya and T. Basak, "A comprehensive analysis on the effect of shape on the microwave heating dynamics of food materials," *Innovative Food Science and Emerging Technologies*, vol. 39, pp. 247–266, 2017.

[38] T. Gulati, H. Zhu, A. K. Datta, and K. Huang, "Microwave drying of spheres: Coupled electromagnetics-multiphase transport modeling with experimentation. Part II: Model validation and simulation results," *Food and Bioproducts Processing*, vol. 96, pp. 326–337, 2015.

[39] H. Zhang and A. K. Datta, "Heating concentrations of microwaves in spherical and cylindrical foods: Part Two: In a cavity," *Food and Bioproducts Processing*, vol. 83, no. 1 C, pp. 14–24, 2005.

Hindawi
Journal of Food Quality
Volume 2018, Article ID 1347513, 12 pages
https://doi.org/10.1155/2018/1347513

Research Article

Effect of Hot-Water Blanching Pretreatment on Drying Characteristics and Product Qualities for the Novel Integrated Freeze-Drying of Apple Slices

Hai-ou Wang[1,2] **Qing-quan Fu**,[1] **Shou-jiang Chen**,[1] **Zhi-chao Hu**,[2,3] **and Huan-xiong Xie**[2,3]

[1]*School of Food Science, Nanjing Xiaozhuang University, Nanjing 211171, China*
[2]*Key Laboratory of Modern Agricultural Equipment, Ministry of Agriculture, Nanjing 210014, China*
[3]*Nanjing Research Institute for Agricultural Mechanization, Ministry of Agriculture, Nanjing 210014, China*

Correspondence should be addressed to Hai-ou Wang; who1978@163.com

Received 14 August 2017; Revised 16 December 2017; Accepted 8 January 2018; Published 1 February 2018

Academic Editor: Hong-Wei Xiao

The effect of hot-water blanching (HWB) on drying characteristics and product qualities of dried apple slices with the novel integrated freeze-drying (NIFD) process was investigated by comparing with 3 different FD methods. Compared with the NIFD process without HWB pretreatment (VF-FD), the NIFD process with HWB pretreatment (HWB-VF-FD) resulted in a significantly higher mass loss and more sufficient freezing in vacuum-frozen samples, significantly higher rehydration ratio (RR), higher shrinkage ratio (SR), smaller Vitamin C (V_C) content and lower hardness and better apparent shape in freeze-dried samples, and fewer change to the color of the dried or rehydrated samples ($p < 0.05$). Compared with the conventional FD process with HWB pretreatment (HWB-PF-FD), HWB-VF-FD cost significantly less processing time and FD time and obtained significantly higher RR ($p < 0.05$), almost the equivalent SR, V_C content, and hardness, and similar appearance in dried samples. The microstructure of apple cell tissues was analyzed by transmission electron microscopy and scanning electron microscopy to interpret the above differences in drying characteristics and product qualities. The results suggested that the NIFD process of apple slices with HWB pretreatment was a promising alternative method to decrease drying time, achieve similar product quality, and simplify the process steps of the conventional FD technology.

1. Introduction

Vacuum freeze-drying (FD) has been considered as one of the best methods for obtaining dehydrated foods with high quality. During FD, the whole dehydrating process is accomplished in the state of high vacuum and low temperature, which almost retains the original color, shape, smell, and nutritional ingredients in fresh materials [1–3]. An industrial-scale FD process for most fruits and vegetables generally consists of 4 main stages, including pretreating, freezing, freeze-drying (primary drying and secondary drying), and packaging. During pretreating in practice, the materials (especially fruits and vegetables) are usually conducted in the sequence steps including selecting, washing, slicing, blanching, quickly cooling, draining residual water, and filling trays. The materials are then transferred into freezing unit and FD unit. In conventional freeze-drying (CFD) processing line, all the individual steps require independent equipment or facility. For example, materials after blanching should be quickly cooled with cold running water, drained with vibratory or centrifugal equipment, frozen with fluidized bed freezer or cold storage, and then dried in vacuum freeze dryer. The CFD process technology is characterized by many disadvantages including complicated process steps, large space occupation, huge equipment investment, frequent materials transferring, long drying time, and high production cost [1, 4]. It was

reported that the production cost of FD was as much as 200–500% higher than that of hot air drying, which greatly reduced economic competitiveness of FD products [5].

In an effort to reduce drying time, researchers attempted to combine FD with other drying methods including vacuum drying, microwave drying, and osmotic drying, and they had achieved good effect in the laboratories [4, 6]. Litvin et al. showed that a considerable saving in FD time and similar quality parameters including color, dimensions, and rehydration ratio were achieved in dried carrot slices which were dried by combining freeze drying with a short microwave treatment and air or vacuum drying [7]. Wang et al. found that salt and/or sucrose osmotic pretreatment prior to microwave freeze-drying resulted in dried products of good quality with shorter processing time as compared with untreated samples [8]. Microwave was used as the heating source to heat the raw materials in FD, which had attracted much attention during the last decades [4]. In order to simplify the food FD processes and shorten the drying time, we proposed a novel integrated freeze-drying (NIFD) processing technology based on the principle of vacuum cooling and vacuum freeze dryer [9, 10]. More specifically, the post-blanching steps in the CFD process including quick cooling, draining, and freezing were replaced with the only step of vacuum freezing, which was conducted in the same vacuum freeze dryer. The step of vacuum freezing is a coupling process of water fast-evaporating and quick-freezing in a closed environment at low pressure, which can remove all the residual water on the material surface and partial internal water in the tissue resulting in rapid reduction of material temperature. The only step of vacuum freezing in the NIFD process can meet the requirements of the steps of cooling, draining, and freezing in the CFD process, which can save the prime-investment and space occupation of the corresponding facilities and equipment and simplify the assembly line and the operation process. Moreover, the water loss during vacuum freezing can reduce the subsequent sublimation load and the FD time. And some experiments of fruits and vegetables including apple were performed by this NIFD processing technology [9, 10]. The above expected effect was achieved. However, further investigation should be carried out on the product quality especially how to maximally retain the original shape of freeze-dried samples.

It is well known that blanching is an important processing step during commercial drying of vegetables and fruits [11]. The use of hot-water blanching (HWB) as a pretreatment is usually carried out to inactivate enzymes and remove air from intercellular space of fruits and vegetables in order to prevent off color and flavor changes during drying [12–14]. And some existent literatures revealed that blanching pretreatment can enhance mass transport in the tissue and affect the drying behavior of fruits and vegetables [15–19]. Apple is one of the most popular fruits worldwide in our life. FD apple slices products are available throughout the world market. However, to our knowledge there are no available reports on the studies on the NIFD processing technology of apple slices pretreated with HWB.

The main objectives of the current study are to evaluate the effect of HWB on the drying characteristics and product qualities of apple slices dried with the NIFD process, including mass loss and frozen temperature of apple samples at the end of freezing treatment, freezing time, freeze-drying time, rehydration ratio (RR), shrinkage ratio (SR), Vitamin C (V_C) content, color, texture, and microstructure of FD apple slice. This study aimed to provide basic knowledge for improving the effect of this NIFD processing and promoting its practical application in fruits and vegetables.

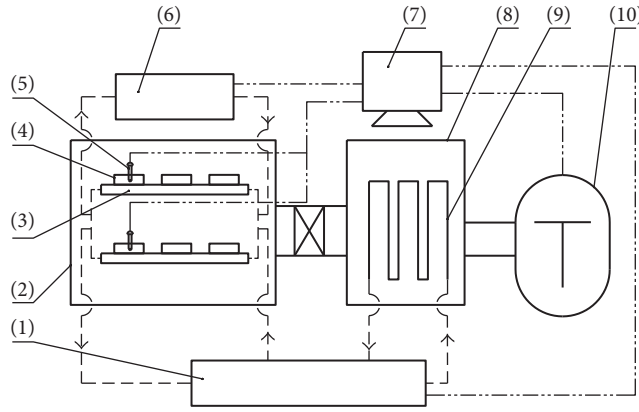

Figure 1: Schematic of the vacuum freeze dryer used. (1) Refrigeration machine; (2) freeze-drying chamber; (3) cooling/heating plate; (4) apple slice samples; (5) thermocouple temperature sensors; (6) heating machine; (7) control system; (8) cold trap; (9) refrigeration coils; (10) vacuum pump.

2. Materials and Methods

2.1. Materials and Samples. Commercial Fuji apples were purchased from a local supermarket (Nanjing, China) and stored at ambient temperature (20°C) until experimental use. The apples with similar dimension were chosen and washed with tap water and hand peeled, cored with a knife, and then cut into slices with about a dimension of 30 mm × 30 mm × 5 mm. The initial moisture content of these apple samples was measured as 86.56 ± 0.59% (w.b.).

2.2. Vacuum Freeze Dryer. In our experiments, the processing steps of the freezing and the freeze-drying of samples were carried out in a laboratory-scale vacuum freeze dryer (SCIENTZ-50F, Ningbo Scientz Biotechnology Co., Ltd., Ningbo, China) which was shown schematically in Figure 1. This equipment consists of a freeze-drying chamber where food samples are put on the cooling/heating plates to perform the freezing and drying steps. During freezing or freeze-drying, the temperature of the cooling/heating plates is controlled by the refrigeration machine or the heating machine; the temperature of food samples is monitored by using the thermocouple sensors. The refrigeration machine also provides refrigerating output to the clod trap to condense the water vapor generated from food samples. The vacuum condition is maintained by the vacuum pump.

2.3. Blanching Treatments. The HWB pretreatment of apple slices was conducted for 1 min in 90°C distilled water that was

heated by an electric heaters, which can inhibit the enzyme activity and retain good color for the fresh slices [20, 21].

2.4. Freezing Treatments. In this study, two different freezing methods were carried out in the vacuum freeze dryer: one was the vacuum freezing (VF) performed under vacuum condition and the other one was the plate freezing (PF) performed under atmospheric pressure condition. When performing the VF treatment, the refrigeration machine was started half an hour earlier to reduce the cold trap temperature below −50°C. The prepared apple samples were then put into the trays on the cooling/heating plates which were not controlled with either heating function or cooling function. The ambient pressure in the freeze-drying chamber was continuously reduced after starting the vacuum pump; then the liquid water evaporating and freezing happened in apple samples. The water vapor flowed into the clod trap and was condensed on the refrigeration coils. The VF treatment was sustained for 30 min and the samples were frozen finally. In case of the PF treatment, the cooling/heating plates temperature was kept around −40°C for 3 h to reduce the temperature of the center of apple slices below −30°C, which was carried out under atmospheric pressure without turning on the vacuum pump and the refrigeration in the clod trap.

2.5. Freeze-Drying Process. The above frozen apple slices were subsequently conducted in-place FD process on the plates in the vacuum freeze dryer. The plate's temperature throughout the FD process was controlled according to the preset automatic heating procedure of temperature-duration time: maintaining the plate's temperature at −20°C for 1 hour (h), then followed by −10°C for 1 h, 0°C for 1 h, 10°C for 2 h, 20°C for 2 h, and 30°C for 2 h, and finally maintaining the plate's temperature at 40°C until the drying end point. Meanwhile, the center temperature of the apple slices was monitored in real time by the control system. It was verified by the early FD experiments using this heating procedure that the moisture content of the dried samples reached about 5% (w.b.) when the center temperature of the apple slices increased to 35 ± 0.5°C, which was determined as the drying end point.

2.6. Three Different Processing Methods. The prepared apple slices samples in Section 2.1 were divided into three groups to perform three different processing methods. There were 50 slices of apple in each group.

2.6.1. VF-FD Method. Apple slices without HWB pretreatment were put into the vacuum freeze dryer to perform the VF treatment and FD process.

2.6.2. HWB-VF-FD Method. Apple slices were pretreated with HWB and then were quickly transferred into the vacuum freeze dryer to perform the VF treatment and FD process.

2.6.3. HWB-PF-FD Method. Apple slices were pretreated with HWB, then were quickly cooled to room temperature using tap water, drained the residual water by air blasting for 15 min with an electric fan at 60 watts power, and were subsequently performed with the PF treatment. This method was an CFD process.

2.7. Analytical Methods

2.7.1. Mass Loss and Temperature of Frozen Samples. At the end of the freezing treatments in the above three processing methods, mass loss of apple slice was calculated by using the following formula:

$$\mathrm{ML} = \frac{m_0 - m_1}{m_0} \times 100\%, \tag{1}$$

where ML (%) is the percentage of mass loss in the apple slice during freezing and m_0 (g) and m_1 (g) are the weight of the apple slice before and after the VF treatment, respectively.

During the VF treatment, the temperature of the geometric center of the apple slice was measured with the thermocouple temperature sensors of the SCIENTZ-50F freeze dryer to determine the temperature variation of apple samples. The measurements of mass loss and frozen temperature were carried out in triplicate for each processing method and the average values were taken for analysis.

2.7.2. Processing Time and FD Time Analysis. The processing time of the individual processing method consisted of two sections: freezing time and FD time. The freezing time in VF-FD and HWB-VF-FD was 30 min, and that in HWB-PF-FD was 3 h. The FD time was determined by the drying terminal temperature of 35 ± 0.5°C in apple slice center. The measurements were carried out in triplicate and the averages are reported.

2.7.3. Rehydration Ratio (RR) Analysis. Rehydration experiments were performed by immersing a weighed amount of dried samples (about 1 g) into a distilled water bath at a controlled temperature of 25°C for 30 min. Then the samples were removed and drained over a mesh for 30 seconds (s) and quickly blotted with the paper towels gently in order to eliminate the surface water and then reweighed. Each rehydration experiment was carried out in triplicate and the averages are reported. The RR was calculated according to the following formula:

$$\mathrm{RR} = \frac{M_r}{M_d} \times 100\%, \tag{2}$$

where RR (%) is the percentage of rehydration ratio of FD samples (%) and M_d and M_r are the mass of the apple sample before and after rehydration tests, respectively (g).

2.7.4. Shrinkage Ratio (SR) Analysis. The sample volume was determined by the volumetric displacement method using glass beads with a diameter in the range (0.105–0.210 mm) as a replacement medium [13, 22]. The measurements were conducted 5 times for the same apple slice sample and the average values were taken for analysis. The SR of the dried sample was calculated as follows:

$$\mathrm{SR} = \frac{V_d}{V_0} \times 100\%, \tag{3}$$

where SR is the percentage of shrinkage ratio of the FD sample (%) and V_0 and V_d are the volume of the sample (cm^3) before freezing and after drying, respectively.

2.7.5. Vitamin C Content Analysis. The V_C content was determined by using the 2,6-dichloroindophenol titration method [23].

2.7.6. Color Analysis. Color measurements of freeze-dried samples and rehydrated samples were carried out by using a colorimeter (NH310, Shenzhen 3nh Technology Co., Ltd., Shenzhen, China). The coordinates of the color CIE-L^* (lightness), a^* (redness), and b^* (yellowness) of the skin of apple slice samples were obtained by reflection. The total color difference (ΔE) was used to characterize the variation of in products color during processing by applying the following equation:

$$\Delta E = \sqrt{\left(L_0{}^* - L^*\right)^2 + \left(a_0{}^* - a^*\right)^2 + \left(b_0{}^* - b^*\right)^2}, \quad (4)$$

where $L_0{}^*$, $a_0{}^*$, and $b_0{}^*$ were the color readings of fresh samples. The measurements were carried out on 5 apple slice samples for each FD method and the average values were taken for analysis.

2.7.7. Hardness Analysis. Hardness of FD apple samples were measured by using a texture analyzer (TA.XTplus, Stable Micro Systems Ltd., Surrey, UK). The cylinder penetrometer probe (5 mm diameter) was passed through the sample with the test parameters set as follows: 2 mm/s of prespeed and postspeed, 2 mm/s of test speed, and 10 g trigger. In the penetration test, hardness was defined as the maximum force (N) required for puncturing the apple slice. The measurements were performed 5 times for samples in each method treatment and the average values were reported.

2.7.8. Transmission Electron Microscopy Analysis. Transmission electron microscopy, TEM (Model JEM-1400; JEOL Inc., Tokyo, Japan), was used to analyze the internal structure of apple slices before and after HWB pretreatment referring to the method in Jiang's research report [24]. Samples of apple tissue were cut into 2 mm × 1 mm pieces, fixed in 3.5% glutaral phosphate buffer, flushed with 0.1 mol/L PBS (pH 7.2), fixed in 1% osmium acid (OsO4), and flushed again in 0.1 mol/L PBS. The samples were then dehydrated in graded ethanol solutions of 35%, 45%, 60%, 70%, 85%, 95%, and 100% (v/v), followed by propylene oxide. The samples were then embedded in Spurr resin and polymerized for 8 h at 20°C. The samples were then pruned and cut into thin slices by using an LKB ultramicrotome. Finally, the samples were double-stained using uranyl acetate and lead citrate. Micrographs were taken at 20000x and 40000x magnification. All the microstructural examinations were performed at 25°C.

2.7.9. Scanning Electron Microscopy Analysis. Cross-sectional observed samples for scanning electron microscopy (SEM) analyses were obtained by naturally fracturing the freeze-dried samples with the aiding of instant freezing by liquid nitrogen. The observed samples were placed on one surface of a two-sided adhesive tape that was fixed to the sample support. Then, they were sputtered immediately (CPD-030; BAL-TEC Company, Liechtenstein). Finally, the specimen fragments were mounted on aluminium stubs, coated with gold under vacuum conditions, and then observed on a scanning electron microscope (EVO-LS10, Cambridge, Germany) for outer surface using an accelerating voltage of 10 kV. In addition, apparent photographs of freeze-dried samples were taken with a camera to compare with the SEM photographs.

In every processing method, 5 SEM images were taken from the dried apple samples to analyze the pores network structure. To quantify the difference in the structure of dried samples, the porosity in the structure was determined. Firstly, the SEM images were turned into gray level and binarized by using an automatic image processing method based on the gray level difference between adjacent pixels, which was performed using Matlab code (Mathworks, Inc., version 7.0.1 Release 14, USA). Then, measurements of pores area (obtained from binarized images) were carried out by the Image Pro-Plus software (Media Cybernetics, Inc., Version 4.0, USA). The porosity of the dried sample was calculated as follows:

$$\mathrm{PR} = \frac{S_p}{S_0} \times 100\%, \quad (5)$$

where PR is the percentage of porosity of the FD sample (%), S_p is the sum of the area of all pores in the image (μm^2), and S_0 is the whole area of the image (μm^2).

2.7.10. Statistical Analysis. Statistical analysis of variance (ANOVA) was performed by using SPSS 20.0 software (IBM, Chicago, IL, USA). Tests of significant differences between means were determined by Tukey's HSD test at a significance level of 0.05 ($p < 0.05$).

3. Results and Discussion

3.1. Mass Loss and Frozen Temperature at the End of Freezing Treatment. Mass loss and frozen temperature of apple samples at the end of freezing treatment in the three processing methods were shown in Figure 2. Mass loss was an inevitable phenomenon for either the VF treatment or the PF treatment. The highest mass loss value at the end of freezing treatment occurred in HWB-VF-FD 32.38%, followed by VF-FD 22.5% and HWB-PF-FD 5.19%, showing significant difference. It was found that mass loss of apple samples at the end of the VF treatment are much higher than that in the PF treatment because they were caused by completely different action principles. During the VF treatment, water on the surface and in the tissue of apple slices evaporated quickly due to exposing to specific vacuum conditions, which resulted in an apparent mass loss and a rapid decrease in the materials temperature [25, 26]. The water evaporation in apple samples during the VF treatment was an intensive and short process of self-dehydration, while no intensive water evaporation happened in the PF treatment because it was performed at atmospheric pressure by using mechanical refrigeration and heat conduction. When apple samples were frozen during the PF

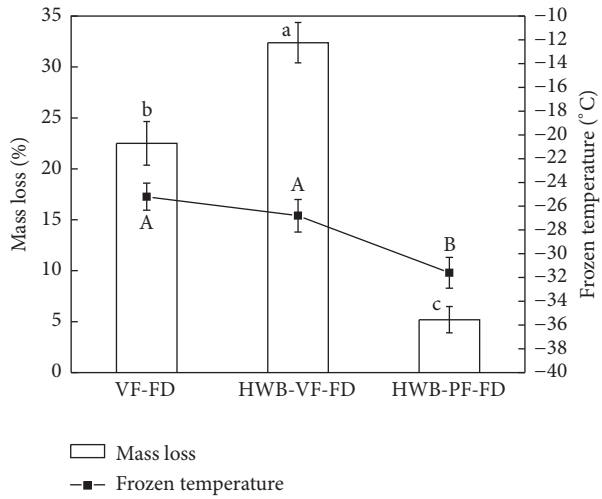

Figure 2: Mass loss and frozen temperature of apple samples at the end of freezing treatment in 3 freeze-drying methods. VF-FD: apple samples without hot-water pretreatment were performed with vacuum freezing treatment and freeze-drying process; HWB-VF-FD: apple samples with hot-water pretreatment were performed with vacuum freezing treatment and freeze-drying process; HWB-PF-FD: apple samples with hot-water pretreatment were performed with plate freezing treatment and freeze-drying process. *Note*. Different letters on the same bar or line indicate significant differences at $p = 0.05$ by Tukey's HSD test.

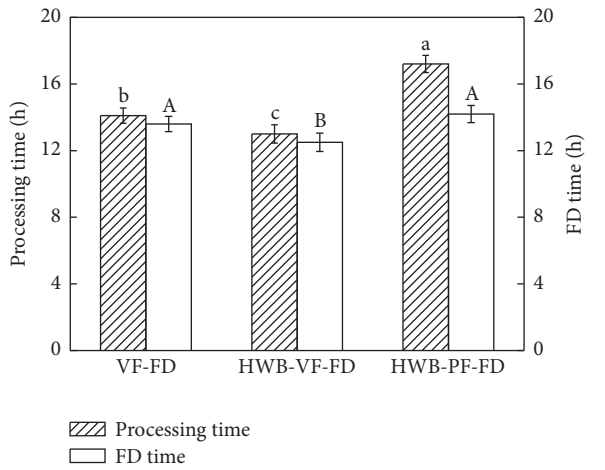

Figure 3: Processing time and FD time in 3 freeze-drying methods. VF-FD: apple samples without hot-water pretreatment were performed with vacuum freezing treatment and freeze-drying process; HWB-VF-FD: apple samples with hot-water pretreatment were performed with vacuum freezing treatment and freeze-drying process; HWB-PF-FD: apple samples with hot-water pretreatment were performed with plate freezing treatment and freeze-drying process. *Note*. Different letters on the same bars indicate significant differences at $p = 0.05$ by Tukey's HSD test.

treatment, a small amount of dehydration also occurred due to the superficial ice sublimation caused by the vapor pressure-temperature environmental interaction [27, 28].

Mass loss of VF treatment in HWB-VF-FD was increased by 43.91% in contrast to that in VF-FD; this significant difference was caused by HWB pretreatment. It can be attributed to the fact that short-time action of high-temperature blanching generally produces profound changes to the cell microstructure including protoplasm coagulation, water loss and shrinkage of intercellular spaces, plasmolysis, increase in permeability or even disruption of cell membranes, and decrease in bound or hydrophilic capacity of extracellular and intracellular water [29–31], which definitely contributed to faster water-evaporating speed and higher mass loss in HWB-VF-FD.

In order to obtain a successful FD performance, the fresh raw materials were required to be fully frozen and keep frozen temperature below their eutectic temperature. The eutectic temperature of the fresh apple in this study was determined as −22.6°C by the electric resistance method [32]. Frozen temperature of samples in VF-FD and HWB-VF-FD was around −26°C with no significant difference and that in HWB-PF-FD was around −32°C, which all can meet the requirements of the eutectic temperature.

Higher mass loss and more temperature decrease in HWB-VF-FD were more favorable for the NIFD process by considering the requirement of the fully freezing and the eutectic temperature of fresh samples as well as the least FD time as possible. Theoretically, the mass loss would be closely corresponding to the frozen temperature of samples complying with the principle of conservation of energy during the VF process. In other words, the higher mass loss, the lower frozen temperature. But no significant difference was observed between the frozen temperatures of the VF treatment in VF-FD and HWB-VF-FD. The reason may be inferred that the removed latent heat by mass loss (water evaporation) in the samples during the VF treatment came from the sensible heat for reducing samples temperature, the latent heat for forming ice crystals in the samples, the foreign heat transmitted from the plates, and the ambient chamber into the apple samples. Before the beginning of the VF treatment in VF-FD method, the temperature of apple samples and the material trays was around the room temperature (20°C) and the plate's temperature in the freeze-drying chamber was around 5°C due to the heat transferring from the cold trap. Before the beginning of the VF treatment in HWB-VF-FD method, the temperature of apple samples and the material trays was around 50°C without precooling treatment and the plate's temperature was also around 5°C. At the end of the VF treatment, the temperature of apple samples, the material trays, and the plates was all around or close to the frozen temperature −26°C. The removed heat either from the material trays or from the plates due to the temperature difference before and after the VF treatment was absorbed mostly by the latent heat of water evaporation from apple samples. So the energy of water evaporation was not only dedicated to the cooling and freezing of apple samples. The inevitable foreign heat transmission might undermine the apparent difference of frozen temperature of apple samples caused by different mass loss.

3.2. Processing Time and FD Time. It is well known that FD is a drying method with high production cost. And the drying time is regarded as one of the main economic indicators of freeze-dried food processing. As shown in Figure 3, HWB-VF-FD cost the shortest FD time and processing time, then

followed by VF-FD and HWB-PF-FD. There was no significant difference between FD time in VF-FD and HWB-PF-FD. But FD time in HWB-PF-FD was significantly longer than that in HWB-VF-FD, which was caused by huge difference in mass loss of apple samples after VF and PF. In other words, the moisture content of samples after VF was much lower than that after PF. And the processing time in HWB-PF-FD was significantly higher than the other two methods. In particular, HWB-VF-FD method reduced 24.42% of the processing time compared with the conventional HWB-PF-FD method, showing an evident economic advantage of the NIFD process. The processing time was the sum of freezing time and FD time. The freezing time of the VF and PF treatment was set as 0.5 h and 3 h, respectively. 2.5 h difference in the freezing time of the two freezing methods probably contributed to the main difference in the processing time. It also can be concluded that HWB pretreatment in the NIFD process (HWB-VF-FD) can shorten FD time and processing time. The similar results had been reported in some available research publications [13, 33, 34]. The reason why blanching pretreatment can accelerate the drying process might be attributed to the fact that high-temperature blanching can relax tissue structure, enhance cell membranes permeability, and reduce water hydrophilic capacity, facilitating faster and more vapor transmission during VF treatment and FD process.

3.3. Rehydration Ratio (RR) and Shrinkage Ratio (SR). The higher values of RR and SR are desired for better quality of FD products. As shown in Figure 4, RR of freeze-dried samples in HWB-VF-FD were obviously higher than that in VF-FD and HWB-PF-FD, showing that the freeze-dried samples with the treatment of HWB and VF were easier to recover nearly to the fresh state by rehydrating. The possible reason was that better porous structure and higher cell membranes permeability were formed in the dried samples in HWB-VF-FD.

There was no significant difference between SR in HWB-VF-FD and HWB-PF-FD. But SR in VF-FD was significantly smaller than the others, which indicated that more shrinkage happened in the tissue of freeze-dried samples. By comparing RR and SR in the two NIFD process (VF-FD and HWB-VF-FD), we can conclude that HWB pretreatment resulted in a significant enhancement on the FD properties of apple slices. The NIFD process of HWB-VF-FD can even acquire a higher RR value and an equivalent SR value in contrast with those in the CFD process of HWB-PF-FD.

3.4. V_C Content. Figure 5 showed the V_C content of freeze-dried samples in the three methods. V_C content in VF-FD was evidently higher than HWB-VF-FD and HWB-PF-FD. It can be concluded that HWB pretreatment was the main factor accounting for the difference in V_C contents, while the freezing method was not. It had been reported that V_C loss was found to occur during the blanching process, which was probably caused by high-temperature thermal degradation, leaching of V_C into the blanch water and involving V_C in the ascorbic acid oxidation [33, 35]. Therefore, HWB pretreatment was not favorable for the V_C retention either in the NIFD process or in the CFD process.

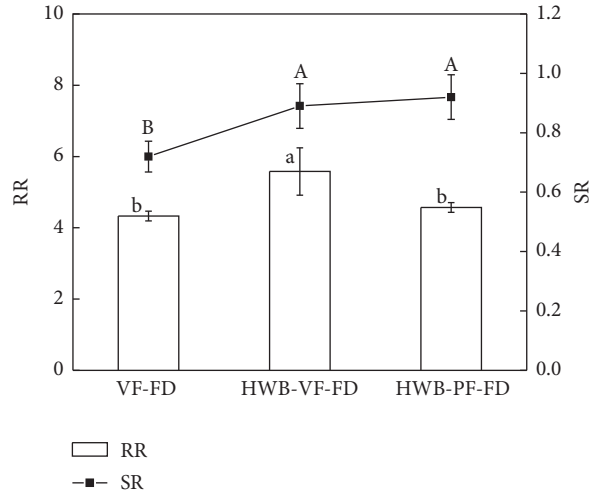

Figure 4: Rehydration ratio and shrinkage ratio of freeze-dried samples in 3 freeze-drying methods. VF-FD: apple samples without hot-water pretreatment were performed with vacuum freezing treatment and freeze-drying process; HWB-VF-FD: apple samples with hot-water pretreatment were performed with vacuum freezing treatment and freeze-drying process; HWB-PF-FD: apple samples with hot-water pretreatment were performed with plate freezing treatment and freeze-drying process. *Note*. Different letters on the same bar or line indicate significant differences at $p = 0.05$ by Tukey's HSD test.

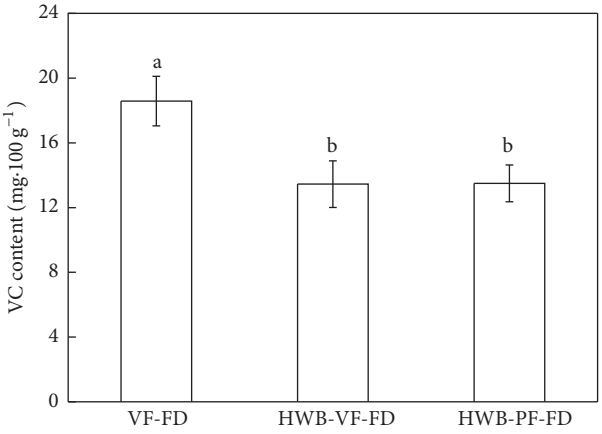

Figure 5: Vitamin C content of freeze-dried samples in 3 freeze-drying methods. VF-FD: apple samples without hot-water pretreatment were performed with vacuum freezing treatment and freeze-drying process; HWB-VF-FD: apple samples with hot-water pretreatment were performed with vacuum freezing treatment and freeze-drying process; HWB-PF-FD: apple samples with hot-water pretreatment were performed with plate freezing treatment and freeze-drying process. *Note*. Different letters on the same bar indicate significant differences at $p = 0.05$ by Tukey's HSD test.

3.5. Color. Color data of freeze-dried and rehydrated samples was shown in Table 1. Among the color parameters, L^*

Table 1: Color difference of freeze-dried and rehydrated samples in 3 freeze-drying methods.

	L^*	a^*	b^*	ΔE
Fresh sample	74.56 ± 0.92	6.72 ± 1.26	21.24 ± 2.20	
Freeze-dried sample				
VF-FD	81.98 ± 2.68^{ab}	7.07 ± 1.89^{a}	29.84 ± 1.92^{a}	11.36 ± 0.76^{a}
HWB-VF-FD	82.89 ± 0.47^{a}	1.83 ± 0.57^{b}	18.07 ± 1.51^{c}	10.16 ± 0.86^{a}
HWB-PF-FD	78.85 ± 2.11^{b}	8.33 ± 0.61^{a}	25.04 ± 1.42^{b}	5.95 ± 0.45^{b}
Rehydrated sample				
VF-FD	56.01 ± 1.37^{b}	14.34 ± 0.31^{a}	30.47 ± 0.75^{a}	22.08 ± 0.68^{a}
HWB-VF-FD	63.41 ± 2.59^{a}	3.41 ± 1.70^{c}	21.00 ± 1.04^{c}	11.63 ± 1.07^{c}
HWB-PF-FD	58.24 ± 2.61^{b}	9.55 ± 1.94^{b}	24.00 ± 2.54^{b}	16.79 ± 1.15^{b}

VF-FD: apple samples without hot-water pretreatment were performed with vacuum freezing treatment and freeze-drying process; HWB-VF-FD: apple samples with hot-water pretreatment were performed with vacuum freezing treatment and freeze-drying process; HWB-PF-FD: apple samples with hot-water pretreatment were performed with plate freezing treatment and freeze-drying process. *Note*. Different letters on the same columns indicate significant differences at $p = 0.05$ by Tukey's HSD test.

expresses the brightness of sample, a higher value of L^* means brighter color; a^* and b^* with decreasing value indicate red to green and yellow to blue, respectively; ΔE shows the color change compared to the original fresh samples.

In case of freeze-dried samples, HWB-VF-FD presented a brighter appearance than HWB-PF-FD based on both visual evaluation and instrumental testing. Instrumentally, L^* value in HWB-VF-FD was higher than that in HWB-PF-FD. Compared with the fresh samples, the dried samples in HWB-VF-FD became slightly more green and blue, and dried samples in VF-FD and HWB-PF-FD became slightly more red and yellow judging from the values of a^* and b^*. The comprehensive parameter ΔE was calculated with the lowest value in HWB-VF-FD and the highest value in VF-FD.

In case of the rehydrated samples, the L^* value in HWB-VF-FD was significantly higher, and ΔE was significantly lower than the two others. Actually, the rehydrated samples in VF-FD appeared visually to be darker in color than that in HWB-VF-FD. The color of rehydrated samples in HWB-VF-FD was most approximate to the fresh samples. The reason why the color difference occurred was very complicated and might be attributed to the comprehensive difference in porosity, density, and other physical properties, activity of oxidation or residual-enzyme browning, and so on. A bright and white appearance of product in HWB-VF-FD is naturally more popular with customers whether for freeze-dried samples or for rehydrated samples.

3.6. Hardness. Hardness (force at fracture) is viewed as one of the important textural properties for dried food products. Fracture of dried food products is a complex phenomenon that depends largely on the components and the microstructure of food materials [36]. As shown in Figure 6, dried samples in VF-FD were measured with significantly higher hardness values than those in HWB-VF-FD and HWB-PF-FD. The fact that blanching pretreatment can lead to some soluble solid loss in fruits tissue had been verified by some available research literatures [37, 38]. In particular, the leaching of soluble solid during blanching would also reduce rigidity to the cell wall in the tissue and the hardness of dried samples [39, 40]. Additionally, high-temperature blanching

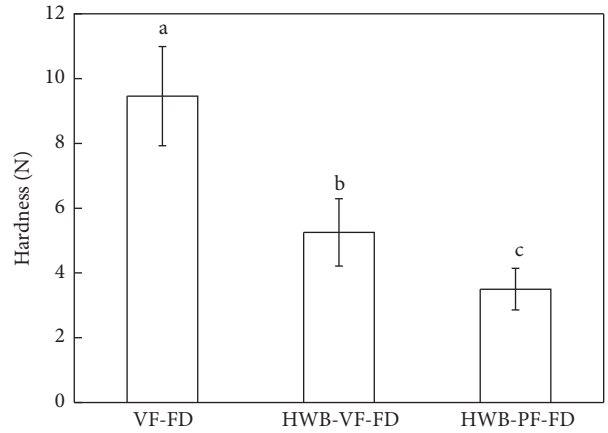

Figure 6: Hardness of freeze-dried samples in 3 freeze-drying methods. VF-FD: apple samples without hot-water pretreatment were performed with vacuum freezing treatment and freeze-drying process; HWB-VF-FD: apple samples with hot-water pretreatment were performed with vacuum freezing treatment and freeze-drying process; HWB-PF-FD: apple samples with hot-water pretreatment were performed with plate freezing treatment and freeze-drying process. *Note*. Different letters on the same bar indicate significant differences at $p = 0.05$ by Tukey's HSD test.

itself can relax and soften the apple tissue and undermine the mechanics properties of porous structure in freeze-dried apple slices [40], which can also contribute to the hardness reduction of dried samples in HWB-VF-FD and HWB-PF-FD. In VF-FD, the most compact and denser porous structure might be formed due to its highest SR of freeze-dried samples (see Figure 4). Thus the highest fracture force in VF-FD (see Figure 6) was reasonably to be expected by considering the microstructure shrinkage as well as the influence of HWB pretreatment.

3.7. TEM Analysis. Representative TEM micrographs of cell wall and membrane in apple slices before and after HWB pretreatment are shown in Figure 7. It was found that HWB pretreatment resulted in evident changes to cell tissue. Before HWB pretreatment, cell wall and membrane were tightly

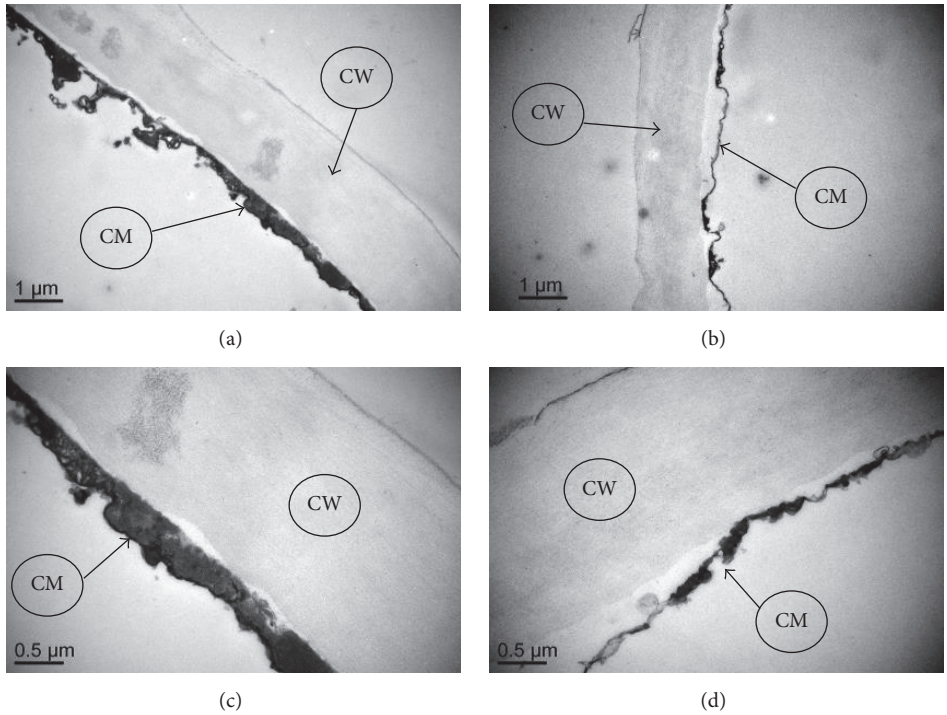

Figure 7: Microphotographs from TEM of cell wall and membrane in apple slices before and after hot-water blanching. (a) Before hot-water blanching at 20000x magnification; (b) after hot-water blanching at 20000x magnification; (c) before hot-water blanching at 40000x magnification; (d) after hot-water blanching at 40000x magnification; CW: cell wall; CM: cell membrane.

bonded with each other, and the cell membrane was thick, intact, and continuous in shape and dimension. After HWB pretreatment, cell membrane was partly detached from cell wall and became thinner and partially broken, which can contribute to the results of the dehydration and softening in cell tissue, the increase of cell membrane permeability, and the decrease in tissue hardness. In some sense, all the changes in cell tissue caused by HWB pretreatment can account for the higher mass loss, shorter FD time, higher SR and RR, and smaller hardness of the freeze-dried samples in HWB-VF-FD.

3.8. SEM Analysis. Representative apparent photographs and SEM micrographs of freeze-dried samples in the three methods were shown in Figures 8 and 9, respectively. Retaining the original shape of the materials is an essential requirement for FD products. In Figure 8, a significant shrinkage and collapse phenomenon was observed in the freeze-dried samples in VF-FD (Figure 8(a)), whose volume was much smaller than the others, while HWB-VF-FD obtained a flat and full appearance in the samples which was almost the same as that in HWB-PF-FD (Figures 8(a) and 8(b)), showing a good performance of retaining the original shape of fresh materials.

In Figure 9, it can be found that the honeycomb network was formed in the tissues of all the samples. VF-FD samples formed the smallest pores and appeared to be the most compact and dense (Figure 9(a)). HWB-VF-FD samples showed a network size with larger pores (Figure 9(b)). HWB-PF-FD samples appeared to be of a network size with the largest pores (Figure 9(c)). The porosity of freeze-dried samples in the three methods was shown as Figure 10. There was significant difference among the porosity of samples in the three methods. HWB-PF-FD samples had the highest porosity, followed by HWB-VF-FD samples and VF-FD samples. The results of the porosity measurement were consistent with the observation results of SEM images in Figure 9, which identified that the VF-FD samples had a dense structure.

The pores of the tissue in SEM images were associated with the size and location of ice crystals [27]. It is well known that ice crystal size is closely related to the freezing rate. Compared with the PF treatment in HWB-PF-FD, the VF treatment in VF-FD and HWB-VF-FD was performed with a much faster freezing rate, resulting in smaller ice crystals in the frozen tissue and forming smaller pores in the dried tissue after ice sublimation. Besides, microvolume distribution of water in the apple tissue during the VF treatment can directly influence the size of ice crystal and the network pores. About 30% water was removed from apple samples during the VF treatment in VF-FD and HWB-VF-FD, which inevitably reduced the water microvolume distribution in the cell tissue and also formed smaller ice crystals and network pores in contrast to that in HWB-VF-FD.

On the other hand, the shape of the honeycomb network was also influenced by HWB pretreatment in the NIFD process. Pores in the samples of VF-FD presented much more shrinkage and collapse than the others, which conform to the results of apparent photographs in Figure 8. Krokida et

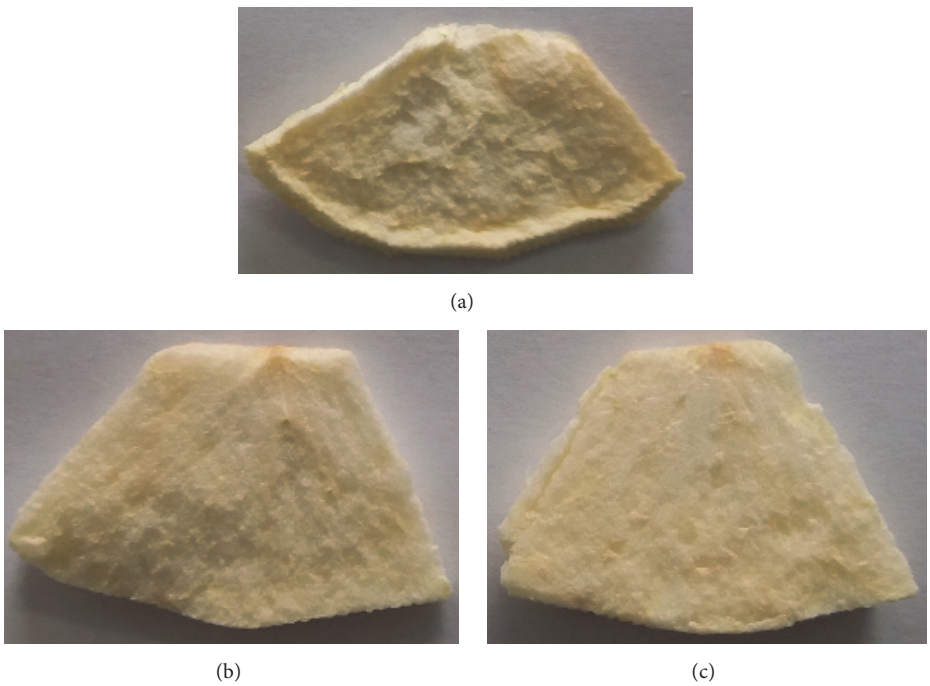

(a) (b) (c)

Figure 8: Apparent photographs of freeze-dried samples with 3 freeze-drying methods. (a) VF-FD; (b) HWB-VF-FD; (c) HWB-PF-FD. VF-FD: apple samples without hot-water pretreatment were performed with vacuum freezing treatment and freeze-drying process; HWB-VF-FD: apple samples with hot-water pretreatment were performed with vacuum freezing treatment and freeze-drying process; HWB-PF-FD: apple samples with hot-water pretreatment were performed with plate freezing treatment and freeze-drying process.

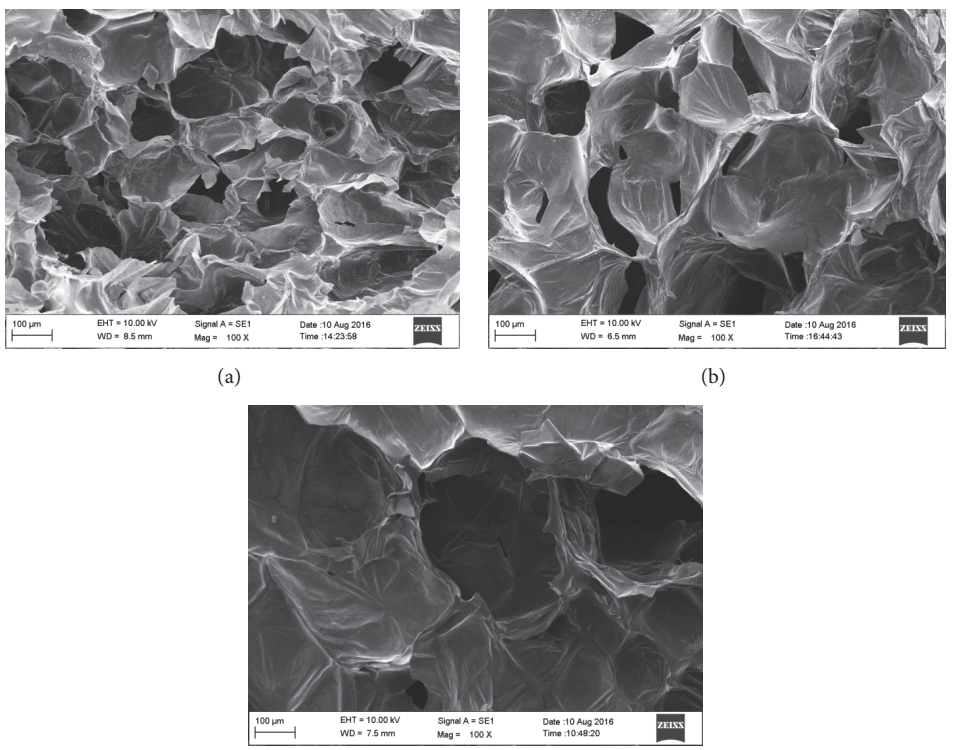

(a) (b) (c)

Figure 9: Microphotographs (at 100 magnification) from SEM of freeze-dried samples with 3 freeze-drying methods. (a) VF-FD; (b) HWB-VF-FD; (c) HWB-PF-FD. VF-FD: apple samples without hot-water pretreatment were performed with vacuum freezing treatment and freeze-drying process; HWB-VF-FD: apple samples with hot-water pretreatment were performed with vacuum freezing treatment and freeze-drying process; HWB-PF-FD: apple samples with hot-water pretreatment were performed with plate freezing treatment and freeze-drying process.

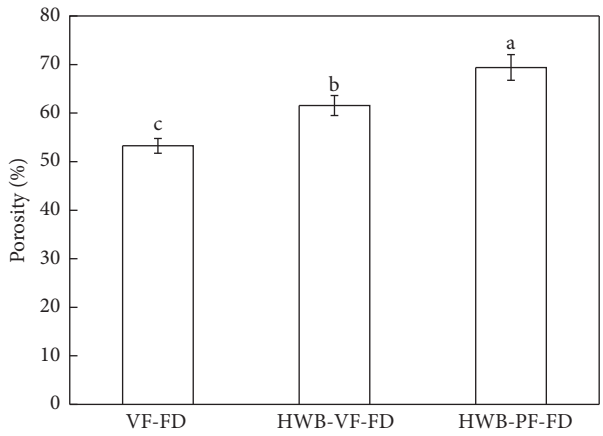

Figure 10: Porosity of freeze-dried samples in 3 freeze-drying methods. VF-FD: apple samples without hot-water pretreatment were performed with vacuum freezing treatment and freeze-drying process; HWB-VF-FD: apple samples with hot-water pretreatment were performed with vacuum freezing treatment and freeze-drying process; HWB-PF-FD: apple samples with hot-water pretreatment were performed with plate freezing treatment and freeze-drying process. *Note*. Different letters on the same bar indicate significant differences at $p = 0.05$ by Tukey's HSD test.

al. showed that serious shrinkage of FD products was often caused by the appearance of the overmuch unfrozen water due to the insufficient freezing treatment of materials and the ice melting in samples during FD process because of unsuitable heating speed [41]. Mass loss during the VF treatment in VF-FD was significantly smaller than HWB-VF-FD because of the HWB pretreatment. It can be inferred that ice melting and collapsing occurred during the FD process because of the incomplete freezing status caused by insufficient mass loss during the VF treatment. VF-FD samples had the lowest SR value and the highest hardness value mainly due to its smallest pores size and porosity, most compact and densest structure of the honeycomb network formed during the VF treatment and the subsequent FD process. So, the NIFD process of VF-FD without HWB cannot be viewed as a successful one especially due to its serious shrinkage and collapse appearance.

4. Conclusions

By comparing the 3 different FD processing methods, we can conclude that HWB pretreatment in the NIFD progress of HWB-VF-FD resulted in lots of changes to the product qualities in contrast to VF-FD, including higher mass loss, shorter FD time, higher SR and RR, lower Vc content, smaller hardness, better apparent colors, and shape in freeze-dried samples, which were desired or acceptable for a successful FD process (except the quality index of V_C content). Compared with the CFD process in HWB-PF-FD, the NIFD process of HWB-VF-FD achieved similar or better product quality and, moreover, showed a considerable time-saving advantage. The observation of apple sample's microstructure was conducted by TEM and SEM, which can account for the above differences in product qualities.

Abbreviations

FD:	Freeze-drying
NIFD:	Novel integrated freeze-drying
CFD:	Conventional freeze-drying
HWB:	Hot-water blanching
VF-FD:	Apple samples without hot-water pretreatment were performed with vacuum freezing treatment and freeze-drying process
HWB-VF-FD:	Apple samples with hot-water pretreatment were performed with vacuum freezing treatment and freeze-drying process
HWB-PF-FD:	Apple samples with hot-water pretreatment were performed with plate freezing treatment and freeze-drying process
V_C:	Vitamin C
VF:	Vacuum freezing
PF:	Plate freezing
RR:	Rehydration ratio
SR:	Shrinkage ratio
TEM:	Transmission electron microscopy
SEM:	Scanning electron microscopy.

Additional Points

Practical Application. Vacuum freeze-drying is one of the best methods for food drying. But in practice, conventional freeze-drying process is characterized by many disadvantages including complicated process steps, large space occupation, huge equipment investment, frequent materials transferring, long drying time, and high production cost, which greatly reduced economic competitiveness of FD products. Therefore the novel integrated freeze-drying processing technology was proposed. In this study, the effect of HWB on the drying characteristics and product qualities of apple slices dried with the novel progress. HWB pretreatment in the novel progress resulted in lots of desired or acceptable changes to the drying characteristics and product qualities such as FD time, rehydration ratio, shrinkage ratio, apparent colors, and shape. The NIFD process of HWB-VF-FD was suggested as a promising alternative method to decrease FD time, simplify the steps, and achieve similar product quality of the CFD process.

Conflicts of Interest

The authors declare that they have no conflicts of interest.

Acknowledgments

The authors would like to acknowledge the financial support from the National Natural Science Foundations of China (no. 31301592) which enabled us to carry out this study. Financial supports from Key Laboratory of Modern Agricultural Equipment of Ministry of Agriculture Funding Program

(201604002) and Changzhou Science and Technology Support Program (CE20152017) are also acknowledged.

References

[1] C. Ratti, "Hot air and freeze-drying of high-value foods: a review," *Journal of Food Engineering*, vol. 49, no. 4, pp. 311–319, 2001.

[2] F. Shishehgarha, J. Makhlouf, and C. Ratti, "Freeze-drying characteristics of strawberries," *Drying Technology*, vol. 20, no. 1, pp. 131–145, 2002.

[3] L. G. Marques, A. M. Silveira, and J. T. Freire, "Freeze-drying characteristics of tropical fruits," *Drying Technology*, vol. 24, no. 4, pp. 457–463, 2006.

[4] M. Zhang, J. Tang, A. S. Mujumdar, and S. Wang, "Trends in microwave-related drying of fruits and vegetables," *Trends in Food Science & Technology*, vol. 17, no. 10, pp. 524–534, 2006.

[5] H. Jiang, M. Zhang, A. S. Mujumdar, and R.-X. Lim, "Comparison of drying characteristic and uniformity of banana cubes dried by pulse-spouted microwave vacuum drying, freeze drying and microwave freeze drying," *Journal of the Science of Food and Agriculture*, vol. 94, no. 9, pp. 1827–1834, 2014.

[6] S. V. Jangam, "An overview of recent developments and some R&D challenges related to drying of foods," *Drying Technology*, vol. 29, no. 12, pp. 1343–1357, 2011.

[7] S. Litvin, C. H. Mannheim, and J. Miltz, "Dehydration of carrots by a combination of freeze drying, microwave heating and air or vacuum drying," *Journal of Food Engineering*, vol. 36, no. 1-4, pp. 103–111, 1998.

[8] R. Wang, M. Zhang, and A. S. Mujumdar, "Effect of osmotic dehydration on microwave freeze-drying characteristics and quality of potato chips," *Drying Technology*, vol. 28, no. 6, pp. 798–806, 2010.

[9] H. Wang, Z. Hu, K. Tu, F. Wu, T. Zhong, and H. Xie, "Application of vacuum-cooling pretreatment to microwave freeze drying of carrot slices," *Transactions of the Chinese Society of Agricultural Engineering*, vol. 27, no. 7, pp. 358–363, 2011.

[10] H. O. Wang, S. J. Chen, and W. Zhang, "An integrated equipment of radiation vacuum freeze-drying and its method," in *Chinese Patent No. 201510017464.8 , Beijing: State Intellectual Property Office of the P.R.C*, in Chinese, C, 2015.

[11] A. A. Adedeji, T. K. Gachovska, M. O. Ngadi, and G. S. V. Raghavan, "Effect of pretreatments on drying characteristics of okra," *Drying Technology*, vol. 26, no. 10, pp. 1251–1256, 2008.

[12] C. Severini, A. Baiano, T. De Pilli, R. Romaniello, and A. Derossi, "Prevention of enzymatic browning in sliced potatoes by blanching in boiling saline solutions," *LWT- Food Science and Technology*, vol. 36, no. 7, pp. 657–665, 2003.

[13] Y. Wang, M. Zhang, A. S. Mujumdar, K. J. Mothibe, and S. M. Roknul Azam, "Effect of blanching on microwave freeze drying of stem lettuce cubes in a circular conduit drying chamber," *Journal of Food Engineering*, vol. 113, no. 2, pp. 177–185, 2012.

[14] M. González-Fésler, D. Salvatori, P. Gómez, and S. M. Alzamora, "Convective air drying of apples as affected by blanching and calcium impregnation," *Journal of Food Engineering*, vol. 87, no. 3, pp. 323–332, 2008.

[15] N. Sanjuán, G. Clemente, J. Bon, and A. Mulet, "The effect of blanching on the quality of dehydrated broccoli florets," *European Food Research and Technology*, vol. 213, no. 6, pp. 474–479, 2001.

[16] J. I. Maté, M. Zwietering, and K. Van't Riet, "The effect of blanching on the mechanical and rehydration properties of dried potato slices," *European Food Research and Technology*, vol. 209, no. 5, pp. 343–347, 1999.

[17] C. Severini, A. Baiano, T. De Pilli, B. F. Carbone, and A. Derossi, "Combined treatments of blanching and dehydration: study on potato cubes," *Journal of Food Engineering*, vol. 68, no. 3, pp. 289–296, 2005.

[18] S. Prakash, S. K. Jha, and N. Datta, "Performance evaluation of blanched carrots dried by three different driers," *Journal of Food Engineering*, vol. 62, no. 3, pp. 305–313, 2004.

[19] K. O. Falade and O. J. Solademi, "Modelling of air drying of fresh and blanched sweet potato slices," *International Journal of Food Science & Technology*, vol. 45, no. 2, pp. 278–288, 2010.

[20] T. Beveridge and S. E. Weintraub, "Effect of blanching pretreatment on color and texture of apple slices at various water activities," *Food Research International*, vol. 28, no. 1, pp. 83–86, 1995.

[21] I. Doymaz, "Effect of citric acid and blanching pre-treatments on drying and rehydration of Amasya red apples," *Food and Bioproducts Processing*, vol. 88, no. 2-3, pp. 124–132, 2010.

[22] R. Thuwapanichayanan, S. Prachayawarakorn, and S. Soponronnarit, "Drying characteristics and quality of banana foam mat," *Journal of Food Engineering*, vol. 86, no. 4, pp. 573–583, 2008.

[23] AOAC, *Official Methods of Analysis*, Association of Official Analytical Chemists, Washington, Wash, USA, 14th edition, 1984.

[24] N. Jiang, C. Liu, D. Li, and Y. Zhou, "Effect of blanching on the dielectric properties and microwave vacuum drying behavior of Agaricus bisporus slices," *Innovative Food Science and Emerging Technologies*, vol. 30, pp. 89–97, 2015.

[25] K. McDonald, D.-W. Sun, and T. Kenny, "Comparison of the quality of cooked beef products cooled by vacuum cooling and by conventional cooling," *LWT- Food Science and Technology*, vol. 33, no. 1, pp. 21–29, 2000.

[26] D. Sun and L. Zheng, "Vacuum cooling technology for the agri-food industry: past, present and future," *Journal of Food Engineering*, vol. 77, no. 2, pp. 203–214, 2006.

[27] Q. T. Pham, "Modelling heat and mass transfer in frozen foods: a review," *International Journal of Refrigeration*, vol. 29, no. 6, pp. 876–888, 2006.

[28] L. A. Campañone, V. O. Salvadori, and R. H. Mascheroni, "Weight loss during freezing and storage of unpackaged foods," *Journal of Food Engineering*, vol. 47, no. 2, pp. 69–79, 2001.

[29] S. M. Alzamora, M. A. Castro, S. L. Vidales et al., "The role of tissue microstructure in the textural characteristics of minimally processed fruits," *Minimally Processed Fruits and Vegetables*, pp. 153–171, 2000.

[30] A. Nieto, D. Salvatori, M. A. Castro, and S. M. Alzamora, "Air drying behavior of apples as affected by blanching and glucose impregnation," *Journal of Food Engineering*, vol. 36, no. 1-4, pp. 63–79, 1998.

[31] A. Nieto, M. A. Castro, and S. M. Alzamora, "Kinetics of moisture transfer during air drying of blanched and/or osmotically dehydrated mango," *Journal of Food Engineering*, vol. 50, no. 3, pp. 175–185, 2001.

[32] Q. Cui, Y. Guo, and Z. Cheng, "Measurement of the eutectic point and melting point of the freeze-dried materials based on electric resistance method," *Transactions of the Chinese Society of Agricultural Machinery*, vol. 39, no. 5, pp. 65–69, 2008.

[33] T. M. Lin, T. D. Durance, and C. H. Scaman, "Characterization of vacuum microwave, air and freeze dried carrot slices," *Food Research International*, vol. 31, no. 2, pp. 111–117, 1998.

[34] R. Moreira, A. Figueiredo, and A. Sereno, "Shrinkage of apple disks during drying by warm air convection and freeze drying," *Drying Technology*, vol. 18, no. 1-2, pp. 279–294, 2000.

[35] Y. Wu, J. H. Qi, M. Q. Huang et al., "Analysis of substrates and products of non-enzymatic browning in Chinese chestnut," *Chinese Agricultural Science Bulletin*, vol. 28, no. 30, pp. 267–271, 2012 (Chinese).

[36] N. C. Acevedo, V. Briones, P. Buera, and J. M. Aguilera, "Microstructure affects the rate of chemical, physical and color changes during storage of dried apple discs," *Journal of Food Engineering*, vol. 85, no. 2, pp. 222–231, 2008.

[37] S. Mizrahi, "Leaching of soluble solids during blanching of vegetables by ohmic heating," *Journal of Food Engineering*, vol. 29, no. 2, pp. 153–166, 1996.

[38] C. Arroqui, T. R. Rumsey, A. Lopez, and P. Virseda, "Losses by diffusion of ascorbic acid during recycled water blanching of potato tissue," *Journal of Food Engineering*, vol. 52, no. 1, pp. 25–30, 2002.

[39] G. Romano, M. Nagle, D. Argyropoulos, and J. Müller, "Laser light backscattering to monitor moisture content, soluble solid content and hardness of apple tissue during drying," *Journal of Food Engineering*, vol. 104, no. 4, pp. 657–662, 2011.

[40] P. P. Lewicki, "Effect of pre-drying treatment, drying and rehydration on plant tissue properties: a review," *International Journal of Food Properties*, vol. 1, no. 1, pp. 1–22, 1998.

[41] M. K. Krokida, V. T. Karathanos, and Z. B. Maroulis, "Effect of freeze-drying conditions on shrinkage and porosity of dehydrated agricultural products," *Journal of Food Engineering*, vol. 35, no. 4, pp. 369–380, 1998.

Hindawi
Journal of Food Quality
Volume 2018, Article ID 6157697, 13 pages
https://doi.org/10.1155/2018/6157697

Research Article

Novel Combined Freeze-Drying and Instant Controlled Pressure Drop Drying for Restructured Carrot-Potato Chips: Optimized by Response Surface Method

Jianyong Yi,[1] **Chunhui Hou**,[1,2] **Jinfeng Bi**,[1] **Yuanyuan Zhao**,[1] **Jian Peng**,[1] **and Changjin Liu**[2]

[1]*Institute of Food Science and Technology, Chinese Academy of Agricultural Sciences/Key Laboratory of Agro-Products Processing, Ministry of Agriculture, Beijing 100193, China*
[2]*College of Food Engineering and Biotechnology, Tianjin University of Science & Technology, Tianjin 300457, China*

Correspondence should be addressed to Jianyong Yi; yijianyong_caas@yeah.net and Jinfeng Bi; bijinfeng2010@163.com

Received 30 September 2017; Accepted 31 December 2017; Published 31 January 2018

Academic Editor: Alex Martynenko

Combined freeze-drying and instant controlled pressure drop process (FD-DIC) for restructured carrot-potato chips was developed and its processing conditions were optimized using response surface methodology (RSM) with the purpose of improving the quality of products and reducing energy consumption. Three critical variables including the amount of carrot, the moisture content of the partially dried product before DIC treatment, and equilibrium temperature of DIC for the restructured chips were considered. Response parameters such as the final moisture content, color value (L, a, and b), and texture properties of restructured carrot-potato chips were investigated. The results showed that the graphical optimal ranges of FD-DIC drying process were as follows: the amount of carrot was 46–54% w/w, the moisture content of the partially dried product before DIC treatment was 0.20–0.35 g/g, and the equilibrium temperature of DIC was 85–95°C. Furthermore, the numerical optimization suggested that conditions were 47.43% w/w, 0.29 g/g, and 90.57°C, respectively. It could be concluded that the combined drying method of FD-DIC provided the restructured carrot-potato chips with higher quality, as compared to the freeze-dried chips. Considering the relatively high production cost of FD, this novel FD-DIC could be an alternative method for obtaining desirable restructured fruit and vegetable chips.

1. Introduction

Carrot and potato are both prolific and common vegetables, which have been widely cultivated and consumed around the world. According to FAO, the production of carrot and potato was 40 million and 3 billion tons in 2015. Carrot is highly nutritious as it contains appreciable amount of vitamins B1, B2, B6, and B12 besides being rich in β-carotene [1]. It is well known that carrots are beneficial for eyesight and could prevent cardiovascular disease [2]. Potatoes are the second staple food in Europe and United States, since they are rich in vitamins, calcium, and potassium and suitable for all ages [3].

Recently, a rapid increase in the consumption of snack food has been witnessed, especially the snack food derived from fruits and vegetables. On the one hand, among these plant-based snack foods, potato and carrot chips are still the most popular products in Chinese market. Many drying technologies have been employed to dry carrots and potatoes with the goal of maintaining their appearance and their nutrients [4]. The fruit and vegetable chips could be simply separated into two categories according to processing methods: fried chips and nonfried chips. In Chinese market, the fried chips which are mainly produced by deep-frying have been mainstream since 1980s. It is generally recognized that the unique texture-flavor combination of fried chips is attributed to the complicated chemical reaction during frying, for example, Maillard reaction and lipid oxidation; meanwhile, frying often leads to a residual oil content ranging from 35.3% to 44.5% wet basis (w.b.) [5]. Due to the possibility of

intake of excessive energy during consumption of fried chips, consumers are becoming more and more interested in healthy products with low amount of fat as well as good taste [6]. On the other hand, restructured chips are recognized as a type of healthier products, which often were mixed together with several different fruits and vegetables followed by remodeling and finally drying through various means. According to the "The Dietary Guidelines for Chinese Residents" published in 2016, it is recommended for Chinese residents to take 200–300 g of fruits and 300–500 g of vegetables daily, and it is suggested that at least 25 different types of food should be consumed every day. Nevertheless, few citizens in China could achieve balanced diet according to the guidelines due to the fast pace of city-life, excessive consumption of animal foods, and abuse of fast foods with simple ingredients. From the view of diet balance, restructured chips derived from various fruits and vegetables could not only guarantee the amount and type of plant foods consumed, but also provide a variety of nutrients, including vitamins, minerals, and dietary fiber, with obvious advantages of meeting the daily nutritional demand of human beings.

Currently, a variety of technologies were developed for producing restructured chips, like extrusion, vacuum frying, freeze-drying, and so on. In Chinese market, restructured chips are often produced by extrusion which has been increasingly popular as a remodeled method, while vacuum frying is mainly applied in restructured potato chips. Generally, in order to enhance the adhesive property of mixture puree, total amount of more than 50%–70% of starch, flour, corn powder, and/or other ingredients were added, leading to a decline of the proportion of fruit and vegetable materials for restructured chips [7]. Moreover, the extruded products have to experience high temperature and high pressure treatments during remodeling, possibly resulting in significant degradation of beneficial nutrients [8]. In contrast, freeze-dried foods were characterized with high qualities such as super crispness, high retention of nutrients, and minimum shrinkage [9], which might be suitable for processing restructured chips. Though the advantages of FD are obvious, one major problem for this technology is the relative long drying time, which in turn leads to high energy consumption and production cost [10]. Fortunately, the high production cost for FD process could be reduced by combining it with some of other drying technologies [11]. Huang et al. [12] found that the restructured chips containing potato and apple dried by combined microwave and freeze-drying (MFD) obtained the best quality, and the drying time of MFD was shorter than that of FD. In addition, the combination of FD and hot-air-drying for apple cubes was confirmed to be a good alternative instead of mere FD treatment [13]. According to these previous reports, the drying time and energy consumption for FD could be significantly reduced through applying several combination methods, with the products comparatively superior to hot-air-dried products and nearer in quality to FD products [14].

Instant controlled pressure drop process (French term: détente instantannée controlee, DIC), also known as explosion puffing drying [15], was defined in 1988 by a French scientist named Allaf and his colleagues as a high-temperature short-time treatment followed by an abrupt pressure drop towards a vacuum (pressure drop rate higher than 0.5 MPa/s) [16]. DIC has been perfectly adapted to texture-sensitive products such as apple and onion and could significantly expand the volume of materials, thus generating porous microstructure and improving crispness, which pointed to superior quality for fruit and vegetable chips [17]. According to the study of Professors T. Allaf and K. Allaf [18], DIC technology requires relatively a low moisture content for materials (around 10–30% d.b.) before using DIC process, which indicates that the fresh materials need predrying first. Due to this unique principle, DIC is not suitable for drying of raw agroproducts with high moisture content such as fresh fruits and vegetables. Consequently, many drying methods have been introduced prior to the DIC treatment with the aim of reducing the moisture content of raw materials, among which the combination of hot-air-drying and DIC is wildly practiced in industry. However, this combination does not scale well to the production of restructured fruit and vegetable chips due to the fact that remarkable shrinkage could occur during hot-air-predrying, which significantly compromises the expansion effects of DIC treatment and yields products with high hardness. Therefore, our previous study on jackfruit chips provides clue for solving this problem by combining FD with DIC treatment, which yields jackfruit chips with comparative overall quality to FD-dried products [19]. However, the feasibility of this combination on restructured chips remains unknown.

The objective of this work was to validate the feasibility and optimize the processing conditions of combined freeze-drying and instant controlled pressure drop process (FD-DIC) on restructured carrot-potato chips by using response surface methodology (RSM). In terms of this, simple formula was adopted which only contained two representative materials, that is, carrots containing high content of dietary fibers and potatoes containing high amount of starch, for preparing restructured chips, because it is easy to develop series of products by adding more types of fruits and vegetables based on the simple formula.

2. Materials and Methods

2.1. Sample Preparation. Fresh carrots (*Daucus carota L.* CV. Heitianwucun) and potatoes (*Solanum tuberosum L.* CV. Dabaihua) were purchased from a local market (Beijing, China) and kept in a refrigerator at $4 \pm 0.5^{\circ}$C. The carrots and potatoes were washed with tap water then peeled and uniformly cut into sticks (4 mm × 4 mm × 50 mm) by an automatic cutter (CL50, Robot Coupe, France) before being used. The initial moisture content of carrot and potato was 10.61 g/g and 4.62 g/g on dry basis (d.b.), respectively. All of the carrot and potato sticks were steamed for 30 minutes and then blended (JYL-C022, Mixer, Joyoung Co., Ltd. Shandong, China) with different mixed ratio according to the experimental design (Table 2). At last, the mixed puree was poured into molds (5 cm × 5 cm × 5 mm) and frozen at -40°C overnight.

2.2. Freeze-Drying Combined with Instant Controlled Pressure Drop Drying. The mixed purees together with the molds were placed into the chamber of a freeze-drying machine (Alpha 1-4 Lplus, Marin Christ Co., Ltd., Osterode, Germany). The pressure of the treatment chamber was set at 0.37 mbar and the chamber was equipped with a condensate collector set at −50°C. Samples were taken out from the chamber when they reached the certain moisture content according to the experimental design (Table 2). Besides, a batch of samples were dried to final state by FD, which was used as control sample for the comparison of microstructure with FD-DIC finished samples.

Partially FD-dried samples were then treated by a DIC reactor (QDPH10-1, Tianjin Qin De Co., Ltd., Tianjin, China). Detailed information of the mechanism and system of DIC reactor were available in a previous publication [19, 20]. Firstly, the treatment chamber was heated to different equilibrium temperature according to the experimental design (Table 2) by heat exchanger. Then the samples were placed into the treatment chamber and kept for a certain time (10 min) at atmospheric pressure. An instant pressure drop towards vacuum (3–5 kPa) was carried out by opening the decompression valve which connected with the vacuum tank. Finally, the samples were dried at 60°C and under continuous vacuum for 1.5 h. Final products were taken out and stored in a desiccator before analysis. The drying process was performed in triplicate.

2.3. Experimental Design and Statistical Analysis. Response surface methodology (RSM) was applied for evaluation of the effects of drying parameters and their optimization for various responses. Central composite experimental design (CCD) with three numeric factors on three levels was used. Factors and levels of the CCD were obtained by single factor experiments. Fourteen different combinations with six replicates at the central point were constituted to run the experiment. Various parameters could affect the FD-DIC process, but the mixed ratio and the moisture content of the partially dried products to be DIC-treated could be distinguished as the most influencing factor. Therefore, the independent variables used in experimental design were the amount of carrot (or mixed ratio), the moisture content of the partially dried product before DIC treatment, and equilibrium temperature of DIC. To affect the response surfaces more evenly, drying parameters were normalized as coded variables according to Table 1.

The response variables were fitted to a second-order polynomial model (see (1)) which is generally able to describe relationship between the responses and the independent variables [21].

$$Y = \beta_0 + \sum_{i=1}^{2} \beta_i X_i + \sum_{i \neq j=1}^{2} \beta_{ij} X_i X_j + \sum_{i=1}^{2} \beta_{ii} {X_i}^2, \quad (1)$$

where Y represents the response variable, X_i and X_j are the independent variables affecting the response, and β_0, β_i, β_{ii}, and β_{ij} are the regression coefficients for intercept, linear, quadratic, and interaction terms, respectively. Analysis of variance (ANOVA) was used in order to evaluate model adequacy and determine regression coefficients and statistical significance. The results were statistically tested at significance level of $P = 0.05$. The adequacy of the model was evaluated by the coefficient of determination (R^2), model P value, and lack-of-fit testing. A mathematical model was established to describe the influence of single process parameter and/or interaction of multiple parameters on each investigated response. Three-dimensional (3D) response surface plots were generated using a software Design-Expert v.8.0 Trial (Stat-Ease, Minneapolis, MN, USA) and drawn by using the function of two factors while keeping the others constant.

Table 1: The factors and levels of central composite design of response surface methodology.

Coded levels	X_1 (the amount of carrot, %)	X_2 (the moisture content of the partially dried product before DIC treatment, g/g)	X_3 (equilibrium temperature of DIC, °C)
−1.68	16.4	0.132	73.2
−1	30.0	0.200	80.0
0	50.0	0.300	90.0
1	70.0	0.400	100
1.68	83.6	0.468	107

2.4. Moisture Content. Moisture content was determined by drying the samples at 105°C until reaching constant weight [22]. The weights were measured in triplicate and the results were shown as the averages.

2.5. Texture. Texture of the samples were analyzed by using a Texture Analyzer (TA.XT 2i/50, Stable Micro System Ltd., Surry, UK), which was loaded with a ball probe. The measurements were operating at a test speed of 1.0 mm/s over a distance of 5.0 mm. The pretest and posttest speeds for compression were set at 1.0 mm/s and 10.0 mm/s, respectively [23]. Data obtained from force-deformation curve were used for the analysis of hardness and crispness of the samples. Hardness is expressed as the maximum force (N) drawn from the highest compression peak, while crispness is the distance (mm) from origin of coordinate to abscissa of the first fracture point [24].

2.6. Color. The CIE Lab color coordinates were measured by using a colorimeter (MINOLTA Chroma Meter, CM-700d, Konica Minolta Ltd, Tokyo, Japan). The apparent (surface) color of the samples was measured in terms of L (degree of lightness and darkness), a (degree of redness and greenness), and b (degree of yellowness and blueness) [25]. Samples were placed on the measure head of the colorimeter and measurements of color were performed for all the prepared samples. Standard white and black colors were used for calibration. Experiments were replicated five times for statistical purpose.

Table 2: The results of central composite design of response surface methodology.

Run	Coded levels			Responses					
	X_1	X_2	X_3	Y_1 (final moisture content, g/g)	Y_2 (hardness, N)	Y_3 (crispness, mm)	Y_4 (L)	Y_5 (a)	Y_6 (b)
(1)	−1	−1	−1	0.046 ± 0.001	7.26 ± 0.25	0.34 ± 0.03	72.27 ± 0.57	22.15 ± 0.54	30.27 ± 0.54
(2)	1	−1	−1	0.054 ± 0.002	6.33 ± 0.14	0.68 ± 0.06	66.64 ± 0.97	28.13 ± 1.46	33.61 ± 0.89
(3)	−1	1	−1	0.041 ± 0.002	5.41 ± 0.30	0.24 ± 0.02	71.63 ± 0.86	22.46 ± 0.55	33.34 ± 0.54
(4)	1	1	−1	0.052 ± 0.005	6.50 ± 0.20	0.61 ± 0.01	65.86 ± 0.79	29.85 ± 1.07	38.42 ± 0.58
(5)	−1	−1	1	0.041 ± 0.001	5.30 ± 0.30	0.76 ± 0.05	74.02 ± 0.55	21.14 ± 0.84	29.21 ± 0.73
(6)	1	−1	1	0.050 ± 0.003	6.41 ± 0.28	1.24 ± 0.27	65.32 ± 0.79	26.18 ± 2.15	34.08 ± 0.84
(7)	−1	1	1	0.032 ± 0.017	5.69 ± 0.13	0.42 ± 0.02	72.69 ± 0.48	23.45 ± 1.51	32.71 ± 0.31
(8)	1	1	1	0.058 ± 0.004	8.57 ± 0.40	1.32 ± 0.21	64.95 ± 0.76	28.51 ± 0.84	34.62 ± 0.88
(9)	−1.68	0	0	0.044 ± 0.005	7.17 ± 1.16	0.27 ± 0.03	72.63 ± 0.48	21.50 ± 0.65	28.81 ± 0.78
(10)	1.68	0	0	0.060 ± 0.002	6.08 ± 0.47	0.57 ± 0.05	62.02 ± 0.38	26.55 ± 1.06	30.96 ± 1.05
(11)	0	−1.68	0	0.041 ± 0.004	9.21 ± 0.79	0.26 ± 0.03	70.40 ± 0.75	24.40 ± 0.68	35.88 ± 2.02
(12)	0	1.68	0	0.047 ± 0.007	6.84 ± 0.44	0.31 ± 0.09	68.34 ± 0.70	27.98 ± 0.25	37.29 ± 1.91
(13)	0	0	−1.68	0.044 ± 0.002	7.90 ± 0.69	0.37 ± 0.04	72.49 ± 0.37	24.83 ± 0.39	32.39 ± 0.76
(14)	0	0	1.68	0.033 ± 0.005	6.84 ± 0.54	0.56 ± 0.08	71.59 ± 0.48	22.13 ± 0.87	35.86 ± 2.14
(15)	0	0	0	0.028 ± 0.002	10.46 ± 0.31	0.36 ± 0.03	69.89 ± 0.72	24.10 ± 0.83	36.63 ± 3.02
(16)	0	0	0	0.025 ± 0.001	9.53 ± 0.26	0.45 ± 0.02	70.07 ± 1.01	24.48 ± 0.23	35.88 ± 0.36
(17)	0	0	0	0.030 ± 0.004	10.37 ± 0.17	0.25 ± 0.03	70.43 ± 0.94	24.52 ± 0.77	35.07 ± 0.93
(18)	0	0	0	0.028 ± 0.002	11.36 ± 0.25	0.18 ± 0.04	70.38 ± 0.41	25.76 ± 1.19	37.89 ± 1.36
(19)	0	0	0	0.031 ± 0.002	10.12 ± 0.21	0.27 ± 0.02	70.06 ± 1.51	25.02 ± 1.34	36.32 ± 1.04
(20)	0	0	0	0.028 ± 0.002	10.05 ± 0.23	0.31 ± 0.03	70.70 ± 1.05	24.99 ± 0.52	35.21 ± 1.01

2.7. Scanning Electron Microscopy. Microstructural analysis of the restructured chips was carried out using a scanning electron microscope (SU8010, Hitachi Co., Ltd., Tokyo, Japan) at an accelerating voltage of 20.0 kV. The samples were fixed on the scanning stub using double sided adhesive tapes and then sputter-coated with gold by ion sputtering apparatus (MCI000, Hitachi Co., Ltd, Tokyo, Japan) for 10 min under low vacuum with argon gas to provide a reflective surface for electron beam. Image analysis was conducted at magnification of 80x.

2.8. Data Analysis. Statistical analysis was performed using RSM software Design-Expert v.8.0 Trial (Stat-Ease, Minneapolis, MN, USA). Analysis of variance (ANOVA) and the coefficient of determination (R^2) were used to assess the validity of the model. Comparison of the mean was considered to be defined at $P < 0.05$.

3. Results and Discussion

3.1. Effect of Amount of Carrot on the Freeze-Drying Characteristic of the Restructured Chips. The evolution of the moisture content of the restructured carrot-potato chips during FD is shown in Figure 1. Due to the differences in mixed ratio, the initial moisture contents of the restructured chips were varied from 10.08 g/g to 7.23 g/g with reducing of the amount of carrot from 70% to 30%. In other words, higher initial moisture content of the mixture was found by increasing the amount of carrot in the formula of restructured chips. This was attributed to the fact that the moisture content of the raw carrots was higher (10.61 g/g d.b.) than that of potatoes.

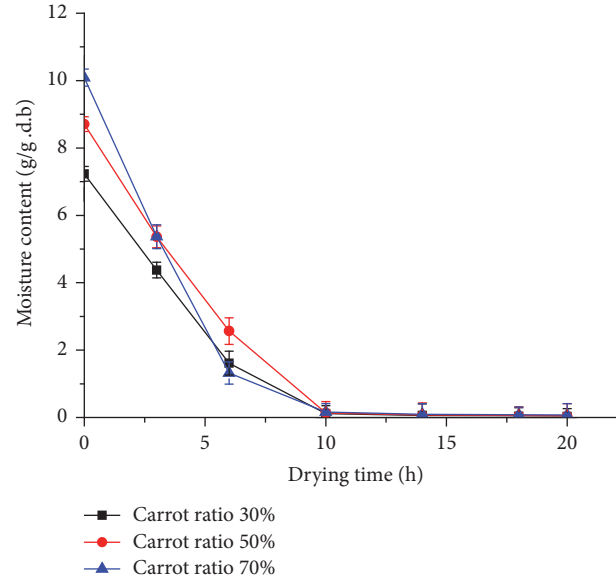

Figure 1: Freeze-drying curves of the restructured carrot-potato chips.

Table 3: Estimated coefficients of the fitted second-order polynomial models for the final moisture content, hardness, and color of the restructured chips.

Regression coefficient	Response				
	Final moisture content	Hardness	L	a	b
β_0	0.028	10.340	70.270	24.800	36.170
Linear					
β_1	$5.924 \cdot 10^{-3}$**	0.170	−3.350**	2.570**	1.380*
β_2	$1.531 \cdot 10^{-4}$	−0.230	−0.480**	0.930**	1.050*
β_3	$-2.233 \cdot 10^{-3}$*	−0.096	−0.068	−0.570*	0.060
Interaction					
β_{12}	$2.500 \cdot 10^{-3}$*	0.470	0.100	0.180	−0.150
β_{13}	$2.000 \cdot 10^{-3}$	0.480	−0.630**	−0.410	−0.200
β_{23}	$7.500 \cdot 10^{-4}$	0.530	−0.035	0.330	−0.480
Quadratic					
β_{11}	$8.561 \cdot 10^{-3}$**	−1.460**	−1.110**	0.130	−2.240**
β_{22}	$5.732 \cdot 10^{-3}$**	−0.960**	−0.390**	0.560*	0.130
β_{33}	$3.788 \cdot 10^{-3}$**	−1.190**	0.550**	−0.400	−0.740
R^2	0.956	0.900	0.989	0.955	0.830

*Significant at the 5% level, **significant at the 1% level.

Notably, it could be seen that the restructured chips with 70% carrot exhibited the fastest trend of water removing in the first 10 h during the FD process among all the samples. This might be due to the lower bulk density of the chips containing 70% carrot, which tend to form large pores and porous structure during FD, and this in turn helped in moisture diffusion [26]. In addition, though the moisture content of all the samples decreased quickly in the first 10 h, a plateau was observed in further drying process, indicating that the samples entered secondary drying stage in which the desorbed water vapor was transported through the pores of the material. Generally, the basic energy used to remove one kilogram of water is almost double for freeze-drying than for conventional drying [27]. In this study, considering the relatively long drying time and high energy cost, DIC drying was applied combined with FD process instead of single FD process in order to improve the efficiency of dehydration for the restructured carrot-potato chips.

3.2. Diagnostic Checking of Predictive Models and Response Surfaces. RSM was used to determine the experimental conditions for optimal response parameters including moisture content, hardness, crispness, and color of the final products. The experimental design and results of the responses for the restructured chips are presented in Table 2. All the response parameters except for the crispness of the samples were fitted well to a second-order polynomial model (see (1)) according to the multiple regression coefficients which were analyzed using the method of least square approach (MLS). In addition, the relationships between the process conditions and the moisture content, hardness, and color of the final products were depicted by means of quadratic polynomial models. The regression coefficients and corresponding statistical significance for each investigated response are summarized in Table 3. The results showed that the models representing the moisture content, hardness, and L and a value of the final products were of high adequacy to the experimental results ($R^2 \geq 0.90$), while the b value of the products was of moderate adequacy ($R^2 = 0.83$). The analysis of variance (ANOVA) of the fitted second-order polynomial models for the moisture content, hardness, and L, a, and b value of the final products are presented in Table 4. According to statistically significant values of P value (<0.05) for the investigated responses of the moisture content, hardness, and L, a, and b value of the samples, it could be concluded that the applied mathematical model provided proper simulation of the experimental results [28]. Additionally, the nonsignificant ($P > 0.05$) effects of lack-of-fit test implied that the prediction of the constant variance was satisfied for all the responses [29]. To sum up, the predictive models selected in this study could be satisfactorily applied to describe the experimental data for the majority of the responses.

3.3. Effect of Processing Variables on the Final Moisture Content of the Restructured Chips. The equation of second-order polynomial model of the final moisture content of products was obtained through RSM and showed as follows:

$$\begin{aligned} Y_1 = {} & 0.028 + 0.0059X_1 + 0.00015X_2 - 0.0022X_3 \\ & + 0.0025X_1X_2 + 0.002X_1X_3 + 0.00075X_2X_3 \\ & + 0.0086{X_1}^2 + 0.0057{X_2}^2 + 0.0038{X_3}^2, \end{aligned} \quad (2)$$

where Y_1 is final moisture content (g/g d.b.); X_1 is the amount of carrot (%); X_2 is the moisture content of the partially dried product before DIC treatment (g/g d.b.); X_3 is equilibrium temperature of DIC (°C).

As shown in Table 2, the final moisture content of the restructured chips in response to the experimental variables was varied from 0.025 g/g to 0.060 g/g d.b. In addition, the results showed in Table 3 suggested that the final moisture content was highly significant ($P < 0.01$) on the linear

Table 4: The results of analysis of variance (ANOVA) of the fitted second-order polynomial models for the moisture content, hardness, and color of the restructured chips.

Source	Sum of squares	DF	Mean square	F value	P value
Moisture content					
Model	$2.129 \cdot 10^{-3}$	9	$2.365 \cdot 10^{-4}$	24.200	<0.0001
Residual	$9.774 \cdot 10^{-5}$	10	$9.774 \cdot 10^{-6}$		
Lack of fit	$7.641 \cdot 10^{-5}$	5	$1.528 \cdot 10^{-5}$	3.580	0.0939
Pure error	$2.133 \cdot 10^{-5}$	5	$4.267 \cdot 10^{-6}$		
Cor total	$2.227 \cdot 10^{-5}$	19			
Hardness					
Model	61.430	9	6.830	7.990	0.0016
Residual	8.540	10	0.850		
Lack of fit	6.700	5	1.340	3.640	0.0913
Pure error	1.840	5	0.370		
Cor total	69.970	19			
L					
Model	185.290	9	20.590	106.890	<0.0001
Residual	1.920	10	0.190		
Lack of fit	1.470	5	0.290	3.280	0.1092
Pure error	0.450	5	0.090		
Cor total	187.220	19			
a					
Model	116.89	9	12.99	23.63	<0.0001
Residual	5.50	10	0.55		
Lack of fit	3.82	5	0.76	2.28	0.1935
Pure error	1.68	5	0.34		
Cor total	122.39	10			
b					
Model	121.82	9	13.54	5.13	0.0087
Residual	26.83	10	2.64		
Lack of fit	20.98	5	4.20	3.88	0.0816
Pure error	5.41	5	1.08		
Cor total	148.21	19			

terms of the mixed ratio of the sample (β_1), as well as on the quadratic terms of the mixed ratio (β_{11}), the moisture content of the partially dried product before DIC treatment (β_{22}), and equilibrium temperature of DIC (β_{33}); meanwhile the moisture content of the final product was significant ($P < 0.05$) on the linear term of the equilibrium temperature of DIC (β_2) and the interaction term of "the amount of carrot and the moisture content of the partially dried product before DIC treatment" (β_{12}). Moreover, positive coefficients were found in the linear terms of the amount of carrot and the moisture content of the partially dried product before DIC treatment and negative linear coefficients were obtained in the equilibrium temperature of DIC (see (2)), as demonstrated by the three-dimensional response surfaces of mixed ratio, the moisture content of the partially dried product before DIC treatment, and equilibrium temperature of DIC on the final moisture content of the restructured chips (Figures 2(a) and 2(b)). The moisture content of the products was slowly raised with increasing the amount of carrot when the equilibrium temperature was fixed (90°C), while it sharply increased with increasing the amount of carrot when the moisture content of the partially dried product before DIC treatment was in the range of 0.35–0.40 g/g d.b. (Figure 2(a)). This might be attributed to the fact that the moisture content of the partially dried product before DIC treatment was increased with adding more amount of carrot in the mixture, which in turn led to the high moisture content of the final products. Additionally, the final moisture content slowly decreased with increasing of the equilibrium temperature of DIC when the amount of carrot was constant (30%) (Figure 2(b)). This could be explained by the fact that the rate of water diffusion is proportional to the material temperature and time of heat during drying process [13]. The R^2 of the regression model of the final moisture content of products was 0.956, which indicated that 95.6% of the total variability in the final moisture content of the restructured carrot-potato chips could be explained by this model (Table 3). The maximum (0.060 g/g d.b.) and minimum (0.025 g/g d.b.) of the final moisture content were observed in the samples mixed with approximately 83.6% and 50.0%

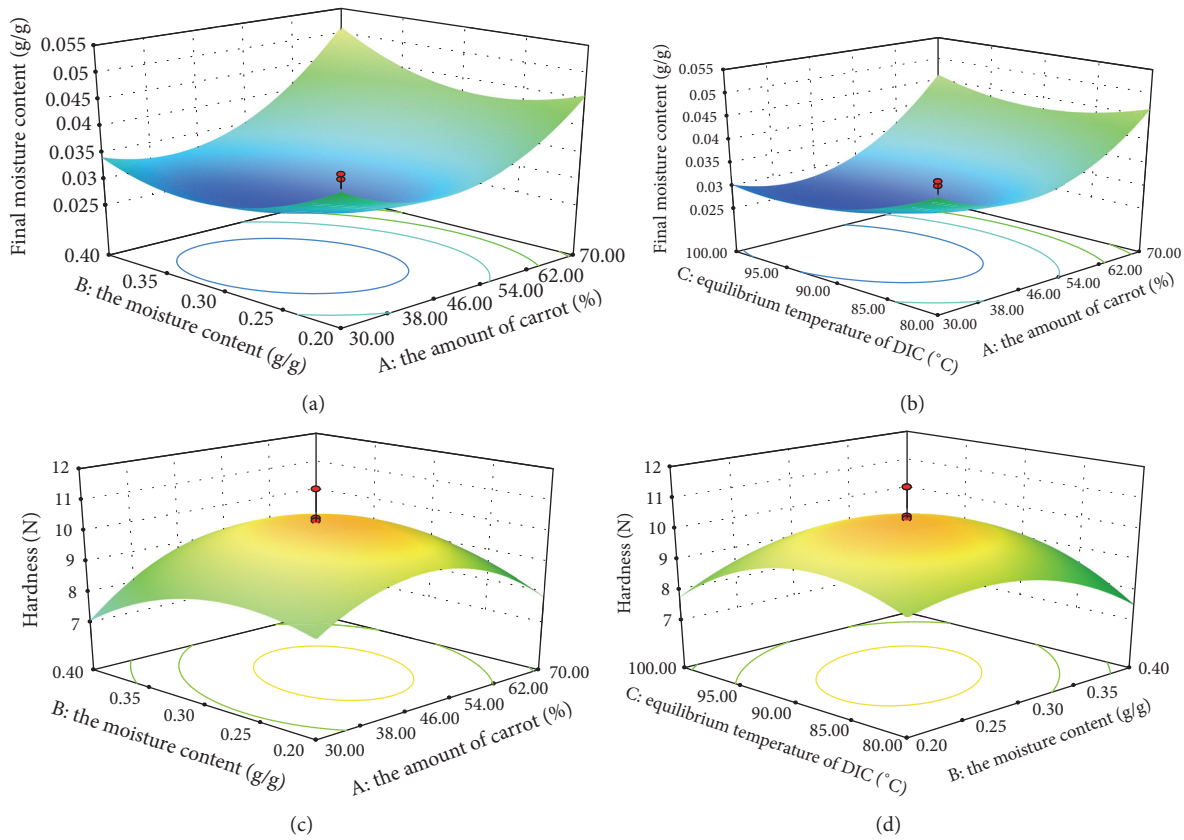

FIGURE 2: Response surfaces for the effects of the amount of carrot, the moisture content of the partially dried product before DIC treatment, and equilibrium temperature of DIC on the moisture content (a-b) and hardness (c-d) of the restructured carrot-potato chips dried by FD-DIC.

carrot, respectively, the moisture content of 0.30 g/g d.b. of the partially dried product, and the equilibrium temperature of 90°C. Considering the hygroscopicity of the restructured chips and with the aim of extending storage time, the lowest final moisture content was chosen as the optimum moisture content of the restructured chips.

3.4. Effect of Processing Variables on the Hardness and Crispness of the Restructured Chips. The equation of the second-order polynomial model for the hardness of the products was obtained through RSM and showed as follows:

$$Y_2 = 10.34 + 0.17X_1 - 0.23X_2 - 0.096X_3 + 0.47X_1X_2 + 0.48X_1X_3 + 0.53X_2X_3 - 1.46{X_1}^2 - 0.96{X_2}^2 - 1.19{X_3}^2, \quad (3)$$

where Y_2 is hardness (N); X_1 is the amount of carrot (%); X_2 is the moisture content of the partially dried product before DIC treatment (g/g d.b.); X_3 is equilibrium temperature of DIC (°C).

The observation for hardness was varied from 11.36 N to 5.30 N and the crispness was from 0.18 mm to 1.32 mm, as shown in Table 2. It is illustrated that the restructured chips with the highest hardness and crispness could be obtained under the condition that the amount of carrot was 50%, the moisture content of the partially dried product before DIC treatment was 0.30 g/g d.b., and the equilibrium temperature of DIC was 90°C. The results in Table 3 suggested that the second-order polynomial model explained 90% of the total variability in hardness; however, it only represented 69% of the total variability in crispness. Therefore, the 3D response surfaces concerning crispness were not shown, except for the experimental results in Table 2. The increase in the amount of carrot, the moisture content of the partially dried product before DIC treatment, and equilibrium temperature of DIC firstly resulted in the increase of crispness of the final products, and subsequently led to a decrease when these parameters exceed certain limits, that is, 50% carrot, the moisture content of 0.30 g/g d.b. of the partially dried product, and equilibrium temperature of 90°C, respectively. This was in accordance with the results of Jiang et al. [30] who reported that higher crispness of the dried products was obtained by adding higher amount of potato in the sample. In Table 3, the interaction terms of all the process parameters showed significantly negative effects ($P < 0.01$), while the linear terms and quadratic terms of all the process parameters exhibited no significance on hardness. However, the linear terms of the moisture content of the partially dried product before DIC treatment (β_2) and the equilibrium temperature of DIC (β_3) showed negative coefficients with hardness of the products,

whereas the linear term of the amount of carrot (β_1) exhibited positive coefficient (see (3)). In Figure 2(c), the hardness of the chips was firstly enhanced by an increase in the amount of carrot and equilibrium temperature of DIC and subsequently decreased after the two parameters reached certain level, that is, 50% carrots and equilibrium temperature of 90°C. Moreover, Figure 2(d) suggested that the hardness slightly increased with decreasing of the moisture content of the partially dried product before DIC treatment. Though Chien et al. [31] claimed that higher quality of the dried product could be featured with relatively low hardness, the maximum of hardness was chosen as the optimum parameter in this study considering that the final products could be crispier when it obtained harder texture after FD-DIC process [12].

3.5. Effect of Processing Variables on the Color Value of the Restructured Chips. The equations of the second-order polynomial model for the *L*, *a*, and *b* value of the products were obtained through RSM and showed as follows:

$$Y_4 = 70.27 - 3.35X_1 - 0.48X_2 - 0.068X_3 + 0.1X_1X_2 - 0.63X_1X_3 - 0.035X_2X_3 - 1.11{X_1}^2 - 0.39{X_2}^2 + 0.55{X_3}^2, \quad (4)$$

$$Y_5 = 24.8 + 2.57X_1 + 0.93X_2 - 0.57X_3 + 0.18X_1X_2 - 0.41X_1X_3 + 0.33X_2X_3 + 0.13{X_1}^2 + 0.56{X_2}^2 - 0.4{X_3}^2, \quad (5)$$

$$Y_6 = 36.17 + 1.38X_1 + 1.05X_2 + 0.06X_3 - 0.15X_1X_2 - 0.2X_1X_3 - 0.48X_2X_3 - 2.24{X_1}^2 + 0.13{X_2}^2 - 0.74{X_3}^2, \quad (6)$$

where Y_4 is *L* value; Y_5 is *a* value; Y_6 is *b* value; X_1 is the amount of carrot (%); X_2 is the moisture content of the partially dried product before DIC treatment (g/g d.b.); X_3 is equilibrium temperature of DIC (°C).

As shown in Table 2, the *L*, *a*, and *b* value of the restructured carrot-potato chips was varied from 62.02 to 74.02, from 21.14 to 28.51, and from 28.81 to 38.42, respectively. According to the *P*-statistics in Table 3, the *L* value exhibited significant ($P < 0.01$) negative relationship with the linear terms of the amount of carrot (β_1) and the moisture content of the partially dried product before DIC treatment (β_2), and the interaction terms of "the amount of carrot and equilibrium temperature of DIC" (β_{13}), as well as all the quadratic terms. However, the equilibrium temperature of DIC showed no significant influence on *L* value. Similarly, Figures 3(a) and 3(b) also depicted that the *L* value sharply increased with decreasing the amount of carrot and slowly increased with decreasing the moisture content of the partially dried product before DIC treatment at high amount of carrot (62%–70%). This might be attributed to the increase of the amount of potato which contributed to the lightness of the products [12]. Table 3 showed that the linear terms of the amount of carrot (β_1) and the moisture content of the partially dried product before DIC treatment (β_2) exhibited significantly ($P < 0.01$) positive influences on the *a* value of the restructured chips, while the linear term of the equilibrium temperature of DIC (β_3) showed negative significance ($P < 0.05$). As shown in Figures 3(c) and 3(d), the *a* value, presenting redness in this case, was improved with increasing the amount of carrot and the moisture content of the partially dried product before DIC treatment. However, the *a* value slowly decreased with increasing the equilibrium temperature of DIC. A possible reason was that the high temperature adopted during DIC process might cause degradation of carotenoids thus leading to the disappearing of redness (*a*) and yellowness (*b*), and this was in accordance with the research of Hornero-Méndez and Mínguez-Mosquera [32] who found that the thermal effects during cooking might bring negative impacts on the stability of carotenoids. According to (6), positive coefficients were found in the linear terms of the amount of carrot and the moisture content of the partially dried product before DIC treatment concerning the *b* value, and negative coefficients were obtained in the quadratic terms of the amount of carrot. In addition, Figures 3(e) and 3(f) also demonstrated that the increase of the amount of carrot resulted in increase of *b* value when the amount of carrot was below 50%, while the increase of the moisture content of the partially dried product before DIC treatment slightly enhances the *b* value. However, the equilibrium temperature of DIC showed no significant impacts on the *b* value. Similarly, Zhang et al. (2011) put forward a point of view that the color of raw materials (especially carrots) might fade and tend to become white during prefreezing of the mixed puree, which suggested that the color of the restructured carrot-potato chips after FD would be lighter and tend to become yellow instead of orange.

3.6. Effect of the Amount of Carrot on the Microstructure of the Restructured Chips. Based on the data obtained from response surface methodology, it was found that the mixed ratios of potato and carrot significantly affected the qualities (especially hardness and crispness) of the restructured carrot-potato chips after the above analysis of qualities. Therefore, the effect of the amount of carrot on the microstructure of the products was investigated. The microstructure of the restructured chips of the FD-DIC dried products is shown in Figure 4. As seen in Figure 4(a), the FD-DIC dried restructured chips with 30% carrot obtained several large pores and the size of these pores was inhomogeneous. Moreover, these samples are easy to collapse, which could be explained by the high proportion of potato. This phenomenon was similar to the microscopic image taken by Gao et al. [33] who revealed that the starch gelatinization during blanching resulted in partially collapsed or broken cell walls in the cross-section of fried sweet potato chips. In Figure 4(b), the FD-DIC restructured chips with 50% carrot obtained more pores, and the distribution of pore size was more uniform than the other mixed ratios. This homogeneous microstructure might be the reason why the FD-DIC dried restructured chips with 50% carrot obtained the highest hardness and crispness among all the samples [34], which are indicated in the 3D surface contour (Figure 2(b)). In addition, more numbers of pores were

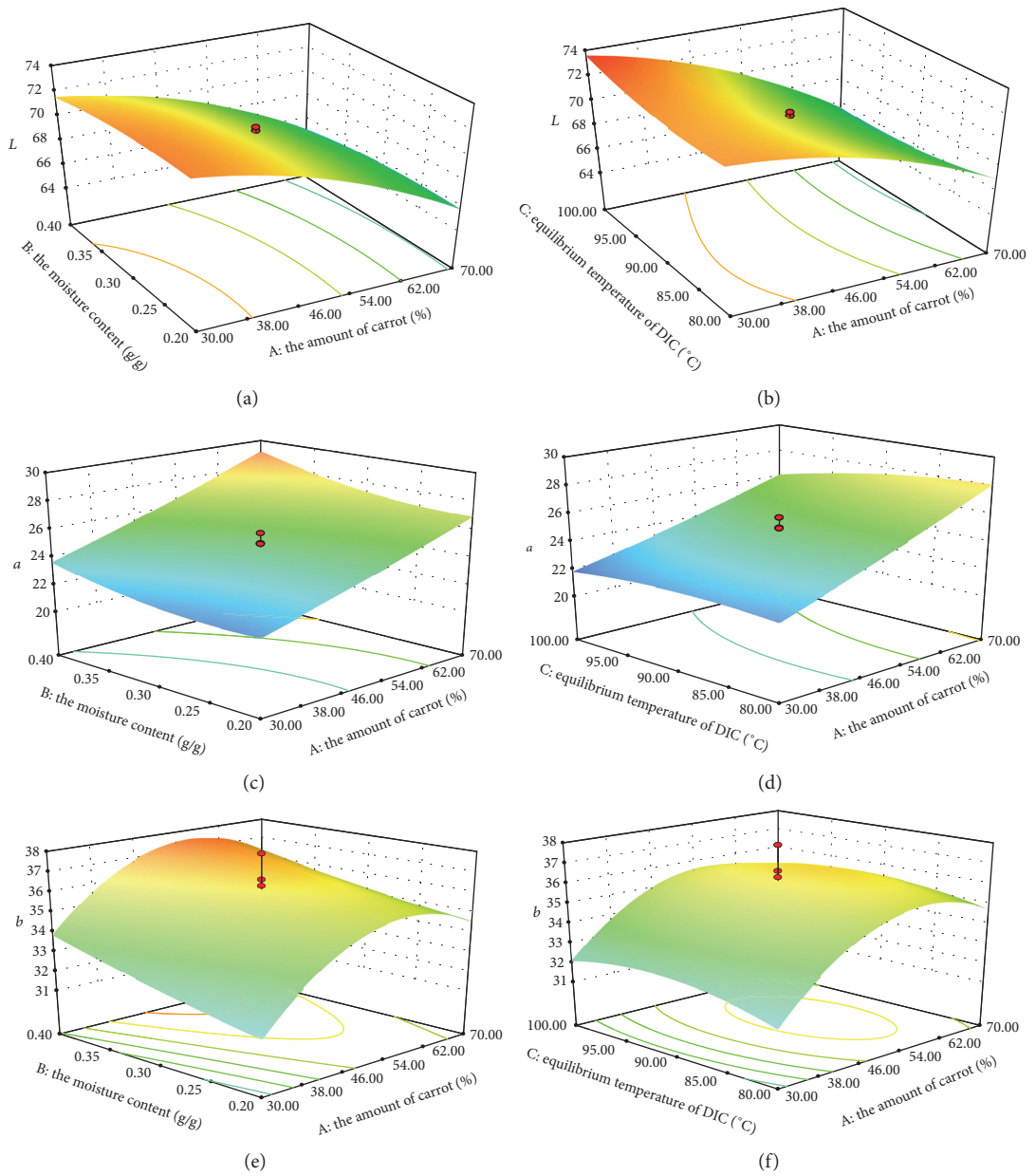

FIGURE 3: Response surfaces for the effect of the amount of carrot, the moisture content of the partially dried product before DIC treatment, and equilibrium temperature of DIC on the color values of L (a-b), a (c-d), and b (e-f) of the restructured carrot-potato chips dried by FD-DIC.

found in the FD-dried restructured chips with 50% carrot (Figure 4(d)), and the distribution of pores was much more regular in comparison to the restructured chips with the same amount of carrot but dried by FD-DIC (Figure 4(b)). During the freeze-drying process, the shrinkage of the sample was limited and the integrity of the microstructure of the raw material could be well maintained [35]. However, the homogenous porous microstructure found in FD-dried samples often pointed to a soft taste or mouth-feel. In contrast, the pores of FD-DIC dried restructured chips expanded and became inhomogeneous after DIC process, which could bring super crispness during masticating. From this point of view, DIC was defined as a texturing operation [17]. Overall, the optimum hardness and crispness of the restructured carrot-potato chips could be obtained by FD-DIC drying when the amount of carrot was 50%.

3.7. Process Optimization and Validation of Predicted Models. Numerical and graphical optimization techniques were adopted to optimize the different drying variables for the production of restructured chips. The main criterion for constraints optimization was the minimum moisture content and the maximum hardness and crispness, with the L, a, and b value of color being in an appropriate range [24]. The results of numerical optimization were listed in Table 5 and verified by experiments. The results showed that the actual values

Table 5: Validation of predicted values for the qualities of the restructured chips.

Variables response	Optimized solutions	Predicted value	Experimental value
Amount of carrot, %	47.43	-	-
The moisture content of the partially dried product before DIC treatment, g/g	0.29	-	-
Equilibrium temperature of DIC, ˚C	90.57	-	-
Moisture content, g/g	-	0.0275	0.028 ± 0.002
Hardness, N	-	10.30	11.30 ± 0.25
Crispness, mm	-	0.28	0.31 ± 0.01
L	-	70.72	70.05 ± 0.64
a	-	24.37	25.62 ± 0.78
b	-	35.88	36.54 ± 0.82

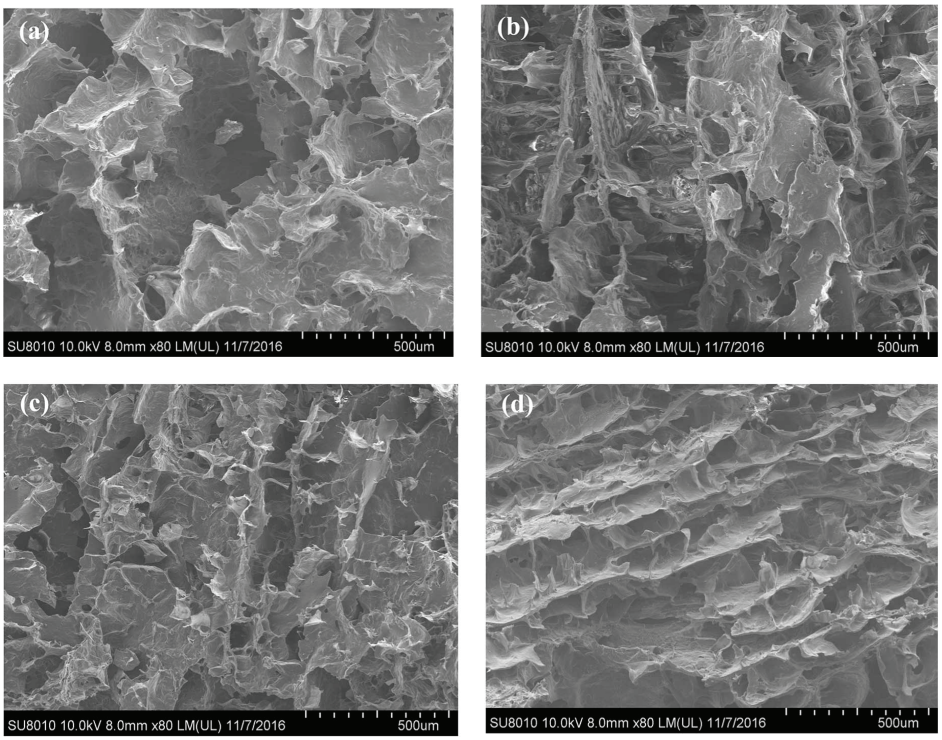

Figure 4: Scanning electron microscopy (SEM) of the restructured carrot-potato chips with different amount of carrot. (a) FD-DIC dried restructured carrot-potato chips with 30% carrot; (b) FD-DIC dried restructured carrot-potato chips with 50% carrot; (c) FD-DIC dried restructured carrot-potato chips with 70% carrot; (d) FD-dried restructured carrot-potato chips with 50% carrot.

for the qualities of the restructured chips were close to the predicted values. For any two given sets of variables, the third one was kept constant, and overlaid contours were obtained between the other two variables in graphical optimization. Figure 5(a) described the overlay plots for the amount of carrot and the moisture content of the partially dried product before DIC treatment when the equilibrium temperature of DIC was set at 90˚C. Similarly, Figure 5(b) described the overlay plots for the moisture content of the partially dried product before DIC treatment and the equilibrium temperature of DIC when the constant amount of carrot was 50%. The yellow area within the overlay plots highlighted the most advantageous range for a given set of variables. The most favorable ranges drawn from the overlay plot were found to be between 46% and 54% for the amount of carrot, from 0.20 to 0.35 g/g for the moisture content of the partially dried product before DIC treatment, and from 85 to 95˚C for the equilibrium temperature of DIC, respectively. Based on the quality parameters, the optimized process parameters could be helpful in manufacturing the restructured carrot-potato chips with superior texture and color, indicating that the combined drying method of FD-DIC might be practicable for industry.

4. Conclusions

RSM was used to optimize the process parameters of FD-DIC for producing restructured carrot-potato chips. All the three

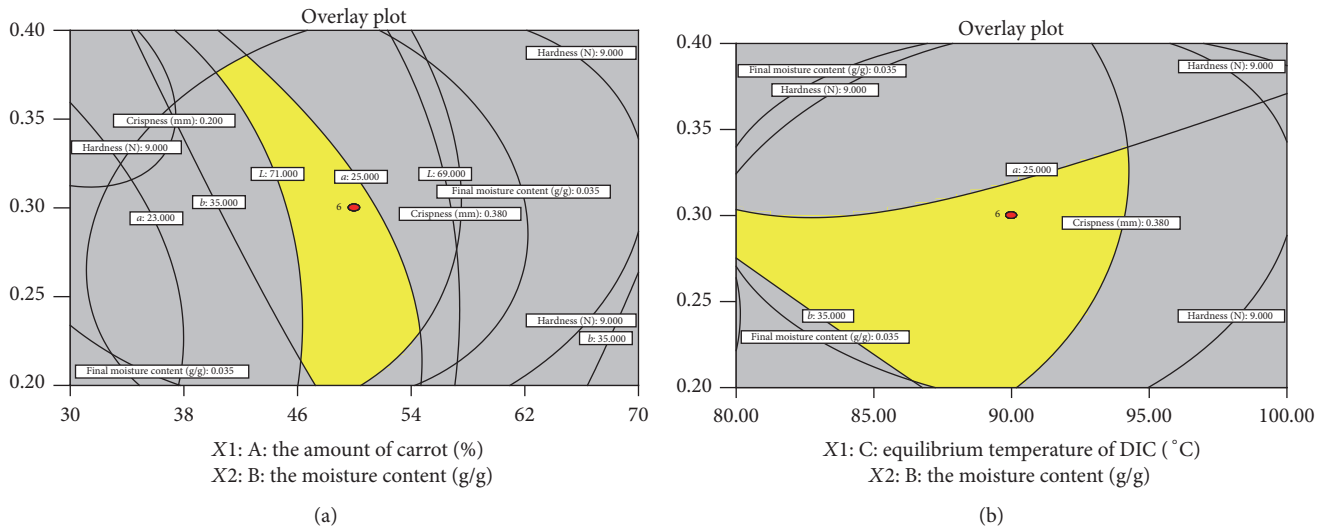

Figure 5: Overlaid contours for (a) the amount of carrot and the moisture content of the partially dried product before DIC treatment to optimize the qualities of the restructured carrot-potato chips at 90°C equilibrium temperature of DIC and (b) for the moisture content of the partially dried product before DIC treatment and equilibrium temperature of DIC to optimize the qualities of the restructured carrot-potato chips at 50% carrot.

targeted parameters, that is, the amount of carrot (mixed ratio), the moisture content of the partially dried product to be DIC-treated, and the equilibrium temperature of DIC, were found to significantly affect the final moisture content, color (L, a, and b), and texture (hardness and crispness) of the restructured chips. For restructured carrot-potato chips, the graphical ranges of the optimized conditions for FD-DIC process were derived as 46–54% w/w for the amount of carrot, 0.20–0.35 g/g for the moisture content of the partially dried product before DIC treatment, and 85–95°C for the equilibrium temperature of DIC, respectively. In addition, the numerical optimization suggested that the optimal solution for the amount of carrot, the moisture content of the partially dried product before DIC treatment, and the equilibrium temperature of DIC were 47.43%, 0.29 g/g, and 90.57°C, respectively, which could yield products with the minimum moisture content, the maximum hardness and crispness, and desirable color. Moreover, the combined drying method was confirmed to have benefits on yielding restructured chips with comparatively superior texture due to the well expanded porous microstructure, as compared to the FD-dried restructured chips. Besides, it is reasonable to speculate that the energy consumption could be significantly reduced due to the reduced drying time during the final stage of drying, and these benefits should be validated in further research and commercial practice. In conclusion, data from the parameter optimization and product quality suggested that instant controlled pressure drop combined with freeze-drying (FD-DIC) could be an alternative method for obtaining high-quality restructured fruit and vegetable chips or processing valuable agroproducts.

Additional Points

Practical Applications. Instant controlled pressure drop (DIC) drying, an emerging drying technology, has been used for a variety of fruit and vegetables, which featured the advantages of yielding products with pleasant crispness and flavor. However, the hot-air-drying combined with DIC drying is not suitable for restructured fruit and vegetable chips owing to the shrinkage of the mixture puree during drying. This problem can be solved by using freeze-drying (FD) which can remove the moisture by sublimation and disadsorption and keep the shape of the samples which were previously frozen in the mold, thus avoiding significant shrinkage. Nevertheless, the application of FD is limited by the relative high consumption of energy and low efficiency of water removing. Considering both the quality of products and energy consumption, the novel combination of FD and DIC with optimized processing conditions could be a practical solution to manufacture restructured fruit and vegetable chips.

Conflicts of Interest

The authors declare that they have no conflicts of interest.

Authors' Contributions

Jianyong Yi and Chunhui Hou contributed equally to the present paper.

Acknowledgments

This work was supported by the National Key R&D Program of China (2016YFD0400700, 2016YFD0400704).

References

[1] M. Planinic, D. Velić, S. Tomas, M. Bilić, and A. Bucić, "Modelling of drying and rehydration of carrots using Peleg's

model," *European Food Research and Technology*, vol. 221, no. 3-4, pp. 446–451, 2005.

[2] R. Estévez-Santiago, B. Olmedilla-Alonso, and I. Fernández-Jalao, "Bioaccessibility of provitamin A carotenoids from fruits: Application of a standardised static in vitro digestion method," *Food & Function*, vol. 7, no. 3, pp. 1354–1366, 2015.

[3] X. L. He, X. H. Tan, X. Y. Xiong, and Y. Zhang, "Recent development situation and prospect of potato foods in china," *Guangzhou Food Science and Technology*, vol. 21, no. 3, pp. 169–171, 2005.

[4] B. Hiranvarachat, S. Devahastin, and N. Chiewchan, "Effects of acid pretreatments on some physicochemical properties of carrot undergoing hot air drying," *Food and Bioproducts Processing*, vol. 89, no. 2, pp. 116–127, 2011.

[5] J. Garayo and R. Moreira, "Vacuum frying of potato chips," *Journal of Food Engineering*, vol. 55, no. 2, pp. 181–191, 2002.

[6] P. F. D. Silva and R. G. Moreira, "Vacuum frying of high-quality fruit and vegetable-based snacks," *LWT - Food Science and Technology*, vol. 41, no. 10, pp. 1758–1767, 2008.

[7] S. Valentina, A. Paul, P. Andrew, and İ. Şenol, "The advantage of using extrusion processing for increasing dietary fibre level in gluten-free products," *Food Chemistry*, vol. 121, no. 1, pp. 156–164, 2010.

[8] A. Peksa, A. Kita, E. Jariene et al., "Amino Acid Improving and Physical Qualities of Extruded Corn Snacks Using Flours Made from Jerusalem Artichoke (Helianthus tuberosus), Amaranth (Amaranthus cruentus L.) and Pumpkin (Cucurbita maxima L.)," *Journal of Food Quality*, vol. 39, no. 6, pp. 580–589, 2016.

[9] T. Antal, B. Kerekes, and L. Sikolya, "Evaluation of various chemical pre-treatments for physical properties of freeze dried apple," in *Proceedings of the In Proceedings of International Multidisciplinary Conference*, pp. 15–20, Nyíregyháza, Hungary, 2013.

[10] J. I. Lombrana, I. Zuaso, and J. Ikara, "Moisture diffusivity behavior during freeze drying under microwave heating power application," *Drying Technology*, vol. 19, no. 8, pp. 1613–1627, 2001.

[11] L.-L. Huang, M. Zhang, A. S. Mujumdar, D.-F. Sun, G.-W. Tan, and S. Tang, "Studies on decreasing energy consumption for a freeze-drying process of apple slices," *Drying Technology*, vol. 27, no. 9, pp. 938–946, 2009.

[12] L.-L. Huang, M. Zhang, A. S. Mujumdar, and R.-X. Lim, "Comparison of four drying methods for re-structured mixed potato with apple chips," *Journal of Food Engineering*, vol. 103, no. 3, pp. 279–284, 2011.

[13] T. Antal, B. Kerekes, L. Sikolya, and M. Tarek, "Quality and Drying Characteristics of Apple Cubes Subjected to Combined Drying (FD Pre-Drying and HAD Finish-Drying)," *Journal of Food Processing and Preservation*, vol. 39, no. 6, pp. 994–1005, 2015.

[14] H. S. P. Kumar, K. Radhakrishna, P. K. Nagaraju, and D. Vijaya Rao, "Effect of combination drying on the physico-chemical characteristics of carrot and pumpkin," *Journal of Food Processing and Preservation*, vol. 25, no. 6, pp. 447–460, 2001.

[15] J.-F. Bi, X. Wang, Q.-Q. Chen et al., "Evaluation indicators of explosion puffing Fuji apple chips quality from different Chinese origins," *LWT- Food Science and Technology*, vol. 60, no. 2, pp. 1129–1135, 2015.

[16] S. Mounir, T. Allaf, A. S. Mujumdar, and K. Allaf, "Swell Drying: Coupling Instant Controlled Pressure Drop DIC to Standard Convection Drying Processes to Intensify Transfer Phenomena and Improve Quality-An Overview," *Drying Technology*, vol. 30, no. 14, pp. 1508–1531, 2012.

[17] S. Mounir, C. Besombes, N. Al-Bitar, and K. Allaf, "Study of instant controlled pressure drop DIC treatment in manufacturing snack and expanded granule powder of Apple and Onion," *Drying Technology*, vol. 29, no. 3, pp. 331–341, 2011.

[18] T. Allaf and K. Allaf, *Instant controlled pressure drop (D.I.C.) in food processing*, Springer, New York, NY, USA, 2014.

[19] J. Yi, P. Wang, J. Bi, X. Liu, X. Wu, and Y. Zhong, "Developing Novel Combination Drying Method for Jackfruit Bulb Chips: Instant Controlled Pressure Drop (DIC)-Assisted Freeze Drying," *Food and Bioprocess Technology*, vol. 9, no. 3, pp. 452–462, 2016.

[20] J. Peng, J. Yi, J. Bi et al., "Freezing as pretreatment in instant controlled pressure drop (DIC) texturing of dried carrot chips: Impact of freezing temperature," *LWT- Food Science and Technology*, vol. 89, pp. 365–373, 2018.

[21] Z. Šumić, A. Vakula, A. Tepić, J. Čakarević, J. Vitas, and B. Pavlić, "Modeling and optimization of red currants vacuum drying process by response surface methodology (RSM)," *Food Chemistry*, vol. 203, pp. 465–475, 2016.

[22] K. Zou, J. Teng, L. Huang, X. Dai, and B. Wei, "Effect of osmotic pretreatment on quality of mango chips by explosion puffing drying," *LWT- Food Science and Technology*, vol. 51, no. 1, pp. 253–259, 2013.

[23] A. Salvador, P. Varela, T. Sanz, and S. M. Fiszman, "Understanding potato chips crispy texture by simultaneous fracture and acoustic measurements, and sensory analysis," *LWT- Food Science and Technology*, vol. 42, no. 3, pp. 763–767, 2009.

[24] A. Saxena, T. Maity, P. S. Raju, and A. S. Bawa, "Optimization of pretreatment and evaluation of quality of jackfruit (Artocarpus heterophyllus) bulb crisps developed using combination drying," *Food and Bioproducts Processing*, vol. 95, pp. 106–117, 2015.

[25] B. Singh, P. S. Panesar, V. Nanda, and J. F. Kennedy, "Optimisation of osmotic dehydration process of carrot cubes in mixtures of sucrose and sodium chloride solutions," *Food Chemistry*, vol. 123, no. 3, pp. 590–600, 2010.

[26] M. Kochs, C. Körber, B. Nunner, and I. Heschel, "The influence of the freezing process on vapour transport during sublimation in vacuum-freeze-drying," *International Journal of Heat and Mass Transfer*, vol. 34, no. 9, pp. 2395–2408, 1991.

[27] X. Duan, X. Yang, G. Ren, Y. Pang, L. Liu, and Y. Liu, "Technical aspects in freeze-drying of foods," *Drying Technology*, vol. 34, no. 11, pp. 1271–1285, 2016.

[28] A. Nath, P. K. Chattopadhyay, and G. C. Majumdar, "High temperature short time air puffed ready-to-eat (RTE) potato snacks: Process parameter optimization," *Journal of Food Engineering*, vol. 80, no. 3, pp. 770–780, 2007.

[29] R. H. Myers, D. C. Montgomery, and C. M. Anderson-Cook, *Response Surface Methodology: Process and Product Optimization Using Designed Experiments*, Wiley Series in Probability and Statistics, Wiley, Hoboken, NJ, USA, 3rd edition, 2009.

[30] H. Jiang, M. Zhang, A. S. Mujumdar, and R.-X. Lim, "Comparison of the effect of microwave freeze drying and microwave vacuum drying upon the process and quality characteristics of potato/banana re-structured chips," *International Journal of Food Science & Technology*, vol. 46, no. 3, pp. 570–576, 2011.

[31] H. C. Chien, L. L. Chung, C. Michael, C. A. Luqman, and R. D. Wan, "Drying kinetics, texture, color, and determination of effective diffusivities during sun drying of chempedak," *Drying Technology*, vol. 26, no. 10, pp. 1286–1293, 2008.

[32] D. Hornero-Méndez and M. I. Mínguez-Mosquera, "Bioaccessibility of carotenes from carrots: Effect of cooking and addition of oil," *Innovative Food Science and Emerging Technologies*, vol. 8, no. 3, pp. 407–412, 2007.

[33] M. Gao, J. Huam, C. Moallic, G. M. Ashu, Q. Xia, and L. Stewart, "Structure-related properties of sweetpotato critically impact the textural quality of fried chips," *African Journal of Agricultural Research*, vol. 9, no. 14, pp. 1113–1123, 2014.

[34] S. Devahastin, "Fractal characterization of some physical properties of a food product under various drying conditions," *Drying Technology*, vol. 25, no. 1, pp. 135–146, 2007.

[35] A. Voda, N. Homan, M. Witek et al., "The impact of freeze-drying on microstructure and rehydration properties of carrot," *Food Research International*, vol. 49, no. 2, pp. 687–693, 2012.

Hindawi
Journal of Food Quality
Volume 2018, Article ID 4510126, 7 pages
https://doi.org/10.1155/2018/4510126

Research Article

Effect of Various Pretreatments on Quality Attributes of Vacuum-Fried Shiitake Mushroom Chips

Aiqing Ren,[1,2] **Siyi Pan**,[1] **Weirong Li**,[2] **Guobao Chen**,[2] **and Xu Duan**[3]

[1]*College of Food Science and Technology, Huazhong Agricultural University, Shizishan Street No. 1, Wuhan, Hubei 430070, China*
[2]*Lishui Academy of Agricultural Sciences, Liyang Street No. 827, Lishui, Zhejiang 323000, China*
[3]*College of Food & Bioengineering, Henan University of Science and Technology, Luoyang 471023, China*

Correspondence should be addressed to Siyi Pan; siyipanshipin@126.com

Received 19 September 2017; Revised 12 December 2017; Accepted 20 December 2017; Published 16 January 2018

Academic Editor: Hong-Wei Xiao

The objective of this study is to investigate the effects of pretreatments on the quality of vacuum-fried shiitake mushroom slices. Four different pretreatments addressed in this study were (1) blanching as control, (2) blanching and osmotic dehydration with maltodextrin (MD) solution, (3) blanching, osmotic dehydration, and coating with sodium carboxymethyl cellulose (CMC), (4) blanching and osmotic dehydration, followed by freezing. All samples were pretreated and then fried in palm oil at 90°C with vacuum degree of −0.095 MPa for 30 min. The results showed that pretreatments significantly ($p < 0.05$) affected the moisture content, oil content, color, water activity (a_w), total phenolic content, and sensory evaluation of shiitake mushroom chips. The blanching, osmotic dehydration, and coating pretreatment could improve color and sensory evaluation and also minimize the oil uptake of fried chips, whereas this treatment caused the highest reduction of total phenolic contents. There were no significant ($p > 0.05$) differences of fried chip in the texture among the four different pretreatments. The a_w values of all the fried chips were less than 0.38, indicating that the products had a long shelf life. Therefore, the blanching, osmotic dehydration, and coating pretreatment before vacuum frying was the most suitable pretreatment for vacuum-fried shiitake mushroom chips.

1. Introduction

Shiitake mushroom is one of the most popular edible mushrooms in the market, which has been valued as a food and medicine for thousands of years in Asia, and China accounts for over 70% of the world's shiitake production [1]. Numerous studies have shown its medicinal attributes including antitumor and antimicrobial activities, improvement of liver function, reduction of cholesterol activity, decrease of blood pressure, and enhancement of the immune system against diseases [2]. However, fresh shiitake mushrooms are highly perishable and start deteriorating within a day after harvest, causing difficulties in their distribution and marketing as fresh products. It is well known that fried products have consumer appeal in all age groups and in virtually all cultures, the process is quick and can easily be made continuous for mass production, and the food appears sterile and dry, with a relatively long shelf life. Furthermore, vacuum frying is one of the latest optional methods applied to fruits and vegetables with low oil content and the desired texture and flavor characteristics [3]. This method processes the fruits and vegetables under pressures well below atmospheric levels, preferably below 8 kPa that can lower the boiling points of frying oil and moisture in food. Moisture can be thus removed from the fried food rapidly once the oil temperature reaches the boiling point of water. As a result, vacuum frying is a feasible option for processing of shiitake mushroom chips.

There were many previous researches focused on preserving nutrients and reducing oil content during the vacuum frying process [4–7]. In fact, some quality deteriorations could take place during the vacuum frying process. To improve the quality of vacuum-fried products, several pretreatments methods, such as blanching, predrying, osmotic pretreatment, coating, and freezing methods, have been applied to the frying of foods [8–12]. Blanching is a highly effective pretreatment method to improve the product quality of fried

food; it brings a considerable improvement in the color of the vacuum-treated samples and less oil absorption [13]; it also could reduce the oil absorption by gelatinization of surface starch [14]. Pedreschi and Moyano have investigated the effect of predrying on texture and oil uptake of potato chips and found that predrying dramatically decreased the oil absorption and significantly increased the crispness of the potato slices after frying [15]. Osmotic dehydration pretreatment influences the quality of the final product by preventing discoloration [16]. Nunes and Moreira have reported that mango chips soaked in 65% maltodextrin (MD) solution resulted in a vacuum-fried product with the highest dehydration efficiency index (water loss/sugar gain), lowest oil content, and highest sensory scores [17]. Food hydrocolloids have been widely used as multifunctional additives in food processing to improve stability, modify the surface, and control the moisture content. It was shown that coating with 1% (m/v) pectin solution for bananas chips decreased the oil content in fried bananas chips by approximately 23% [18]. In addition, Sothornvit found that banana chips coated with guar gum maintained better quality and lower oil content after vacuum frying [19]. The hydrocolloid pretreatment provided more mechanical strength to the fruit tissue that could enhance sensory scores by improved structural integrity, while the difference in the behavior of color values of different chips upon hydrocolloid treatment might be related to the nature of the product, modification of surface property of the tissue, or differences in the frying process [20]. Freezing is an alternative pretreatment for increasing the rate of frying and improving the quality of fried products. During freezing pretreatment, the size of ice crystals was largely dependent on the freezing rate. Lower freezing rate resulted in the formation of larger ice crystals; large ice crystals may cause the mechanical damage, remarkable drip loss, and structural deformation of cellular structure of many biological materials [21].

Vacuum frying technology has been extensively investigated for lots of fruits and vegetables products [5–29]. However, to the best of our knowledge, there was no literature concerning the vacuum frying of shiitake mushroom (*Lentinus edodes*), especially for the effect of different pretreatments on physical-chemical properties of shiitake mushroom chips. Therefore, the objectives of this study were (1) to investigate the influence of different pretreatments (blanching, osmotic dehydration, coating, and freezing) prior to vacuum frying on the variations of moisture and oil content of the shiitake mushroom slices and (2) to evaluate the effect of pretreatments on the physicochemical properties of final vacuum-fried shiitake mushroom chips, such as texture, color, a_w, total phenolic content, and sensory evaluation.

2. Materials and Methods

2.1. Materials. Fresh shiitake mushrooms were purchased from local market in Lishui, Zhejiang, China, and kept in refrigerator at 4-5°C before frying. palm oil was supplied by the Jia-li Co. Ltd., Shanghai, China. The vacuum fryer equipped with a centrifuge (model VF2I, Hai Rui Company, Yantai, China) had a capacity of 100 L and a maximum

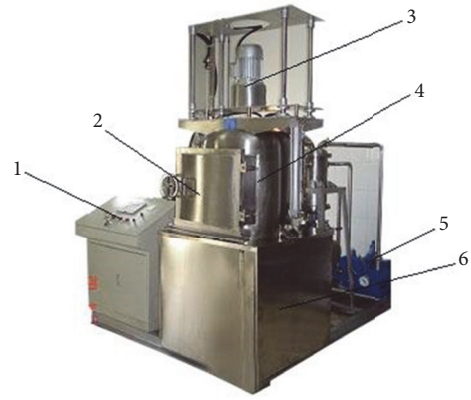

Figure 1: The vacuum frying equipment ((1) control center which controls the oil temperature, vacuum degree, frying time, deoiling speed, deoiling time, (2) the door of vacuum fryer, (3) frying basket lift and centrifugal deoiling machine, (4) frying chamber, (5) vacuum pump, (6) sandwich pot, storage oil, and steam heating).

temperature (the sandwich pot is heated by steam) and vacuum degree of 150°C and −0.096 MPa, respectively, for an oil capacity of 50 L. The vacuum frying equipment was shown in Figure 1. A Model WSC-S colorimeter (Shanghai Medical Appliance Factory, Shanghai, China) was used to measure the color of the samples. A texture analyzer (TA-XT2i, Stable Micro System Co. Ltd., Surrey, UK) was used for measurement of the breaking force of the samples. A a_w detector Ms-1 (NOVASINA Company, Switzerland) was used to measure the a_w of the samples. A Model SP-721E Visible Spectrometer (Shanghai Guanpu company, Shanghai, China) was used to measure the total phenolic content of the samples.

2.2. Pretreatment of Shiitake Mushroom Slices. Fresh shiitake mushrooms were washed and then cut into 6 ± 0.5 mm slices after removing the stalks. The shiitake mushroom slices were treated as follows: blanching for 3 min in water (95°C), cooling under running tap water for 3 min, and draining on absorbent paper until the surface was nearly dry. The shiitake mushroom slices were divided into the following four different pretreatments: (1) blanched as control, (2) blanched and immersed in MD solution (50% w/v) at 25°C for 60 min, (3) blanched, immersed in the solution, and then immersed in a dilute CMC solution (0.5% w/v) at 25°C for 15 min, (4) blanched, immersed in the MD solution, and then freezed at −20°C for 12 h.

2.3. Vacuum Frying. A batch of 100 g shiitake mushroom slices, after the pretreatment, was fried in 50 L of palm oil. The oil temperature was 90 ± 2°C and vacuum degree was −0.095 MPa during frying (it is the best parameter based on our previous experiment). A centrifuging step (300 rpm for 2 min) before pressurizing the vessel after frying was added and its aim is to remove the excess surface oil. The moisture and oil content of the shiitake mushroom slices were measured at 0, 2, 4, 6, 8, 10, 15, 20, 25, and 30 min of frying. On the other hand, texture, color, a_w, and sensory evaluation were measured at 30 min of frying.

2.4. Analysis of Samples

2.4.1. Moisture Content. The shiitake mushroom chips were ground with a mortar at the end of each vacuum frying operation. Moisture content was determined using approximately 10 g of the ground shiitake mushroom chips and oven-dried at 102 ± 3°C until the weight stabilized [10]. The test was performed in triplicate.

2.4.2. Fat Content. The vacuum-fried shiitake mushroom chips were ground and oven-dried. Fat content of shiitake mushroom chips was determined by Soxhlet extraction with diethyl ether [30]. The test was performed in triplicate.

2.4.3. Color. The color parameters (L^*, a^*, b^*) of the shiitake mushroom chips were measured using a colorimeter Model WSC-S. The measuring aperture diameter was 10 mm, and the colorimeter was calibrated by a standard white board. Hunter L^* (lightness), a^* (redness/greenness), and b^* (yellowness/blueness) values were obtained from each color measurement. The samples were scanned at three different positions of the shiitake mushroom section, and the data were reported as average values of the three measurements.

2.4.4. Texture. Measurement of the texture of shiitake mushroom chips was carried out using a texture analyzer. Breaking force of the shiitake mushroom chips was performed at room temperature by a puncture test. The shiitake mushroom chips were placed over the end of a hollow cylinder. A stainless steel ball probe (P/0.25 s), moving at a speed of 5.0 mm/s over a distance of 5.0 mm, was used to break the chip. All numerical results were expressed in grams. The test was performed in triplicate.

2.4.5. a_w. The a_w of vacuum-fried shiitake mushroom chips was measured using a a_w detector Model MS-1 with a measurement range from 0.03 to 0.098 a_w. The test was performed in triplicate.

2.4.6. Total Phenolic. Total phenolics were determined using the Folin–Ciocalteu reagent [31]. Samples (2 g) were homogenized in 80% aqueous ethanol at room temperature and centrifuged in cold at 10,000 ×g for 15 min, and the supernatant was saved. The residue was reextracted twice with 80% ethanol and supernatants were pooled, put into evaporating dishes, and evaporated to dryness at room temperature. Residue was dissolved in 5 mL of distilled water. One-hundred microlitres of this extract was diluted to 3 mL with water, and 0.5 mL of Folin–Ciocalteu reagent was added. After 3 min, 2 mL of 20% of sodium carbonate was added and the contents were mixed thoroughly. The color was developed and absorbance measured at 650 nm by a spectrometer after 60 min using catechol as a standard. The results were expressed as mg catechol/100 g of dry weight material.

2.4.7. Sensory Evaluation. Fifty nonsmoking, self-confessed healthy panelists were trained to evaluate the quality of vacuum-fried shiitake mushroom chips in terms of appearance, color, flavor, texture, oiliness, and overall acceptability using a nine-point hedonic scale for likeness. The scores were assigned from extremely liked (9) to extremely disliked (1). Each sample was presented to the panelists for identification. Spring water was provided between samples for mouth rinsing by each panelist [29].

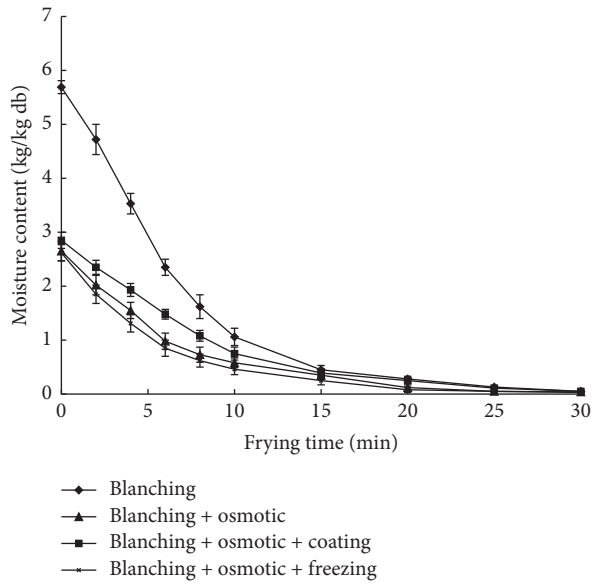

Figure 2: Effect of different pretreatments on moisture content of vacuum-fried shiitake mushroom chips.

2.5. Statistical Analysis. Data were analyzed by using the Statistical Analysis System (SAS, version 8.0, SAS Institute Inc., Cary, North Carolina). Analyses of variance were performed by the ANOVA procedure. Mean values were considered significantly different when $p < 0.05$.

3. Results and Discussion

3.1. Effects of Pretreatment on Moisture Content. The variation of moisture content during vacuum frying of shiitake mushroom chips with different pretreatments is shown in Figure 2. It can be seen that the initial moisture contents of shiitake mushroom slices were 5.69, 2.65, 2.85, and 2.62 kg/kg db, respectively. This could be attributed to the fact that MD osmotic treatment reduced the moisture content of materials, and after coating with CMC the moisture content was increased. The free water evaporated from the shiitake mushroom slices rapidly at the beginning of 10 min. The moisture contents of shiitake mushroom slices from high to low were blanching, osmotic, osmotic + freezing, and osmotic + coating during the frying process. The moisture content of blanching treatment was the highest because of its high initial moisture content. The moisture content of osmotic + freezing treatment was the lowest; this might be due to the fact that freezing could increase cell membrane penetrability of the material and cause the water to more easily evaporate [10]. The moisture content of blanching + osmotic + coating treatment was higher than the samples without coating. This is because CMC coating provided effective moisture retention

Table 1: The color value of shiitake mushroom chips for different pretreatments.

Pretreatment	L^*	a^*	b^*
Blanching	36.62 ± 0.36^{a}	5.37 ± 0.32^{c}	12.37 ± 0.28^{c}
Blanching + osmotic	41.23 ± 0.35^{c}	4.42 ± 0.42^{ab}	10.47 ± 0.56^{ab}
Blanching + osmotic + coating	45.21 ± 0.34^{d}	4.14 ± 0.21^{a}	9.85 ± 0.45^{a}
Blanching + osmotic + freezing	39.60 ± 0.85^{a}	4.76 ± 0.18^{b}	11.17 ± 0.98^{b}

Note. Means with different letters within a column are significantly different ($p < 0.05$) by Duncan's multiple range test.

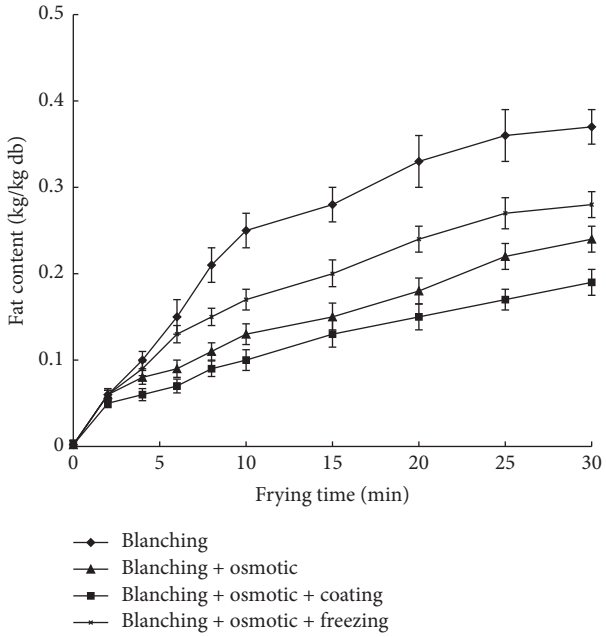

Figure 3: Effect of different pretreatments on oil content of vacuum-fried shiitake mushroom chips.

of the shiitake mushroom due to a strong interaction of hydrogen bonds between water molecules [32]. This is also consistent with the research of Maity et al. [20]. After 25 min, the moisture content in the products decreased slowly. When frying was finished, the moisture contents of four fried shiitake mushroom chips were 0.05 kg/kg db, 0.03 kg/kg db, 0.04 kg/kg db, and 0.05 kg/kg db, respectively.

3.2. Effects of Pretreatment on Oil Content. The variation of oil content during vacuum frying of shiitake mushroom chips with different pretreatments was shown in Figure 3. It can be observed that the rate of fat absorption increased with increasing vacuum frying time at the first 10 min, and the rate of oil absorption increased slowly after 25 min. This coincided with the period of time at which water evaporated from the shiitake mushroom slices at the fastest rate (Figure 2). The final oil content of the chips was 0.37, 0.24, 0.19, and 0.28 kg/kg db, respectively. Shiitake mushroom chips coated with the CMC exhibited a reduction in oil absorption with content of 0.19 kg/kg db. This result correlated with previous studies for CMC having the ability to form edible coatings to barrier lipids into chips [20, 29, 33]. Figure 3 shows that shiitake mushroom slices treated with osmotic and osmotic followed by freezing also could reduce the oil uptake compared to only blanched products. This might suggest that osmotic treatment significantly reduced the initial moisture content of samples, and high initial free moisture content resulted in high final oil content [34]. The fat content of shiitake mushroom chips treated with freezing was higher than that without freezing. This might be because freezing destroys the cell wall structure and induces greater disruption of the shiitake mushroom cells, making the fat more easily absorbed and retained during the vacuum frying [10].

3.3. Effects of Pretreatment on Color Value. The effects of pretreatments on the color of vacuum-fried shiitake mushroom chips can be seen in Table 1. In the present study, the color values of shiitake mushroom chips ranged from 36.62 to 45.21 (L^*), 4.14 to 5.37 (a^*), 9.85 to 12.37 (b^*). The statistical analysis showed that pretreatments significantly affected the color values of shiitake mushroom chips ($p < 0.05$). Maillard reaction which occurs between reducing sugars and protein sources and oil uptake affects the final color of the fried products [35]. The pretreatment for coating showed the least browning and oil uptake, so the L^* value was the highest and the a^* value and the b^* value were the lowest.

3.4. Effects of Pretreatment on a_w, Breaking Force and Total Phenolic. As shown in Table 2, pretreatment significantly affected the value of a_w of shiitake mushroom chips ($p < 0.05$). Osmotic treatment can increase the solid content of products and bind up more free water [36]. This made the value of a_w of shiitake mushroom chips treated with osmotic dehydration greatly decrease. Water activity is an important property that can be used to predict the stability and safety of food with respect to microbial growth, rates of deteriorative reactions, and chemical/physical properties. The limiting value of a_w for the growth of any microorganism is less than 0.6 [37]. In the present work, all the chips had a_w of less than 0.38, which indicated vacuum frying is a good method to maintain quality and prolong the shelf life of the products. Breaking force is an indicator of the extent of crispness of vacuum-fried chips, with lower breaking force corresponding with higher crispiness. There were no significant ($p > 0.05$) differences in breaking force of shiitake mushroom chips treated with different pretreatments.

Antioxidant activity correlated significantly and positively with total phenolic [38]. Table 2 shows that total phenolic contents in the shiitake mushroom chips by different pretreatments were 3.32 mg/100 g (db), 3.15 mg/100 g (db), and 3.41 mg/100 g (db), respectively, and they were lower than that of the control (4.32 mg/100 g (db)). Polyphenols

Table 2: Effects of pretreatments on a_w, breaking force, and total phenolic content of shiitake mushroom chips.

Pretreatments	a_w	Breaking force (g)	Total phenolic (mg/g, db)
Blanching	0.38 ± 0.02^b	975.9 ± 17.5^a	4.32 ± 0.11^c
Blanching + osmotic	0.25 ± 0.01^a	960.2 ± 22.9^a	3.32 ± 0.09^b
Blanching + osmotic + coating	0.25 ± 0.01^a	978.7 ± 14.9^a	3.15 ± 0.08^a
Blanching + osmotic + freezing	0.26 ± 0.01^a	980.5 ± 18.2^a	3.41 ± 0.08^b

Note. Means with different letters within a column are significantly different ($p < 0.05$) by Duncan's multiple range test.

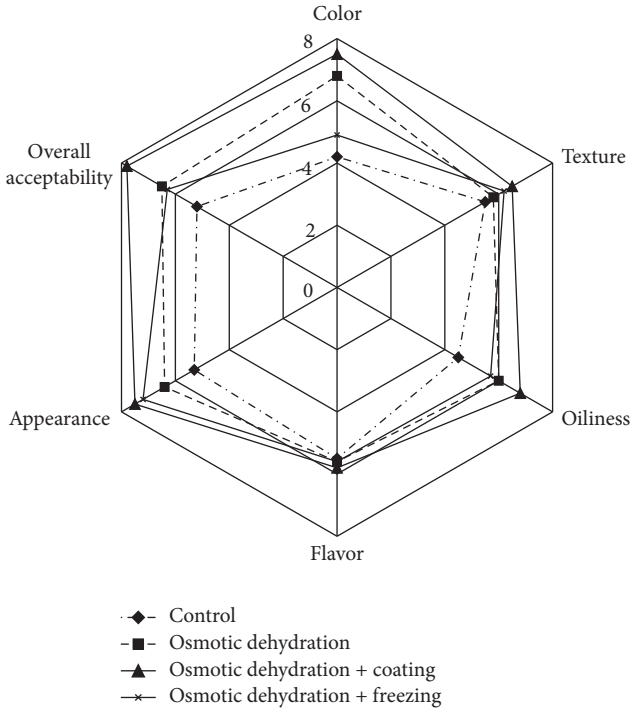

Figure 4: Sensory evaluation of the quality of vacuum-fried shiitake mushroom chips in four experimental conditions.

entered into water, when shiitake mushroom slices were dipped into MD and CMC solution, resulting in the reduction of content, while the control samples retained more total phenolic contents.

3.5. Effects of Pretreatment on Sensory Evaluation. A sensory analysis was performed to determine the consumer preference of vacuum-fried shiitake mushroom chips. Figure 4 showed that the panelists liked the products as indicated by overall acceptability scores. All groups received scores of over 4 on a 1–9 point hedonic scale. No significant ($p < 0.05$) differences were found in flavor or textures detected by the judges, since vacuum frying can preserve the natural flavor and keep crisp of shiitake mushroom chips. In addition, all panelists considered that the untreated shiitake mushroom chips were more oily, with worse appearance and color, compared to others. This indicates that the three pretreatments before vacuum frying could reduce the oil absorption, preserve the natural color, and reduce shrink. As can be seen from Figure 4, blanching, osmotic dehydration, and coating pretreatment had the highest values of appearance, color, flavor, texture, and overall acceptability, indicating that this pretreatment was the most suitable for vacuum-fried shiitake mushroom chips.

4. Conclusions

In the present study, the influence of different pretreatments (blanching, osmotic dehydration, coating, and freezing) prior to vacuum frying on the variations of moisture and oil content, as well as the quality attributes of the shiitake mushroom slices, was investigated. Results showed that the drying rate of blanching, osmotic dehydration, and freezing pretreatment was the highest. As the frying time increased, the oil content of vacuum-fried products increased. The products obtained from blanching, osmotic dehydration, and coating pretreatment had the lowest oil content. In addition, all the pretreatments can significantly ($p < 0.05$) improve the quality attributes, including the color, sensory evaluation. All the fried shiitake mushroom chips had extremely low a_w values. Furthermore, blanching, osmotic dehydration, and coating pretreatment had the highest values of appearance, color, flavor, texture, and overall acceptability. Therefore, the vacuum-fried shiitake mushroom slices from the blanching, osmotic dehydration, and coating pretreatment had the lowest oil uptake and best color property and sensory evaluation, indicating that it was the most suitable for vacuum-fried shiitake mushroom chips.

Conflicts of Interest

The authors declare that there are no conflicts of interest regarding the publication of this paper.

Acknowledgments

The authors acknowledge the financial support provided by Lishui Talents Project no. 2016RC30, the National Natural Science Foundation of China under Contract no. 31671907, and the National Key Research and Development Program of China under Contract no. 2017YFD0400900.

References

[1] M. Zhang, S. W. Cui, P. C. K. Cheung, and Q. Wang, "Antitumor polysaccharides from mushrooms: a review on their isolation process, structural characteristics and antitumor activity," *Trends in Food Science & Technology*, vol. 18, no. 1, pp. 4–19, 2007.

[2] H. Kantrong, A. Tansakul, and G. S. Mittal, "Drying characteristics and quality of shiitake mushroom undergoing

microwave-vacuum drying and microwave-vacuum combined with infrared drying," *Journal of Food Science and Technology*, vol. 51, no. 12, pp. 3594–3608, 2014.

[3] L. M. Diamante, S. Shi, A. Hellmann, and J. Busch, "Vacuum frying foods: Products, process and optimization," *International Food Research Journal*, vol. 22, no. 1, pp. 15–22, 2015.

[4] V. Dueik and P. Bouchon, "Development of polyphenol-enriched vacuum and atmospheric fried matrices: Evaluation of quality parameters and in vitro bioavailability of polyphenols," *Food Research International*, vol. 88, pp. 166–172, 2016.

[5] R. Yamsaengsung, S. Yaeed, and T. Ophithakorn, "Vacuum frying of fish tofu and effect on oil quality usage life," *Journal of Food Process Engineering*, vol. 40, no. 6, p. e12587, 2017.

[6] M. G. Vernaza and Y. K. Chang, "Survival of resistant starch during the processing of atmospheric and vacuum fried instant noodles," *Food Science and Technology*, vol. 37, no. 3, pp. 425–431, 2017.

[7] A. B. Oyedeji, O. P. Sobukola, F. Henshaw et al., "Effect of frying treatments on texture and colour parameters of deep fat fried yellow fleshed cassava chips," *Journal of Food Quality*, vol. 2017, Article ID 8373801, 10 pages, 2017.

[8] I. Albertosa, A. B. Martin-Dianaa, M. A. Sanza et al., "Effect of high pressure processing or freezing technologies as pretreatment in vacuum fried carrot snacks," *Innovative Food Science & Emerging Technologies*, no. 33, pp. 115–122, 2016.

[9] L. M. Diamante, G. P. Savage, L. Vanhanen, and R. Ihns, "Effects of maltodextrin level, frying temperature and time on the moisture, oil and beta-carotene contents of vacuum-fried apricot slices," *International Journal of Food Science & Technology*, vol. 47, no. 2, pp. 325–331, 2012.

[10] L.-P. Fan, M. Zhang, and A. S. Mujumdar, "Effect of various pretreatments on the quality of vacuum-fried carrot chips," *Drying Technology*, vol. 24, no. 11, pp. 1481–1486, 2006.

[11] S.-L. Shyu, L.-B. Hau, and L. S. Hwang, "Effects of processing conditions on the quality of vacuum-fried carrot chips," *Journal of the Science of Food and Agriculture*, vol. 85, no. 11, pp. 1903–1908, 2005.

[12] E. Troncoso, F. Pedreschi, and R. N. Zúñiga, "Comparative study of physical and sensory properties of pre-treated potato slices during vacuum and atmospheric frying," *LWT—Food Science and Technology*, vol. 42, no. 1, pp. 187–195, 2009.

[13] P. García-Segovia, A. M. Urbano-Ramos, S. Fiszman, and J. Martínez-Monzó, "Effects of processing conditions on the quality of vacuum fried cassava chips (Manihot esculenta Crantz)," *LWT—Food Science and Technology*, vol. 69, pp. 515–521, 2016.

[14] M. Zhang, C. Li, X. Ding, and C. W. Cao, "Optimization for preservation of selenium in sweet pepper under low-vacuum dehydration," *Drying Technology*, vol. 21, no. 3, pp. 569–579, 2003.

[15] F. Pedreschi and P. Moyano, "Effect of pre-drying on texture and oil uptake of potato chips," *LWT—Food Science and Technology*, vol. 38, no. 6, pp. 599–604, 2005.

[16] F. A. Afjeh, A. Bassiri, and A. M. Nafchi, "Evaluation of the effects of osmotic dehydration pretreatment at low pressure on texture, colour and oil absorption of vacuum fried kiwi slices," *Food Technology & Nutrition*, no. 12, pp. 5–12, 2015.

[17] Y. Nunes and R. G. Moreira, "Effect of osmotic dehydration and vacuum-frying parameters to produce high-quality mango chips," *Journal of Food Science*, vol. 74, no. 7, pp. E355–E362, 2009.

[18] J. Singthong and C. Thongkaew, "Using hydrocolloids to decrease oil absorption in banana chips," *LWT—Food Science and Technology*, vol. 42, no. 7, pp. 1199–1203, 2009.

[19] R. Sothornvit, "Edible coating and post-frying centrifuge step effect on quality of vacuum-fried banana chips," *Journal of Food Engineering*, vol. 107, no. 3-4, pp. 319–325, 2011.

[20] T. Maity, A. S. Bawa, and P. S. Raju, "Use of hydrocolloids to improve the quality of vacuum fried jackfruit chips," *International Food Research Journal*, vol. 22, no. 4, pp. 1571–1577, 2015.

[21] A. A. Adedeji and M. Ngadi, "Impact of freezing method, frying and storage on fat absorption kinetics and structural changes of parfried potato," *Journal of Food Engineering*, vol. 218, pp. 24–32, 2018.

[22] J. Garayo and R. Moreira, "Vacuum frying of potato chips," *Journal of Food Engineering*, vol. 55, no. 2, pp. 181–191, 2002.

[23] P. F. Da Silva and R. G. Moreira, "Vacuum frying of high-quality fruit and vegetable-based snacks," *LWT—Food Science and Technology*, vol. 41, no. 10, pp. 1758–1767, 2008.

[24] C. Granda, R. G. Moreira, and S. E. Tichy, "Reduction of acrylamide formation in potato chips by low-temperature vacuum frying," *Journal of Food Science*, vol. 69, no. 8, pp. E405–E411, 2004.

[25] G. Pan, H. Ji, S. Liu, and X. He, "Vacuum frying of breaded shrimps," *LWT—Food Science and Technology*, vol. 62, no. 1, pp. 734–739, 2015.

[26] H. Chen, M. Zhang, and Z. Fang, "Vacuum frying of desalted grass carp (Ctenopharyngodon idellus) fillets," *Drying Technology*, vol. 32, no. 7, pp. 820–828, 2014.

[27] M. Mariscal and P. Bouchon, "Comparison between atmospheric and vacuum frying of apple slices," *Food Chemistry*, vol. 107, no. 4, pp. 1561–1569, 2008.

[28] M. R. Perez-Tinoco, A. Perez, M. Salgado-Cervantes, M. Reynes, and F. Vaillant, "Effect of vacuum frying on main physicochemical and nutritional quality parameters of pineapple chips," *Journal of the Science of Food and Agriculture*, vol. 88, no. 6, pp. 945–953, 2008.

[29] Y.-Y. Zhu, M. Zhang, and Y.-Q. Wang, "Vacuum frying of peas: effect of coating and pre-drying," *Journal of Food Science and Technology*, vol. 52, no. 5, pp. 3105–3110, 2015.

[30] H. Zeng, J. Chen, J. Zhai, H. Wang, W. Xia, and Y. L. Xiong, "Reduction of the fat content of battered and breaded fish balls during deep-fat frying using fermented bamboo shoot dietary fiber," *LWT—Food Science and Technology*, vol. 73, pp. 425–431, 2016.

[31] C. Kaur and H. C. Kapoor, "Anti-oxidant activity and total phenolic content of some asian vegetables," *Journal of Food Science and Technology*, vol. 37, no. 2, pp. 153–161, 2002.

[32] N. Akdeniz, S. Sahin, and G. Sumnu, "Functionality of batters containing different gums for deep-fat frying of carrot slices," *Journal of Food Engineering*, vol. 75, no. 4, pp. 522–526, 2006.

[33] S. Albert and G. S. Mittal, "Comparative evaluation of edible coatings to reduce fat uptake in a deep-fried cereal product," *Food Research International*, vol. 35, no. 5, pp. 445–458, 2002.

[34] X.-J. Song, M. Zhang, and A. S. Mujumdar, "Effect of vacuum-microwave predrying on quality of vacuum-fried potato chips," *Drying Technology*, vol. 25, no. 12, pp. 2021–2026, 2007.

[35] A. Bunger, P. Moyano, and V. Rioseco, "NaCl soaking treatment for improving the quality of french-fried potatoes," *Food Research International*, vol. 36, no. 2, pp. 161–166, 2003.

[36] D. Torreggiani, "Osmotic dehydration in fruit and vegetable processing," *Food Research International*, vol. 26, no. 1, pp. 59–68, 1993.

[37] A. J. Fontana, "Water activity: why it is important for food safety," in *Proceedings of the 1st NSF International Conference on Food Safety*, pp. 177–185, 1998.

[38] C. Kaur and H. C. Kapoor, "Anti-oxidant activity and total phenolic content of some Asian vegetables," *International Journal of Food Science & Technology*, vol. 37, no. 2, pp. 153–161, 2002.

Hindawi
Journal of Food Quality
Volume 2017, Article ID 1612708, 7 pages
https://doi.org/10.1155/2017/1612708

Research Article

Comparative Study on Different Drying Methods of Fish Oil Microcapsules

Yuqi Pang, Xu Duan, Guangyue Ren, and Wenchao Liu

College of Food & Bioengineering, Henan University of Science and Technology, Luoyang 471023, China

Correspondence should be addressed to Xu Duan; duanxu_dx@163.com

Received 26 May 2017; Accepted 10 October 2017; Published 31 October 2017

Academic Editor: Prabhat K. Nema

Microencapsulation is widely used to minimize the oxidation of fish oil products. This study compared the effects of different drying methods, for example, spray drying (SD), freeze drying (FD), and spray freeze drying (SFD) on the microencapsulation of fish oil. Spray drying (SD) is the most common method for producing fish oil microcapsules, and it has low operation cost and short processing time, while the product yield and quality are poor. Freeze drying (FD) can be used to produce oil microcapsules with high quality, but it takes long time and high overall cost for drying. Spray freeze drying (SFD) is a new method for the preparation of microcapsules, which combines the SD and FD processes to obtain high quality powder. The yield of powder reached 95.07% along with porous structure by SFD. The stability and slow-release property of SFD products were better than those of SD and FD, which showed that SFD improved product storage stability and potential digestibility.

1. Introduction

Omega-3 polyunsaturated fatty acids (ω-3-PUFA), especially docosahexaenoic acid (DHA, C22:6 ω-3) and eicosapentaenoic acid (EPA, C20:5 ω-3), are considered necessary for human health because of some health beneficial effects. The ω-3-PUFA can prevent cardiovascular disease and improve the cardiovascular activity, anti-inflammatory reaction, and development of brain and eye retina in infants and young children [1, 2]. The main food sources of ω-3-PUFA are fish and fish oil, and particularly fish oil is considered as the most important supplement of ω-3-PUFA [3]. In fact, ω-3 fatty acids biosynthetic pathways are slow in human body [4]; therefore, it could be beneficial to human health by consumption of fish oil which is rich in ω-3 fatty acid [5].

However, the oxidative instability of ω-3-PUFA during storage restricts its use in foods owing to lipid oxidation [6]. At present, the main products of fish oil are soft capsule and oral liquid, but, because of their short storage period, the further processing of fish oil has been limited. Nowadays, encapsulation has appeared to be an essential technique to incorporate such valuable sensitive ingredients into food systems which can be efficiently used to protect food ingredients (i.e., flavors, essential oils, lipids, oleoresins, and colorants) against deterioration, volatile losses, and interaction with other ingredients [7]. As a result, microencapsulation of fish oil could be an alternative method to solve the above issues. It has been reported that microencapsulation of functional foods is an effective approach to achieve the desired attributes of stability, storability, and delivery [8]. Microencapsulation is mainly used to encapsulate a gel, solid, liquid, or gas core by a coating shell [9], which is a promising technique for maintaining the viability of fish oil during the process and covering the smell of fish [10]. Microencapsulation technology could isolate functional oils from deteriorating effects of air, mitigate the evaporation rate of volatile cores, mask the taste or odor of core materials, and isolate reactive core materials from chemical attacks [11]. The key step is the selection of the microencapsulation process and the coating materials in microencapsulation of foods [12, 13].

The spray drying is one of the most frequently used operations for drying of emulsions and slurries containing oils and flavors during microencapsulation process [14, 15]. Spray drying (SD), which is used to prepare dry, stable, and small volume food material, has characters of low operation cost and short processing time. Nevertheless, due to the high temperature drying strategy during SD process, this drying method was not suitable for the preparation of

heat sensitive products [16]. Aghbashlo et al. [17, 18] and Ramakrishnan et al. [19] have reported that SD can be used to prepare fish oil microcapsules, and Kalkan et al. [20] used SD to prepare hazelnut oil microcapsules. But the product quality was not good enough because of high temperature and oxygen stresses. Anwar and Kunz [12] confirmed that although SD only needed a few seconds to produce a desirable size of granules, it had a high chance of lipid degradation by oxidation due to high drying temperature in the SD process. Leung et al. used SD and spray freeze drying (SFD) to produce inhalation phage powders and found that SD powders loss was much higher than the SFD powders during the aerosolization process [21]. Her et al. reported that SD had the advantage of low operation cost as a common technology used in the food industry, while most of flavoring compounds were easily lost during SD operation [14]. Freeze drying (FD) can remove the water by sublimation under vacuum condition to prepare the high quality dried products [22]. However, it takes long time and high overall cost for drying [23]. To avoid drawbacks of both methods, a new method, SFD, is gradually being applied to prepare stable and uniform volume food materials.

SFD combines advantages of SD and FD to obtain fine flavor powders without heat damage, which prevents the powders from agglomeration in turn. SFD is a two-step process, that is, spray freezing followed by freeze drying of the resultant frozen particles in a freeze drier [10]. Ishwarya et al. [24] reported that, compared with other drying technologies, the potential applications in product structure, quality, retention of volatiles, and biologically active compounds of SFD are better. The selection of encapsulation method is governed by important variables, such as the desired size of the microcapsules and the controlled release of oil from microcapsules in foods or in gastrointestinal tract. It was reported that the microcapsule powders by SFD had a uniform particle size, larger specific surface area, and a better porous character than freeze-dried and spray-dried powders. The powders retained their spherical and porous morphology and could be further coated with an enteric food grade biological polymer and conducive to be absorbed [1, 25, 26]. Her et al. [14] reported that SFD combined the SD and FD processes to obtain fine flavor powder without heat damage, which in turn prevented the drying of the agglomerates, while flavor powder produced by the SFD process typically had a larger surface area and higher fine particle fraction than the particles produced by the SD process, so it could be more quickly and easily rehydrated. In addition, the effective embedding capability of SFD powders can mask unpleasant flavor. In conclusion, SFD can be introduced to prepare fish oil microcapsules with better product quality and less oxidation.

Up to date, there is no report about the application of SFD on fish oil microcapsulation. The objective of this research was to compare the performance of spray drying, freeze drying, and spray freeze drying for fish oil microcapsule preparation, and, then, a suitable method of fish oil microcapsule manufacture for different application fields can be suggested.

2. Materials and Methods

2.1. Materials. In this study, refined fish oil was purchased from Zebang Biological Technology Co. Ltd. (Xi'an, Shanxi, China). Acacia gum (food grade) and sodium alginate (food grade) were used to build the microcapsules, and the Tween-80 was used as emulsifier. The rest of the reagents used in this study, such as ethanol absolute and light petroleum, were of analytical grade and obtained from the Deen Chemical Reagent Co. Ltd. (Tianjin, China).

2.2. Emulsion Preparation. Two kinds of materials with opposite charge—acacia gum with negative charge and sodium alginate with positive charge—are selected as wall material. Acacia gum, sodium alginate, and Tween-80 at the ratio of 3 : 1 : 0.1 which was determined by the research from Ramakrishnan et al. [19] were added in distilled water, and then the solution was homogenized at 3000 r/min for 3 min by a homogenizer (AD500S-H, Onnen Instrument Co., Ltd., Shanghai, China) at 60°C. Finally, a certain flask proportion of fish oil was added to the solution and the ratio of the core and wall was 1 : 4, and some water was added to ensure the final solids content to be 15% which was determined by the research from Li et al. [27], and then it was homogenized at 8000 r/min for 5 min by emulsification homogenizer to obtain emulsion liquid reserved.

2.3. Drying Procedure

2.3.1. Spray Drying (SD). The pretreated materials were dried by a pressure spray dryer (YC-015, Pilotech Instrument & Equipment Co., Ltd., Shanghai, China) with two-fluid spray atomization and cocurrent air flow which was 1200 mm in height, 650 mm in length, and 500 mm in width. The emulsion was fed into the chamber through a peristaltic pump at a feed flow rate (1×10^3 mL/h). The inlet air temperature was set at 180°C while outlet air temperature was 80°C, and the air flow rate was 35 m^3/h.

2.3.2. Freeze Drying (FD). The emulsion was placed into aluminum plates and frozen at −25°C for 24 h and then was put into the FD chamber (LGJ-10D, Si Huan Scientific Instrument Factory Co., Ltd., Beijing, China) at the pressure of 20 Pa. During the drying process, the temperature of heat shelf was set as 40°C and the cold trap was set at lower than −50°C. The frozen emulsion was dried for 36 h.

2.3.3. Spray Freeze Drying (SFD). Figure 1 shows the spray freeze dryer (YC-3000, Pilotech Instrument & Equipment Co., Ltd., Shanghai, China) used in this study. The emulsion liquid was sprayed through a two-fluid nozzle (nozzle tip lift: 0.5 mm opening) and a peristaltic pump with a flow rate of 15 mL/min. The ultimate vacuum pressure can be set at less than 20 Pa and atomization air pressure can be set from 2 Bar to 5 Bar while it was set at 5 Bar in this study. During this process, spray droplets were frozen while passing through the cryogenic gas. After the spraying process, the samples were treated by FD process. FD process used natural

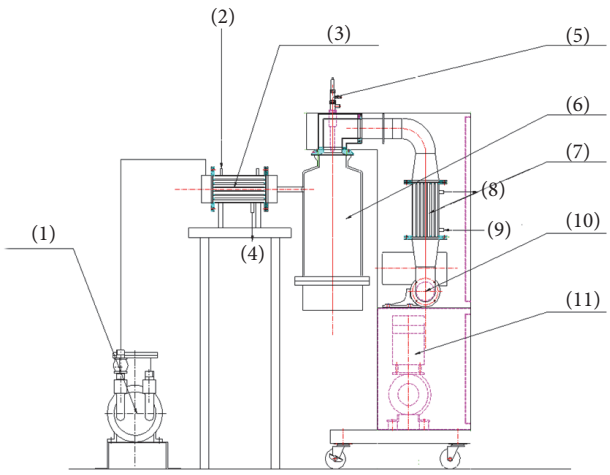

(1) Vacuum pump
(2) Coolant inlet
(3) Cold trap
(4) Coolant outlet
(5) Atomizer
(6) Spray freeze drying chamber
(7) Heat exchanger
(8) Coolant outlet
(9) Coolant inlet
(10) draught fan
(11) Air compressor

Figure 1: The schematic diagram of vacuum spray freeze drier.

air heating, and the pressure (20 Pa) was maintained by a vacuum pump. The cold trap was set at −65°C, which was sufficient to condense all vapor generated during FD.

2.4. Analysis of Sample

2.4.1. Moisture Content. Moisture content was determined by the gravimetric method. At regular time intervals during the drying processes samples were taken out and dried in the oven for 7-8 h at 105°C until constant weight. Weighing was performed on a digital balance, and then moisture content was calculated. The tests were performed in triplicate.

2.4.2. Drying Yield. The yield of different drying methods was calculated according to formula (1) as follows:

$$\text{Yield} = \frac{(M_1 - M_2)}{M_0} \times 100\%, \quad (1)$$

where M_1 was the weight (g) of samples after drying; M_2 was the moisture content (g); and M_0 was the solids content (g) of emulsion liquid.

2.4.3. Encapsulation Efficiency (EE). The encapsulation efficiency was obtained by determining the total oil content and surface oil content of microcapsules, respectively [28], and was calculated according to formula (2) as follows:

$$\text{EE} = \frac{(\text{Total oil content} - \text{Surface oil content})}{\text{Total oil content}} \times 100\%. \quad (2)$$

Extraction of Total Oil. Ten millilitres of water was added to 2 g of fish oil microcapsule (M_1, g) followed by homogenization for 5 times and the homogenizer was rinsed with ethanol. The emulsion was sealed by plastic film after 20 mL ethanol and 20 mL petroleum ether were added in the beaker (M_2, g). The oil was extracted by a magnetic stirrer at 70°C for 10 min followed by centrifuging for 5 min at 3000 r/min by a high speed centrifuge (TG16-WS, Xiangyi Laboratory Instrument Development Co., Ltd., Hunan, China). The liquid layer was discarded followed by drying of solid residue and weighing (M_3, g). Each treatment was determined in triplicate:

$$\text{Total oil content} = \frac{(M_3 - M_2)}{M_1}, \quad (3)$$

where M_1 was the weight (g) of samples; M_2 was the weight (g) of beaker; and M_3 was the weight (g) of beaker containing barrier residue (g) after drying.

Extraction of Surface Oil. Twenty millilitres of petroleum ether was added to 2 g of fish oil microcapsule (M_1, g) in an Erlenmeyer flask (M_4, g) followed by shaking at 25°C for 2 min and standing for 8 min. The suspension was then filtered through filter paper (M_5, g) and the residue was rinsed three times with 15 mL petroleum ether. The Erlenmeyer flask and filter paper were transferred to an oven (101-2, Kewei Yongxing Instrument Co., Ltd., Beijing, China) and heated at 75°C for 6 h until petroleum ether was completely evaporated and then weighed (M_6, g). Each treatment was determined in triplicate:

$$\text{Surface oil content} = \frac{(M_1 + M_4 + M_5 - M_6)}{M_1}, \quad (4)$$

where M_1 was the weight (g) of samples; M_4 was the weight (g) of the Erlenmeyer flask; M_5 was the weight (g) of filter paper; M_6 was the total weight (g) after drying.

2.4.4. Color. The color of dried samples was measured using a spectrocolorimeter (Xrite Color i5, X-Rite Inc., MI, USA). The results were expressed as Hunter L^*, a^*, and b^*, respectively, where L^* was the degree of lightness, a^* the degree of redness (+) and greenness (−), and b^* the degree of yellowness (+) and blueness (−). The Hunter L^*, a^*, and b^* values of each treatment were determined in triplicate.

2.4.5. Sensory Evaluation. The sensory evaluation of dried samples was judged by 9 persons who were untrained. They were asked to indicate their preference for each sample, based on the quality attributes of color, appearance, texture, flavor, and overall acceptability. Score was divided into five grades: 9-10 denoted "like very much"; 7-8 "like"; 5-6 "neutral"; 3-4 "dislike"; and 1-2 "dislike very much." They were asked to give their remarks about each of the samples.

2.4.6. Stability. The samples of the microcapsules produced by different drying methods (FD, SD, and SFD) were kept in brown bottle closed containers at 30°C for 2 months. Samples were taken to determine the oil stability by detecting the propanal formation every 15 days. A static headspace sampler (G1888 from Agilent Tachnologies, Waldbronn, Germany)

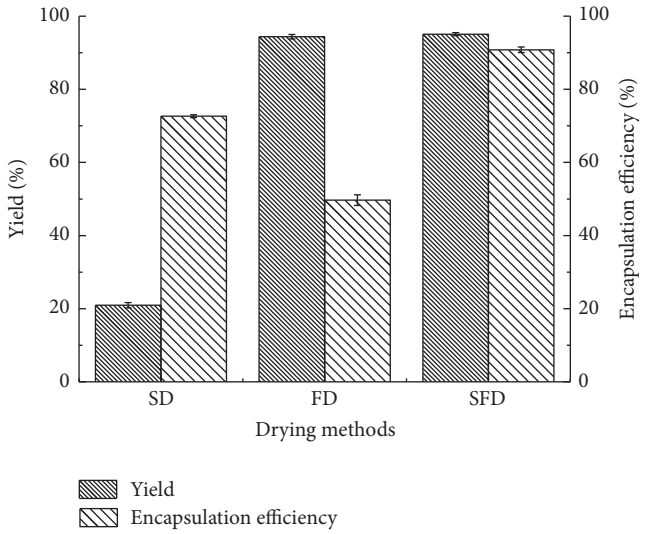

Figure 2: The productivity and encapsulation efficiency of different drying methods of fish oil microcapsules.

coupled to a gas chromatograph (HP 6890 from Hewlett-Packard, Waldbronn, Germany) was used to determine the propanal content of the microcapsules [15].

2.4.7. Scanning Electron Microscopy. The fish oil microcapsules with different treatments were sprinkled onto a two-sided adhesive tape and sputter-coated with gold in a sputter coater. The microstructural properties of the fish oil microcapsules was observed with a Quanta-250 feg scanning electron microscope (FEI Co., Eindhoven, Netherlands) at an accelerating voltage of 10 kV.

2.4.8. Slow-Release Property. The fish oil microcapsule was added to 100 mL simulated gastric fluid (pH 1) for 2 h in a constant temperature oscillator with 90 r/min at 37°C, which was followed by transferring into simulated intestinal fluid (pH 7.1) that contained 0.025 mol/L Na_2HPO_4 and 0.025 mol/L KH_2PO_4. The released fish oil was extracted and weighed while the release rate was calculated.

2.5. Statistical Analysis. Analysis of variance and the test of mean comparison, according to Tukey's honestly significant difference, were conducted at the level of significance of 0.05. The statistical software SPSS (version 10.0) for Windows was used for the analysis.

3. Results and Discussion

3.1. Characteristics of SFD. Figure 2 shows the yield and encapsulation efficiency of the products obtained by SD, FD, and SFD, respectively. It was found that the yields of SFD (95.07%) and FD (94.39%) were close and far greater than that of SD (20.93%). The yield of FD and SFD showed no significant difference ($P > 0.05$). The possible reason was that SD underwent higher temperature resulting in part of products lost through the exhaust system and some of products wall sticking during the liquid drop was heated to evaporate. In comparison, SFD and FD could effectively avoid this phenomenon because of lower drying temperature. On the other hand, the encapsulation efficiency of SFD reached 90.80%, while that of FD and SD was 49.7% and 72.64%, respectively. The encapsulation efficiency of SD was higher than that of Aghbashlo et al. [18] and lower than that of Aghbashlo et al. [29] which may be related to the changes in selection of wall materials and the application of different analytical methods of SFD atomized the emulsion into small droplets under the condition of negative pressure, which promoted the embedment process. Thus, it can be concluded that SFD ensured the highest yield and encapsulation efficiency than SD and FD.

For color of the fish oil microcapsules, L^* value exhibits the brightness of sample, and higher L^* means brighter color, which implies the product can obtain a good commodity value. As shown in Table 1, it was found that L^* value of SD fish oil microcapsules was much lower than the others. This meant SD samples have a darker color than that of the other two methods because high processing temperature could lead to browning effects. It was observed that there was significant difference between the L^* values of SFD and FD products ($P \leqq 0.05$). The sensory value of FD was also lower than that of SFD because FD powder was irregular in structure and had a large surface area [12]. The moisture content of three samples was similar, but when the three samples were exposed to air for a period of time to observe their mobility, it was found that FD powder had stronger moisture absorption, and the SD powder was easy to agglomerate, while the SFD powder can better maintain the original state. The moisture content of SD powder in the study of Aghbashlo et al. [18] was slightly lower than this study, and the possible reason was the difference of feed flow rate. The higher feed flow rate (1×10^3 mL/h) in this study reduced the contact time between the emulsion and the hot air that made the emulsion not fully dried, which resulted in the higher moisture content. Therefore, it can be concluded that SFD can ensure good appearance and product quality. Moreover, as shown in Table 1, compared to FD, SFD greatly reduced drying time.

3.2. Slow-Release Property. Figure 3 shows slow-release curves of various samples. It was found that the slow-release property of SFD was much higher than that of SD and FD. The microcapsules exhibited fast release rate of 27.2% within the first 1 h, and then the release rate reached about 67.2% within 8 h. The slow release indicated release of the fish oil from the core of microcapsules. The slow-release rate of FD products was the lowest, which was related to the irregular structure of FD samples, and the thickness of the wall materials was not uniform. As a result, the fish oil was difficult to release from the pore of wall. It was reported that microcapsules released fish oil through diffusion rather than dissolution of the shell material [8]. The release rate of SFD samples was 84.2% within 12 h, which indicated that the release rate of SFD products was higher. This property was conducive to the absorption of the intestines. The slow-release rate of SD products also increased fast in the

Table 1: Effect of different drying methods on color, sensory value, moisture content, and drying time of fish oil microcapsules.

Drying method	L^*	a^*	b^*	Sensory value	Moisture content	Drying time
FD	92.98 ± 0.05^b	0.90 ± 0.02^b	8.20 ± 0.01^b	7.13 ± 0.08^c	4.05 ± 0.03^a	36 ± 1.0 h
SD	66.06 ± 0.01^c	12.24 ± 0.02^a	20.30 ± 0.06^a	7.94 ± 0.14^b	3.60 ± 0.06^b	2.0 ± 0.5 h
SFD	95.33 ± 0.01^a	0.40 ± 0.03^c	1.64 ± 0.01^c	9.54 ± 0.04^a	3.38 ± 0.09^b	24 ± 1.5 h

*Different letters indicated a significant difference ($P \leqq 0.05$) in a column.

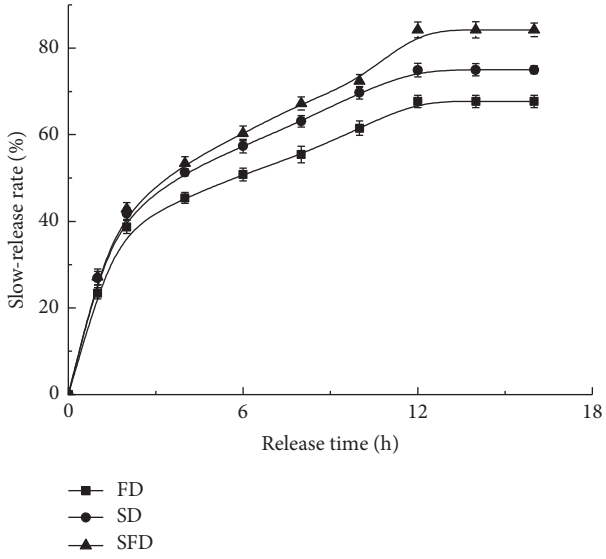

Figure 3: Release profile of fish oil microcapsules by different drying methods.

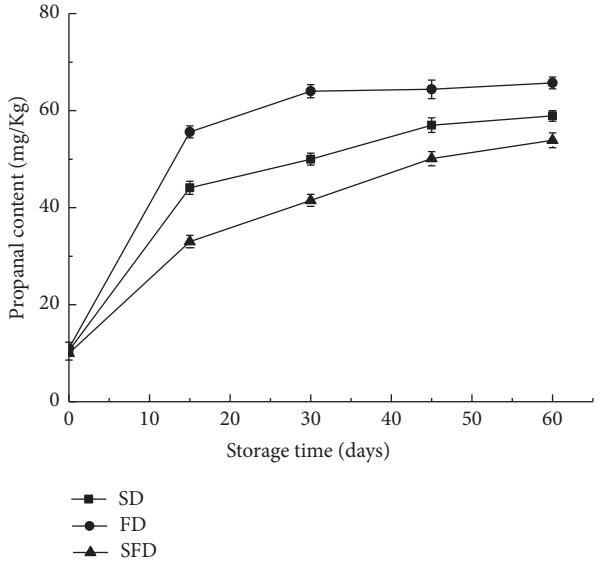

Figure 4: The relationship between the storage time and propanal content of fish oil microcapsules by different drying methods.

early stage, and then the curve exhibited a gentle trend. The maximum slow-release rate of SD was 75%.

3.3. Stability. Propanal is one of the main volatile compounds generated during the oxidative decomposition of omega-3 fatty acids and it has been recommended to evaluate the oxidation stability of foods that are rich in this type of fatty acids [19].

As shown in Figure 4, at the beginning of this process, the propanal contents of the three kinds of microcapsules were all close to 11 mg/kg. During the first 15 days, the propanal content had a fast growth trend, particularly the FD powder, which had the highest growth rate. Then the growth rate was slowed down slightly, and it tended to be stable after 30 days, which implied almost no subsequent oxidation proceeding. It was found that the propanal content of SFD products was lower than that of SD and FD samples. The possible reason was that the propanal content was related to surface oil content and moisture content. The surface oil content of FD and SD samples was relatively high resulting in a high propanal content. A number of studies have been reported on the oxidative stability of microencapsulated fish oil obtained either by SD or by FD, and the results were inconsistent [30, 31]. These inconsistent results may be due to changes in conditions of storage and different analytical methods. As a result, SFD could ensure fish oil microcapsules with good stability.

3.4. Scanning Electron Microscopy. Microcapsule's microstructure and morphology are important to determine their stability, functionality, and flowability [32]. Figure 5 shows the scanning electron microscopy (SEM) images of fish oil microcapsules obtained by different drying methods (SD, FD, and SFD) in order to investigate the surface morphology and microstructure. As shown in Figures 5(a) and 5(b), SFD sample exhibited a clearer porous structure. The porous structure was possibly formed by cavities left from ice crystals or air bubbles retained during the freezing [33]. As water was removed by sublimation during the freeze drying process, the SFD could obtain a porous structure [21]. The image showed the microcapsules of SFD powders had spherical shape and porous surface structure. From Figures 5(b), 5(c), and 5(d), it was found that the microstructure of SD was similar to that of SFD with spherical shape structure but had smooth surface and occurrence of dents and cracks was less, which was similar to the spray granulation (SG) powder done by Anwar et al. [32]. Aghbashlo et al. [34] reported that the microcapsules produced by SD were almost spherical in shape and had a slightly smooth surface without any particle expansion, which was consistent with the results of this study. FD microcapsules had porous surface, but their structure was highly heterogeneous. The reason for the difference of microstructure between FD and SFD was the spray drying process of SFD, which can spray the emulsion liquid to

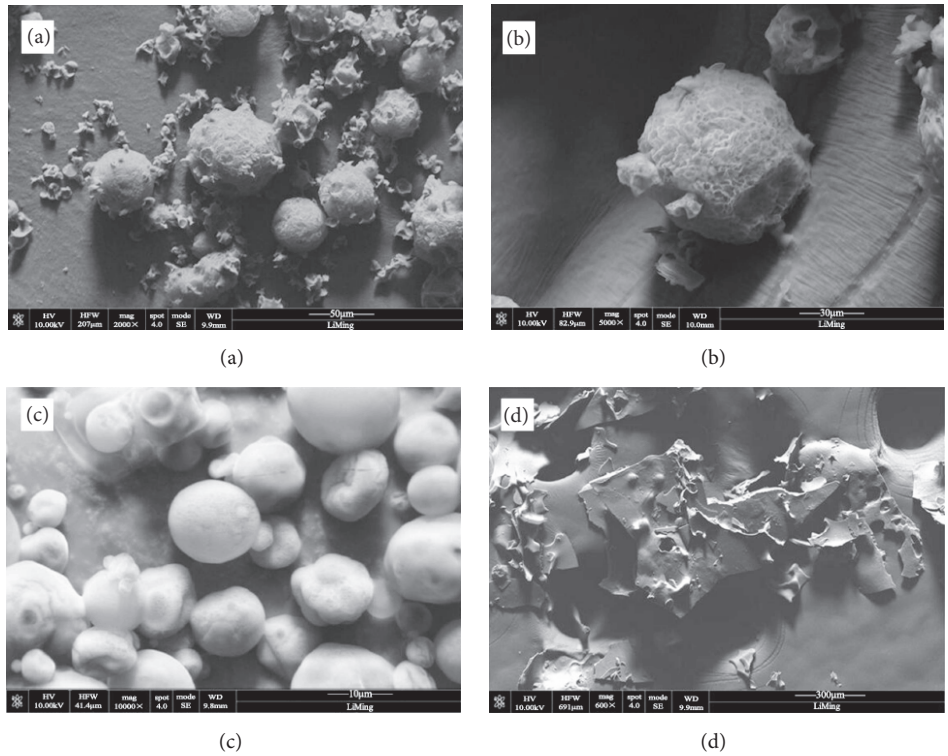

FIGURE 5: Comparison of the morphology of (a) spray-freeze-dried (2000x); (b) spray-freeze-dried (5000x); (c) spray-dried (10000x); and (d) freeze-dried (600x) fish oil microcapsule.

spheroid. Anwar et al. [32] pointed that the absence of cracks is critically important to wall functionality in limiting fish oil deterioration or oxidation during storage. Therefore, SD and SFD can effectively avoid the deterioration and oxidation of fish oil. In conclusion, SFD produced high quality fish oil microcapsules.

4. Conclusions

Freeze drying fish oil microcapsule takes long time and high overall cost for drying. Spray drying has low operation cost and short processing time, while the yield and quality of products are poor under the experimental conditions of this study. Spray freeze drying can replace conventional freeze drying and microcapsule powders produced by SFD have a uniform particle size, large specific surface area, and a great porous character. In addition, SFD improves the slow-release effect and storage stability of the products, and it combines the SD and FD processes to obtain higher quality powder and reduces the drying time.

Conflicts of Interest

The authors declare that they have no conflicts of interest.

Acknowledgments

The authors acknowledge that this project was financially supported by the National Natural Science Foundation of China under Contract no. 31671907 and National Key R&D Program of China under Contract no. 2017YFD0400900. The authors also acknowledge the support of the Program for Science and Technology Innovation Talents in Universities of Henan Province, no. 14HASTIT023, and the support of the Program for Science and Technology Innovation Team in Universities of Henan Province, no. 16IRTSTHN009.

References

[1] C. Encina, C. Vergara, B. Giménez, F. Oyarzún-Ampuero, and P. Robert, "Conventional spray-drying and future trends for the microencapsulation of fish oil," *Trends in Food Science & Technology*, vol. 56, pp. 46–60, 2016.

[2] P. J. García-Moreno, K. Stephansen, J. Van Der Kruijs et al., "Encapsulation of fish oil in nanofibers by emulsion electrospinning: Physical characterization and oxidative stability," *Journal of Food Engineering*, vol. 183, pp. 39–49, 2016.

[3] A. Jeyakumari, G. Janarthanan, M. K. Chouksey, and G. Venkateshwarlu, "Effect of fish oil encapsulates incorporation on the physico-chemical and sensory properties of cookies," *Journal of Food Science and Technology*, vol. 53, no. 1, pp. 856–863, 2016.

[4] I. Peinado, W. Miles, and G. Koutsidis, "Odour characteristics of seafood flavour formulations produced with fish by-products incorporating EPA, DHA and fish oil," *Food Chemistry*, vol. 212, pp. 612–619, 2016.

[5] L. Sanguansri, P. Udabage, S. Bhail et al., "Microencapsulated Fish Oil Powder Formulation with Improved Resistance to Oil

Leakage During Powder Compression," *Journal of the American Oil Chemists' Society*, vol. 93, no. 5, pp. 701–710, 2016.

[6] P. J. García-Moreno, A. Guadix, E. M. Guadix, and C. Jacobsen, "Physical and oxidative stability of fish oil-in-water emulsions stabilized with fish protein hydrolysates," *Food Chemistry*, vol. 203, pp. 124–135, 2016.

[7] S. Shamaei, A. Kharaghani, S. S. Seiiedlou, M. Aghbashlo, F. Sondej, and E. Tsotsas, "Drying behavior and locking point of single droplets containing functional oil," *Advanced Powder Technology*, vol. 27, no. 4, pp. 1750–1760, 2016.

[8] S. Chatterjee and Z. M. A. Judeh, "Impact of encapsulation on the physicochemical properties and gastrointestinal stability of fish oil," *LWT- Food Science and Technology*, vol. 65, pp. 206–213, 2016.

[9] A. Ghaemi, A. Philipp, A. Bauer, K. Last, A. Fery, and S. Gekle, "Mechanical behaviour of micro-capsules and their rupture under compression," *Chemical Engineering Science*, vol. 142, pp. 236–243, 2016.

[10] R. Rajam and C. Anandharamakrishnan, "Spray freeze drying method for microencapsulation of Lactobacillus plantarum," *Journal of Food Engineering*, vol. 166, pp. 95–103, 2015.

[11] S. Shamaei, S. S. Seiiedlou, M. Aghbashlo, and H. Valizadeh, "Mathematical modeling of drying behavior of single emulsion droplets containing functional oil," *Food and Bioproducts Processing*, vol. 101, pp. 100–109, 2017.

[12] S. H. Anwar and B. Kunz, "The influence of drying methods on the stabilization of fish oil microcapsules: Comparison of spray granulation, spray drying, and freeze drying," *Journal of Food Engineering*, vol. 105, no. 2, pp. 367–378, 2011.

[13] P. K. Binsi, N. Nayak, P. C. Sarkar et al., "Structural and oxidative stabilization of spray dried fish oil microencapsulates with gum arabic and sage polyphenols: Characterization and release kinetics," *Food Chemistry*, vol. 219, pp. 158–168, 2017.

[14] J.-Y. Her, M. S. Kim, M. K. Kim, and K.-G. Lee, "Development of a spray freeze-drying method for preparation of volatile shiitake mushroom (Lentinus edodes) powder," *International Journal of Food Science & Technology*, vol. 50, no. 10, pp. 2222–2228, 2015.

[15] S. Shamaei, S. S. Seiiedlou, M. Aghbashlo, E. Tsotsas, and A. Kharaghani, "Microencapsulation of walnut oil by spray drying: effects of wall material and drying conditions on physicochemical properties of microcapsules," *Innovative Food Science and Emerging Technologies*, vol. 39, pp. 101–112, 2017.

[16] J.-Y. Her, M. S. Kim, and K.-G. Lee, "Preparation of probiotic powder by the spray freeze-drying method," *Journal of Food Engineering*, vol. 150, pp. 70–74, 2015.

[17] M. Aghbashlo, H. Mobli, S. Rafiee, and A. Madadlou, "An artificial neural network for predicting the physiochemical properties of fish oil microcapsules obtained by spray drying," *Food Science and Biotechnology*, vol. 22, no. 3, pp. 677–685, 2013.

[18] M. Aghbashlo, H. Mobli, A. Madadlou, and S. Rafiee, "Influence of Wall Material and Inlet Drying Air Temperature on the Microencapsulation of Fish Oil by Spray Drying," *Food and Bioprocess Technology*, vol. 6, no. 6, pp. 1561–1569, 2013.

[19] S. Ramakrishnan, M. Ferrando, L. Aceña-Muñoz, M. Mestres, S. De Lamo-Castellví, and C. Güell, "Influence of Emulsification Technique and Wall Composition on Physicochemical Properties and Oxidative Stability of Fish Oil Microcapsules Produced by Spray Drying," *Food and Bioprocess Technology*, vol. 7, no. 7, pp. 1959–1972, 2014.

[20] F. Kalkan, S. K. Vanga, R. Murugesan, V. Orsat, and V. Raghavan, "Microencapsulation of hazelnut oil through spray drying," *Drying Technology*, vol. 35, no. 5, pp. 527–533, 2017.

[21] S. S. Y. Leung, T. Parumasivam, F. G. Gao et al., "Production of Inhalation Phage Powders Using Spray Freeze Drying and Spray Drying Techniques for Treatment of Respiratory Infections," *Pharmaceutical Research*, vol. 33, no. 6, pp. 1486–1496, 2016.

[22] J. Barbosa, S. Borges, M. Amorim et al., "Comparison of spray drying, freeze drying and convective hot air drying for the production of a probiotic orange powder," *Journal of Functional Foods*, vol. 17, pp. 340–351, 2015.

[23] C. Chranioti, S. Chanioti, and C. Tzia, "Comparison of spray, freeze and oven drying as a means of reducing bitter aftertaste of steviol glycosides (derived from Stevia rebaudiana Bertoni plant) - Evaluation of the final products," *Food Chemistry*, vol. 190, pp. 1151–1158, 2016.

[24] S. P. Ishwarya, C. Anandharamakrishnan, and A. G. F. Stapley, "Spray-freeze-drying: A novel process for the drying of foods and bioproducts," *Trends in Food Science & Technology*, vol. 41, no. 2, pp. 161–181, 2015.

[25] T. Okuda, Y. Suzuki, Y. Kobayashi et al., "Development of biodegradable polycation-based inhalable dry gene powders by spray freeze drying," *Pharmaceutics*, vol. 7, no. 3, pp. 233–254, 2015.

[26] D. Semyonov, O. Ramon, Z. Kaplun, L. Levin-Brener, N. Gurevich, and E. Shimoni, "Microencapsulation of Lactobacillus paracasei by spray freeze drying," *Food Research International*, vol. 43, no. 1, pp. 193–202, 2010.

[27] J. Li, S. Xiong, F. Wang, J. M. Regenstein, and R. Liu, "Optimization of Microencapsulation of Fish Oil with Gum Arabic/Casein/Beta-Cyclodextrin Mixtures by Spray Drying," *Journal of Food Science*, vol. 80, no. 7, pp. C1445–C1452, 2015.

[28] P. Pourashouri, B. Shabanpour, S. H. Razavi, S. M. Jafari, A. Shabani, and S. P. Aubourg, "Impact of Wall Materials on Physicochemical Properties of Microencapsulated Fish Oil by Spray Drying," *Food and Bioprocess Technology*, vol. 7, no. 8, pp. 2354–2365, 2014.

[29] M. Aghbashlo, H. Mobli, A. Madadlou, and S. Rafiee, "The correlation of wall material composition with flow characteristics and encapsulation behavior of fish oil emulsion," *Food Research International*, vol. 49, no. 1, pp. 379–388, 2012.

[30] W. Kolanowski, M. Ziolkowski, J. Weißbrodt, B. Kunz, and G. Laufenberg, "Microencapsulation of fish oil by spray drying - Impact on oxidative stability. Part 1," *European Food Research and Technology*, vol. 222, no. 3-4, pp. 336–342, 2006.

[31] S. Drusch, Y. Serfert, and K. Schwarz, "Microencapsulation of fish oil with n-octenylsuccinate-derivatised starch: flow properties and oxidative stability," *European Journal of Lipid Science and Technology*, vol. 108, no. 6, pp. 501–512, 2006.

[32] S. H. Anwar, J. Weissbrodt, and B. Kunz, "Microencapsulation of fish oil by spray granulation and fluid bed film coating," *Journal of Food Science*, vol. 75, no. 6, pp. E359–E371, 2010.

[33] Y. Zhang, C. Tan, S. Abbas, K. Eric, S. Xia, and X. Zhang, "Modified SPI improves the emulsion properties and oxidative stability of fish oil microcapsules," *Food Hydrocolloids*, vol. 51, pp. 108–117, 2015.

[34] M. Aghbashlo, H. Mobli, A. Madadlou, and S. Rafiee, "Fish oil microencapsulation as influenced by spray dryer operational variables," *International Journal of Food Science & Technology*, vol. 48, no. 8, pp. 1707–1713, 2013.